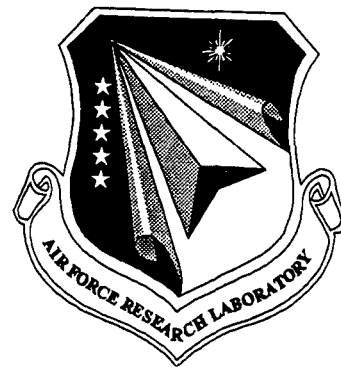


AFRL-ML-WP-TR-1998-4008

**RUN-IN FINISHING AND TRIBOLOGICAL
PERFORMANCE EVALUATION OF
CERAMIC BEARINGS**



O.O. AJAYI
L.D. WEDEVEN

WEDEVEN ASSOCIATES, INC.
5072 WEST CHESTER PIKE
EDGMONT, PA 19028-0646

JANUARY 1998

FINAL REPORT FOR 09/01/1991 – 12/31/1994

APPROVED FOR PUBLIC RELEASE; DISTRIBUTION IS UNLIMITED.

19980915 088

**MATERIALS DIRECTORATE
WRIGHT LABORATORY
AIR FORCE MATERIEL COMMAND
WRIGHT-PATTERSON AFB, OH 45433-7734**

19980915 088

NOTICE

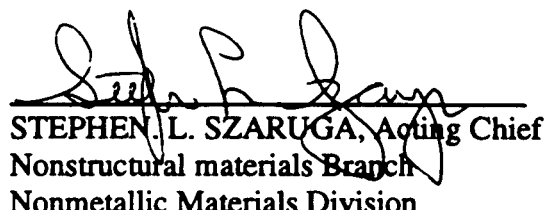
Using government drawings, specifications, or other data included in this document for any purpose other than government procurement does not in any way obligate the US government. The fact that the government formulated or supplied the drawings, specifications, or other data does not license the holder or any other person or corporation; or convey any rights or permission to manufacture, use, or sell any patented invention that may relate to them.

This report is releasable to the national technical information service (NTIS). At NTIS, it will be available to the general public, including foreign nations.

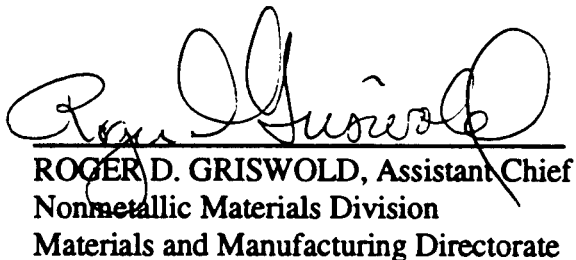
This technical report has been reviewed and is approved for publication.



SHASHI K. SHARMA, Project Engineer
Nonstructural materials Branch
Nonmetallic Materials Division



STEPHEN L. SZARUGA, Acting Chief
Nonstructural materials Branch
Nonmetallic Materials Division



ROGER D. GRISWOLD, Assistant Chief
Nonmetallic Materials Division
Materials and Manufacturing Directorate

If your address has changed, if you wish to be removed from our mailing list, or if the addressee is no longer employed by your organization please notify AFRL/MLBT, 2941 P Street, Suite 1, Wright-Patterson AFB OH 45433-7750 to help maintain a current mailing list.

Do not return copies of this report unless contractual obligations or notice on a specific document requires its return.

| REPORT DOCUMENTATION PAGE | | | Form Approved OMB No. 0704-0188 | |
|--|---|--|---|--|
| Public reporting burden for this collection of information is estimated to average 1 hour per response, including the time for reviewing instructions, searching existing data sources, gathering and maintaining the data needed, and completing and reviewing the collection of information. Send comments regarding this burden estimate or any other aspect of this collection of information, including suggestions for reducing this burden, to Washington Headquarters Services, Directorate for Information Operations and Reports, 1215 Jefferson Davis Highway, Suite 1204, Arlington, VA 22202-4302, and to the Office of Management and Budget, Paperwork Reduction Project (0704-0188), Washington, DC 20503. | | | | |
| 1. AGENCY USE ONLY (Leave blank) | | 2. REPORT DATE JAN 1998 | 3. REPORT TYPE AND DATES COVERED FINAL 09/01/1991--12/31/1994 | |
| 4. TITLE AND SUBTITLE RUN-IN FINISHING AND TRIBOLOGICAL PERFORMANCE EVALUATION OF CERAMIC BEARINGS | | | 5. FUNDING NUMBERS C F33615-92-C-5925 PE 62712 PR 8355 TA 00 WU 03 | |
| 6. AUTHOR(S) O.O. AJAYI L.D. WEDEVEN | | | | |
| 7. PERFORMING ORGANIZATION NAME(S) AND ADDRESS(ES) WEDEVEN AND ASSOCIATES, INC. 5072 WEST CHESTER PIKE EDGEMONT, PA 19028 | | | 8. PERFORMING ORGANIZATION REPORT NUMBER | |
| 9. SPONSORING/MONITORING AGENCY NAME(S) AND ADDRESS(ES) MATERIALS AND MANUFACTURING DIRECTORATE AIR FORCE RESEARCH LABORATORY AIR FORCE MATERIEL COMMAND WRIGHT PATTERSON AFB OH 45433-7734 POC: MR. MECKLENBURG, AFRL/MLBT (937) 255-4860 | | | 10. SPONSORING/MONITORING AGENCY REPORT NUMBER AFRL-ML-WP-TR-1998-4008 | |
| 11. SUPPLEMENTARY NOTES | | | | |
| 12a. DISTRIBUTION/AVAILABILITY STATEMENT APPROVED FOR PUBLIC RELEASE; DISTRIBUTION IS UNLIMITED. | | | 12b. DISTRIBUTION CODE | |
| 13. ABSTRACT (Maximum 200 words) The objective of this effort was to assist in the development of ceramic bearing technology, particularly hybrid bearings. The focus was to address major obstacles to the implementation and use of hybrid bearings. The two areas addressed were cost reduction and qualification of hybrid bearings systems. The effort was divided into three task areas: Task I: The development of run-in finishing procedures to address cost reduction by finishing Si ₃ N ₄ rolling elements and the steel race ways of bearing in-situ; Task II: Chemical conditioning of surfaces to improve the tribological performance of hybrid contacts under boundary lubrication conditions; Task III: Assessment of tribological attributes of a hybrid contact under conditions relevant to bearing operation. | | | | |
| 14. SUBJECT TERMS | | | 15. NUMBER OF PAGES 164 | |
| | | | 16. PRICE CODE | |
| 17. SECURITY CLASSIFICATION OF REPORT UNCLASSIFIED | 18. SECURITY CLASSIFICATION OF THIS PAGE UNCLASSIFIED | 19. SECURITY CLASSIFICATION OF ABSTRACT UNCLASSIFIED | 20. LIMITATION OF ABSTRACT SAR | |

Table of Contents

Page

| | | |
|---------|--|----|
| 1. | Introduction | 1 |
| 2. | Background | 2 |
| 3. | Objectives | 4 |
| 4. | TASK I: RUN-IN FINISHING | 5 |
| 4.1 | Introduction | 5 |
| 4.2 | Technical Approach | 6 |
| 4.2.1 | Test Machine | 7 |
| 4.2.2 | Current Si_3N_4 Ball Finishing Operation | 7 |
| 4.2.3 | Si_3N_4 Ball Blank Materials | 14 |
| 4.2.4 | Test Details | 16 |
| 4.2.5 | Procedure | 16 |
| 4.3 | Results and Observations | 16 |
| 4.3.1 | Effect of Working Fluid | 16 |
| 4.3.1.1 | Synthetic Ester Basestock Oil | 17 |
| 4.3.1.2 | Water and Water-Oil Mixtures | 17 |
| 4.3.1.3 | Ester Basestock Oil-Water-Isopropyl Alcohol Mixture | 17 |
| 4.3.1.4 | Hydroperoxide-Water Fluid | 22 |
| 4.3.1.5 | Mineral Oil-Water NaOH Mixture | 22 |
| 4.3.1.6 | Mineral Oil-Lauric Acid | 25 |
| 4.3.1.7 | Mineral Oil-Lauric Acid-Hydrogen Peroxide Mixture | 25 |
| 4.3.1.8 | Summary of Effect of Working Fluid | 25 |
| 4.3.2 | Effect of Ball Blank Materials | 32 |
| 4.3.2.1 | Oil-Water Mixture Fluid | 32 |
| 4.3.2.2 | Oil-Water Hydrogen Peroxide Mixture | 36 |
| 4.3.2.3 | Oil-Water Sodium Hydroxide Fluid | 36 |
| 4.3.3 | Further analysis of Run-In Finished Surfaces | 40 |
| 4.3.3.1 | X-Ray Diffractometry | 40 |
| 4.3.3.2 | Raman Spectroscopy | 44 |
| 4.3.4 | Discussion | 45 |
| 4.4 | Disc (Raceway) Run-In Finishing | 50 |
| 4.4.1 | Test Procedure | 50 |
| 4.4.2 | Run-In Finishing of M50 and 9310 Steel Discs | 51 |
| 4.5 | Effect of Metallic Coatings on Steel Disc Run-In finishing | 56 |
| 4.5.1 | Silver Coatings | 56 |
| 4.5.2 | Copper Coatings | 58 |
| 4.5.3 | Nickel Coatings | 58 |
| 4.5.4 | Chromium Coatings | 61 |
| 4.5.5 | Summary of Coating Effects | 61 |
| 4.5.6 | Si_3N_4 Ball on Si_3N_4 Disc Combination | 63 |
| 4.6 | Summary of Disc (Raceway) Run-In Finishing | 63 |
| 5. | Task II: TRIBOLOGICAL SURFACE CONDITIONING | 67 |
| 5.1 | Introduction | 67 |
| 5.2 | Metallic Coatings | 67 |
| 5.2.1 | Reduction of Traction (Friction) | 68 |
| 5.2.2 | Enhancement of EHD Lubrication | 69 |
| 5.2.3 | Modification of Contact Stresses | 69 |
| 5.2.4 | Frictional Heat Management | 69 |

| | |
|--|-----|
| 5.3 Polymeric Materials Coating | 70 |
| 5.4 Summary | 71 |
| 6.Task III: - Tribological Performance Evaluation | 73 |
| 6.1 Introduction | 73 |
| 6.2 Technical Approach | 73 |
| 6.3 Preliminary Traction Test with Steel Ball on Si ₃ N ₄ Disc | 74 |
| 6.3.1 Traction Tests Under Flooded Conditions | 75 |
| 6.3.2 Starved Lubrication | 78 |
| 6.3.3 Experimental Details | 78 |
| 6.3.4 Procedure | 78 |
| 6.3.5 Results and Discussion | 79 |
| 6.3.6 Summary | 83 |
| 6.4 Load Capacity Test | 83 |
| 6.4.1 Experimental Details | 84 |
| 6.4.2 Procedure | 84 |
| 6.4.3 Results and Discussion | 84 |
| 6.4.3.1 Basestock Oil (Herco-A) | 84 |
| 6.4.3.2 Formulated Oil | 87 |
| 6.4.4 Summary | 98 |
| 6.5 Oil-Off Test | 99 |
| 6.5.1 Experimental Details | 99 |
| 6.5.2 Procedure | 99 |
| 6.5.3 Results and Discussion | 101 |
| 6.5.3.1 Ester Oils | 101 |
| 6.5.3.2 PFPE Fluid (Krytox 143AB) | 101 |
| 6.5.3.3 Polyphenylether (PPE) | 108 |
| 6.5.3.4 Synthetic Hydrocarbon (Formulated) | 108 |
| 6.5.4 Summary | 115 |
| 6.6 Grease Lubrication Test | 115 |
| 6.6.1 Test Details | 118 |
| 6.6.2 Procedure | 118 |
| 6.6.3 Results and Discussion | 120 |
| 6.6.4 Summary | 125 |
| 6.7 Performance Mapping | 128 |
| 6.7.1 Approach | 128 |
| 6.7.2 Test Details | 129 |
| 6.7.3 Procedure | 129 |
| 6.7.4 Results and Discussion | 130 |
| 6.7.5 Summary and Implications of Performance Mapping Results | 142 |
| 7. Conclusions | 143 |
| 8. Recommendations | 145 |
| 9. References | 146 |

List of Tables

| Table | | Page |
|---------|--|------|
| Table 1 | Mechanical Properties of Toshiba TSN-03H and Cerbec NBD200 Si ₃ N ₄ materials | 16 |
| Table 2 | Fluids (Lubricant) evaluated and a summary of results | 30 |
| Table 3 | Some properties of coating materials and 9310 steel | 58 |
| Table 4 | Summary of test results | 71 |
| Table 5 | Mechanical properties of three Si ₃ N ₄ materials | 74 |
| Table 6 | Traction coefficients with hybrid materials (M50/NBD200) | 75 |
| Table 7 | Oil-off test results table | 105 |
| Table 8 | Various grease material properties | 119 |
| Table 9 | Grease lubrication results | 124 |

List of Figures

| Figure | | Page |
|------------|--|------|
| Figure 1a | Schematic diagram of a ball-on-disc contact configuration | 8 |
| Figure 1b | Photograph of a ball-on-disc specimen contact during testing | 9 |
| Figure 2 | Schematic diagram and photograph of the WAM3 test machine | 10 |
| Figure 3 | Photomicrograph of the surface of a Si_3N_4 (TSN-03H) ball blank | 12 |
| Figure 4a | Si_3N_4 ball surface after step 1 | 12 |
| Figure 4b | Si_3N_4 ball surface after step 2 | 13 |
| Figure 4c | Si_3N_4 ball surface after step 3. (Final finish shown in Figure 23) | 13 |
| Figure 5 | As received surfaces of the two different Si_3N_4 ball blanks | 15 |
| Figure 6 | Polishing wear of silicon nitride (a) ball and (b) discoloration of disc following run-in finishing test (DA60) with ester basestock oil | 18 |
| Figure 7 | Polishing wear of silicon nitride (a) ball and (b) disc following run-in finishing with water (DA61) | 19 |
| Figure 8a | Traction plot during run-in with 50-50 oil and water mixture | 20 |
| Figure 8b | Traction plot during run-in test with 20-80 oil and water mixture | 21 |
| Figure 9 | Run-in test with water-hydrogen peroxide | 23 |
| Figure 10 | Run-in finishing of (a) ball and (b) disc with hydrogen peroxide | 24 |
| Figure 11 | Si_3N_4 ball run-in finished in water+NaOH+mineral oil | 26 |
| Figure 11a | Test with mineral oil-water-NaOH mixture | 27 |
| Figure 12 | Run-in finishing of (a) ball and (b) disc with Lauric acid | 28 |
| Figure 13 | Traction plot for test run with mineral oil, lauric acid, hydrogen peroxide mixture | 29 |
| Figure 14 | Run-in finishing of ball (A) and disc (B) with mineral oil-Lauric acid-hydrogen peroxide | 31 |
| Figure 15a | Traction plot for run-in test with oil-water mixture with TSN-03H ball | 33 |
| Figure 15b | Traction plot for run-in test with oil-water mixture with NBD 200 ball | 34 |
| Figure 16 | Si_3N_4 ball run-in finished in oil+ H_2O fluid | 35 |
| Figure 17a | Traction plot for run-in finishing test with oil-water-hydrogen peroxide mixture | 37 |
| Figure 17b | Traction plot for run-in finishing test with oil-water-hydrogen peroxide mixture | 38 |
| Figure 18 | Si_3N_4 ball run-in finished in oil+ H_2O + H_2O_2 fluid | 39 |
| Figure 19 | Si_3N_4 ball run-in finished in oil+ H_2O +NaOH fluid | 41 |
| Figure 20a | X-ray diffraction from the run-in finished surface | 42 |
| Figure 20b | X-ray diffraction pattern outside run-in finished surface | 43 |
| Figure 21 | Raman Spectra for α and β Si_3N_4 | 46 |
| Figure 22 | Raman Spectra for run-in finished Si_3N_4 surface | 47 |
| Figure 23 | Surface of a commercially finished Si_3N_4 ball | 48 |
| Figure 24a | Traction behaviour during M50 steel disc run-in finishing with a run-in finished Si_3N_4 ball | 52 |
| Figure 24b | Traction behavior during M50 steel disc run-in finishing with a commercially finished ball | 53 |
| Figure 25a | M50 steel disc run-in finished with Si_3N_4 ball | 54 |
| Figure 25b | | 55 |

| | | |
|------------|--|-----|
| Figure 26 | Photomicrograph of the wear track on silver (Ag) coated steel disc surface that has been tested against finished Si_3N_4 ball..... | 57 |
| Figure 27 | Traction curve for test 1 with Si_3N_4 ball and Cu-coated 9310 steel disc | 59 |
| Figure 28 | Wear track on the Cu coating on 9310 steel after 30 min. test time..... | 60 |
| Figure 29 | Wear track on the Ni-coated 9310 steel disc after a total time of 90 min. showing the coating worn through..... | 60 |
| Figure 30a | Wear track on Si_3N_4 after a test time of 60 min. showing Cr transfer from disc | 62 |
| Figure 30b | Wear track on Cr coated disc after a test time of 60 min. showing coating wearing through in the middle | 62 |
| Figure 31 | Original surface of ground Si_3N_4 disc | 64 |
| Figure 32a | Si_3N_4 disc run-in finished in oil and water mixture fluid | 65 |
| Figure 32b | Si_3N_4 disc run-in finished in oil+water+NaOH mixture | 65 |
| Figure 33a | Traction curve for M50 ball run against NBD200 disc under flooded lubricated condition: 93 lb_f contact loads | 76 |
| Figure 33b | Traction curve for M50 ball run against Dow Chemical self-reinforced Si_3N_4 (APS 1182-1); 93 lb_f | 77 |
| Figure 34a | Traction behavior during starved lubrication tests with hybrid contact | 80 |
| Figure 34b | Traction behavior during starved lubrication tests with all-steel contact..... | 81 |
| Figure 35 | Ball worn surface after starved lubrication test (a) M50 steel and (b) Si_3N_4 | 82 |
| Figure 36 | Load capacity comparison of all-steel and hybrid contacts..... | 85 |
| Figure 37 | All-steel load capacity test | 86 |
| Figure 38 | Hybrid load capacity test..... | 88 |
| Figure 39a | All-steel load capacity test | 89 |
| Figure 39b | Hybrid load capacity test..... | 90 |
| Figure 40 | All-steel load capacity test with formulated oil..... | 91 |
| Figure 40b | Hybrid load capacity test with formulated oil | 92 |
| Figure 41a | All-steel load capacity test with formulated oil and $R = 150$ in/sec..... | 94 |
| Figure 41b | Hybrid load capacity test with formulated oil and $R = 150$ in/sec | 95 |
| Figure 42 | Ball worn surface after load capacity test (a) M50 steel and (b) Si_3N_4 | 96 |
| Figure 43 | Variation of the entraining and sliding velocities during the oil-off test | 100 |
| Figure 44a | All-steel contact pair | 102 |
| Figure 44b | Hybrid contact pair | 103 |
| Figure 45 | Summary chart of hybrid and all-steel contacts during oil-off tests | 104 |
| Figure 46a | Oil-off test with Herco-A for all-steel pair..... | 106 |
| Figure 46b | Oil-off test with Herco-A for hybrid pair | 107 |
| Figure 47a | Oil-off test with Krytox 143AB for all-steel pair..... | 109 |
| Figure 47b | Oil-off test for hybrid contact with Krytox 143AB..... | 110 |
| Figure 48a | Oil-off with PPE B.S. for all-steel pair | 111 |
| Figure 48b | Oil-off test with PPE B.S. for all Hybrid pair | 112 |
| Figure 49a | Oil-off test with the formulated synthetic hydrocarbon oil for all-steel..... | 113 |
| Figure 49b | Oil-off test with the formulated synthetic hydrocarbon oil for hybrid..... | 114 |
| Figure 50a | Oil-off test with NYE 176A for all-steel pair..... | 116 |
| Figure 50b | Oil-off test for Hybrid contact with oil NYE 176A | 117 |
| Figure 51a | All-steel contact grease lubrication test..... | 121 |

| | | |
|------------|--|-----|
| Figure 51b | Hybrid contact grease lubrication test | 122 |
| Figure 52 | Summary chart of grease lubrication tests..... | 123 |
| Figure 53 | Mobilith SHC 100 grease lubricated hybrid contact pair | 126 |
| Figure 54 | Mobilith SHC 100 grease lubricated all-steel contact pair..... | 127 |
| Figure 55a | Performance map for all-steel contact..... | 131 |
| Figure 55b | Performance map for hybrid contact pair | 132 |
| Figure 56a | Average traction coefficient as a function of sliding velocity for all-steel . | 133 |
| Figure 56b | Average traction coefficient as a function of sliding velocity for hybrid.... | 134 |
| Figure 57a | Ball temperature as a function of friction heat input for all-steel..... | 136 |
| Figure 57b | Ball temperature as a function of friction heat input for hybrid..... | 137 |
| Figure 58 | Ball and disc in all-steel contact for performance map at $R = 30$ in/sec after failure..... | 138 |
| Figure 59 | Ball and disc in hybrid contact for performance map at $R=30$ in/sec after failure. Oil: Herco-A..... | 139 |
| Figure 60 | Ball and disc in all-steel contact for performance map at $R = 170$ in/sec after failure. Oil: Herco-A..... | 140 |
| Figure 61 | Ball and disc in hybrid contact for performance map at $R = 170$ in/sec. Contact did not fail. Oil: Herco-A | 141 |

FOREWORD

This document is the final report covering the work performed under U.S. Air Force Systems Command Contract F33615-92-C-5925. The project was sponsored by the Materials Directorate, Wright Laboratory, Air Force Systems Command, Wright Patterson AFB OH 45433-7750. The Advanced Research Projects Agency (ARPA), Arlington, VA, was the original source of the funding. The Air Force Project Engineer was Karl R. Mecklenburg of Wright Laboratory.

1. Introduction

Wedeven Associates submitted a proposal to DARPA, in response to the BAA #91-11, "Ceramic Bearing Technology Program." The proposal (CB-43), titled "Run-in finishing and Tribological Performance Evaluation of Ceramic Bearing" consisting of the following of three inter-related task areas: (1) In-situ or run-in finishing of Ceramic rolling elements and raceway surfaces, (2) Surface pre-conditioning to establish a chemical boundary layer, (3) Development of test methodology and tribological performance evaluation that is efficient and relevant to ceramic bearings.

All of the above test areas are now completed. The following report documents the accomplishments and findings of the effort in the three task areas. Some shifts in emphasis and focus were made at the suggestion of the program monitor during the course of the performance of this effort. These shifts will be discussed as appropriate in later sections of this report.

2. Background

Rolling element bearings are among the most common machine and mechanical system elements. These bearings consist of the inner and outer rings, and often cage or retainer in addition to the rolling elements, which are either balls or rollers.

Bearing components are usually manufactured separately, often at different facilities. The manufacturing process for precision bearings may require more than 40 operations. Conventional metallic ball manufacturing starts with a blank made from wire or rod. This blank is then made into headed spheres, a process, which involves compression and work hardening. The headed sphere then goes through a soft grinding plate. The process could take between 4 and 30 hours, depending on the material. In some cases, this step is followed by heat treatment to harden the ball. The final finishing is done in a series of lapping process done on a lapping machine. This consists of two grooved matched plates. The lapping is usually performed with oil and Al₂O₃ abrasive slurry. Different ball manufactures have different proprietary variations of the above steps.

The rings (inner and outer) are usually made from cylindrical bars. First, the center of the bar is drilled and the outside diameter of the outer ring is machined. The inner and outer rings are then taken off at the same time having the necessary concentricity. Electron Discharge Machine (EDM) process is well situated for this operation. The raceways are produced on both rings by grinding. Raceway finishing through abrasive polishing or honing is the final step. Again, various bearing manufacturers have different proprietary variation of the above steps. In almost all cases, the final finishing of the raceways is done in multi-steps.

Most current bearings rolling elements and rings are manufactured from AISI 52100 steel. Case hardened 4320, 4620 and 8620 steels are also sometimes used. For bearings operating in corrosive environments, AISI 440C stainless steel is preferable. For elevated temperature bearings, tool steel M50 and sometimes the Carburning version M50 NiL are used. Various materials are used for cages. The use of low carbon steels, such as 1010, 1020 than can be easily stamped, are quite common. Other cage materials include brass, Nylon (Polyamide 6/6), bronze 4340 and 4140.

Due to technological advancements, there are several areas of application where even the best of the existing bearings are not adequate. Recent improvements in ceramic materials, specifically Silicon Nitride (Si₃N₄) fabrication and characterization has resulted in their being used as rolling elements. Although all ceramic bearings are now available, the most prominent configuration is the hybrid bearings with steel rings and ceramic balls.

When compared to steel balls, the Si₃N₄ balls have several desirable properties that contribute to better performing bearing. Some of these characteristics include high temperature strength, low density, high hardness, corrosion resistance, long fatigue life, etc. All these attributes make hybrid bearings well suited for machines and hardware operating under severe conditions.

Currently, hybrid bearings are not being used extensively. The two primary reasons are high cost

and the resistance on part of designers, who more "comfortable" with the conventional bearing configuration. In general hybrid bearings cost between three and six times more than conventional all steel bearings. Many designers are reluctant to pay that stiff a price for an "exotic" bearing. There is a persistent uncertainty by many bearing designers on the durability of a ceramic bearing. In many cases, hybrid bearings are used as a last resort when an all-steel bearing is unable to perform satisfactorily. In spite of the reluctance, to the best of our knowledge, we do not know of any reported instance of a hybrid bearing not performing as well as an all-steel bearing. On the contrary, we are aware of many instances in which a hybrid bearing is doing very well and an all-steel bearing has failed.

For hybrid bearings to find more usage, the two limitations described above must be addressed. The present effort is directed at a means of hybrid bearing manufacturing cost reduction and performance evaluation.

3. Objectives

The main objective of this effort was to assist in the development of ceramic bearing technology, particularly hybrid bearings. The focus was to address some of the major obstacles to extensive use of hybrid bearings. The two areas addressed were the high cost and performance qualification of hybrid systems. Cost reduction can be achieved through manufacturing process modification or improvement. Elimination of time consuming, machine intensive final finishing steps without sacrificing performance could translate to significant cost saving. A comprehensive comparative performance evaluation between the conventional and hybrid or even all-ceramic bearings under conditions that can be effectively related to bearing operating conditions will be useful. Such information will give designers and users of bearings greater confidence in the "new" type of bearing.

Efforts to accomplish the above goals were divided into three task areas. Task I was the development of run-in finishing procedure addresses cost reduction by finishing the Si_3N_4 rolling elements and the steel raceways of bearing in-situ. Task II was the chemical conditioning of surfaces to improve the tribological performance of hybrid contacts, especially under boundary lubrication conditions. Due to the relatively chemical inertness of Si_3N_4 ball oil formulated for the conventional all steel bearing may not be as effective. Task III was the evaluation of performance aimed at efficiently accessing the tribological attributes of a hybrid contact vis-a-vis on all steel contacts under conditions that are relevant to bearing operation.

The findings and results of each of the three task areas are now presented. In the course of this work, new things were learned and the emphasis and focus were shifted as needed in order to get the maximum technological benefit from the program. These were done, of course, in consultation with the program monitors. Details will be given as appropriate in the respective sections.

4. TASK I: RUN-IN FINISHING

4.1 Introduction

Hybrid bearings consist of ceramic rolling elements and steel races have significant advantages over all-steel bearings. Currently, silicon nitride (Si_3N_4) is the ceramic material of choice for bearing applications. The ARPA ceramic bearing technology program focuses on the application of Si_3N_4 ceramic material rolling elements in hybrid bearing. The kinematics advantage of hybrid bearings is due primarily to the properties of the Si_3N_4 rolling elements.

The density of Si_3N_4 material is about 40% that of steel. This considerably lower density will result in lighter weight (which is very desirable in aerospace industry), faster response, and higher rotational speed in the bearing due to lower initial. Furthermore, a considerable reduction in the centrifugal load, especially during high-speed operation will occur due to the low density of the Si_3N_4 ball-rolling element. This will reduce the stress between the balls and outer race during bearing operation. The Si_3N_4 material also have an elastic modulus this is about 50% higher than steel. This will make hybrid bearings with Si_3N_4 balls stiffer than all steel bearings.

In addition to kinematic advantages imported to the hybrid bearings by Si_3N_4 ball, there are other benefits that can be derived from hybrid bearings. Si_3N_4 has higher hardness than typical bearing steels (typically 58-64 Rc for bearing steels Vs 75-80 Rc for Si_3N_4), which will make the Ceramic material more resistant to abrasion. Compared to steel, Si_3N_4 material is highly corrosion resistant and has a high temperature capability (800°C for Si_3N_4 Vs 200°C for steel). Thus ceramic bearings will function reasonably well in chemically and thermally aggressive environments. Also, Si_3N_4 is non-magnetic, which makes hybrid bearings ideal for use in applications involving magnetic field. These are just some of the advantage of hybrid bearings over all-steel bearings.

In spite of the many advantages of hybrid bearings over all-steel bearings, it has not found an extensive use. Currently, most engineers and designers will consider hybrid bearings only if the all-steel bearing is inadequate for the intended application. One major reason for this lack of interest is cost. Hybrid bearings cost 3 to 6 times more than the conventional all-steel bearing. If the cost of hybrid bearing could be made more comparable to the all-steel bearings, hybrid bearings certainly will find more use.

The current manufacturing practices of all-ceramics and hybrid bearings is essentially the same as the conventional bearing. This is especially so with regard to race manufacturing and finishing and the ball finishing. Because of Si_3N_4 relative high hardness, and as such abrasive wear resistance, the ball finishing operation in this material takes a lot longer than the finishing of the steel balls. It is also often necessary to use the more expensive diamond paste slurry instead of SiC or/and Al_2O_3 abrasives. The steel races for the hybrid bearing are also usually machined and finished to the same standards as obtains in conventional all-steel bearings. This usually involves intricate sequence of machining and surface finishing operations, all of which add to the overall cost of the bearings.

From our experience with marginally lubricated all-ceramic and hybrid contacts under rolling/sliding conditions, smooth contact areas can be generated without a large-scale damage. This observation suggest that the final finishing operations of the rolling elements and the raceways in hybrid bearing may not be necessary as a manufacturing step, but achieved in-situ during the bearing early operation. This can translate to overall cost savings without sacrificing performance.

The main inpetus for Task I (run-in finishing) is the manufacturing cost savings of hybrid and all ceramic bearings. This, we propose, could be done by omitting the final finishing operations by having such finishing done in-situ during the run-in stage of the bearing operation, hence the term "run-in finishing."

If successful, the development of run-in finishing methodology, among many benefits will eliminate costly finishing operations of individual rolling element and raceway surfaces at the manufacturing stage. There could be a reduction in risk of damage to components, particularly the races, during the high-speed abrasive machining operations. This translates to lower cost for hybrid bearings.

4.2 Technical Approach

Rolling element bearings essentially consists of two surfaces (inner and outer ring) in relative motion with a row of balls or rollers in between and in contact with both. Ideally, during bearing operation, the rolling elements roll on the raceway and there is little or no frictional force involved. Hence, rolling element bearings are sometimes referred to as anti-friction bearings. In real life, sliding does occur in the contact zones, resulting in friction. Also, elastic hysteresis during rolling contact does produce friction, but the magnitude is insignificant when compared to that caused by sliding motions.

Ball finishing operations involves a kinematics identical to that of a rolling element bearing. The ball blanks to be finished are loaded between two lapping plates (one of the plates grooved) and subjected to a rolling motion. Like in bearings, there is also some small amount of sliding at the contact interfaces. Using this operation, ball blanks with surface roughness of 10-15 μin R_a can be polished to a surface roughness of $R_a < 1 \mu\text{in}$.

Current commercial raceway final finishing involves different processes. This finishing is usually done by a high sliding speed abrasive machining/polishing process. Because of this relatively more severe contact condition during raceway finishing, the component is more prone to damage. To forestall such event, raceway final finishing involves intricate processes, which are often costly.

Under marginal or mixed film lubrication regimes, polishing wear occurring at the peak of asperities. This is because the lubricant film thickness is significantly less than the composite surface roughness of the contacting surfaces. The result is a direct interaction between the surfaces and consequently the occurrence of wear. The mode and extent of wear is determined by the severity of surface interaction. Polishing wear mode occurs with mild surface interaction.

The idea behind the 'run-in' finishing is to operate incompletely finished balls and raceways under contact kinematics of a rolling element bearing, but with marginal lubrication. Extensive interaction between the surface asperities under such condition will result in the generation of smoother topography on both surfaces without the risk of severe damage that is typical of high sliding operations. The technical approach that will be taken in the run-in finishing process/procedure development will be to produce a smooth topography on the balls and/or raceways, without the risk of severe damage. This will be done by operating the contact under rolling with some sliding with marginal lubrication.

Although the implementation of the 'run-in' finishing procedure will ultimately involve finishing the rolling elements and/or raceway surfaces in-situ during bearing operation, the development of the process was done by a single element contact. A ball on disc contact configuration was used.

4.2.1 Test Machine

All the tribological testing during this effort were done on the Wedeven Associates Machines (WAM1 and WAM3). The machines use a ball-on-disc contact configuration as shown schematically in Figure 1a. A picture of ball and disc specimens in contact during a test is shown in Figure 1b.

The design of WAM test machines allows the ball and disc specimen motions to be independently controlled. All these flexibility's make it possible to operate the contact between ball and disc in WAM machines under a wide range of tribological conditions ranging from pure rolling to pure sliding, and everything in between. Furthermore, there is the flexibility of imposing linear slip (no spin) to imposing different degree of "Spin" to the contact. Also the off-center alignment of the ball and disc rotation axis can provide differential rolling and sliding condition. In essence, the flexibility of the WAM machines makes the simulation of any tribological hardware contact kinematics with a single point contact possible.

The traction force at the contact interface can be measured under desired contact load and rolling and sliding velocities. The ball and disc specimen can also be measured during each test. Figure 2 shows the picture and schematic diagram respectively of the top WAM3 machine. The application of load in the machine is done by a stepper motor device, which allows for a precise control of load application. Up to 50 different test parameters and measured variables can be controlled and/or measured by the machine.

Both WAM1 and WAM3 machine operations are computer controlled. The test data can be monitored in real time during testing and are also stored for post-test analysis.

4.2.2 Current Si_3N_4 Ball Finishing Operation

Almost all the bearing ball manufacturers are into ceramic ball finishing now. They all get their supply of ball blanks often from the same ceramics material manufacturers. The ball finishing is then done by adapting their proprietary methods/procedures used for steel ball finishing to the ceramic materials. The technology and art of steel ball finishing is quiet mature and different

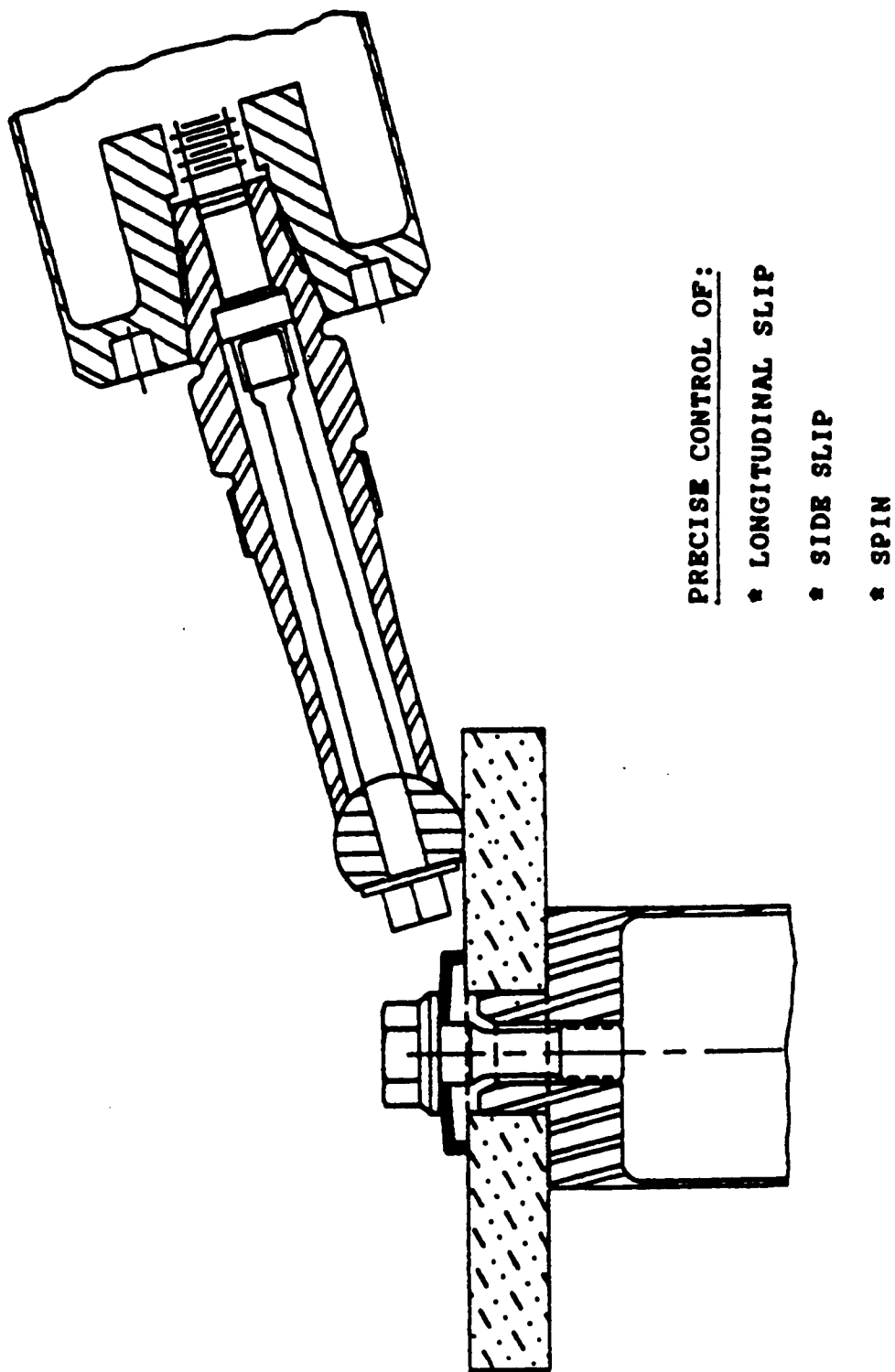


Figure 1a Schematic diagram of a ball-on-disc contact configuration



Figure 1b Photograph of a ball-on-disc specimen contact during testing

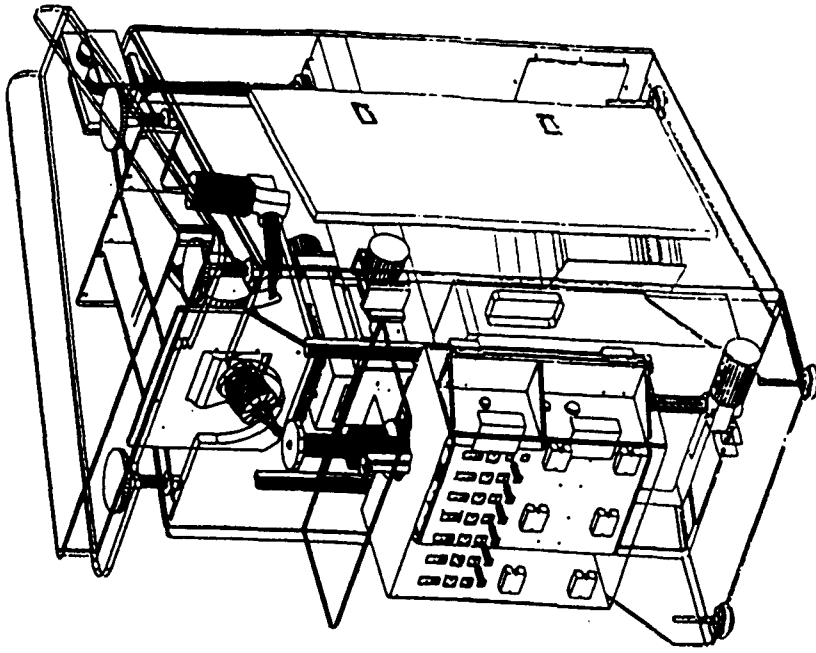


Figure 2 Schematic diagram and photograph of the WAM3 test machine

companies engaged in ball finishing may do things slightly differently, but the essence of the process remains the same.

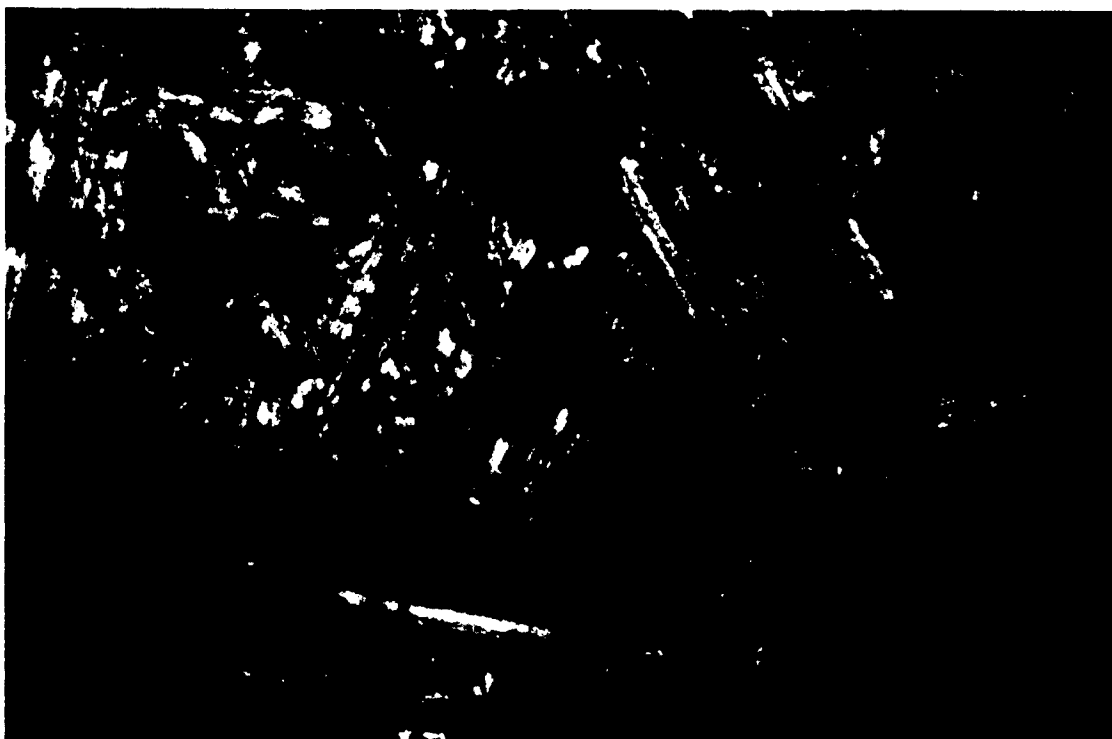
In adopting steel ball finishing to Si_3N_4 ball blank finishing, some significant changes are made. The changes are also different and proprietary for different companies. In general, Si_3N_4 ball finishing involves multi-step processes using abrasive particles of different size. The processes are given different names by different ball finishers. Some companies performed the operations in the same set of plates, but change the abrasive charge after each operation. Others performed each operation in a different set of plates, with each plate dedicated to a single abrasive particle size charge.

In spite of the differences, most changes made to finishing operations for Si_3N_4 balls are very similar for all ball finishers. Among these common changes are:

- (1) Longer lapping time. Due to the relatively high hardness of Si_3N_4 balls compared to steel ones, their abrasive resistance is high. Consequently, the Si_3N_4 balls require longer time to finish than the steel balls do.
- (2) As a result of high abrasive wear resistance of the Si_3N_4 balls, industrial diamond abrasives are used for the lapping process instead of the less expensive SiC and Al_2O_3 abrasives often used for steel ball finishing.
- (3) The wear/finishing rate cannot be accelerated in Si_3N_4 ball by increasing plate pressure. Increasing plate pressure will result in the formation of Hertzian cracks, detrimental to the ball quality and performance. In steel balls on the other hand, the plate pressure increase is one practical way of increasing rate of stock removal during ball finishing.

All these changes, and many others, suggest the cost of finishing Si_3N_4 balls should be significantly higher than the cost of finishing a similar steel ball. One ball finisher who is willing to share the process with us (something that is rare in the industry for each company like to keep their secret to themselves), uses a four step process. Each of the four processes was performed in different plates. The first two steps are to produce the desired geometry of good sphericity, while the last two are for good surface finish topographically. Figure 3 shows the photomicrograph of an incoming Si_3N_4 ball blanks. Figures 4a-c show the surface features of the ball after each of the four steps. The processing steps outlined here are for a specific Si_3N_4 ball blank. For a different kind of Si_3N_4 ball blank, the processing steps may be slightly different. In fact, a desire expressed by all the ball finishes contacted with during the course of the work is to be able to use the same procedure for all Si_3N_4 material as currently done with steel balls.

The primary aim of the ball run-in finishing was to generate a surface finish comparable to the commercially produced ones on Si_3N_4 ball, by make use of the wear occurring during contact. This was to be done with a contact kinematics akin to that of the ball bearing. It also was to be done without the use of abrasives. If successful, the procedure could substantially reduce the overall cost of hybrid bearing by eliminating some of the difficult and perhaps costly finishing steps.



100x

Figure 3 Photomicrograph of the surface of a Si₃N₄ (TSN-03H) ball blank



100x

Figure 4a Si₃N₄ ball surface after step 1

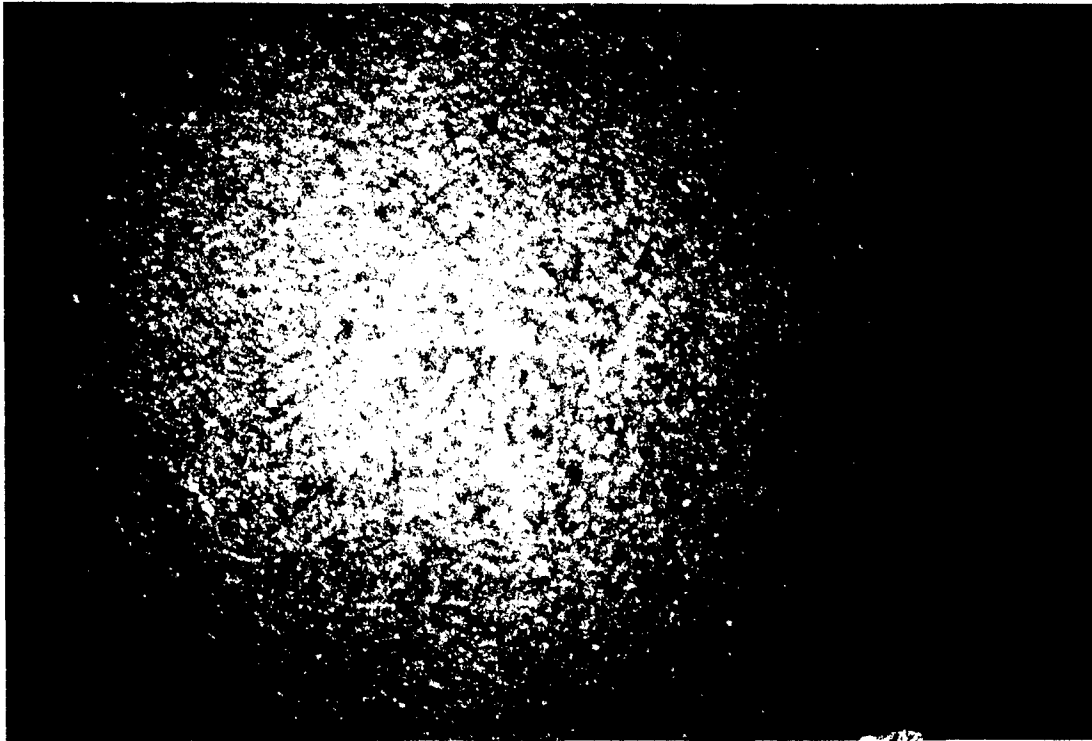


Figure 4b Si₃N₄ ball surface after step 2

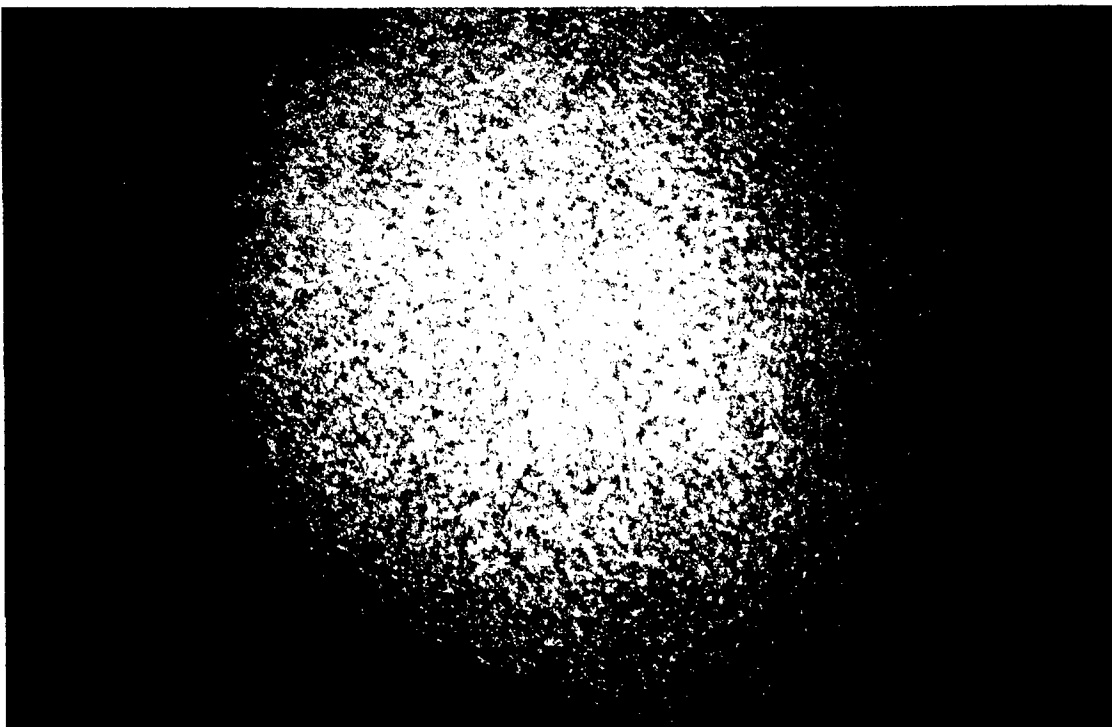


Figure 4c Si₃N₄ ball surface after step 3. (Final finish shown in Figure 23)

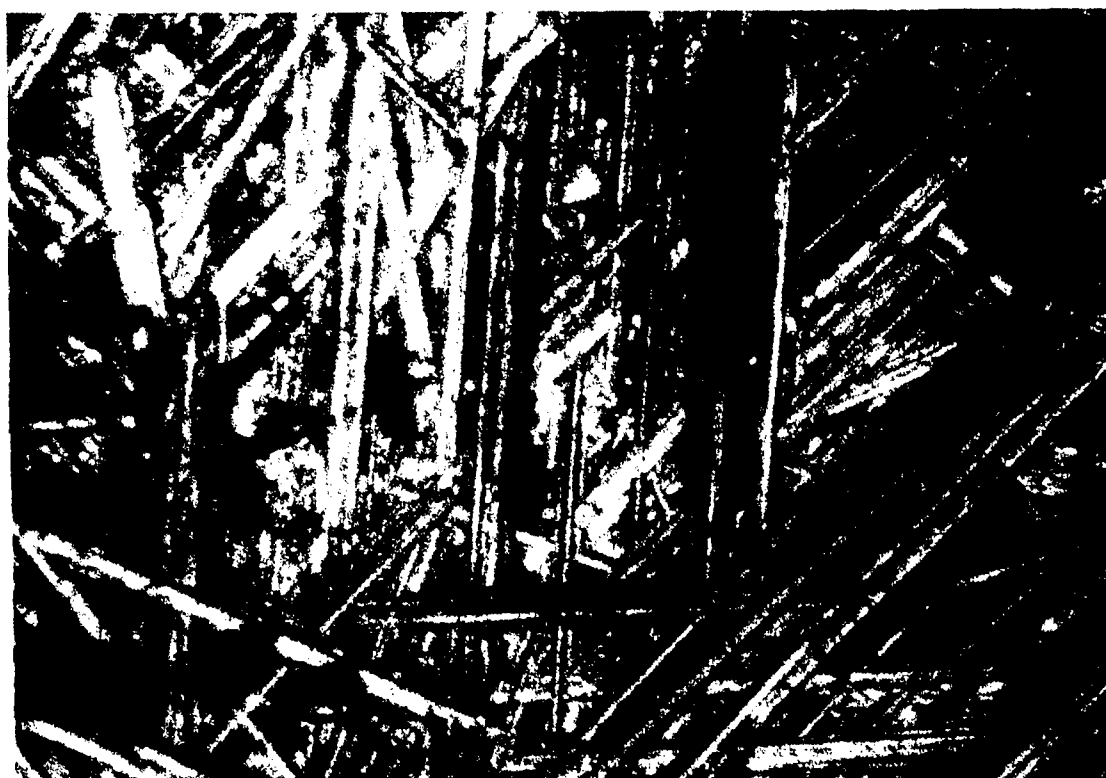
4.2.3 Si₃N₄ Ball Blank Materials

Two different ball blank materials were used in this ball run-in finishing studies. These were Toshiba Si₃N₄ TSN-03H and Cerbec's NBD200 materials. Because we were able to get larger quantity of the TSN-03H materials, the Toshiba material was used for the development of the run-in process. Once the procedure were established, ball blanks of both materials were run-in finished under same conditions to compare their performance.

The two kinds of ball blanks are different in two major ways:

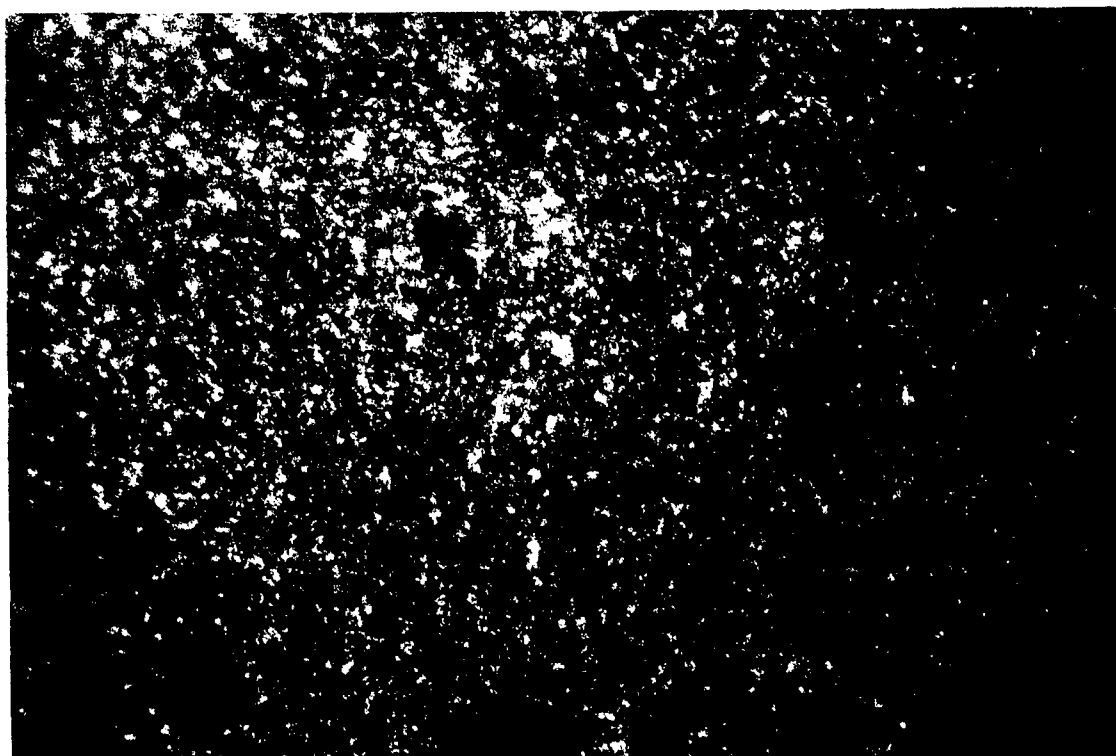
(1) They have different as-received surface morphology. Figures 5a and 5b show the photomicrograph of the as received surfaces of the TSN-03H and the NBD200 ball blanks, respectively. The TSN-03H material has randomly oriented scratches and grooves, suggesting that this material ball blank surface has been machined or ground. This surface morphology may indicate that the ball blanks are machined from a block or rod made of the material. It could also be from the grinding of the skin layer from a shaped fabrication method. The NBD200 ball blanks on the other hand, has a nearly isotropic surface morphology. This may suggest the balls are fabricated with a near net shape method and the skin layer, if removed is done by a tumbling process. In any case, the surface morphology of the two types of Si₃N₄ material ball blanks is significantly different.

(2) The processing, Chemistry (with regards to the sintering aid additives), microstructure (especially the grain boundary phase) and some properties of the two types of materials are also different. Both the Toshiba and Cerbec balls have a very similar appearance, although the Toshiba material is a little darker than the Cerbec material. NBD200 was fabricated by hot isostatic pressing (HIP); TSN-03H was also hot isostatically pressed after pressure-less sintering. The major differences between the two materials however, are in their chemistry and properties. The NBD200 has MgO added as sintering aid while TSN-30H has Y₂O₃+Al₂O₃ added as sintering aid. The microstructure of both materials consists of randomly elongated Si₃N₄ grains, but with very different grain boundary phases. With MgO additive, the grain boundary phase is usually amorphous (glassy), while it consists of amorphous and crystalline components when Y₂O₃+Al₂O₃ are used as sintering aid. The differences in microstructure of the two materials result in differences in their properties. A summary of some mechanical properties of both materials is shown in Table 1. From the table, it can be seen there is significant difference between the properties of the two materials. Notable among these differences are the density, hardness and fracture toughness. The TSN-03H material has a higher density than the NBD200 probably due to lower porosity in the TSN-03H material. This lower porosity, coupled with a higher strength grain boundary phase, may account for the higher fracture toughness of this material. On the other hand, the NBD200 material has a higher hardness, which could be beneficial for abrasive wear resistance. If the grain boundary phases have a significant role to play in the tribological behavior of these materials, one would expect differences in their performances in the three task areas.



200 μm

(A)



200 μm

(B)

Figure 5 As received surfaces of the two different Si_3N_4 ball blanks

TABLE 1: Mechanical Properties of Toshiba TSN-03H and Cerbec NBD200 Si₃N₄ materials.

| <i>Property</i> | <i>TSN-03H</i> | <i>NBD200</i> |
|--|----------------|---------------|
| Density (g/cc) | 3.24 | 3.16 |
| Hardness (GPa) | 15 | 16.6 |
| Flexural Strength (MPa) | 910 | 800 |
| Compressive Strength (GPa) | 4 | 3 |
| Young's Modulus (GPa) | 295 | 320 |
| Poisson's ratio | 0.27 | 0.26 |
| Fracture Toughness (MPa m ^{1/2}) | 6.6 | 4.1 |

4.2.4 Test Details

The development of run-in finishing procedure for Si₃N₄ ball blank was conducted on the WAM3 test machine using 1/2" diameter ball blanks made from TSN-03H material. A Si₃N₄ disc with lower surface roughness than the ball was used as the counter face. The tests were run with the following parameters:

Contact Stress = 300 - 350 ksi

Rolling Velocity = 75 - 100 in/sec.

Contact Slip = Variable

Test Duration = 2500 - 3600 sec.

Temperature = Ambient R.T. (23°C)

Relative Humidity = 40 - 70%

Lubricant = Working fluid - applied by drip-feeding.

4.2.5 Procedure

The ball and the disc specimens, mounted on their respective spindle on the test machine, are set to the desired surface rolling velocity. The specimens are then loaded to the desired contact stress with the working fluid continuously drip feed into the contact interface. The first 200 seconds of the test are operated under pure rolling. At 200 seconds, and every subsequent 300 seconds, the contact slip is increased by 5%. This is continued until 2900 seconds total test time and 50% contact slip. The test is then run with the contact slip constant until termination point at 3600 seconds (1 hr.). At the conclusion of each test, both the ball and the disc surfaces are examined with an optical microscope to characterize the evolution of surface topography.

4.3 Results and Observations

4.3.1 Effect of Working Fluid

Several working fluids were used in the run-in finish procedure development. The results

obtained with each fluid are now given in detail.

4.3.1.1 Synthetic Ester Basestock Oil

The first series of tests were conducted using smooth Si_3N_4 disc and ball blank specimens. Initial contact pressure of 300 ksi, rolling velocity of 100 in/sec and ester basestock synthetic oil (Herco-A) were used. At the conclusion of this test series, some polishing wear had occurred in the contact area of the ball as shown in Figure 6a. The track on the disc showed some dark coloration, with little or no change in the surface topography (Figure 6b). Similar colorations have been attributed to lubricant decomposition product by many investigators.

4.3.1.2 Water and Water-Oil Mixtures

The next test was conducted under an identical condition, but lubricated with water instead of basestock oil. Figures 7a and 7b show the tracks on the ball and the disc, respectively. There was more wear on both the ball and the disc when compared to the test lubricated with oil. But more importantly, the contact areas were much smoother when lubricated with water. The goal of run-in finishing was to produce a smooth topography by the wear process without the use of abrasive. Water lubrication is achieving this goal.

More tests were conducted using the procedure described about with 50 - 50 mixture of water and basestock oil and a 20 -80 water-oil mixture. Figure 8 shows the traction variation during these tests. The traction coefficient showed an increase with the introduction of contact slip to values of about 0.14 for 50 - 50 mixture and about 0.18 for 20 -80 mixture. This initial increase was followed by a decreasing trend throughout the test duration in both cases with more pronounced decrease with the 20 - 80 mixture. A significant fluctuation was also observed during both tests. The surface topography of the ball and the disc at the conclusion of the two tests was very similar and almost identical to the ones lubricated with water as shown in Figure 7.

In an attempt to accelerate the wear and finishing process further, some tests were run under a more severe contact condition using the 20-80 oil-water mixture fluid. The severity of contact was increased by using a disc with rougher surface finish, a lower rolling velocity of 75 in/sec and a higher contact pressure of 334 ksi. These changes reduced the ratio of fluid film thickness to the composite surface roughness of the ball and the disc and imposed higher contact stresses.

The traction behavior during this test is shown in Figure 8. More wear occurs on the ball with the more severe contact conditions as one would expect, but there are also areas on the track where materials had been removed in flake form. Some polishing wear occurred on the disc surface as well.

4.3.1.3 Ester Basestock Oil-Water-Isopropyl Alcohol Mixture

The next fluid was a mixture of 15% basestock oil (Herco-A), 62% water and 23% isopropyl alcohol. Isopropyl alcohol is often used as a grinding media for ceramic powder processing,



(A)

200 μm



(B)

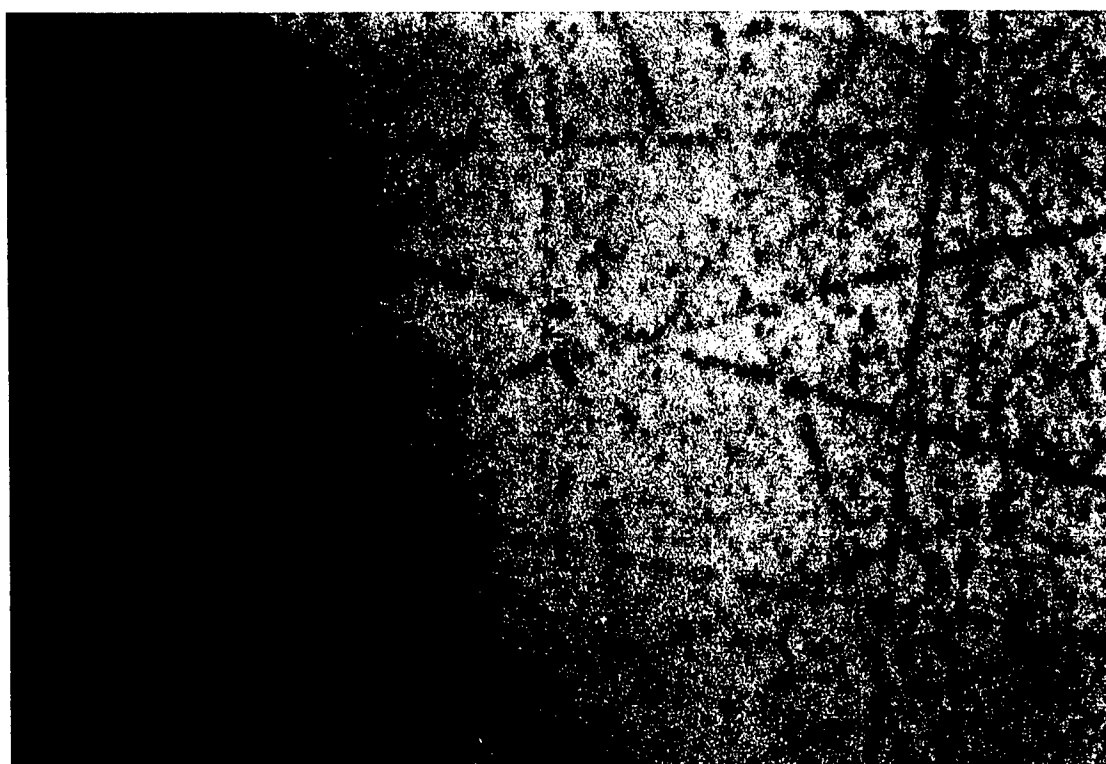
200 μm

Figure 6 Polishing wear of silicon nitride (a) ball and (b) discoloration of disc following run-in finishing test (DA60) with ester basestock oil.



(A)

200 μm



(B)

200 μm

Figure 7 Polishing wear of silicon nitride (a) ball and (b) disc following run-in finishing with water (DA61).

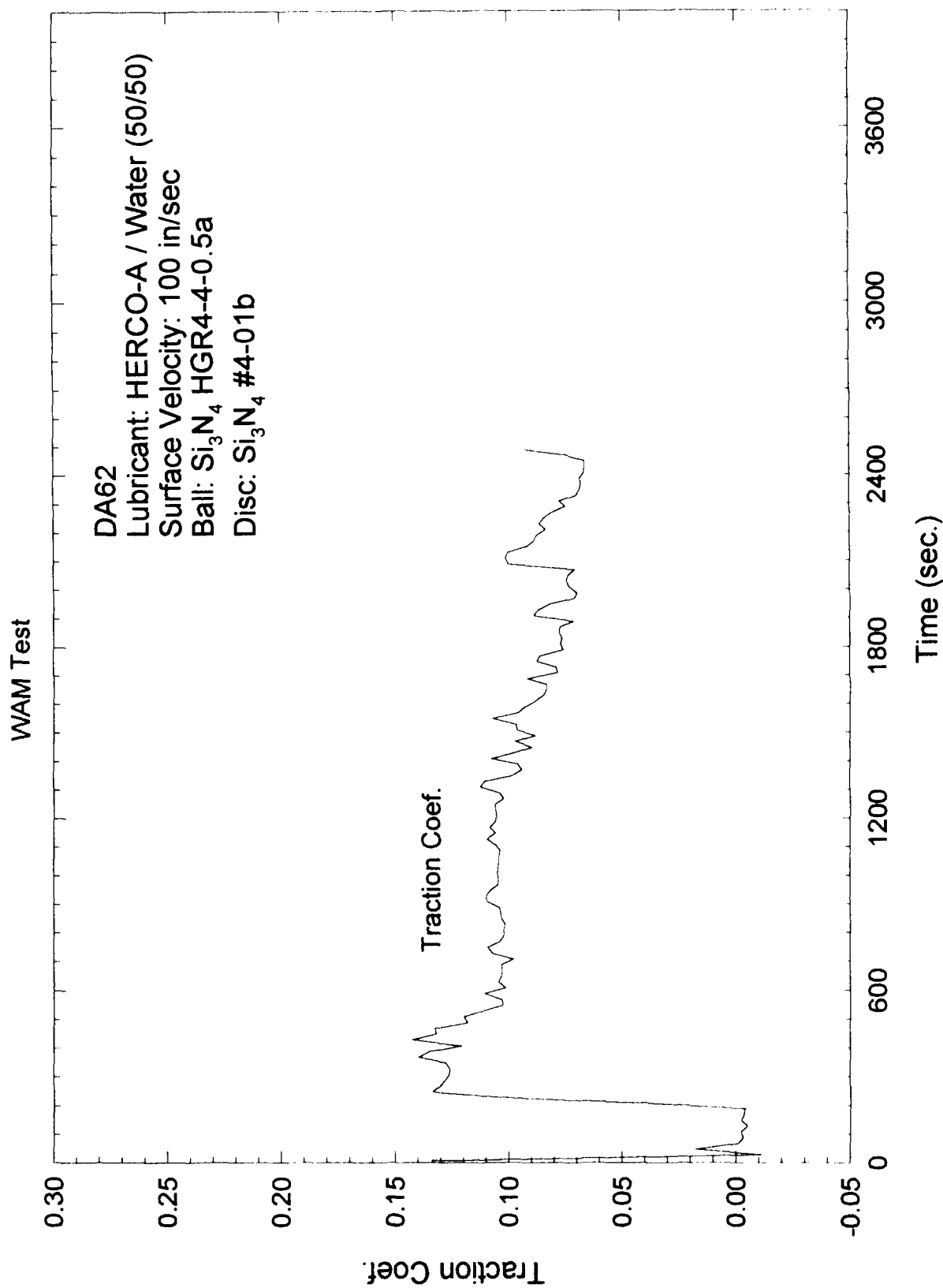


Figure 8a Traction plot during run-in test with 50-50 oil and water mixture

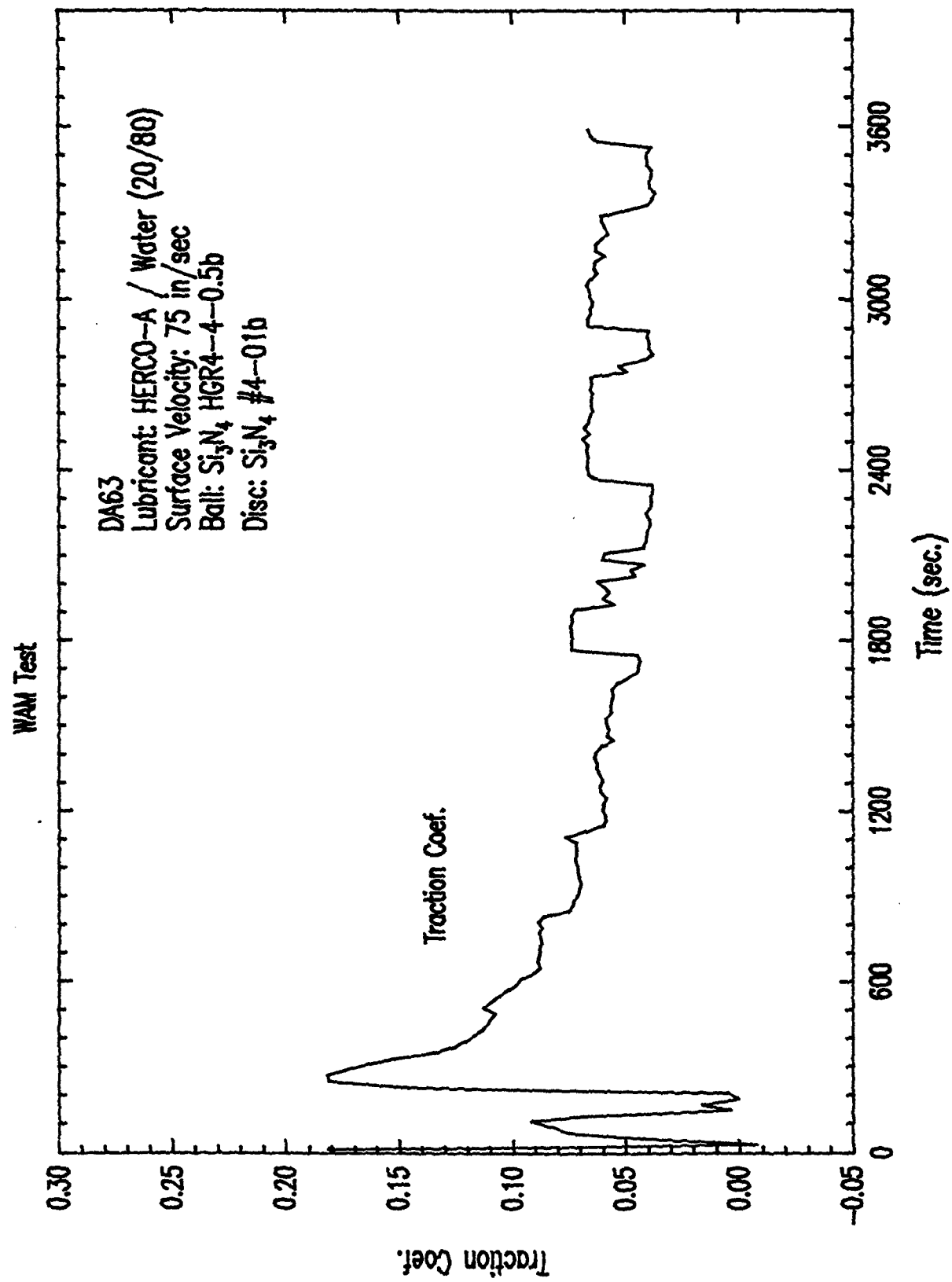


Figure 8b Traction plot during run-in test with 20-80 oil and water mixture

<DA63.SPW>

including Si_3N_4 . The traction coefficient shows a behavior typical of water-containing fluids. With the introduction of 5% contact slip at 200 sec, the traction coefficient increased to about 0.16. This was followed by a near exponential decrease to a steady value of about 0.04 after about 1500 seconds. The traction coefficient showed significant fluctuation throughout the test with unusually large spikes in the early stages of the test. The ball-worn surface shows the same characteristics as the surfaces generated in other oil-water mixtures. The addition of alcohol did not seem to have a major effect on the finishing process, at least under the present test conditions and in the concentration used.

One significant observation with this fluid, however, was the lack of temperature increase of the ball and the disc during the test. This could be a useful attribute of the fluid when used under severe contact conditions wherein frictional heating could be very significant. The track on the disc also showed areas of polishing wear, producing a smooth topography.

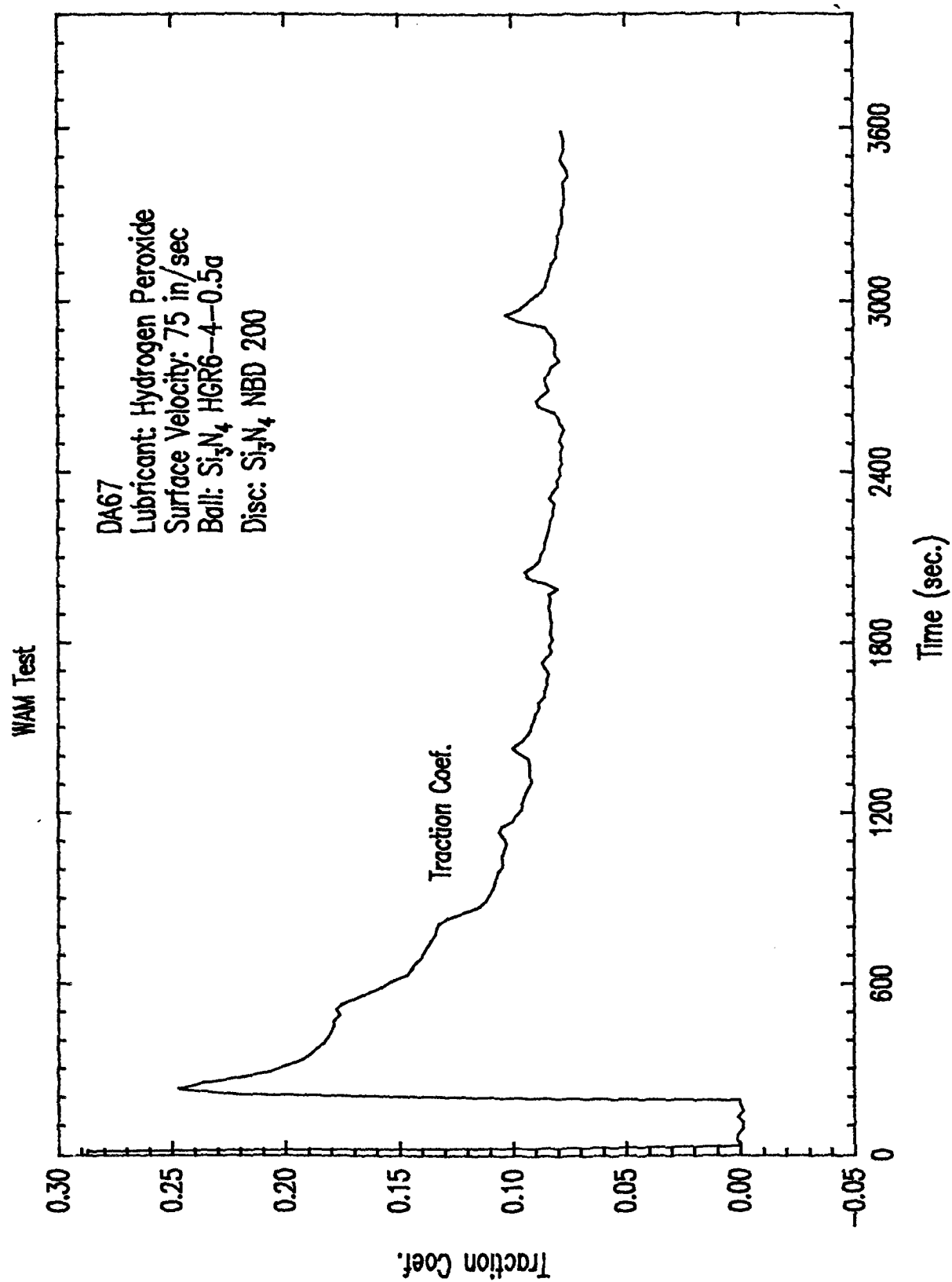
4.3.1.4 Hydroperoxide-Water Fluid

Hydroperoxides, which are usually formed as a by-product of oxidation processes in lubricating oil, are known to accelerate the wear process in ferrous materials through chemical interactions. The next series test was conducted to determine if a hydroperoxide could accelerate the finishing process in Si_3N_4 ball blanks. The test was conducted with a fluid made up of 3% hydrogen peroxide (HOOH) and 97% water. The traction curve for the test with this fluid is shown in Figure 9. The traction coefficient increased to about 0.25 upon the introduction of 5% contact slip at 200 seconds. This is followed by the characteristic rapid decrease in traction, attaining a nearly steady value of about 0.08 at about 1800 seconds. In general, both the starting traction coefficient (when contact slip is introduced) and steady traction coefficient in this test are higher than the ones in the tests performed with the other water containing fluids. Also, there is a periodic small increase and decrease in traction coefficient throughout the duration of the test, as shown in Figure 9.

Wear tracks on the ball and the disc are shown in Figure 10. The wear track on the ball (Figure 10a) is wider, perhaps indicating more wear than the ones in previous tests with other fluids under similar test conditions. The wear mechanisms involved in the generation of a smooth topography are desirable, but there is also material removal in flake form, which results in surface craters. Furthermore, there were networks of random cracks on the surface. The more extensive damage process on the ball surface with this fluid is probably reflected in the relatively high measured traction coefficients. The wear track on the disc was similar to the ones with the other fluids, consisting of some smooth areas, but also some of the original features remaining (Figure 10b).

4.3.1.5 Mineral Oil-Water NaOH Mixture

The next fluid evaluated was a mixture of 20% mineral oil and 80% water with a small amount of NaOH pellets added. Molten NaOH is often used for chemical etching of Si_3N_4 ceramic materials to reveal their microstructure. The etching occurs by the chemical dissolution of the glassy grain boundary phase by the NaOH. Such weakening of the grain boundary phase could



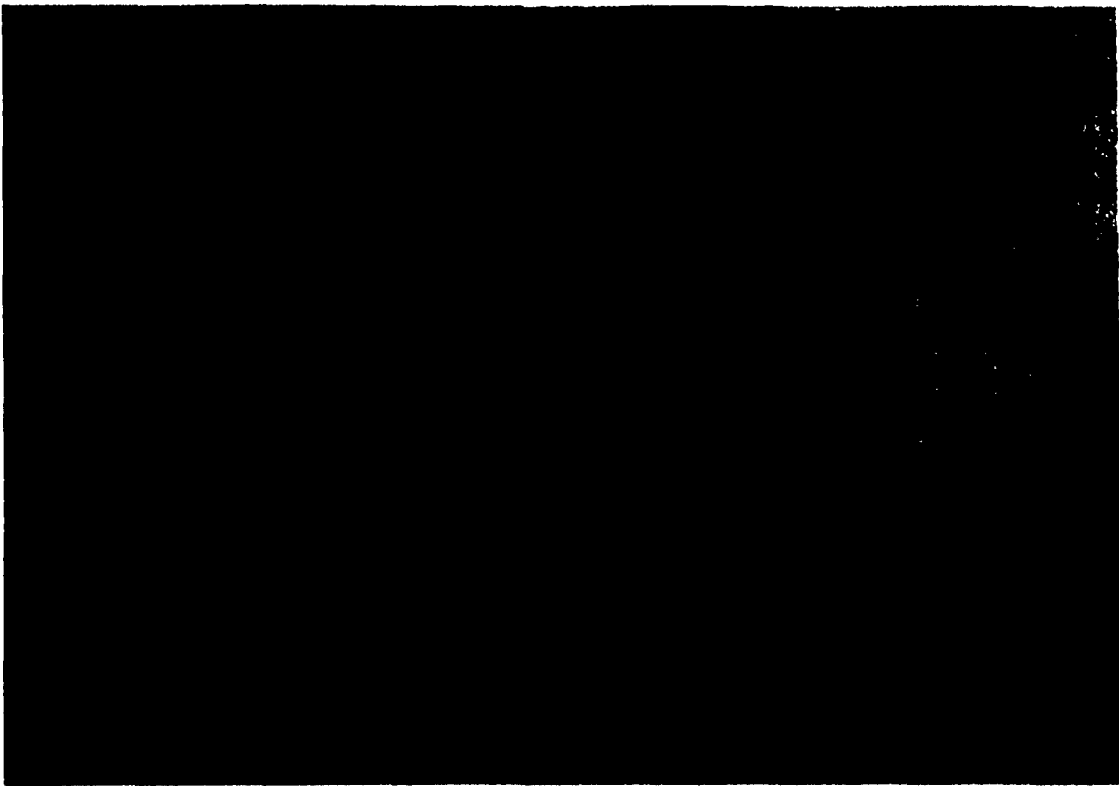
<DA67.SPW>

Figure 9 Run-in test with water-hydrogen peroxide



(A)

200 μm



(B)

200 μm

Figure 10 Run-in finishing of (a) ball and (b) disc with hydrogen peroxide

accelerate the rate of material removal during finishing.

The traction behavior for the test (DP68) conducted with this fluid is shown in Figure 11a. When contact slip is introduced, the traction coefficient increases to about 0.25, then decreases over the next 400 seconds to a value of about 0.15. Following this decrease is a gradual increase in the traction coefficient and an increase in the contact noise level as well. By 1470 sec, when the test was terminated, the traction coefficient had increased to about 0.24 and the contact noise became very loud. Both the ball and the disc surfaces at the conclusion of this test show evidence of severe wear (Figure 11b and 11c). The ball tracks still have areas that are topographically smooth, in addition to areas where large chunks of materials have been removed.

4.3.1.6 Mineral Oil-Lauric Acid

In a lubricated study of tribological behavior of different ceramic materials, it was observed that Lauric acid ($\text{CH}_3(\text{CH})_{10}\text{COOH}$), when used as an additive in mineral oil, accelerated the wear rate of Si_3N_4 ceramic materials. The next fluid evaluated was mineral oil with about 5% Lauric acid. The traction coefficient increased to about 0.17 with 5% contact slip. The traction decreased gradually thereafter throughout the test, the decrease being more rapid at the early stages. The degree of fluctuation in the traction during this test is less than the ones for tests with other fluids.

A smooth track was produced on the ball as shown in Figure 12. There were also brown discoloration spots on the track. The wear on the disc is relatively small with the wear mostly occurring at high asperity peaks (Figure 12b). In general, there was less wear with this fluid compared to the other ones, especially the water containing fluids.

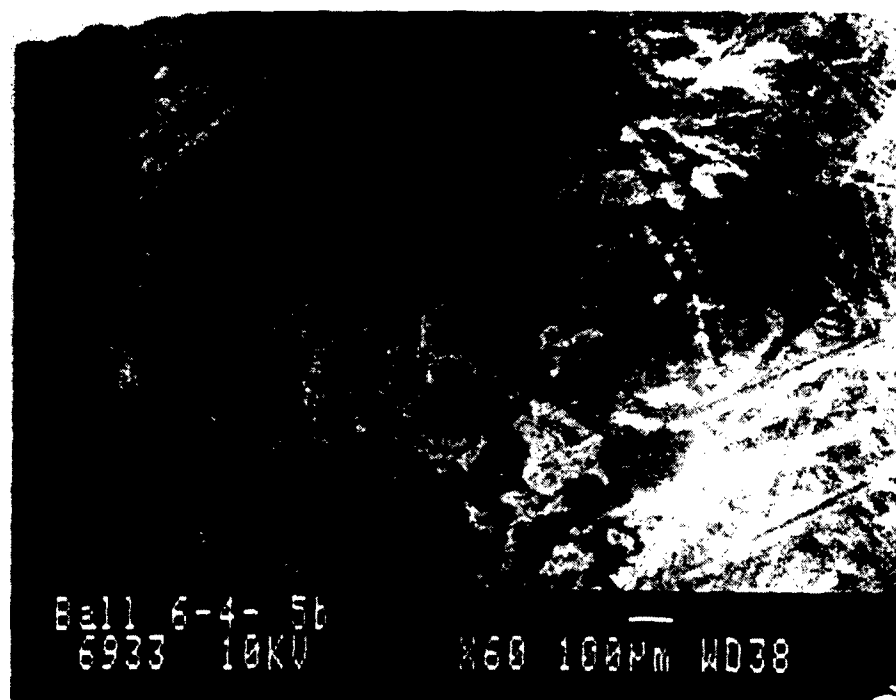
4.3.1.7 Mineral Oil-Lauric Acid-Hydrogen Peroxide Mixture

The last fluid evaluated was a mixture of mineral oil, Lauric acid and hydrogen peroxide. The traction curve for the test (DP70) conducted with this fluid is shown in Figure 13. The traction coefficient shows a near exponential decrease to a near steady value of about 0.05 after an initial rise of about 0.24 with the introduction of contact slip. There is also significant fluctuation in traction coefficient throughout the test, occurring more so at the early stages. This traction behavior is typical for tests in which smooth wear tracks are generated on the ball.

Examination of the ball and disc surfaces indeed show the relatively smooth surface topography is produced on both surfaces at the conclusion of this test (Figure 14). In addition to polishing wear on the ball, material removal in form of flakes also occurred as shown in Figure 14a.

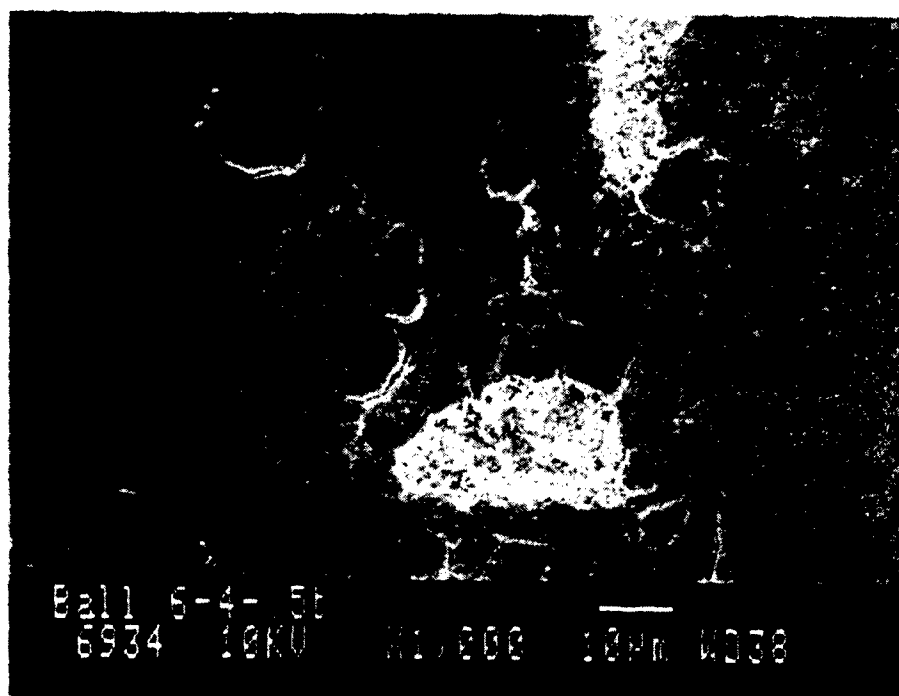
4.3.1.8 Summary of Effect of Working Fluid

A summary of the results of the tests run with various working fluids on the run-in finishing process of Si_3N_4 balls is shown on Table 2. The test results with various working fluids show clearly that the working fluid has a significant effect on the run-in finishing process. Although alcohol did not change or accelerate the finishing mechanism when compared with water, (which



(B)

200 µm



(C)

200 µm

Figure 11 Si_3N_4 ball run-in finished in water + NaOH + mineral oil

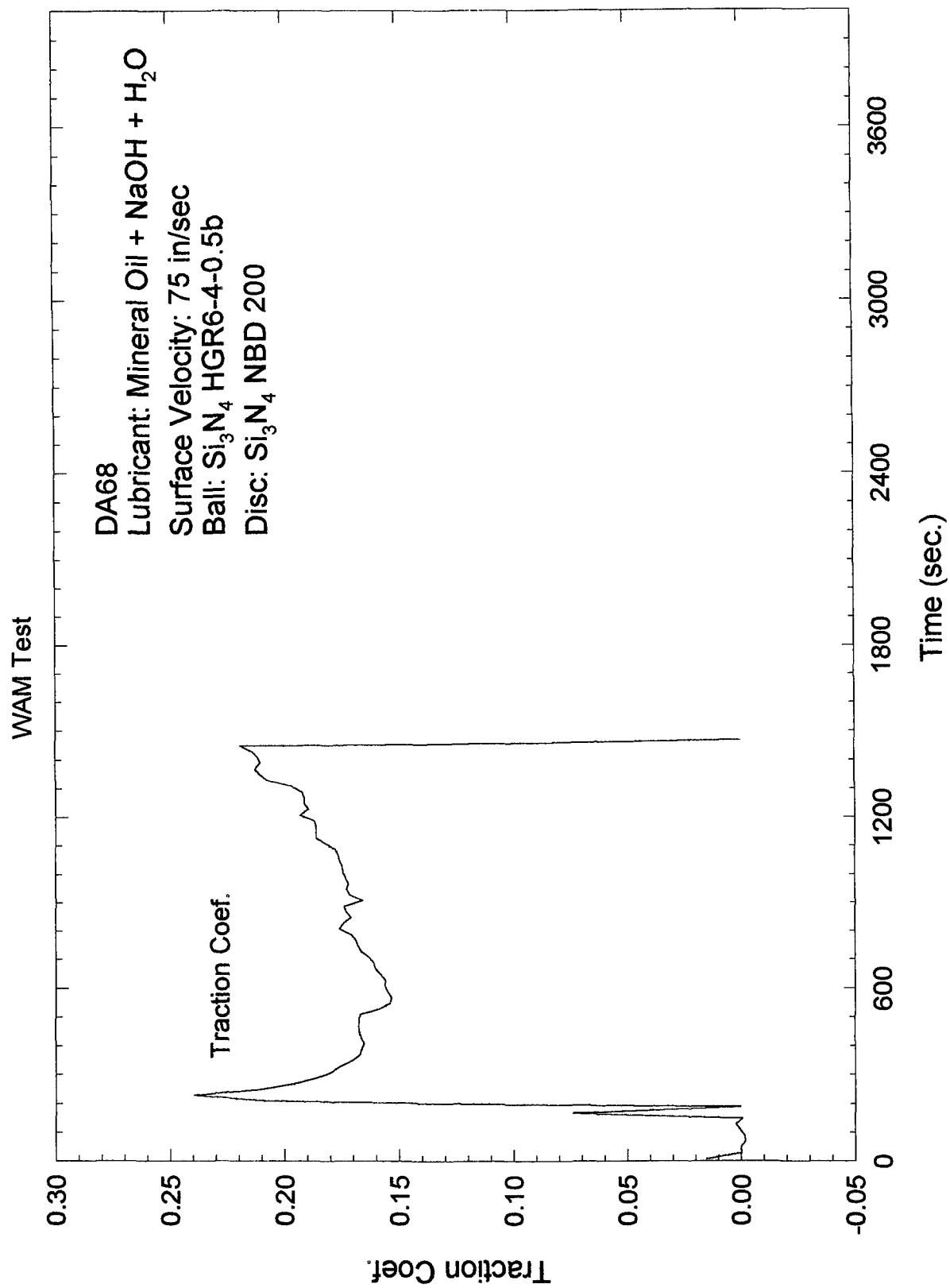


Figure 11a Test with mineral oil-water-NaOH mixture



(A)

200 μm



(B)

200 μm

Figure 12 Run-in finishing of (a) ball and (b) disc with Lauric acid

DARPA TEST SERIES

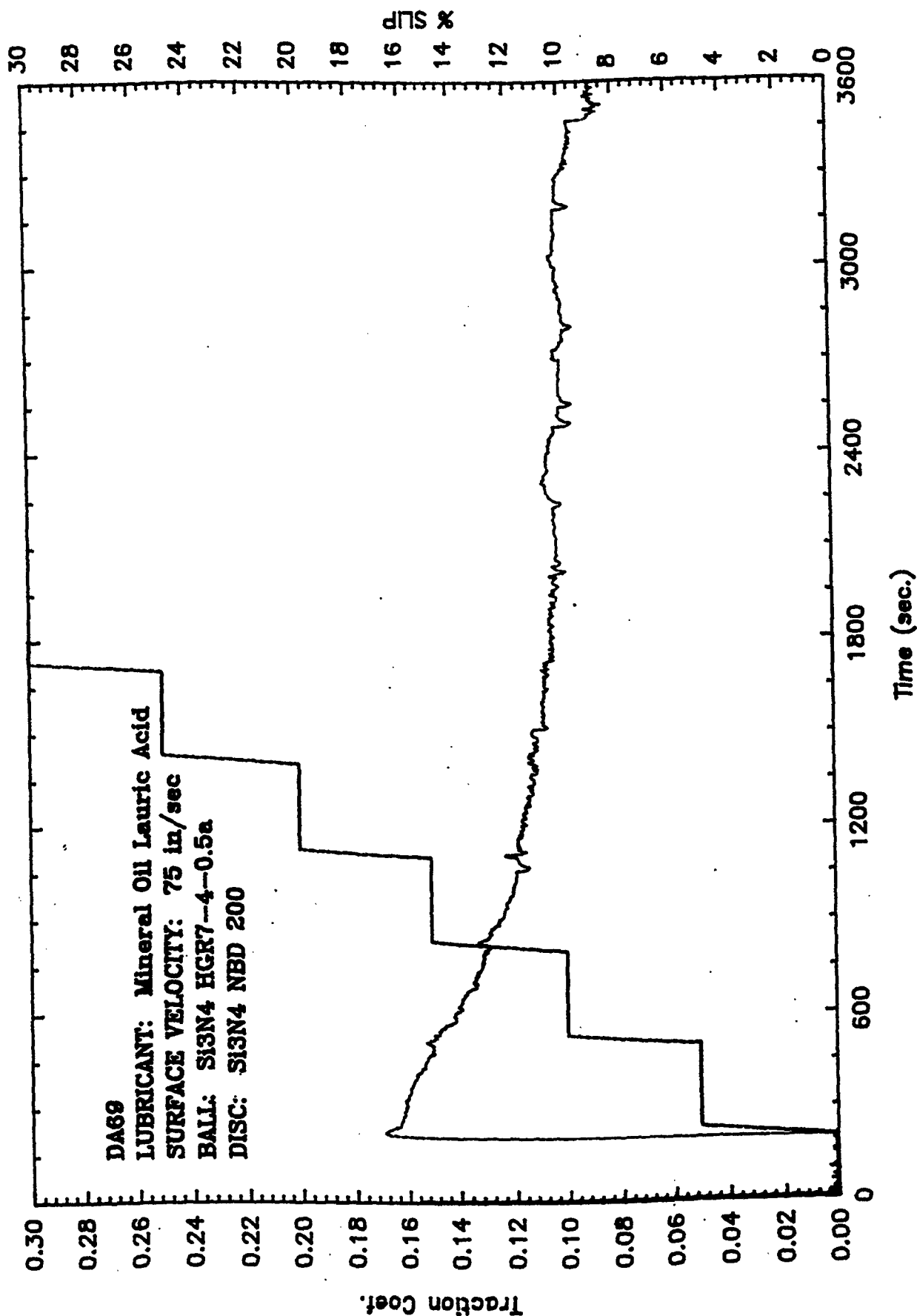
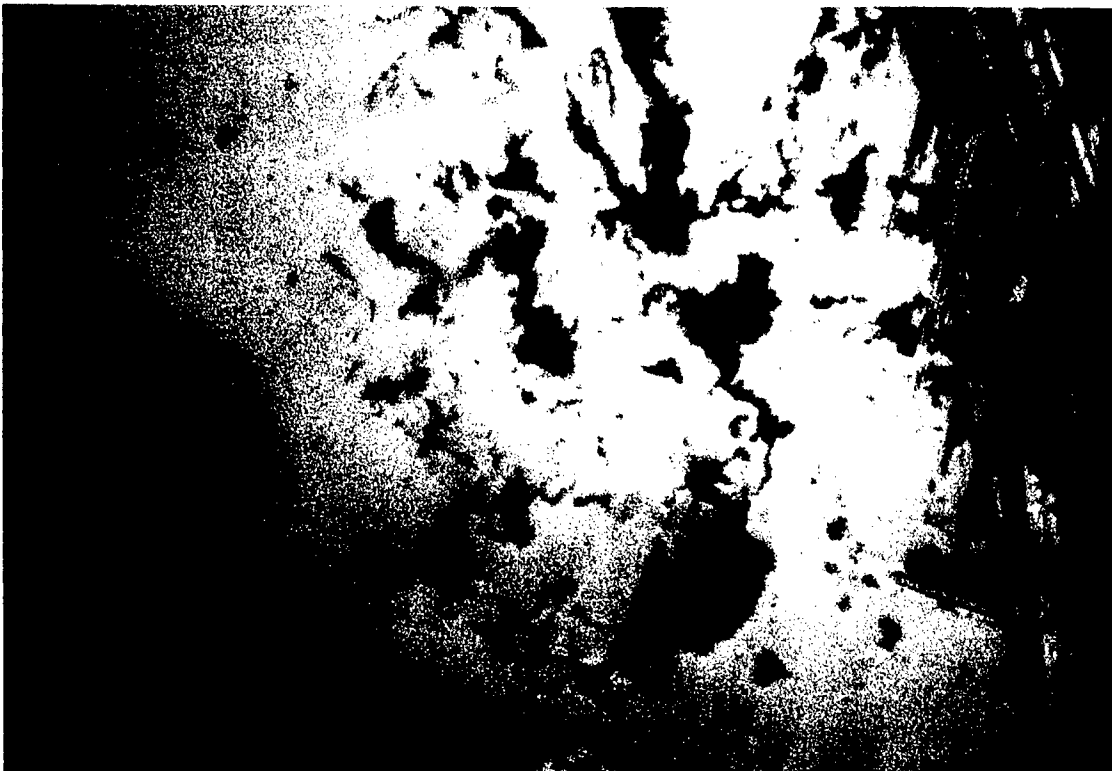


Figure 13 Traction plot for test run with mineral oil, lauric acid, hydrogen peroxide mixture

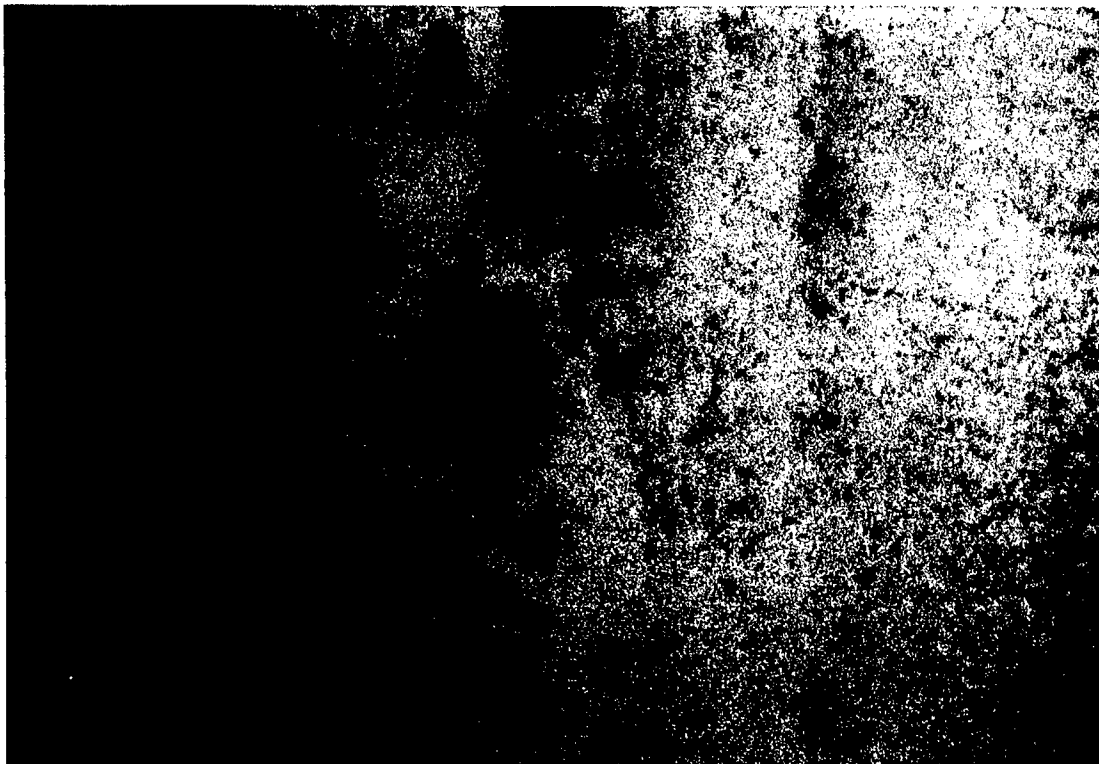
Table 2
Fluids (Lubricant) Evaluated
And a Summary of the Results

| <u>FLUID</u> | <u>RESULTS</u> |
|---|--|
| Synthetic Ester basestock | Some polishing wear at the asperity peaks on the ball blanks |
| Water | Polishing wear on the ball and disc generating a smooth topography |
| Water + Oil Mixture | Polishing wear on the ball and disc generating a smooth topography |
| Water + Oil + Isopropyl Alcohol | Polishing wear on the ball and disc generating a smooth topography |
| Water + Hydrogen Peroxide (HOOH) | Polishing wear and flaking |
| Oil + Water + Sodium Hydroxide | Severe wear |
| Oil + Lauric Acid (CH ₃ (CH) ₁₀ COOH) | Polishing wear |



(A)

200 μ m



(B)

200 μ m

Figure 14 Run-in Finishing of ball (A) and disc (B) with mineral oil - lauric acid - hydrogen peroxide

is a good finishing fluid) it did provide a significant amount of cooling. This could allow the finishing to be done under a more severe condition without concern for excessive frictional heating. Hydrogen peroxide and presumably hydroperoxide in general, accelerated the finishing process, but also promoted the wear mechanisms involving material removal in flake form. Sodium hydroxide (NaOH), which is an etchant for the glassy grain boundary phase, promotes the occurrence of severe wear rather than polishing wear. This may be the consequence of the weakening of the near surface region through the weakening of the grain boundaries.

4.3.2 Effect of Ball Blank Materials

The effect of the ball blank material on the run-in finishing process is investigated by using ball blanks made from two different Si_3N_4 . These were TSN-03H from Toshiba and NBD200 from Cerbec. Details of these materials already were presented above. Three working fluids (lubricants) are used in this comparative run-in finishing of the two kinds of materials. The fluids were oil + water + hydrogen peroxide (H_2O_2) and oil + water + NaOH. The 'run-in' finishing of these two materials was done with a Si_3N_4 (TSN-03H) counterface with a ground surface finish. The disc surfaces were also examined for their run-in finishing. Details of the observation on the disc surfaces will be presented later under the disc (raceway) finishing. Results for the ball finishing are presented.

4.3.2.1 Oil-Water Mixture Fluid

The traction behaviors during the run-in finishing tests with oil and water (20:80) mixture working fluid for the TSN-03H and the NBD200 ball blanks are shown in Figures 15 a and 15b, respectively. The traction behaviors in the tests with the two materials are very similar. In both cases, there was a rapid increase in the traction coefficient as the contact slip of 5% was introduced at 200 seconds. This was then followed by an exponential decrease in the traction coefficient with time, reaching a nearly steady value of about 0.03 at about 300 seconds in tests conducted with both materials. The traction coefficient in both cases also showed some fluctuation during the tests.

There are only two noticeable differences between the traction characteristics of the two materials. (1) When the contact slip is introduced, the traction coefficient in the test with TSN-03H increased to a maximum value of about 0.193, while it is about 0.18 for the test with NBD200. (2) The traction coefficient showed a more rapid decrease during the first 600 seconds in the test run with the TSN-03H material compared to the NBD materials. Tests with the TSN-03H ball blank with higher roughness start with a lower value of h/σ . This results in more intimate interaction between the ball and the disc surfaces, hence the higher traction coefficient, and possibly higher wear rate. The consequence is the quicker generation of a smoother surface and a rapid decrease in traction. In fact, the occurrence of this sequence of events was verified by video monitoring the run-in finishing process in both balls. It was observed that the smoothening of the contact area of the TSN-03H ball occurred more quickly than the NBD200 ball.

Figure 16 shows the tracks produced on the two kinds of material at the conclusion of the 1 hour

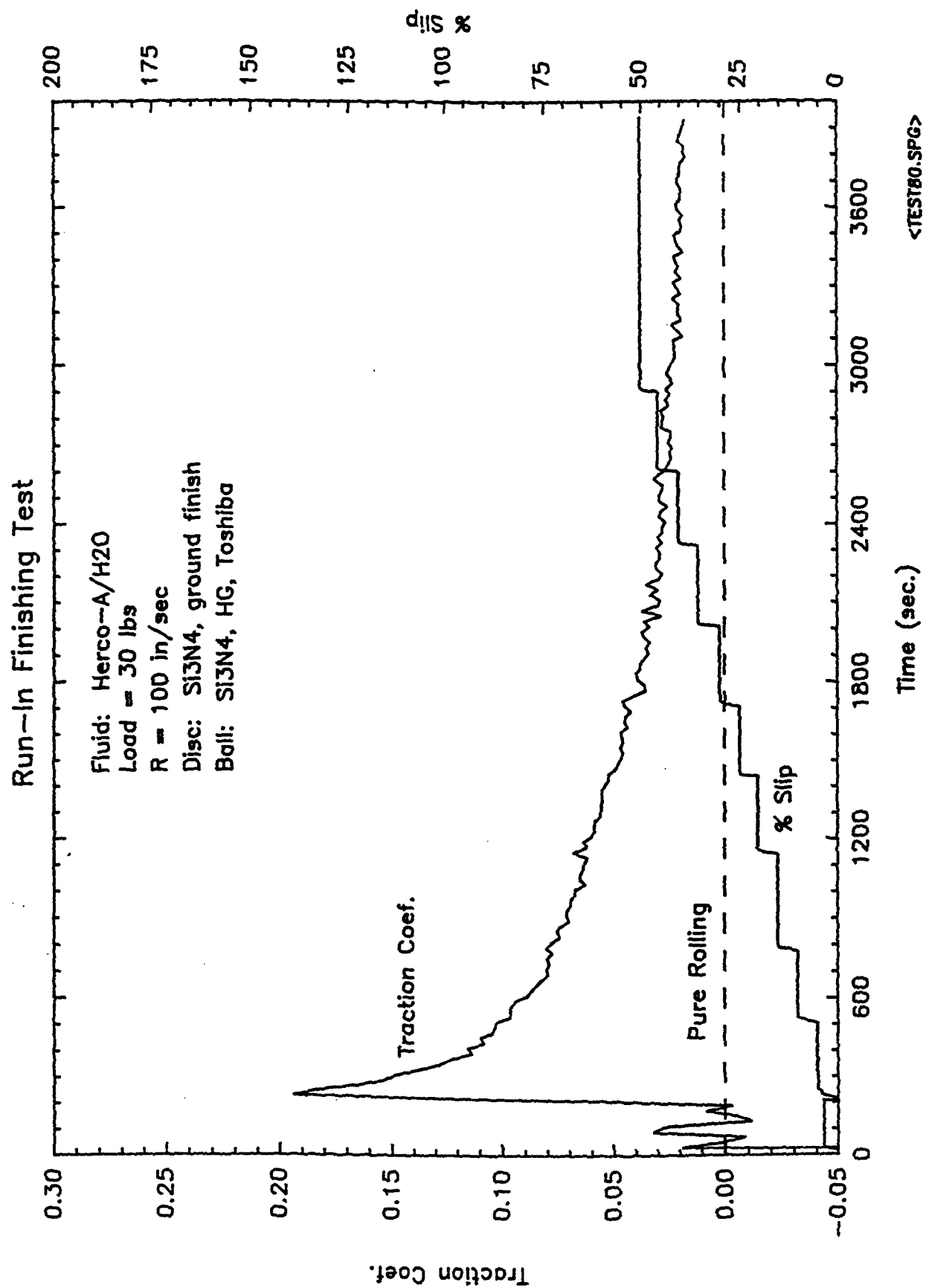


Figure 15a Traction plot for run-in test with oil - water mixture with TSN-03H ball

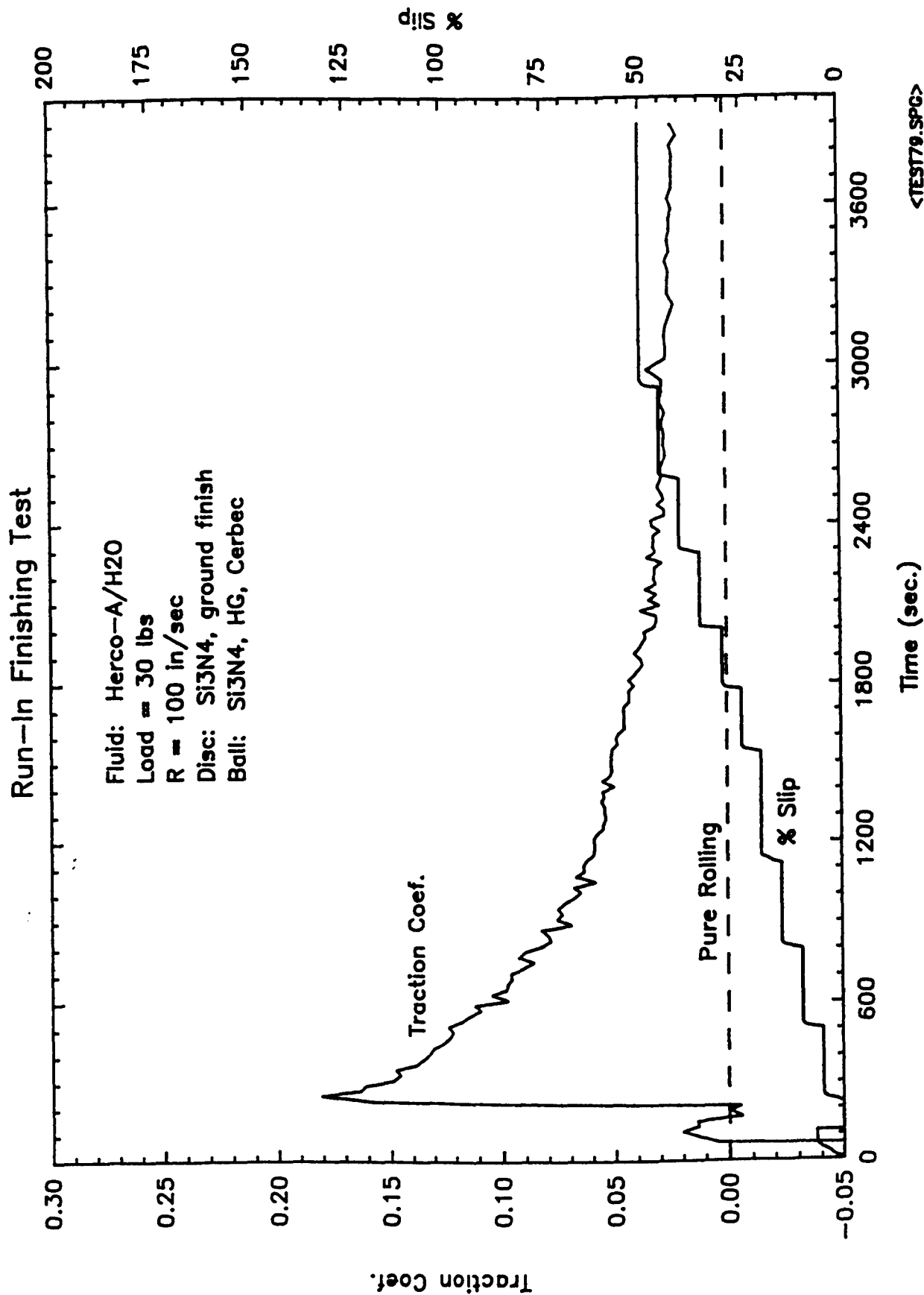
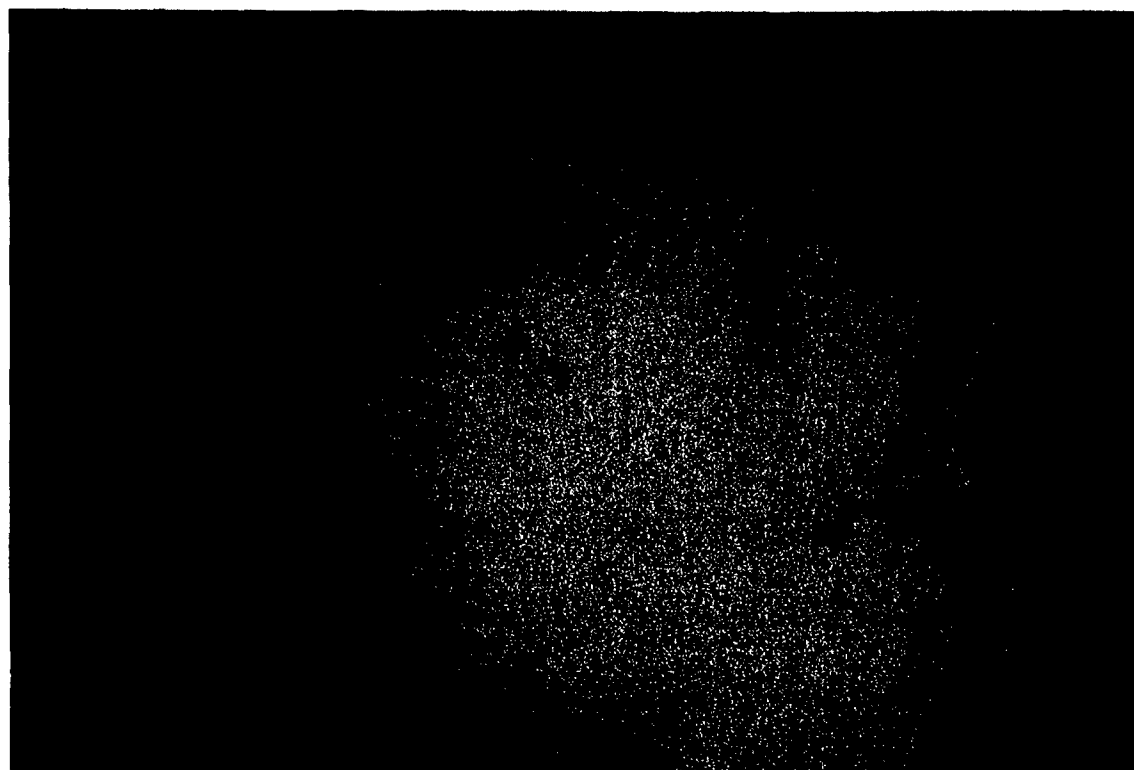


Figure 15b Traction plot for run-in test with oil - water mixture with NBD 200 ball



(A)
TSN-03H

200 μm



(B)
NBD200

200 μm

Figure 16 Si_3N_4 ball run-in finished in Oil + H_2O fluid

run-in finishing test. Smooth track was generated on both surfaces, with the TSN-03H ball having a marginally better finish. This was probably more connected with the differences in their original surface conditions. In any case suffice to say that good run-in finishing is accompanied in both the TSN-03H and the NBD200 ball blanks with this working fluid.

4.3.2.2 Oil-Water Hydrogen Peroxide Mixture

Significant differences are seen in the run-in finishing of the two kinds of Si_3N_4 materials when done in this working fluid. Figures 16 a and 16b shows the traction coefficient behavior during the tests with TSN-03H and NBD200 ball blanks respectively. The traction behavior for the TSN-03H showed the same characteristics as the oil and water mixed fluid. Upon the introduction of contact slip at 200 seconds, the traction coefficient increased to a relatively high value of 0.21. This was immediately followed by a rapid exponential decrease in traction coefficient, ending with a value of about 0.02 after 1 hr. test time. In the test with the NBD200 ball, on the other hand, the traction coefficient increased to only a value of 0.09 with the introduction of contact slip (Figure 17a). Instead of the exponential form, the traction coefficient decreased linearly to a value of about 0.05 at 3000 seconds. This is then followed by a sudden drop to a value of 0.02, which is maintained until the end of the test.

The exact reason for the differences in the traction behavior is not fully understood at this time. Its effect on the run-in finishing process is quite substantial. Through the video monitoring of the finishing process, it was observed that smooth topography was quickly generated on TSN-03H ball while only slight changes occurred on the NBD200 ball for the first 3000 seconds. Rapid "polishing" of NBD200 ball did occur and was accompanied by a sudden drop in traction coefficient at 3000 seconds. The appearance of the track on both balls is shown in Figure 18. A good finish was achieved on both balls, with the finish in the TSN-03H ball a little better than that of NBD200 ball.

The most significant difference between the two kinds of Si_3N_4 balls in the tests with this fluid is the rate of finishing. For the TSN-03H ball, the smooth topography is generated by 1200 seconds into the test. In the NBD200 ball however, the smooth topography is generated at about 3000 seconds. This despairing rate of finishing could be related to the traction behavior differences in the test run with the two different kinds of ball. The high traction coefficient (0.21) with the TSN-03H ball when contact slip is introduced will impose high shear stress at the contact interface. This will result in high wear rate. Since polishing wear mode is the main material removal mechanism, quick generation of smooth surface is expected. If the traction coefficient is too high, however, formation of Hertzian stress at the contact interface can be accompanied by polishing wear. With the NBD200 ball, the traction coefficient with the introduction of contact slip is relatively low (0.09). The resulting lower shear stress will also translate to lower material removal rate as observed especially in the earlier part of the test.

4.3.2.3 Oil-Water Sodium Hydroxide Fluid

The traction behavior during the run-in finishing with this fluid was nearly identical for tests run with the TSN-03H and the NBD200 balls. In both cases, the traction coefficient increased to

Run-In Finishing Test

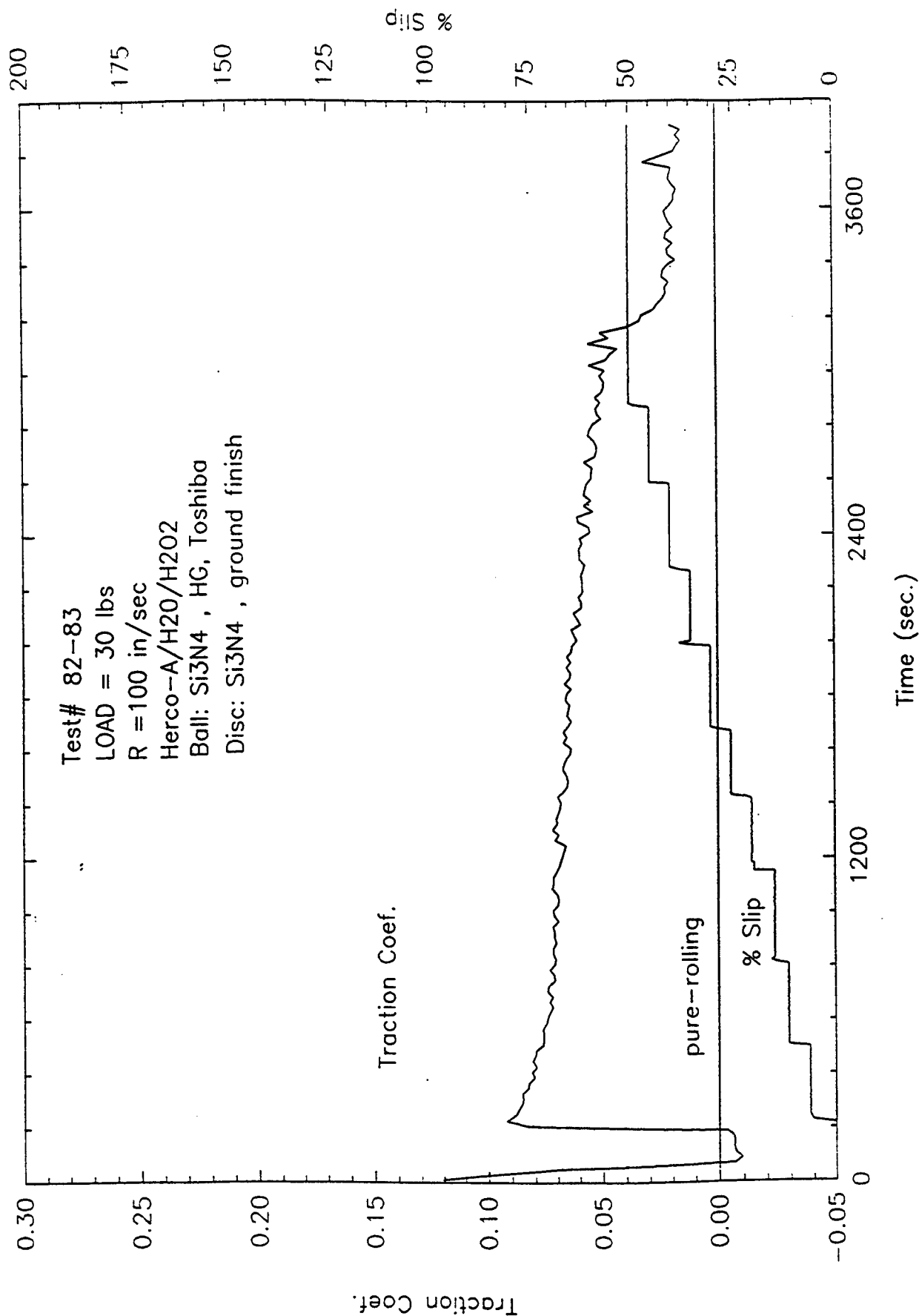


Figure 17a Traction plot for run-in finishing test with oil - water - hydrogen peroxide mixture <TEST82-83.SPG>

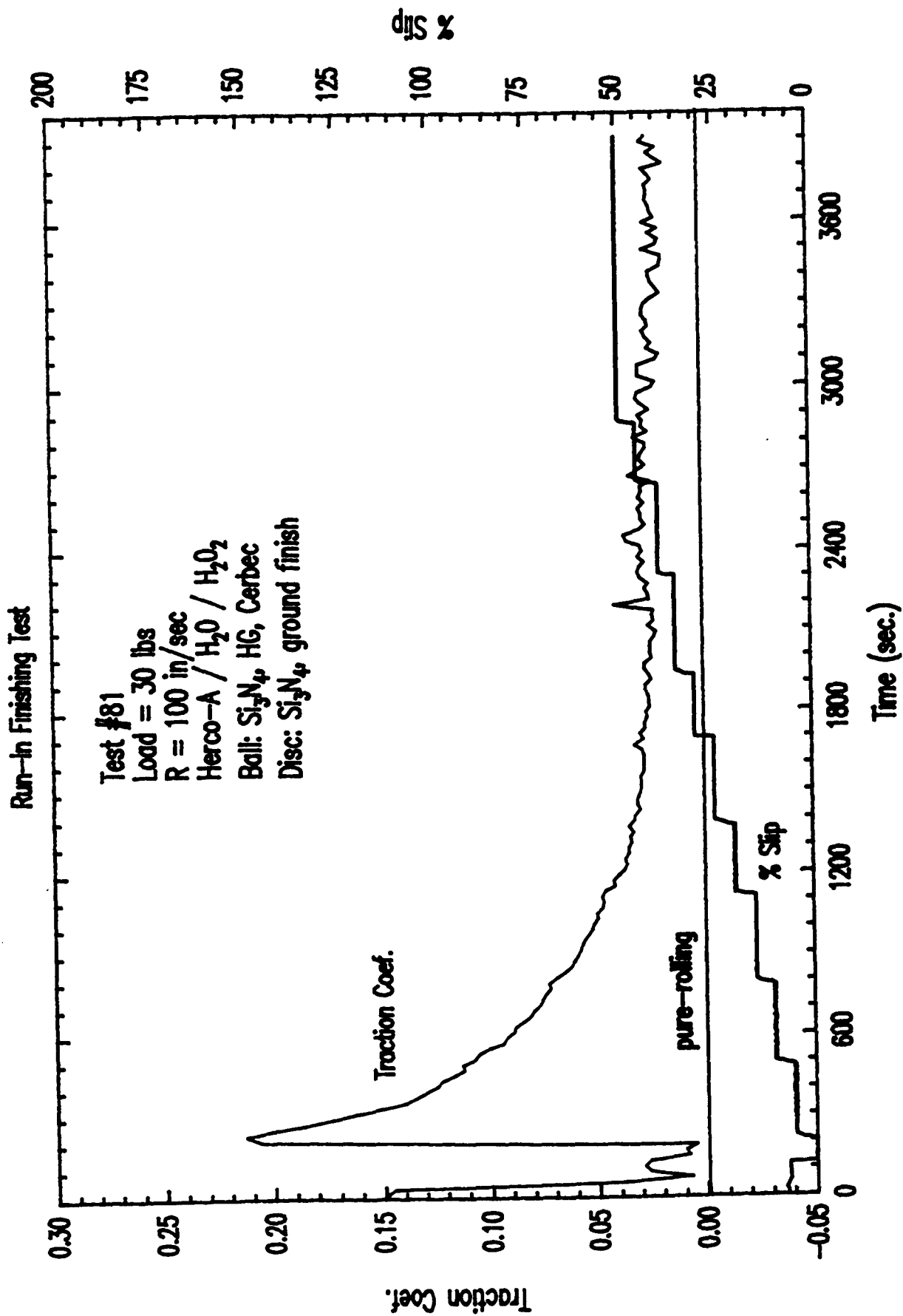
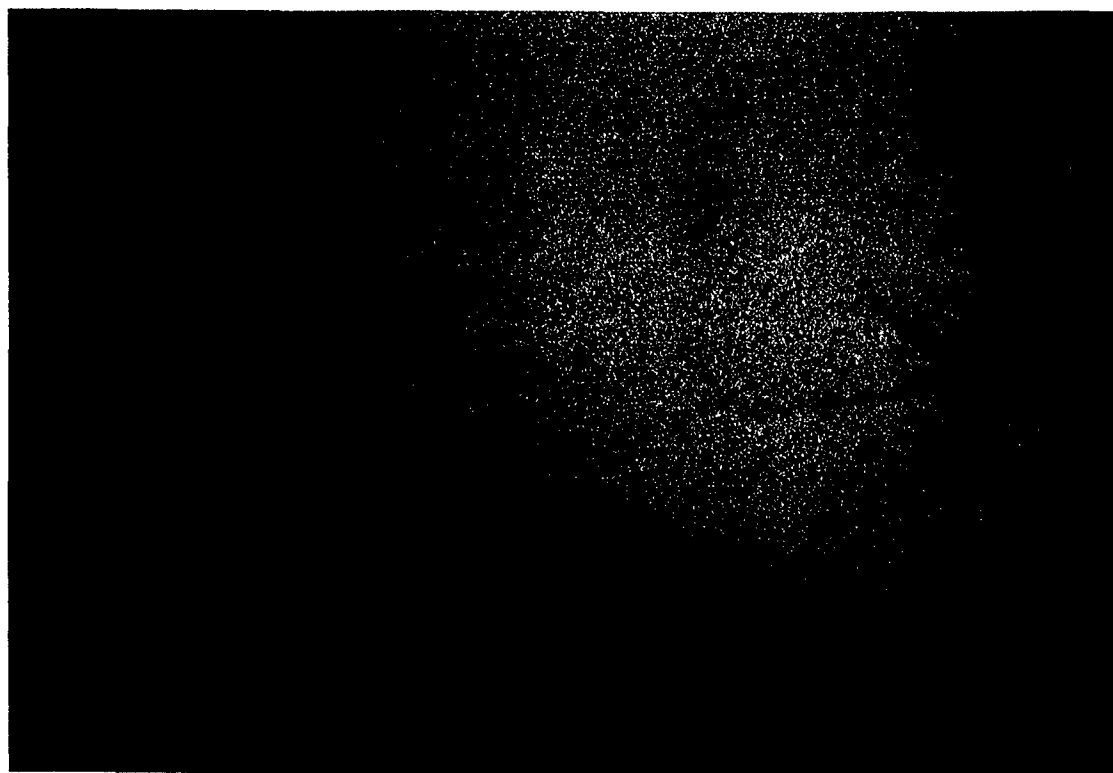
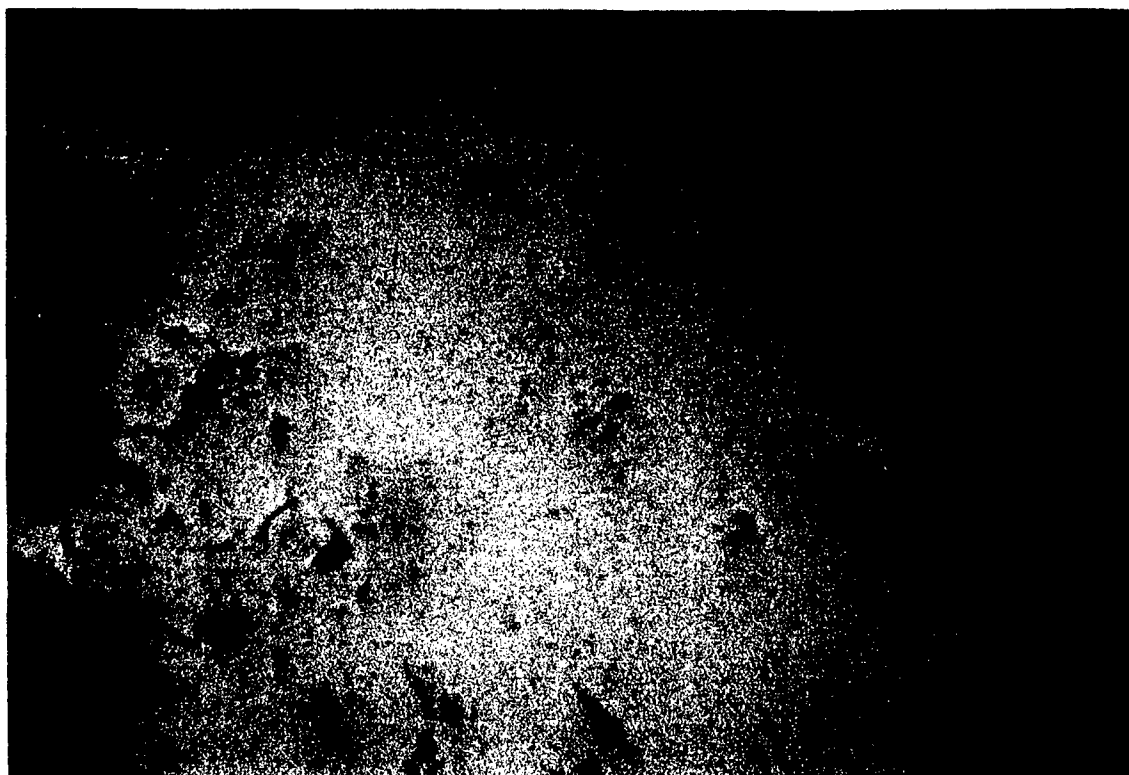


Figure 17b Traction plot for run-in finishing test with oil - water - hydrogen peroxide mixture <TEST181.SPW>



(A) 200 μm



(B) 200 μm

Figure 18 Si_3N_4 ball run-in finished in Oil + H_2O + H_2O_2 fluid

about 0.15 upon the exponential decrease of traction followed this initial event and the end of each test; the traction coefficient had value of about 0.025.

In spite of the similarity of the traction characteristics in the two tests, noticeable difference are seen on the finished surface. In both materials, two competing material removal mechanisms occur in tests with this fluid. One mechanism is the desirable polishing wear, and the other is wear by flaking. The flaking wear mode is more prominent in the TSN-03H material when compared to the NBD200 material as shown in Figure 19. In fact, in NBD200 balls, only surface cracking that proceeds the flaking process is seen (Figure 19b), while areas of material removal by flaking in TSN-03H ball are prominent as indicated in Figure 19a and 19c SEM micrographs.

With this fluid, the occurrence of flaking wear mode is due to the interaction of the NaOH with the grain boundary phase. As previously explained, often NaOH is a common etchant for the glassy grain boundary phase in Si_3N_4 materials. Under the tribological contact employed in the run-in finishing procedure, interaction of the grain boundary phase with the NaOH ions in the solution occurs. This weakens the grain boundaries in the surface layer resulting in material removal by flaking. This difference in the extent of this mode of material removal in the two materials, reflect the differences in the chemistry and interaction with NaOH of their grain boundary phase.

This observation could be useful in ball finishing or machining operation for Si_3N_4 materials where high material removal rate is desirable. Small additions of NaOH and possibly other chemical etchant of Si_3N_4 to the working fluid could significantly accelerate material removal rate by chemically weakening the grain boundary phase in the wear surface layer. The use of such an approach, however, requires a stringent control of the depth of the surface layer that is chemically modified.

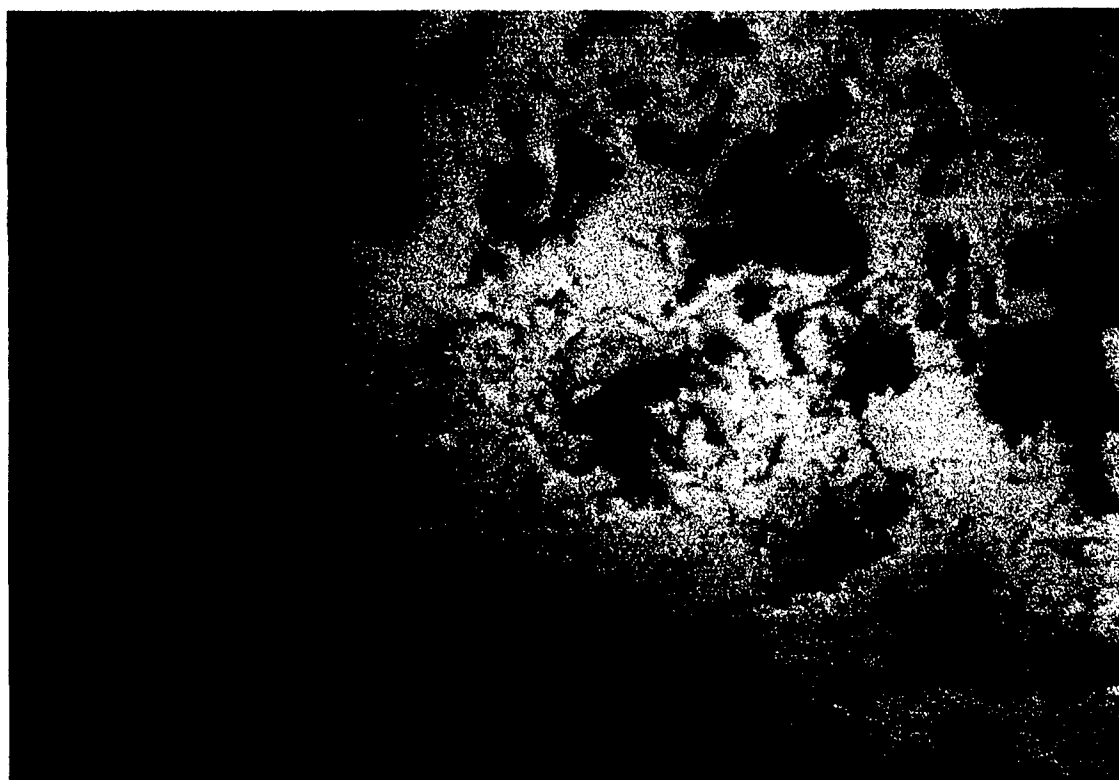
4.3.3 Further analysis of Run-In Finished Surfaces

In order to elucidate some of the mechanisms involved in the generation of smooth surface topography during the run-in finishing of the Si_3N_4 ball blanks, analysis of the surface layer structures were done. The tracks generated in the best run-in fluid, which oil and water mixture, on the TSN-03H ball were analyzed. Two methods used for the surface analysis were X-ray diffractometry and Ramon Spectroscopy.

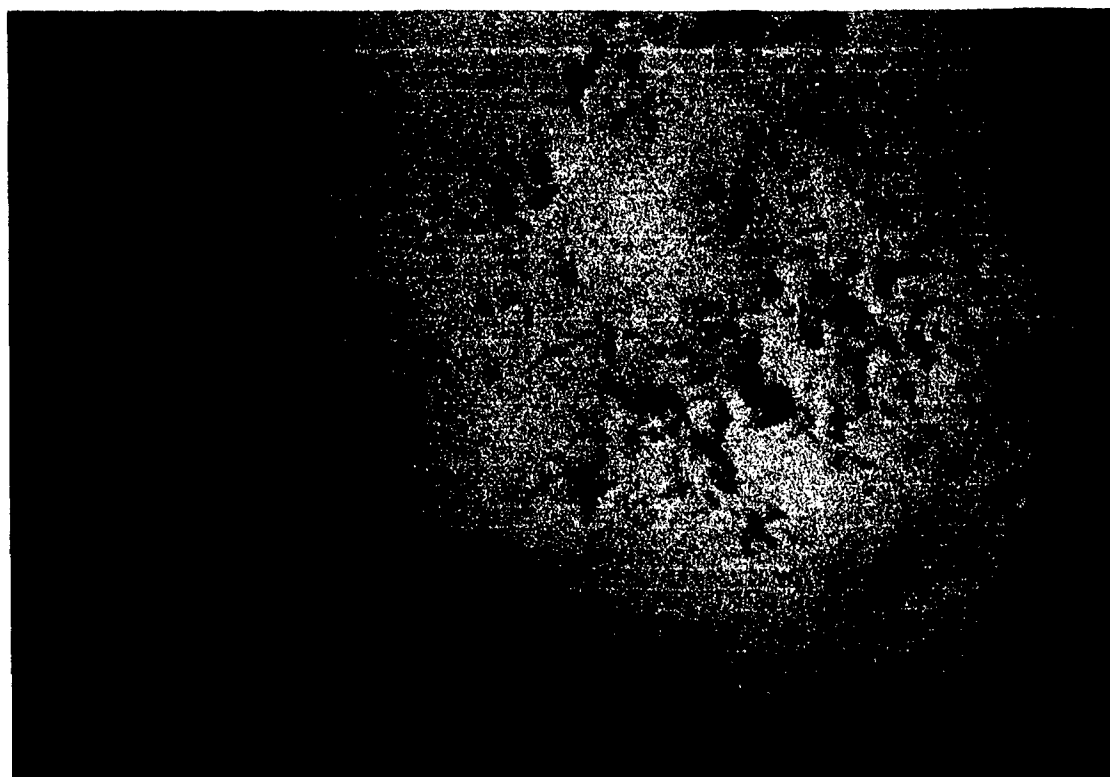
4.3.3.1 X-Ray Diffractometry

X-ray diffraction patterns are acquired from areas within and outside the run-in finished track on the Si_3N_4 ball. Figure 20 shows the two diffraction patterns. The patterns from the area inside and outside the tracks are essentially the same. This would suggest that the crystalline phases in the two regions are the same.

A significant difference between the diffraction patterns is the lower intensity of the peaks from the area that is run-in finished. This attenuation of intensity is a result of X-ray absorption. The absorption could be from two possible sources: (1) The presence of a non diffracting layer on

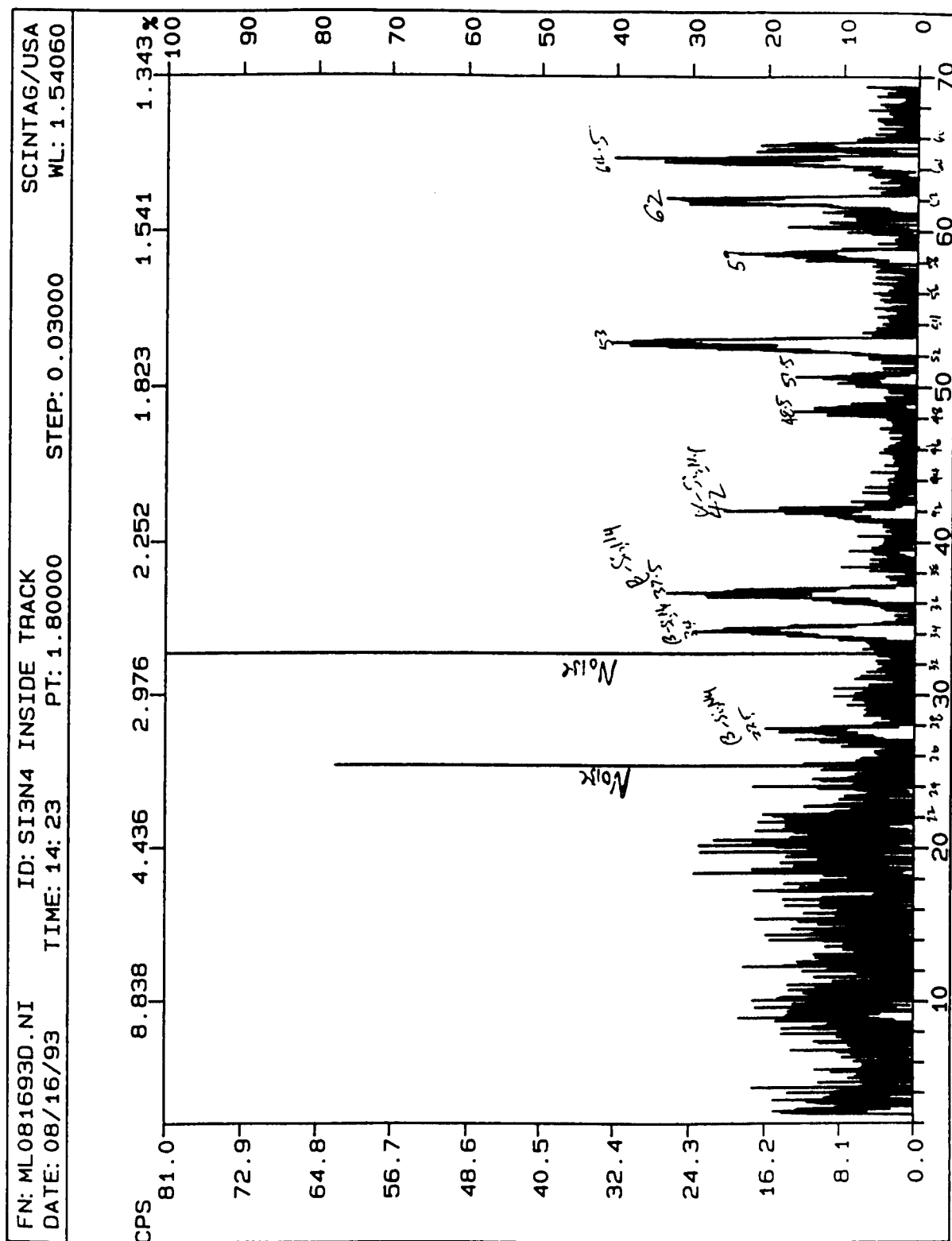


(A) Toshiba
200 μm



(B) Cerbec
200 μm

Figure 19 Si_3N_4 ball run-in finished in Oil + H_2O + NaOH fluid



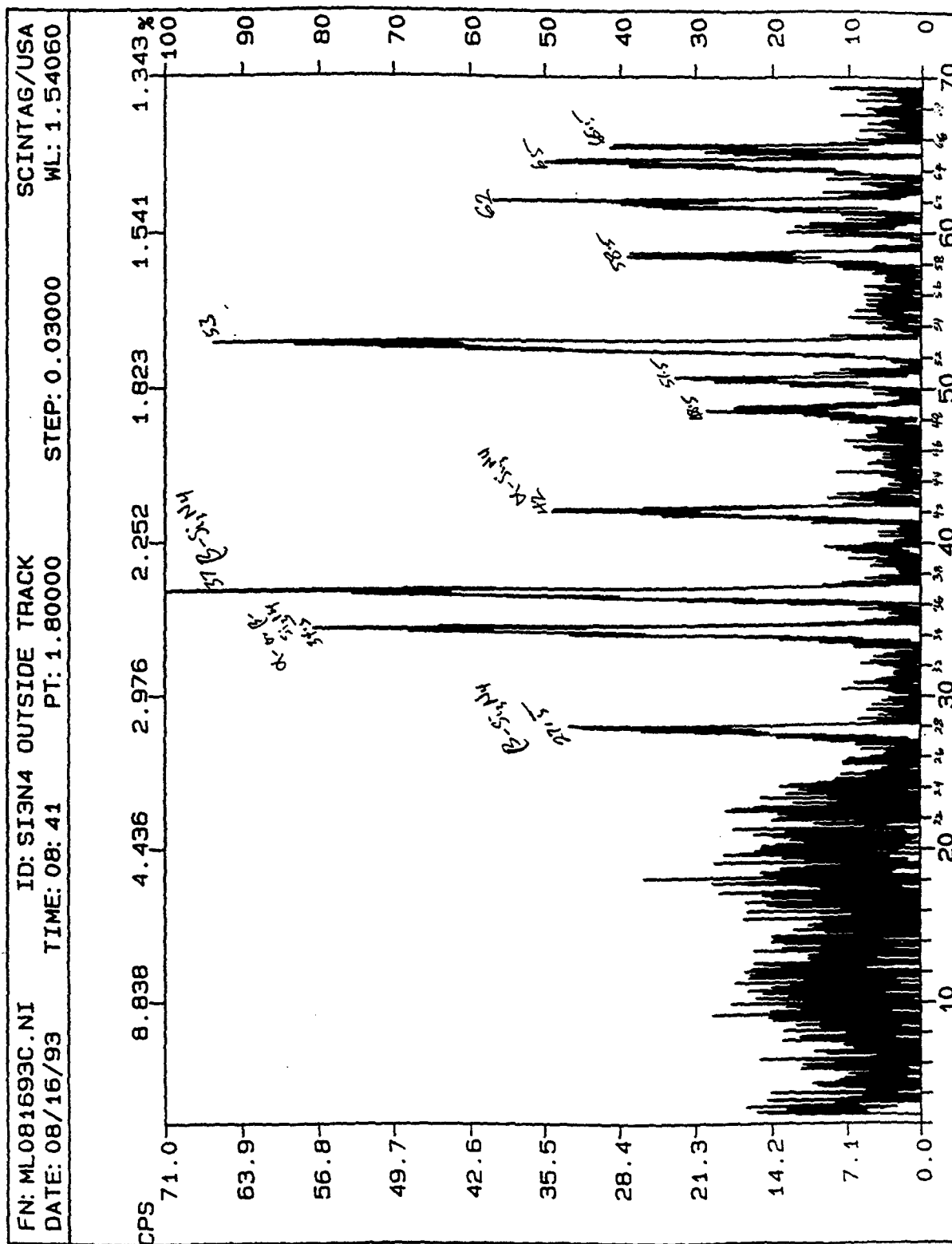


Figure 20b: X-ray diffraction pattern outside run-in finished surface

the surface, or (2) the diffraction pattern being produced by a mixture.

If there is a non-diffracting layer uniform thickness (x) is present on the surface and the X-ray has to pass through the layer. The intensity reduction due to the presence of this layer can be estimated by the equation:

$$I = I_0 \exp - [(\mu/) x]$$

Where I = measured intensity;
 I_0 = initial intensity before absorption,
 $\mu/$ = mass absorption coefficient of the layer,
 ρ = density of the layer.

On the other hand, if the X-ray peak intensity attenuation is due to the fact that the diffraction pattern is being generated by a phase mixture, the intensity can be estimated by the equation:

$$I = I_p \frac{(\mu/)}{(\mu/)_m} f$$

where I_p = intensity of pure phase
 I = intensity of phase in mixture
 f = weight fraction of the phase in the mixture
 $(\mu/)$ = mass absorption coefficient of the phase
 $(\mu/)_m$ = mass absorption coefficient of the mixture

From the diffraction patterns in Figure 20, it is not possible to determine the source of peak attenuation. However it is very likely there is the presence of a X-ray non-diffracting phase i.e. an amorphous phase. This phase could be present as a layer on the surface or as a mixture with Crystalline phases in the original material. If the chemical composition of the amorphous phase is known, and the form in which it exists is also known, its quantity in terms of thickness (if a layer) or its volume fraction (if a mixture) can be estimated by the appropriate equation above.

4.3.3.2 Raman Spectroscopy

Raman Spectroscopy is a material analytical method that uses light scattering phenomenon occurring during the interaction of a light beam with known characteristics with the material of interest. Raman Spectroscopy can provide information on the material/sample characteristics that produce light scattering. In the present study, the two useful material characteristics that this method can provide are the chemical bond nature and the crystal structure.

Raman Spectroscopy is usually done by laser light of known frequency impinging on the surface/specimen. The scattering of the light after interaction with the specimen is then characterized. The result is displayed as a plot of scattered light intensity as a function of frequency shift. The shift is calculated relative to the incoming laser line frequency, which is, assigned a zero value.

Figure 21 shows the Raman Spectra for the standard and phases of Si_3N_4 . The α -phase crystals has two peak shifts at 202 and 260 cm^{-1} frequencies while β -phase crystal has four major peaks shifts at 180, 200, 223 and about 255 cm^{-1} as shown in Figure 21.

Raman Spectra were also acquired from the Si_3N_4 ball surface that were run-in finished in oil and water mixture working fluid. An Argon (Ar^+) laser (with 514.5nm line, and 100 m Watt power) light was used for the analysis. The spectra is shown in Figure 22. The peak shift for the β -phase Si_3N_4 crystal at 180, 200, and 223 cm^{-1} are present. This will be consistent with other analysis of the micro structure of the Si_3N_4 material used for this study. Ref.]. The micro structure consists of primarily β - Si_3N_4 grains and a grain boundary phase. Several other peak shifts are present in Figure 22. Some of these peaks could be associated with the presence of Silica glass. Raman peak shift for silica glass are known to occur at 440 cm^{-1} frequency and several frequencies greater than 800 cm^{-1} [mat'l. handbook]. The high frequency bands ($>800 \text{ cm}^{-1}$) are associated with local distribution of metallic solute atoms in SiO_2 glasses. Thus several of the peaks in Figure 22 are due to the glassy grain boundary phase in the original Si_3N_4 material and also from the Silica glass that may be formed during run-in finishing of the ball.

4.3.4 Discussion

By operating a Si_3N_4 on Si_3N_4 contact under a kinematic condition similar to a rolling element bearing and by using appropriate working fluids as lubricants, smooth surface topography is generated. The surface finish generated by this process, termed run-in finishing, which uses no abrasives, is comparable and sometimes better than that produced by commercial finishing process. Figure 23 shows the surface features of a commercially finished TSN-03H ball. The surface finish material with oil and water mixture working fluid (Figure 16a) is slightly better than one commercially finished (Figure 23). Furthermore, the run-in finishing is accomplished in a 1 hour single test, while commercial Si_3N_4 ball finishing involves 4 to 6 operations, all of them using abrasives.

The generation of smooth surface topography on the Si_3N_4 ball blank in the two processes i.e., run-in finishing and commercial finishing is accomplished by different mechanisms. Finishing in commercial processes occurs primarily by abrasive wear; while in run-in finishing processes, chemically controlled polishing wear appears to be the dominant mechanism. Depending on the working fluid, other processes besides the chemical polishing wear occurs.

X-ray diffractometry and Raman Spectroscopy of the ball surface run-in finished in oil and water mixture fluid showed the presence of a Silica-based layer on the track. The layer is amorphous since no diffraction pattern is produced by it. This Silica layer is formed by the oxidation of Si_3N_4 material on the surface. This observation of chemical reaction of Si_3N_4 material during tribological contact is consistent with the experience of several other investigators [e.g., 2-4]. During the run-in finishing process, the contact condition is under the mixed/boundary lubrication regime. Where in extensive direct interaction occurs between the surface features on ball and the disc. The lubrication condition is in fact more severe, because all the working fluid contained a large fraction of water (70-80%). It is known that water oil mixture (emulsion) tend

Spectra of High Purity Silicon Nitride Power

Aldrich 99.9%

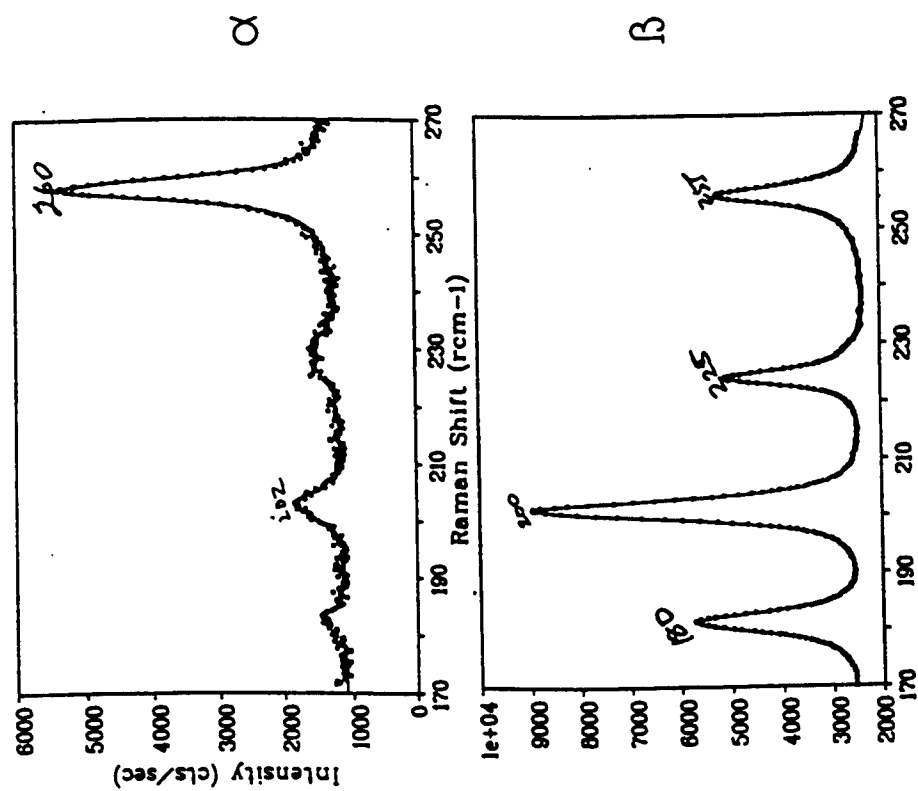


Figure 21: Raman Spectra for α - and β - Si_3N_4

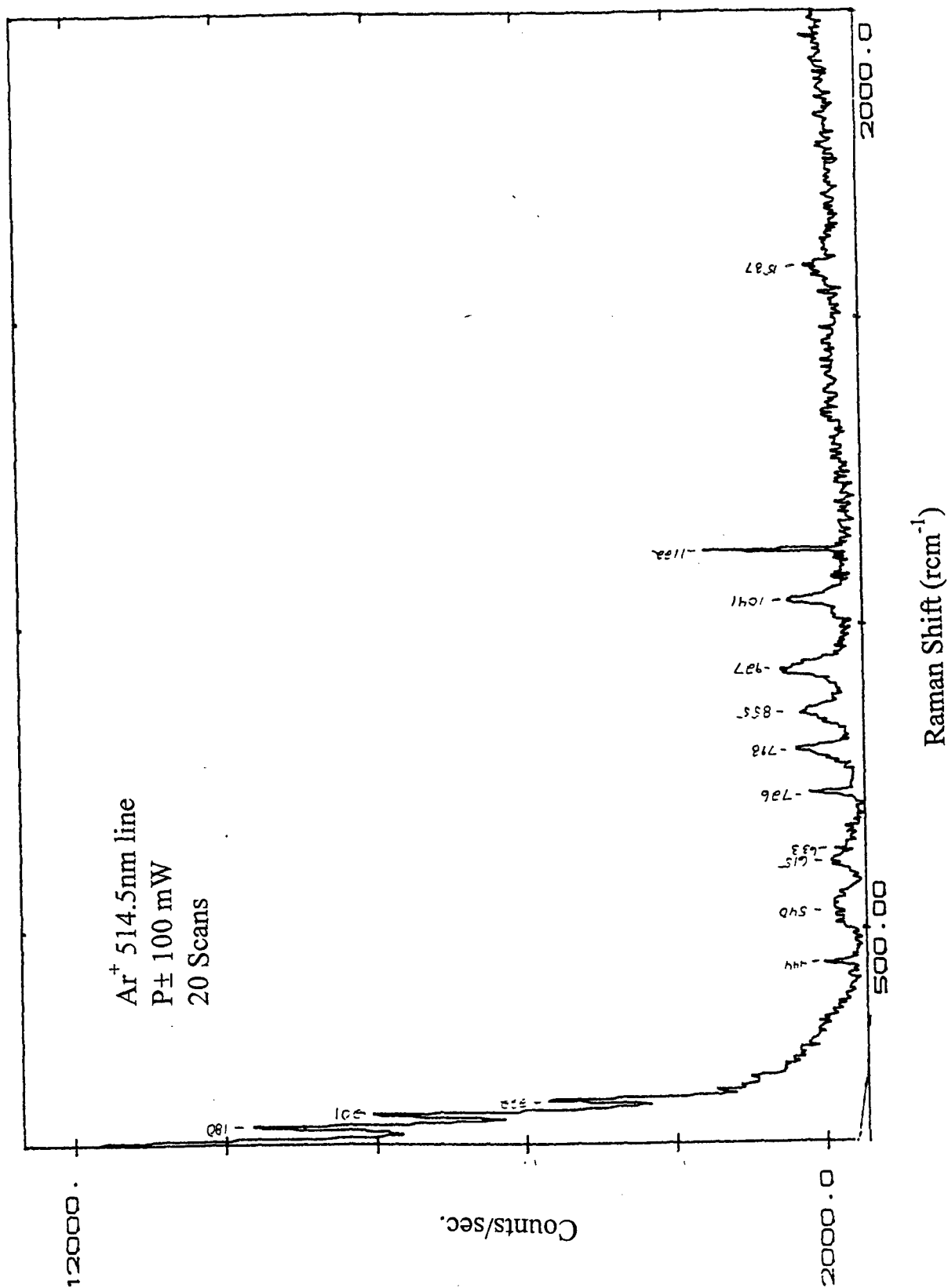


Figure 22: Raman Spectrum for run-in finished Si_3N_4 surface.

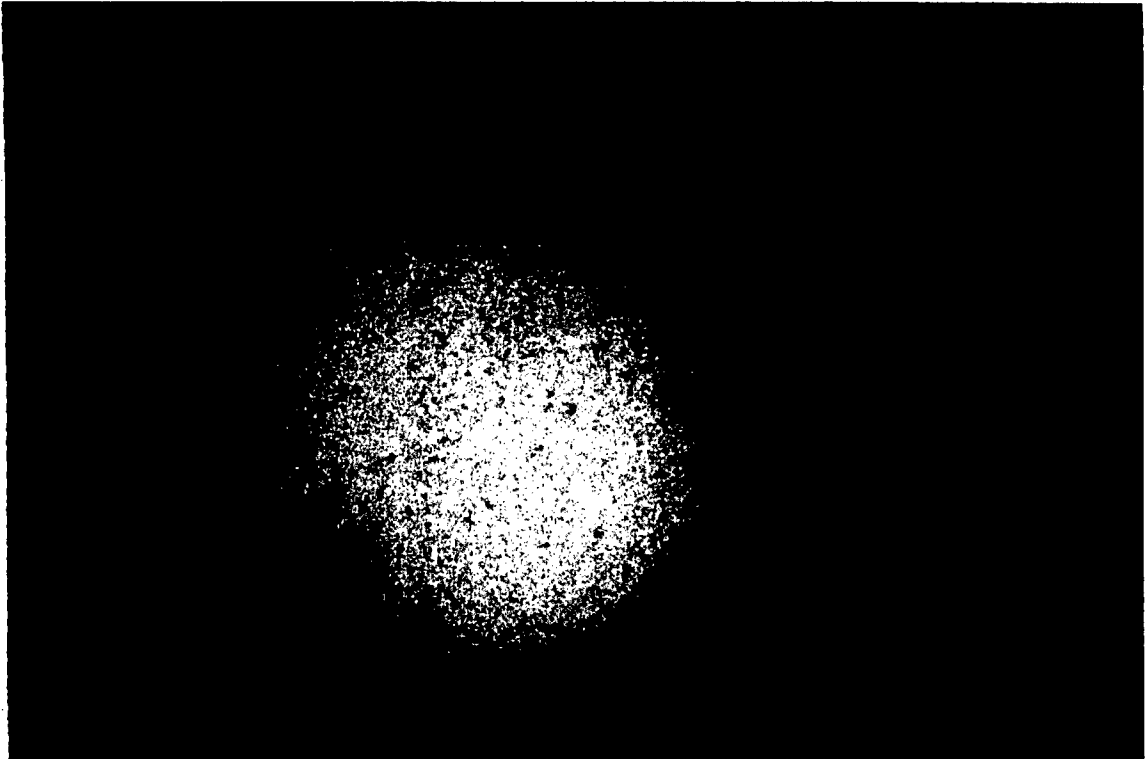


Figure 23: Surface of a commercially finished Si₃N₄ ball.

to form a much thinner EHD film. Furthermore, as the entraining velocity increases, contacts lubricated with water oil emulsion goes in to starvation. As result of this contact condition, wear is expected. Also, due to this severe tribological contact condition, the activation and rate of oxidation of the Si_3N_4 will be increased. It is the combination of these two processes occurring simultaneously that accounts for the run-in finish in Si_3N_4 material.

The observed effects of the various working fluid and ball blank materials on the run-in finishing process can be rationalize in terms of the above mechanisms. When a working fluid that contains no water is used, the run-in finishing occurs primarily by wear, without the benefit of chemical reaction effect. Furthermore, the EHD fluid film is thicker, which will reduce the wear rate. This is responsible for the relatively pure run-in finish of the Si_3N_4 ball blank in the synthetic ester basestock oil and mineral oil + 5% Lauric acid. In the presence of water in the working fluid the synergism of polishing wear and the surface reaction considerably accelerated the generation of smooth surface topography.

Besides the oxidation of Si_3N_4 to form Silica, other kind of chemical reaction did occur in the working fluid that contained NaOH. This reaction involves the weakening of the grain boundary phase in the near surface region. This result is the introduction of another material removal mechanism in the form of a large flake formation. In such fluids, three competitive mechanisms are simultaneously occurring on the surface during run-in finishing.

Between the two kinds of ball blanks tested, the major differences that will influence the run-in finishing processes are the surface condition and the grain boundary phase chemistry. Surface topography will influence run-in wear due to the degree of EHD lubrication. The use of water containing fluids will influence run-in wear by modifying grain boundary strength. Consequently, small differences are seen in the run-in finishing process in the oil and water mixture running fluid for the TSN-03H and NBD200 materials. The effect of the grain boundary phase is highlighted in results of the tests conducted in the fluid containing NaOH. In both material, the weakening of the grain boundaries occurred. It did, however, to a larger extent in the TSN-03H ball, resulting in more material removal by flaking compared to the NBD200 material ball.

The traction coefficient behavior during run-in finishing is a very good indicator of the progression of surface morphology evolution. In all the tests with working fluids where good run-in finishing occur, the traction coefficient usually shows an exponential decrease from the initial high value following the introduction of contact slip. This trend of traction behavior is attributed to a quick decrease in the surface roughness of both the ball and the disc. Such change in the surface topography will improve the EHD lubrication of the contact by increasing the h/o ratio. The improvement in fluid lubrication is manifested in the decrease of traction coefficient. Once the surface are worn smooth enough such that the h/o ratio is greater than 1 and the surfaces are completely separated, little change in the traction coefficient is expected. In the working fluids where relatively poor run-in finishing occurs, the traction coefficient shows only a gradual decrease from the initial high value upon the introduction of contact slip. This slow chain reflects the little change in the ball and disc surfaces during run-in finishing.

The findings reported are the run-in finishing of ball blank coils, which have a major impact on the commercial ball finishing operation. Many of the commercial ball finishers are using oil working fluids with abrasives that they normally use for steel balls for finishing Si_3N_4 ball as well. However, they observed that the use of diamond abrasives and much longer finishing time is required for Si_3N_4 compared to steel. From the results of this study, the used of a water containing working fluid could significantly improve the Si_3N_4 ball finishing rate. The synergism of the run-in finishing process and abrasive wear will account for this finishing rate acceleration. In fact, a commercial ball finisher willing to talk with us during this course of this work did notice a major improvement in the ball finishing rate by change the working fluid from oil to water based fluid. This field observation validates the idea combining run-in finishing process and abrasive wear as a means of improving Si_3N_4 ball finishing rate.

4.4 Disc (Raceway) Run-In Finishing

The concept of run-in finishing is more beneficial to the raceway finishing, especially in an all-ceramic bearing. The outer and inner ring manufacturing requires series of matching operations to attain the desired geometry. Once the geometry is satisfactory, the raceways are honed, and put through series of lapping operation in the final finishing step.

For hybrid bearings, the inner and outer rings are made of steel. Consequently, the manufacturing of steel races for hybrid bearing application should present no problem. Nonetheless, some cost saving could be achieved by omitting the last set of finishing steps during production and the raceways run-in finished instead. The run-in finishing can be implemented as the last stage/step of bearing production or as the first step of bearing operation. Due to the relatively high hardness of the Si_3N_4 balls compared to the steel races in hybrid bearing, polishing wear of the raceway could be accomplished in a reasonable time.

In the all ceramic bearing, the manufacturing of the inner and out rings is move difficult. Because Si_3N_4 cannot be easily machined into the ring geometry, a near-net shape fabrication technique is required. This is then followed also by series of surface finishing operations. Just as the Si_3N_4 balls are harder to finish using the methods for steel ball finishing, the Si_3N_4 compared to steel. Development and implementation of a run-in finishing procedure for the final finishing of the ceramic raceways could indeed be a big cost saver.

Run-in finishing of the disc surface in our single element, ball-on-disc contact configuration was undertaken. The hybrid combinations of steel ball on Si_3N_4 disc and Si_3N_4 ball on steel discs was investigated. The later configuration is the most common one in commercially available hybrid bearings. The Si_3N_4 ball on Si_3N_4 disc was also examined, using essentially the results from the run-in finishing of Si_3N_4 ball, paying particular attention to the Si_3N_4 disc surface.

4.4.1 Test Procedure

Tests were conducted using the WAM 1 machine. The primary objective of the tests was to create a smooth topography on the steel disc without any significant damage or wear on the finished ball, i.e., run-in finishing of the disc by the ball. Test conditions are as follows.

| | |
|------------------|-----------------------------|
| Rolling Velocity | 1.27-2.54 m/s (50-100 in/s) |
| Contact Load | 83-282 N (18.6-63.5 lbs.) |
| Contact Stress | 1.38-2.07 GPa (200-300 KSI) |
| Lubricant | ester basestock (HERCO-A) |
| % Slip | 3-15% |

In addition to the test parameters above, the lubricant (HERCO-A is basestock oil with no performance enhancing additives) supply was another variable. For the most part, tests were performed under starved lubrication; oil was, however, added whenever the traction coefficient was getting too high in order to prevent Hertzian cracking in the ball. Excess oil was also expelled whenever full EHD film was established, even without lubricant replenishment. This was done by spinning the specimens without contact at, or higher than, the test speed.

4.4.2 Run-In Finishing of M50 and 9310 Steel Discs

The traction behavior during the test with a run-in finished Si_3N_4 ball and a ground M50 steel disc ($R_a = 6 \mu\text{in}$) is shown in Figure 24a. Upon the introduction of contact slip, the traction coefficient increased to about 0.10. The traction remains nearly constant for the test duration, except for some minor fluctuations. At the conclusion of this test, very little change has occurred on the ball surface. A well-defined track with a different topographical layer and a relatively smooth topography is generated on the M50 disc during the test (Figure 25a). Thus, run-in finishing did occur on the M50 disc without any significant change in the Si_3N_4 ball.

Tests are also conducted with a commercially finished Si_3N_4 ball. The traction curve for this test is shown in Figure 24b. The traction coefficient increased to only 0.08 with the introduction of contact slip. The traction decreased very gradually starting from about 1000 seconds into the test. At the conclusion of the test, very little change occurred on the ball surface. A track almost identical to the one in Figure 25a, but a little smoother, was produced on the disc.

Tests were also performed using a finished Si_3N_4 ball to run-in finish a ground AISI 9310 steel disc ($R_a = 6 \mu\text{in}$). With the introduction of contact slip in this test, the traction coefficient increased to about 0.083, but decreased very gradually and steadily to a final value of 0.07 at the conclusion of the test. Visual and optical microscopic examination of both the ball and the disc showed no discernible wear track. The slight decrease in traction is probably due to frictional heating of the contact interface resulting in the lowering of oil viscosity. This suggests the test was operating under full EHD film, even though the specimens were wet only at the beginning of the test with no additional supply of oil during the test.

In order to create a more marginal lubrication condition, both the wetted disc and ball were rotated unloaded for about 2 minutes prior to testing. This was done to expel excess oil from the surface and leave only a thin layer of oil on the surface. During this test, the traction coefficient was constant at about 0.075 upon the introduction of the contact slip. At the conclusion of the test, there is no wear on the ball. The original grinding marks are still pronounced within the disc wear track, three high grinding ridges have been polished smooth (Figure 25b). Conceivably, if

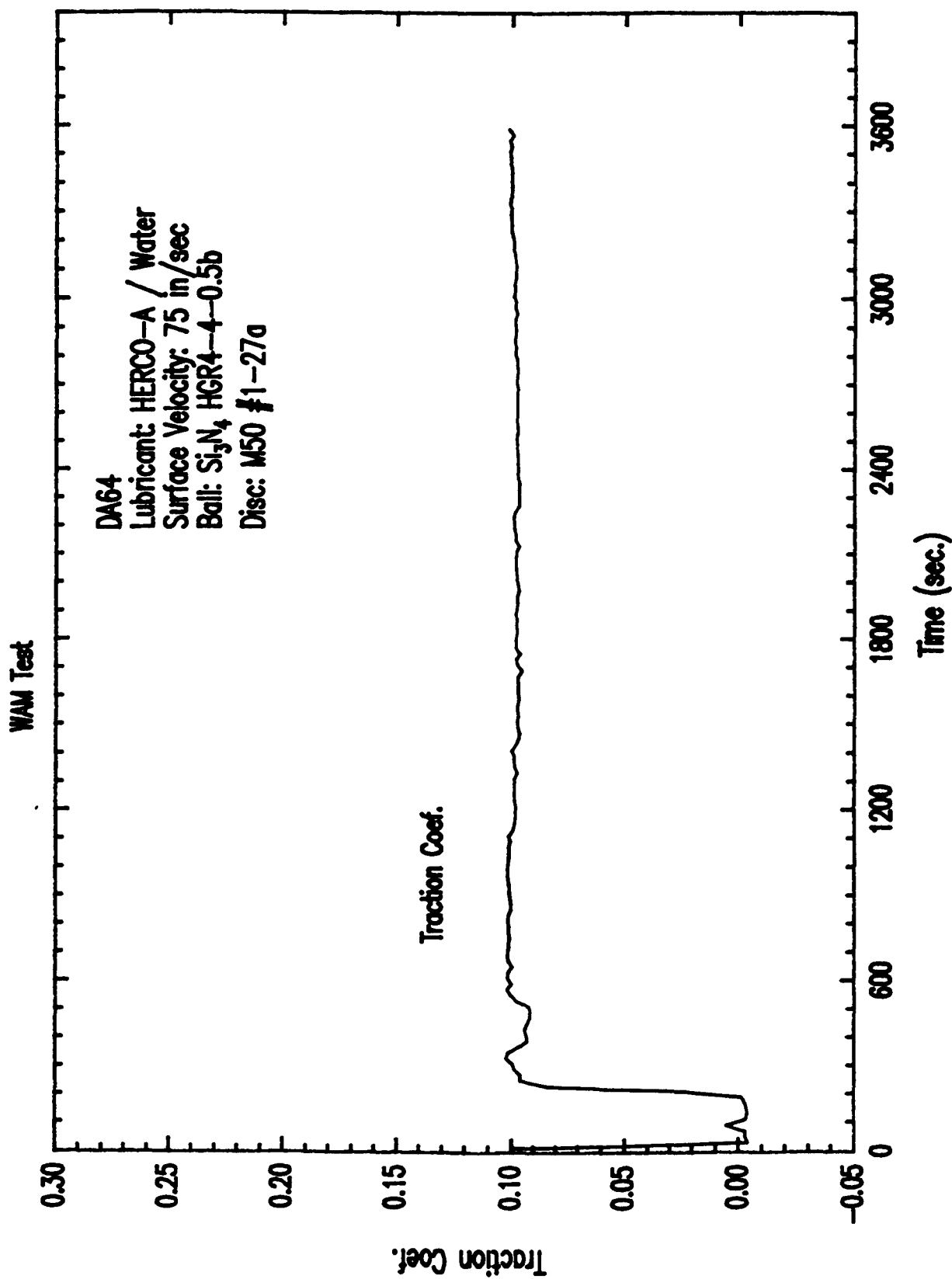


Figure 24a Traction behavior during M50 steel disc run-in finishing with a run-in finished

<DA64.SPW>

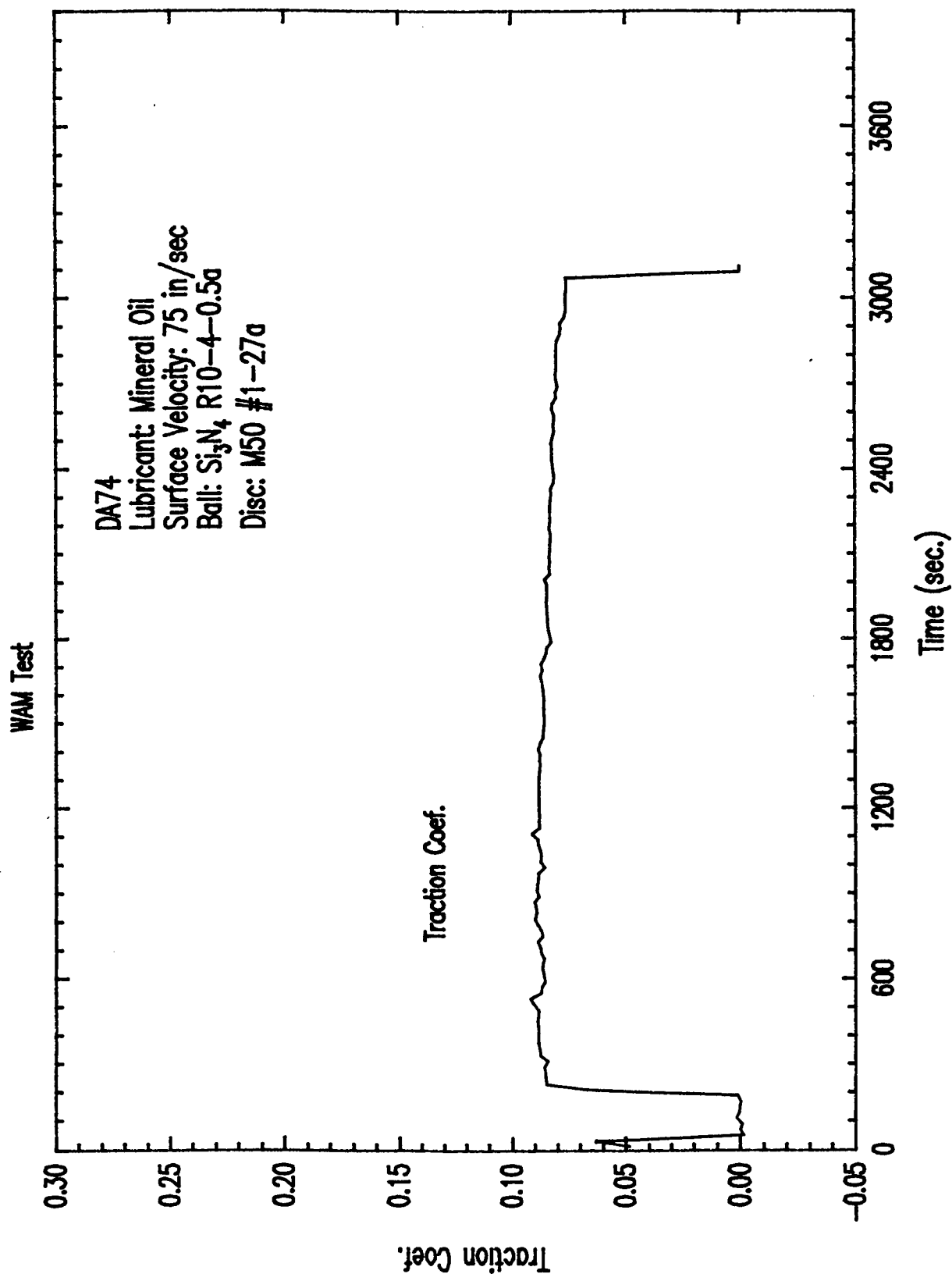


Figure 24b Traction behavior during M50 steel disc run-in finishing with a commercially finished ball

<DA74.SPW>

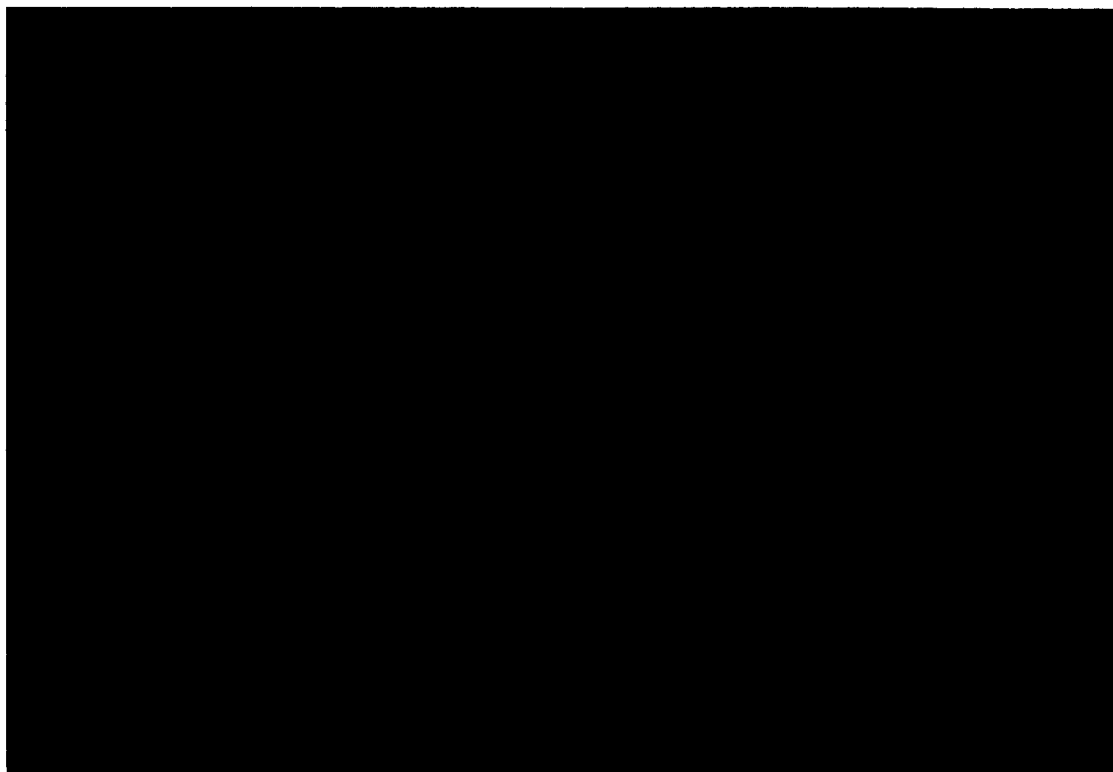
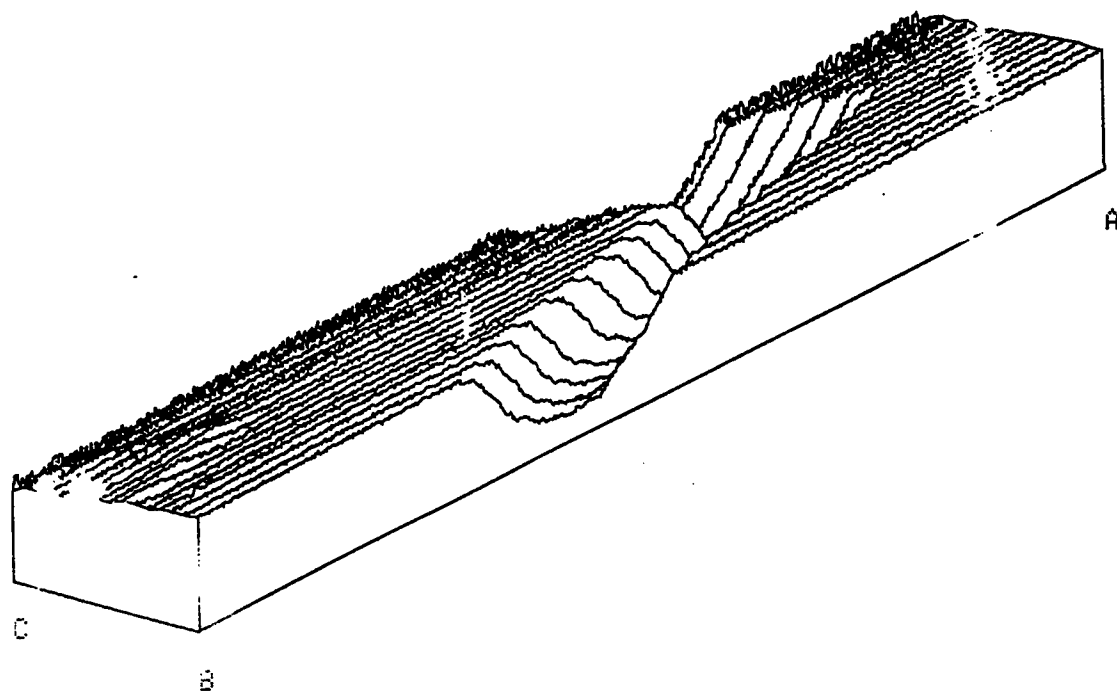


Figure 25 (a): M50 steel disc run-in finished with Si_3N_4 ball.

Id: runin finis

1-27 disc



Normal View
Number of Runs : 16

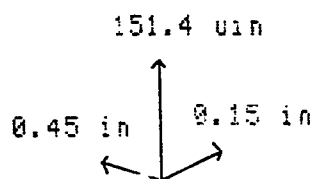


Figure 25b

testing is continued, a continuously smooth track will eventually be generated. Two of the ridges have a blue-brown coloration to them, which may be due to oxide formation or surface films from metal/oil interaction.

4.5 Effect of Metallic Coatings on Steel Disc Run-In finishing

4.5.1 Silver Coatings

Soft metallic coatings, including silver (Ag) are commonly used as solid lubricants. In one of our previous studies, we observed that Ag coatings on a steel disc enhanced the generation of a very smooth wear track after the coatings was worn through, compared to uncoated disc. In this study, steel balls were used. One might expect similar topographical changes on the steel disc surface when Si_3N_4 balls are used. The use of Ag coatings as a means of accelerating the topographical run-in of the steel disc surface in a hybrid contact with Si_3N_4 ball was investigated.

The initial test with an Ag-coated disc was conducted using the above procedure. During the test, with the introduction of contact slip, the traction coefficient increased to about 0.048 but showed a slight decrease throughout the duration of the test, ending with a final value of 0.042. The traction value throughout the test was less than that of tests involving uncoated discs.

In order to increase the severity of contact, the surface velocity was decreased to 1.27 m/s (50 in/s) during the next test. This reduced the lubricating fluid film thickness. The same ball, disc and tracks were used. Upon introduction of contact slip, the traction coefficient increased to about 0.045 and remained nearly constant for the duration of the test. No visible wear or damage was observed on the ball, but a relatively smooth track was observed on the AG coatings. The coating was still intact in terms of adhesion to the steel surface at the end of this test.

More tests were run with the degree of contact severity progressively increased, through an increase in the amount of contact slip, and more lubricant starvation by the rotation of ball and disc specimens prior to testing to expel excess oil. As the contact severity was progressively increased in subsequent tests, the average traction coefficient increased and more wear occurred on the Ag coating of the disc.

In the final test, the traction coefficient increased to about 0.085 upon the introduction of contact slip and remained nearly constant for about 800 seconds. It increased gradually to about 0.12 at the end of the test. At the end of this test, the Ag coatings have been removed from nearly half of the wear track (Figure 26).

Results of the test series with Ag-coatings showed that coated steel races in hybrid bearings with Si_3N_4 balls can be run-in finished. Although the run-in finishing occurs on the Ag coating layer on the steel disc, the smoothness transferred to the steel disc surface at the conclusion of the present test series. However, significant improvement in the tribological performance in the hybrid contact was observed. The damage on the Ag-coated disc after a cumulative test time of 5 hours is less than the damage after 2 hours for an uncoated disc. In both coated and uncoated disc cases there was little or no wear on the Si_3N_4 balls. This improvement of tribological

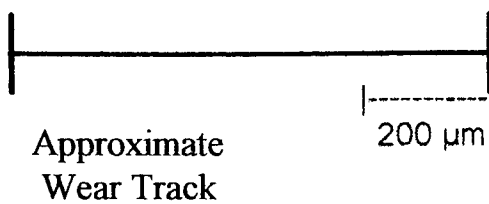
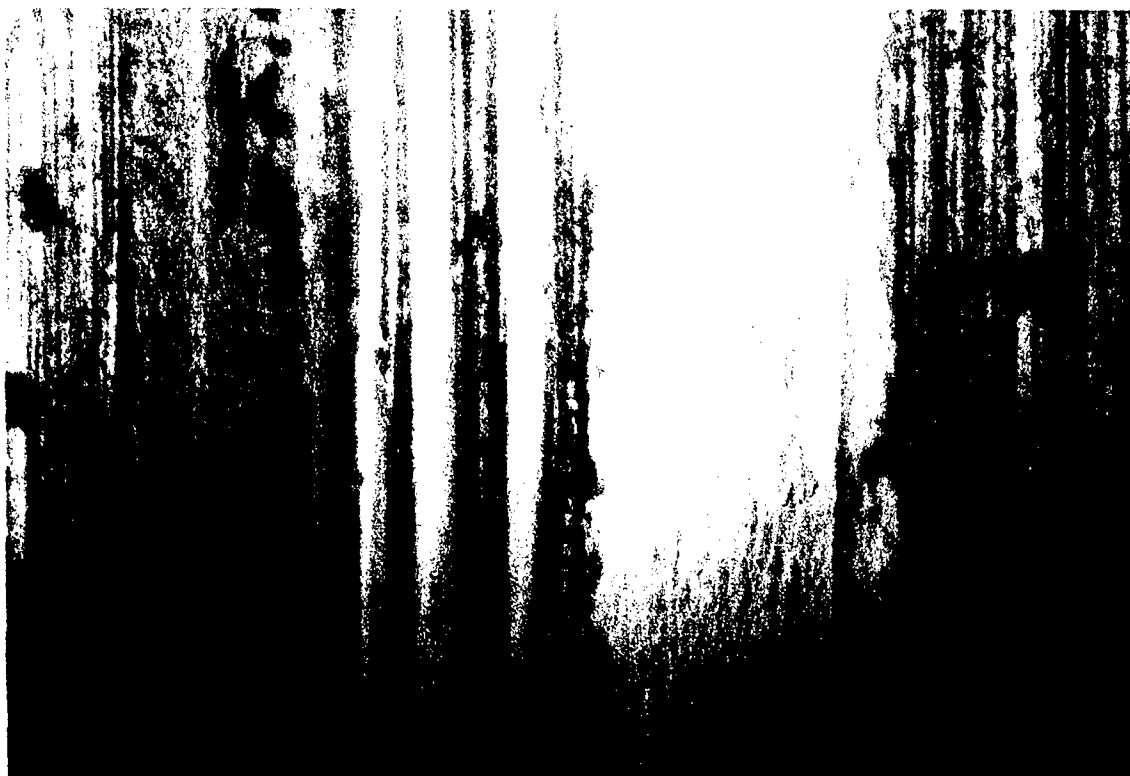


Figure 26: Photomicrograph of the wear track on silver (Ag) coated steel disc surface that has been tested against finished Si_3N_4 ball.

behavior of Ag-coated disc fits well into the main objective of Task II of this project and hence, will be examined in more detail under the Task II section.

In addition to silver coatings, other metallic coatings were evaluated as a means of accelerating the finishing process. Some of the properties of metallic coating materials evaluated are shown in Table 3. Also included in the table are the properties of AISI 9310 steel.

Table 3: Some properties of coating materials and 9310 steel.

| Material | Young's modules E (GPa) | Hardness H (GPa) | Yield Strength YS (MPa) | Thermal conductivity (WM-1K-1) |
|---------------|----------------------------|---------------------|----------------------------|-----------------------------------|
| Silver (Ag) | 82.7 | 0.25 | --- | 425 |
| Copper (Cu) | 129 | 0.50 | 48 | 397 |
| Nickel (Ni) | 199.5 | 1.03 | 150 | 88.5 |
| Chromium (Cr) | 279 | 2.21 | 362 | 91.3 |
| 9310 Steel | 201 | 2.80 | 571 | 33.6 |

The tests with the coatings were performed on WAM1 machine using the same procedure as described above, but at a lower entraining (rolling) velocity of 1.28 m/s (50 in/sec). The contact severity was also progressively increased through lubricant starvation.

4.5.2 Copper Coatings

The CU coatings used in this study had a thin Ni interlayer to enhance adhesion to the steel substrate. Figure 27 shows the traction curve of the first test with CU-coated steel disc and finished Si_3N_4 ball. With the introduction of 15% slip, the traction coefficient increased to about 0.06 and remained constant for the duration of test. Although there was no wear or damage on the ball, the track on the disc coatings was easily visible. Like the AG coating, the CU coating smeared, producing a relatively smooth contact area. The coating was intact at the conclusion of the first test. The traction behavior in subsequent tests with higher contact severity was essentially the same as in the first test. The traction coefficient increased to about 0.06 upon the introduction of contact slip and remained constant for the test duration.

At the end of the test series, the Cu coating was worn through in most of the wear track. In addition, a relatively smooth region was generated in the middle of the track, shown in Figure 28.

4.5.3 Nickel Coatings

The traction behavior during the first test with the Ni-coated steel disc was similar to that of the Ag-coated and Cu-coated discs. The traction coefficient increased to about 0.065 with the introduction of contact slip, and remained constant. The wear track on the disc can be easily seen at the end of this test. The Ni coating was still intact and there was no damage or wear on the ball.

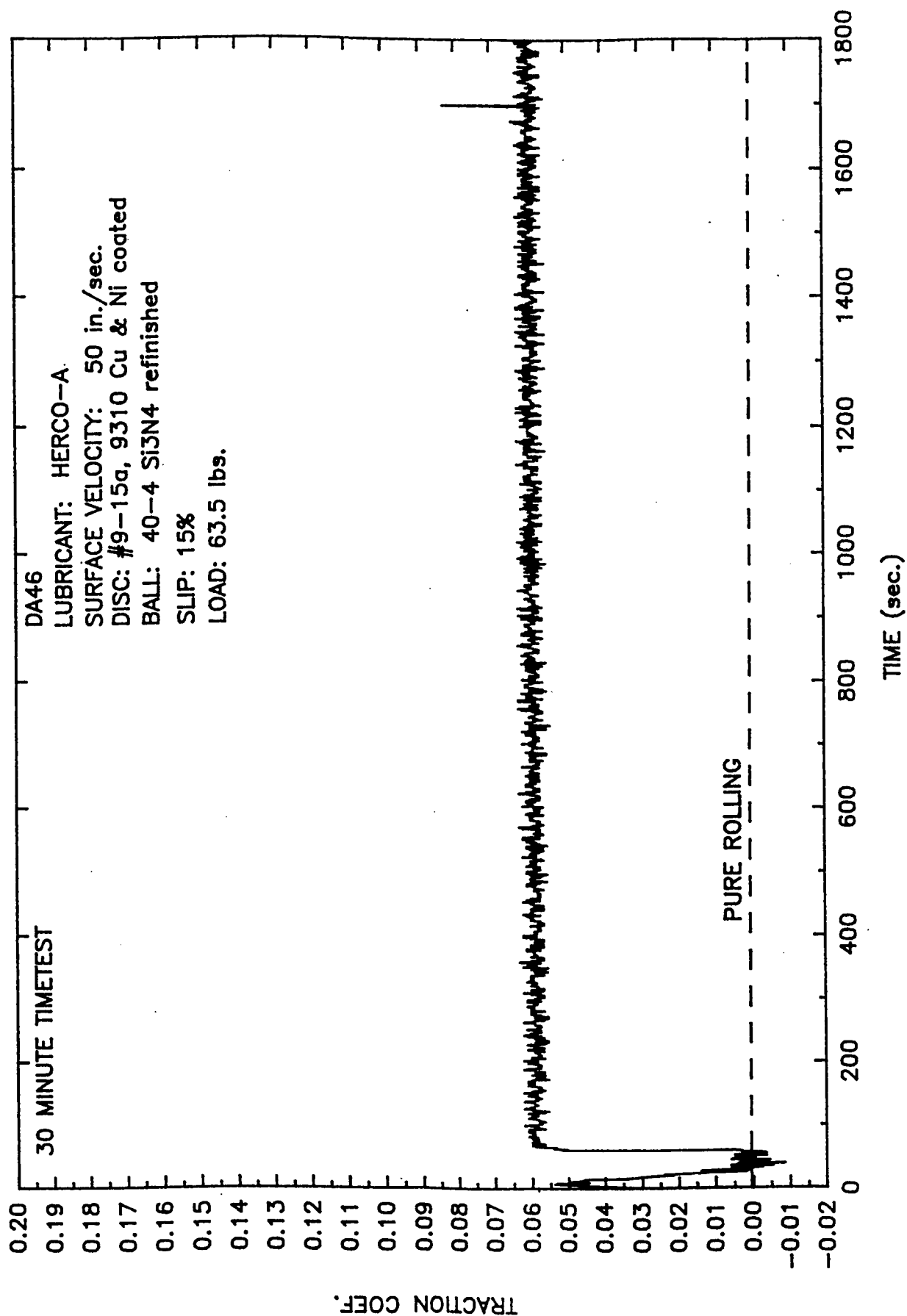


Figure 27: Traction curve for test 1 with Si_3N_4 ball and Cu-coated 9310 steel disc.



Figure 28: Wear track on the Cu coating on 9310 steel after 30 min. test time.

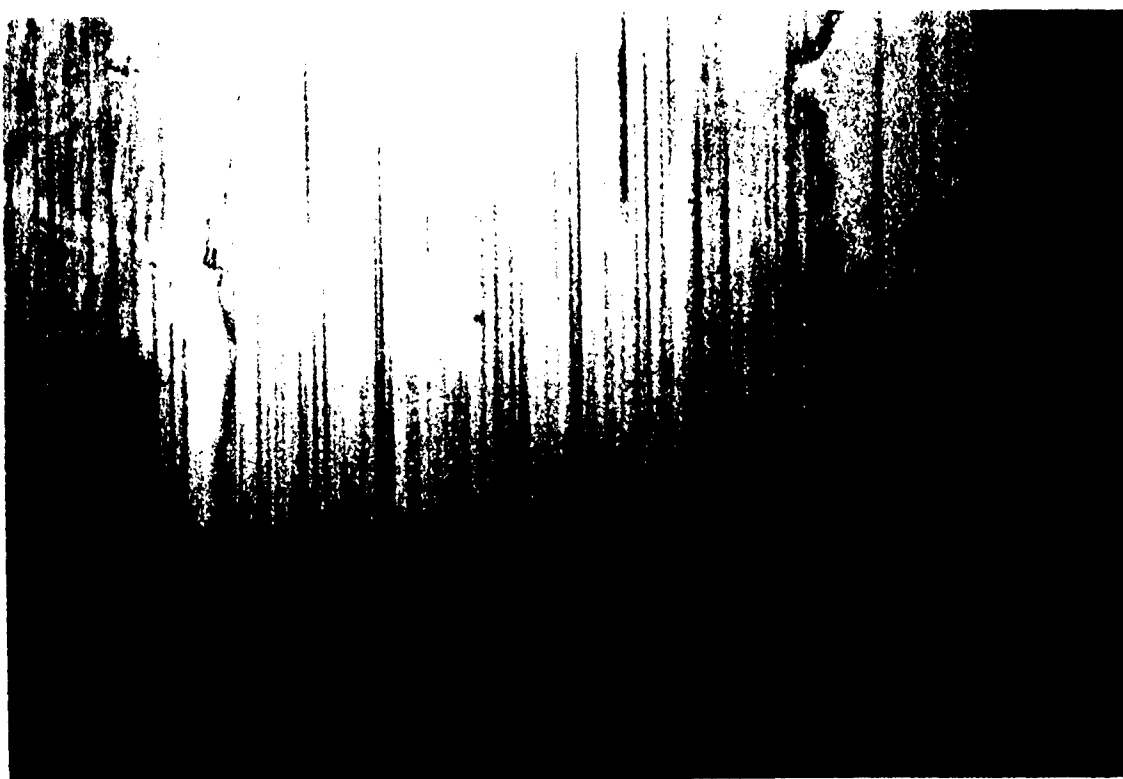


Figure 29: Wear track on the Ni-coated 9310 steel disc after a total time of 90 min. showing the coating worn through

Subsequent tests were run with a higher degree of contact severity, resulting in slightly higher traction and wear on the coated disc. At the conclusion of this test series, the Ni coating was worn through, but there was little (if any) change in the roughness of the steel substrate in the wear track (Figure 29). The original grinding mark prior to coating appears unchanged. It thus appears that Ni coating neither accelerates the run-in finishing process nor significantly improves the tribological performance of the hybrid contact.

4.5.4 Chromium Coatings

A test series was conducted with a thin dense chrome (TDC) coating on the steel disc and Si_3N_4 balls. In the first series of the tests, both ball and disc were wetted with oil prior to testing. Upon the introduction of contact slip, the traction coefficient increased to about 0.075 but decreased gradually over the next 300 seconds of test to a steady value of about 0.065 for the duration of the test. Visual examination showed there was a wear track on the disc and some Cr transfer to the ball.

For the next test with Cr coating, pretest rotation of the disc and ball was done. However with introduction of slip, the traction increased rapidly and oil had to be added to forestall the Hertzian cracking of the Si_3N_4 ball. The traction decreased, sharply to about 0.06 with the addition of oil and remained steady until the end of the test. At the end of this second test with Cr coating, there was a visible track on the ball consisting of some wear and a lot of Cr transfer as shown in Figure 30a. The coating surface on the disc showed a non-uniform wear. While the coating was worn through at some spots in the middle of the track, it was barely worn around the edges of contact (Figure 30b).

4.5.5 Summary of Coating Effects

Results presented show the presence of a coating has a significant effect on the run-in finishing process. The effect of each coatings is dependent on its properties, as one might expect.

Although it took a long time to wear through the AG coating during the run-in finishing test, the presence of the coating significantly improved the tribological performance of the hybrid contact interface. Lower traction and wear were observed with AG coating. In fact, the AG coating essentially fulfilled the role of a boundary film proposed in Task II. A more detailed discussion of the subject matter will be given under the Task II section of this report.

Copper (Cu) coatings also improved the tribological performance of the system, but not to the same extent as Ag coatings. The traction and the wear were a little higher with Cu coatings when compared with Ag coatings. The reasons for the improvement are essentially the same as for Ag. However, Cu coatings accelerated the run-in finishing process upon wearing through, in addition to performance enhancement. After having been worn through, the exposed steel surface is topographically smoother than the initial surface finish.

Nickel (Ni) coating appeared not to have much effect on either tribological performance or run-in finishing. The traction coefficient was about the same in tests involving Ni coated and uncoated



Figure 30 (A): Wear track on Si_3N_4 after a test time of 60 min. showing Cr transfer from disc.



Figure 30 (B): Wear track on Cr coated disc after a test time of 60 min. showing coating wearing through in the middle.

steel discs. A smooth track was generated on the Ni coating surface at the early stage of testing. Once the coating was worn through however, the roughness is about the same as original surface finish.

Chromium (Cr) coatings were the only ones that produced any damage or wear on the Si₃N₄ ball. This is probably due to the higher hardness of this coating than that of the others. It was also the only coating that transferred into the Si₃N₄ ball. This might be connected to chemical affinity of Cr for Si or N. While the details of the mechanisms of the process observed are uncertain, Cr coatings would not be a good candidate for run-in finishing acceleration of the steel disc.

4.5.6 Si₃N₄ Ball on Si₃N₄ Disc Combination

The run-in finishing of the Si₃N₄ disc in this combination was done concurrently with the Si₃N₄ ball blanks. Details of the test procedures have already been described during the discussion of the ball blank run-in finishing. Toshiba's TSN-03H Si₃N₄ disc with a ground surface finish is used for this study.

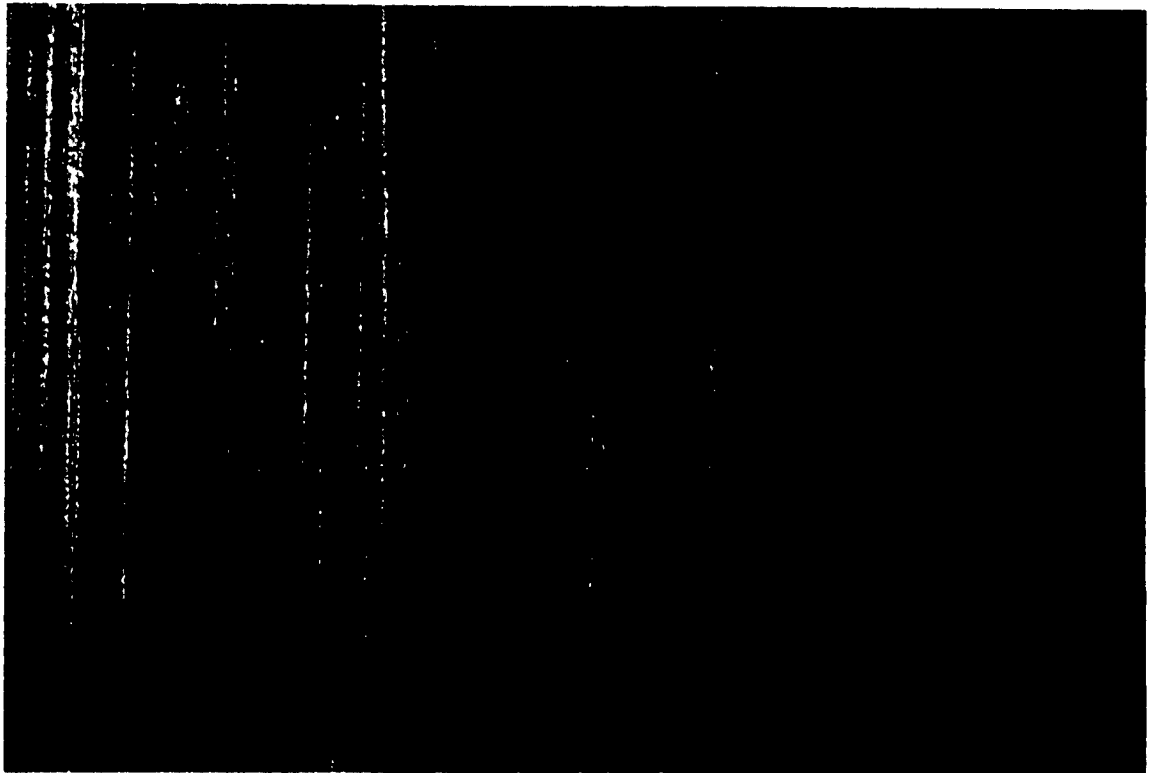
The original surface characteristic of the Si₃N₄ disc is shown in Figure 31. The surface had a roughness of Ra of 25 µin, and the grinding lay was concentric on the disc. After the 1 hour run-in finishing procedure, the relative degree of finishing in the various working fluids was very similar to ones in the balls. The best finishing on the disc was achieved with water containing fluids.

Figure 32a shows the track on the disc run-in finished with the oil and water mixture fluid. Smooth topography was generated in the contact area with some residual grinding marks still visible. In the oil + water + hydrogen peroxide working fluid, smooth topography was generated also, but not to the same extent as in oil and water mixture. The wear track appeared narrower. It can thus be deduced from these observations that the presence of hydrogen peroxide reduces the rate of polishing wear in Si₃N₄ disc. The Si₃N₄ disc, run-in finished with the oil + water + sodium hydroxide mixture is shown in Figure 32b. The extent of disc finishing in this fluid was about the same as the oil and water mixture fluid. Smooth topography and some residual grind marks/grooves were the main features of the track.

Although no separate analysis was done for the Si₃N₄ disc run-in finished in various fluids, the mechanism and processes responsible for the generation of smooth surface topography are the same as for the Si₃N₄ balls. Without repeating the details, the wear process involved the simultaneous occurrence of tribochemical reaction and polishing wear.

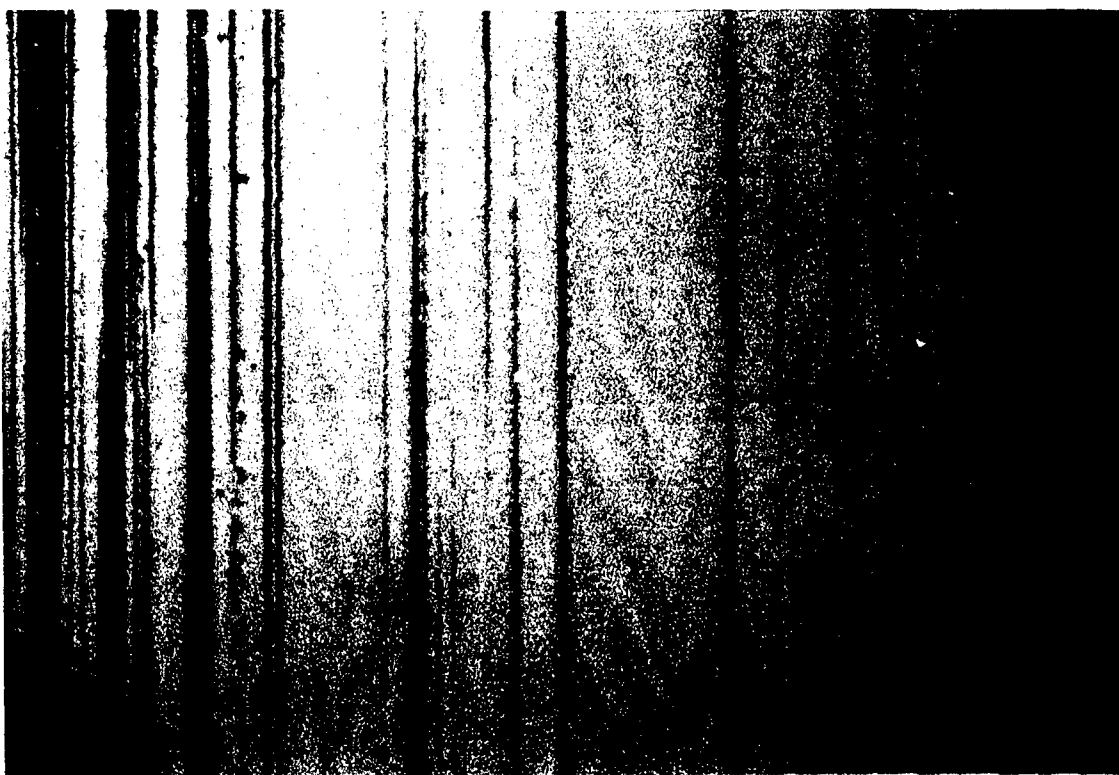
4.6 Summary of Disc (Raceway) Run-In Finishing

Run-in finishing of disc surfaces was accomplished in both the hybrid and all-ceramic materials combination. In the hybrid combination, good run-in finishing of the steel disc surface was accomplished with both commercially finished and run-in finished Si₃N₄ balls. Due to more wear occurring on the steel disc in the hybrid contact during run-in finishing tests, a well-defined



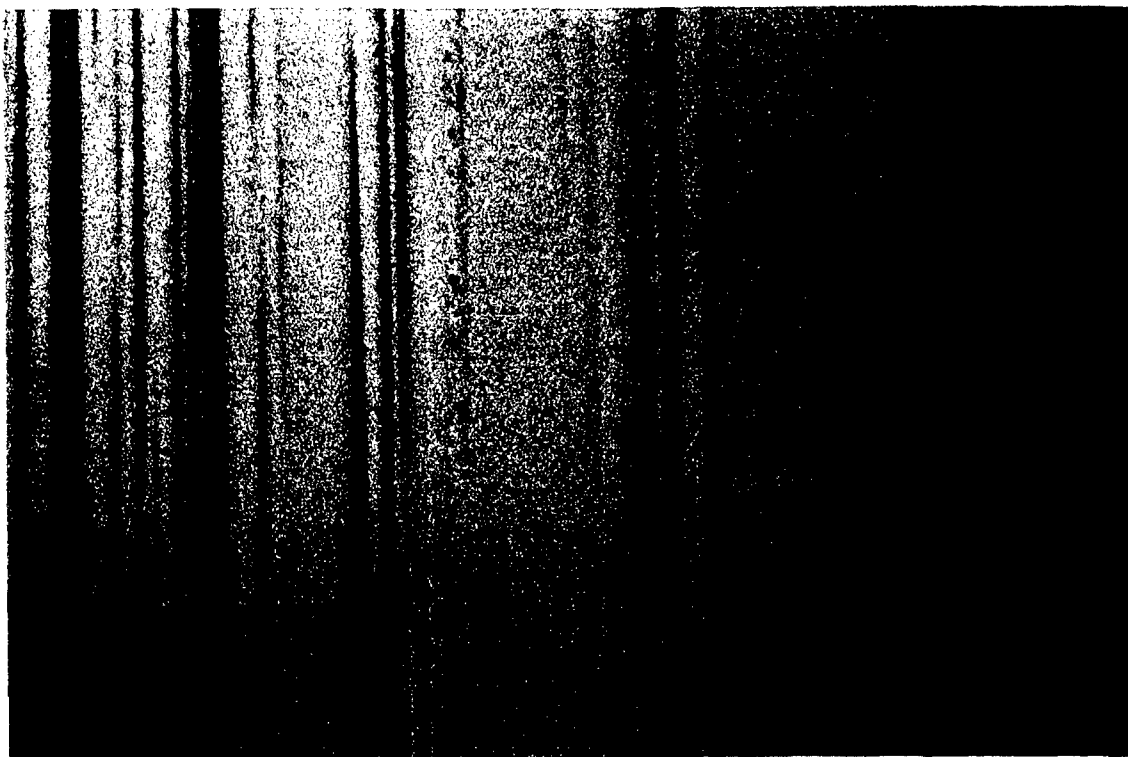
100x

Figure 31: Original surface of ground Si₃N₄ disc



100x

Figure 32 (A): Si₃N₄ disc run-in finished in oil and water mixture fluid.



100x

Figure 32 (B): Si₃N₄ disc run-in finished in oil + water + NaOH mixture.

ball path groove was generated on the disc surface. The presence of a relatively soft metallic layer on the disc surface significantly influenced the disc run-in process. A smooth topography was quickly generated on the soft layer coating. This smooth topography was maintained and transferred into the underlying steel surface when the coating wore through. Consequently, the quality of the run-in disc surface in terms of smooth topography was improved by the presence of a soft metallic film. On the other hand, because the soft film through quick topographical run-in, significantly improves the EHD lubrication, it takes a longer time to achieve the run-in finishing of the underlying steel disc surface.

Run-in finishing of a Si_3N_4 disc was also accomplished during the Si_3N_4 ball blanks run-in finishing tests. The results on the disc surface were nearly identical to those in the ball blanks, as would be expected. All water containing fluids produced good finishing on the disc. The smooth topography is accomplished through the simultaneous occurrence of tribochemical reactions and polishing wear.

5. Task II: TRIBOLOGICAL SURFACE CONDITIONING

5.1 Introduction

In contacts involving Si_3N_4 material, the formation of Hertzian stress cracks occurs at traction coefficients 0.4. Such crack formation occurs in hybrid and all-ceramic contacts. This is due primarily to the inability of the Si_3N_4 material to accommodate the shear strain and the ensuing tensile stress on the surface as a result of the high traction coefficient. The presence of cracks in structural components made from Ceramic materials is undesirable, because these cracks will substantially lower the fracture strength of the component and increase the probability of catastrophic failure.

In metallic materials, the high shear strain in high traction contacts is accommodated by plastic flow. In the extreme case, scuffing or seizure could occur. Although scuffing is a well-known tribological phenomenon, there is no consensus as to its mechanisms. It has been attributed to the collapse of EHD fluid film [7,8], contact interface thermal instability [9,10], and failure of the surface chemical films [11,12]. In spite of the ambiguous nature of scuffing, lubricant oils are formulated with additive packages to protect metallic materials (especially ferrous materials) surfaces against failure under tribologically severe contact conditions of high traction.

The additives act by forming a surface film or the so called boundary film/layer at the contact interface. This layer often possesses low shear strength. Consequently, the layer/film in addition to preventing metal-to-metal contact and as such wear lowers the friction at the contact interface. The reduced friction also translates to a reduced amount of frictional heating.

In general, several studies have shown that boundary films do not readily form on Si_3N_4 materials and ceramic materials. This is expected since ceramic materials are relatively chemically inert. In lubricated hybrid contacts of ceramics and steel, all the additive reaction and film formation occur on the metallic component [13].

The primary goal of Task II of the present effort is the conditioning of the ceramics on ceramics and hybrid contacts for the main purpose of lowering the friction, wear and scuffing under severe tribological contact conditions. The idea is to generate a surface layer/film that will perform the functions of a boundary film. The approach in the original proposal was that of chemical conditioning following, or in conjunction with the run-in finishing process.

Preliminary tests were conducted with two different oils to assess the chemical condition of the Si_3N_4 material surface. Tests were run under boundary conditions of low h/σ ratio with an all-ceramic and a hybrid contact pair. A fully formulated aviation oil (ETO-25) and mineral oil with about 5% TCP were used. In these tests, no visible surface films were observed on the Si_3N_4 surface, either in the all-ceramics or the hybrid contact pairs.

In view of the poor chemical reactivity of Si_3N_4 with many, if not all, of the existing oil additives, attention for this task was focused on a physical approach rather than a chemical approach to the interface conditioning. Results and a discussion are presented on the effect of a thin

metallic coating and a polymeric coating on the tribological characteristics of a hybrid contact interface.

5.2 Metallic Coatings

In the Task I section of this report, results are present of test conducted with the Si_3N_4 ball running against the steel disc with various metallic material thin coatings. The coating materials include Ag, Cu, Ni and Cr. Some of these coatings, especially Ag and Cu were observed to significantly improve the hybrid contact tribological performance, in addition to improving the quality of the run-in finished disc surface. Ni coating only produced a marginal improvement in the tribological performance, but good run-in finishing of the disc is aided by the coating. Extensive transfer of the Cr. coating, material onto the Si_3N_4 ball occurred under the marginal lubrication condition for run-in finishing.

From these results, already given in details under Task I, it can be concluded that the relatively soft metallic coatings, notably Ag and Cu adds boundary films under marginal lubrication conditions. Conceivably, deposition of soft metallic coating layer on the hybrid contact pair surfaces is means of physical surface conditioning, which will perform a function similar to the originally proposed chemical conditioning. We shall now examine how the soft metallic layer functions to improve tribological performance under severe contact condition. The following are some of the effects of soft metallic coatings.

5.2.1 Reduction of Traction (Friction)

When two surfaces in contact are in relative motion, the resistance to the motion usually quantifies as the friction or traction coefficient is given as the ration of the shear strength of the contact interface to the normal force. Lubrication is a means of reducing the interface shear strength and hence the traction coefficient. The presence of any layer, be it solid, liquid or gas at the contact interface that has a lower shear strength will reduce the friction/traction coefficient.

As noted in Table 3, all the coating materials have a lower hardness than the 9310 steel substrate. The shear strength under compression (S) is about 1/3 of the hardness (Hv). Ideally, the presence of any of coating is expected to result in the reduction of traction. The extent of reduction is proportion to difference between the harnesses of the coating and the steel. Soft metals such as lead, silver and indium are known to be good solid lubricants because of the low hardness and hence shear strength.

In the tests we conducted with coated discs, oil was used as a lubricant. Thus, both solid and liquid lubricants were acting simultaneously, which is responsible for the lower traction coefficients in tests run with Ag and Cu coated discs. Since friction reduction is one of the main functions of chemical boundary films, it is clear that a soft metallic coating adequately fulfill this role.

5.2.2 Enhancement of EHD Lubrication

Occurrence of plastic flow in the soft metallic coating layer usually result in the generation of smoother topography at the contact interface. In uncoated steel disc, smooth surfaces can eventually be generated through wear, but over a much longer time frame. This plasticity-accelerated topographical run-in will have a major impact on the operating fluid lubrication regime. As the composite surface roughness is reduced through the smoothening of the coating surface the $h/$ or the so called λ ratio will increase. This will enhance the formation and the maintenance of an EHD fluid film.

Thus, a contact starting out under a severe contact condition of boundary or mixed-film lubrication regime with a low h/σ can quickly be transformed into a soft metallic layer on one of the surfaces. This is a function that a chemical boundary film cannot perform since the original topography is usually preserved during the formation of boundary films.

5.2.3 Modification of Contact Stresses

The presence of rigid layer/films on surfaces in contact will significantly influence the contact stresses. If the coating or film thickness is very large relative to the Hertzian contact size, the contact stresses are nearly Hertzian between the coating material and the uncoated component. If the coating thickness is comparable to or less than the contact size, stresses are imposed on both the coating and the substrate. The coating has the effect of spreading the contact load over a large contact area and thereby reducing the magnitude of the contact pressure. If the coating is a relatively soft material, such as Ag and Cu in the present study, the plastic flow occurring in the coating during contact will increase the contact area move, resulting in further lowering of the contact pressure.

This stress modification by the presence of a soft metallic coatings could have a significant impact on the tribological performance of the Si_3N_4 steel hybrid contacts. Reduced stresses under boundary condition would translate to less wear, especially in the steel component. Also the probability of Hertzian crack in the Si_3N_4 component is reduce through the lowering of contact stress. From a practical stand point a hybrid bearing with soft metallic coating on the raceways can operate at a higher load and still have the rolling elements and the races as the bearing without the coating.

5.2.4 Frictional Heat Management

Frictional force from a loaded contact in relative motion is normally converted into heat. This heat is generated at the contact interface and leads to temperature rise in the contacting components. Under boundary lubrication or severe contact conditions, the temperature rise is substantial. There are scuffing theories based on thermal instability of contacts at some critical temperatures resulting from frictional heating.

The rate of frictional heat generation per unit contact area (q) is given as:

$$q = \mu P_{av} V$$

where μ is the friction coefficient, P_{av} is the average nominal contact pressure, and V is the relative sliding velocity of the surfaces in contact. The heat is partitioned between the two bodies depending on their thermal properties. The temperature increase is manifested at the bulk, surface, and asperity levels. Frictional heating plays a significant role in the tribological behavior of contact interface. Any process that influences the frictional heat characteristics also will strongly influence the tribological behavior.

The incorporation of soft metal coating or film into a hybrid contact interface will influence the frictional heat characteristics in two major ways.

- (1) Reduction of frictional heat generated. As previous discussed, the presence of soft metallic coating reduces the traction (friction) coefficient due to its low shear strength. Also, soft coating reduces the average nominal contact pressure. According to the equation for friction heat generation above, these two effects will result in lower rate of heat generation.
- (2) Dissipation of frictional heat. If the metallic coating has a high thermal conductivity, like Ag and Cu the frictional heat will be more effectively dissipated laterally. This will prevent the occurrence of very high temperatures usually encountered in the real areas of contact. Prevention of localized high temperatures is particularly important for ceramic materials, which are often susceptible to thermal shock cracking and fatigue.

Frictional heat management attributes of Ag and Cu coatings could be very article for hybrid and all-ceramic bearings. Reduction of the probability of thermal instability or undesirable thermally activated process, such as thermal shock will translate to longer life and better tribological performance of hybrid and all-ceramic bearings.

5.3 Polymeric Materials Coating

Polymeric coatings that have low shear strength and can bond adequately well to a contacting surface may also be able to perform the function of a boundary film. The two main functions are the lowering of friction and reduction of wear. A good polymeric candidate for this purpose is the polytetrafluoroethylene (PTFE) common referred to as Teflon. PTFE is a widely used solid lubricant, just like the soft metallic material Ag.

Some tests were conducted to evaluate the lubricating capabilities of PTFE surface film for Si₃N₄-on-steel hybrid contact. The tests were run with Si₃N₄ balls and 440C discs with a polymeric material Polytetrafluoroethylene (PTFE) or Teflon as a solid lubricant. Two forms of PTFE were used, both individually and simultaneously as lubricants. One form consisted of a bronze + PTFE "alloy" (Salox), and the other form consisted of PTFE particles suspended in a volatile carrier fluid (Vydax). The PTFE + bronze was applied as a 'transfer' layer on the disc, while the PTFE suspension was brushed onto the disc or ball surface and allowed to dry. The volatile carrier fluid evaporated, leaving behind a layer of PTFE particles. Tests were performed at normal contact pressures of 300 ksi (load of 63 lbs. for Si₃N₄ on 440C contact) and a constant rolling velocity of 100 in/sec. Upon loading, the tests were operated under pure rolling for 100

seconds after which 1% contact slip was introduced. This condition was maintained until failure, characterized by a transition in the traction coefficient (increase) and wear.

A summary of test results is shown in Table 4 below.

| <i>Lubricant</i> | <i>Time to failure (sec)</i> |
|---------------------------------|------------------------------|
| None | 120 |
| PTFE+bronze | 300 |
| (PTFE+bronze) + PTFE dispersion | 66,600 |

Without any lubricant film on the surface, failure occurred shortly after the introduction of contact slip. The failure was due primarily to the formation of an oxide layer on the disc. With the PTFE + bronze lubricant alone, the test ran for awhile with low traction and no wear, until the lubricant film was removed and failure occurred; again involving oxide build-up on the disc. Similar results were obtained with PTFE dispersion alone. When both kinds of PTFE were used simultaneously however, the test ran for 66,600 seconds (18.5 hr.). During this extended time of running, the traction coefficient was nearly constant at about 0.045 with 1% contact slip. The traction coefficient increased gradually from the steady value of about 0.05 to about 0.3 when lubrication was lost at the end of test.

The detailed mechanisms by which the remarkable improvement in the performance of the $\text{Si}_3\text{N}_4/440\text{C}$ hybrid contact was achieved through two layers of PTFE films is not understood yet. In any case, the double layer prevented the growth of oxides on the 440C surface, which was observed to cause an increase in traction and loss of lubrication [2]. The double layer, after run-in, provided a very durable low shear strength film, which eliminates direct interaction between the ball and the disc. Good lubrication is maintained until the film was gradually removed by wear. A solid PTFE film, with good adhesion produced by running-in or other means may perform the same function of separating the surfaces even during liquid lubrication.

5.4 Summary

Lubrication and protection of hardware components such as bearings made from metallic materials are usually accomplished through chemical interaction between the additives in the lubricating oil and the metal surface to form a boundary film. The film acts by preventing direct metal-to-metal contact and interaction and reduce the friction by its low shear strength. In contacts involving ceramic materials, the low traction is very important for the durability and reliability of the component. When the traction coefficient is higher than 0.4, Hertzian stress cracks form on the Si_3N_4 component, which can eventually lead to catastrophic failure.

Instead of the usual chemical approach of performance enhancement of boundary lubrication of metallic materials, the role of physically-produced metallic and polymeric film on the tribological performance of Si_3N_4 -on-Steel hybrid contact was examined. The presence of a soft metallic films, notably Ag and Cu significantly improved the tribological performance of Si_3N_4 on steel contact under marginal lubrication condition. The soft metallic coating essentially perform the function of the chemical boundary films of reducing the traction and wear, through

its low shear stress and prevention of direct contact between the Si_3N_4 and steel surfaces. Furthermore, the smoothening of the coating surface as a result of plastic flow leads to the enhancement of formation and maintenance of EHD film due to the increase in h/σ ratio. By spreading the contact load over a larger contact area due to its plastic flow, the soft metallic coating/film lowers the nominal contact pressure and stresses between the Si_3N_4 ball and steel disc. Lower contact stresses will translate to lower wear rate and lower probability of stress crack formation. The presence of the soft metallic film also helps the contact interface thermal management. By reducing traction and by lowering the nominal contact pressure, the presence of soft metallic film results in less generation of frictional heat. If the coating has a good thermal conductivity like Ag and Cu do, it will help in dissipating the frictional heat laterally. This will substantially reduce the occurrence of thermal instability and the probability of thermal shock cracking of the Si_3N_4 component.

Polymeric material coating of Teflon also provided an effective lubrication for the Si_3N_4 ball and steel disc contact. By the virtue of its low shear strength, the presence of the coating reduced the traction in the hybrid contact interface. Also, by separating the surfaces, the film lowered the wear in both the ball and the disc material. When use in configuration with a liquid lubricant, the polymeric coating will adequately perform the function of boundary film.

In conclusion, a viable and effective alternative to a chemical boundary films for ceramics and steel hybrid and all-ceramic bearing that are operating under a severe contact condition is the use of a physically-generate soft metallic and polymeric material coating. The only possible shortcoming of such an approach is the durability and replenishment of the film. Where as the chemical film is being formed in-situ during contact and is continuously replenished through chemical reactions, the physically deposited film cannot be replenished insitu. For a short life application this will not be an issue.

6.Task III: - Tribological Performance Evaluation

6.1 Introduction

In addition to the high cost, the other main reason why hybrid bearings consisting of ceramic specifically Si_3N_4 rolling elements and steel raceways and all-ceramics bearing are not being used extensively is the uncertainty of their performance. All-steel bearings have been around for a long time, and their performance characteristics and prediction adequately known. Consequently, system design engineers are more comfortable with all steel bearings. One way to address this reluctance in using hybrid bearing is to convince the designers that hybrid bearings with Si_3N_4 rolling elements tribologically perform better than all-steel bearings.

There are many reports of hybrid bearing tribological performance evaluation in the literature [e.g., 14,15]. All these studies were designed primarily to evaluate the viability of hybrid bearings of Si_3N_4 rolling elements and steel races. In all the reported studies, the hybrid bearing performed well tribologically. There has been little or no comparative performance evaluation of the hybrid and the all-steel bearings. Such evaluation and the database generated thereby can connect performance-wise the less known hybrid bearing and the well known all steel bearing.

During the course of this work, it became apparent through our interaction with bearing manufacturers and through the program review with program monitor Mr. Karl Mecklenburg that the real cost saving of hybrid bearings will be in terms of performance. To the best of our understanding, manufacturing costs, particularly the ball and raceway finishing, are only a small fraction of the total hybrid bearing cost. The bulk of the cost is in the expensive Si_3N_4 material. A significant performance gain by hybrid over all-steel bearing could, however, translate into a major cost saving and justification for the initial higher cost of hybrid bearing.

Besides cost justification, an extensive comparative performance evaluation of Si_3N_4 /Steel hybrid and all-steel bearings can address some of the concerns and uncertainties about hybrid bearings. Some of these uncertainties include the performance and structural reliability of "brittle" Si_3N_4 rolling element material. The durability of steel races when operating in contact with a much harder Si_3N_4 rolling element is often another source of concern.

In view of the foregoing consideration, it was decided during our program review with the program monitor that more of our efforts should be devoted to the comparative performance evaluation of hybrid and all-steel contact pairs than was originally proposed. To this end, several types of bearing life-limiting tribological tests were done to evaluate Si_3N_4 and steel hybrid contacts and all-steel contacts under such conditions.

6.2 Technical Approach

The primary aim of this task was to evaluate, in a realistic way, the performance of Si_3N_4 /steel hybrid and all-steel contact under conditions similar to those in a rolling element bearing. Traditionally, surface and/or subsurface initiated fatigue damage is the major life limiting process in steel bearing materials. Consequently, rolling contact fatigue (RCF) tests are

commonly used to evaluate new bearing materials. Most of the early and current evaluation of Si_3N_4 ceramic materials for bearing application focused on their rolling contact fatigue resistance. The tests are usually run by operating the contacts under pure rolling for an extended period of time, until surface fatigue occurs.

The rolling contacts in bearings, however, are often subjected to both normal and tangential (shear) stresses. Tests without the shear component (such as RCF) may give an unrealistic evaluation with respect to performance in a bearing. The role of the shear stress at the contact interface is particularly critical to a useful evaluation of Si_3N_4 ceramic material for bearing applications. The inability of ceramics materials to accommodate the shear strain by plastic flow must be taken into consideration. If the tangential stress, which is always present in a bearing contact, is too high, Hertzian crack formation can occur in the ceramic materials. The cracks can propagate and interact to cause severe wear and loss of surface integrity or in the extreme case, a catastrophic fracture of the component.

All the performance evaluations in the present effort were conducted using a single element contact of ball-on-disc configuration. The contacts were operated under rolling motion with both the normal and tangential stresses imposed. The tests were conducted on the WAM1 and WAM3 machines described in details earlier in this report. The approach was to drive the contact to failure, by progressively increasing the severity of contacts. Hybrid pairs of Si_3N_4 ball on steel disc and steel ball on steel disc contact pairs were tested under identical conditions. The performance of each contact pair in terms of failure point was compared. Where possible, differences and similarities between the failure mechanisms were assessed. Details of each kind of tests conducted and their results are now presented.

6.3 Preliminary Traction Test with Steel Ball on Si_3N_4 Disc

Preliminary experiments were conducted with hybrid metal/ceramic material pairs consisting of M50 balls running against a Si_3N_4 disc. The contacts were lubricated with different fluids so as to assess the traction behavior of the hybrid pair. Tests were also run with different types of Si_3N_4 discs. Three variations of a Dow Chemical self-reinforced Si_3N_4 disc were used in addition to the referenced NBD200 material. This allows a determination of possible material effects on measured traction. The three self-reinforced materials had different processing and composition. Their mechanical properties are given in Table 5.

Table 5: Mechanical Properties of Three Si_3N_4 Materials

| Material Code | Elastic Modulus | Shear Modulus | Poisson's Ratio | Toughness (K_{Ic}) |
|---------------|-----------------|---------------|-----------------|------------------------|
| 1182-1 | 315 GPa | 124 GPa | 0.28 | 7 |
| 1182-2 | 313 GPa | 122 GPa | 0.28 | 7-8 |
| 1184-1 | 300 GPa | 118 GPa | 0.27 | 9 |

6.3.1 Traction Tests Under Flooded Conditions

Lubricated tests were conducted with an ester base reference fluid, Herco-A. The purpose was to determine the level of traction (tangential stress) when the surfaces are separated with a full EHD film. Traction curves were developed over a slip range of $\pm 10\%$ with a rolling speed of 100 in/s. Traction curves were developed for three different loads: 93lbs, 63lbs, 30lbs. The contact loads correspond to the Hertzian stresses of 341ksi, 300ksi and 234ksi.

Typical traction curves for a M50 ball run against a NBD200 and Dow Chemical 1182 discs are shown in Figures 33a and b, respectively. The following summarizes general observations about the traction behavior of the steel ball on Si_3N_4 disc hybrid contact:

1. The maximum traction coefficient increases slightly with contact stress.
2. The slope of the traction curve under incipient sliding conditions increases slightly with contact stress.
3. The maximum traction coefficients for the two types of ceramics are essentially the same. The Dow material seems to give a slightly greater traction coefficient than NBD200 by 2%.

The above traction results are primarily a function of the shear properties of the oil in the contact region. Since the high contact stress causes the oil to "solidify" in the contact, the maximum traction coefficient reflects a "plastic" shear limit, or limiting shear strength, of the oil. The initial slope of the traction curve is also influenced by the elastic shear properties of the hybrid material pair. Since the elastic modulus of M50 is much lower than Si_3N_4 , it will have a greater influence on the elasticity of the contact in both normal and tangential directions.

The role of lubricant was demonstrated by conducting the same traction tests with a lubricant of different molecular structure. This was done with a polyperfluoropolyalkylether (PFPE) oil (KRYTOX 143AB). PFPE's have a higher limiting shear strength than esters. The measured maximum traction coefficients are shown in Table 6.

Table 6: Traction Coefficients with Hybrid Materials (M50/NBD200)

| Ester Oil, HERCO-A | PFPE Oil, KRYTOX 143AB |
|--------------------|------------------------|
| 0.0611 | 0.107 |
| 0.0582 | 0.099 |
| 0.0493 | 0.095 |

The results of these preliminary tests provided a baseline for the traction characteristics of the hybrid contacts under full EHD film lubricated conditions.

TRACTION VS SLIP

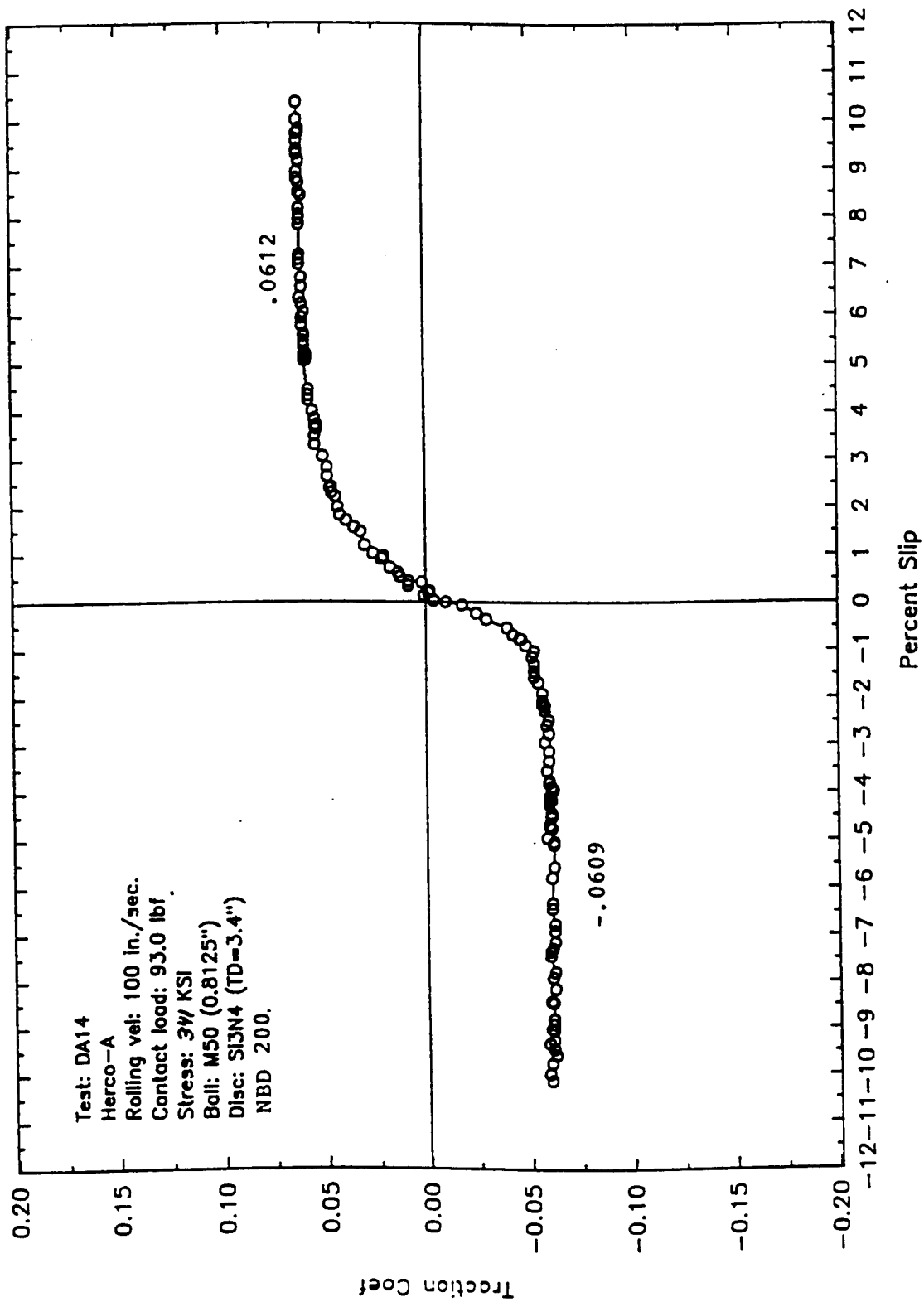


Figure 33a: Traction curve for M50 ball run against NBD 200 disc under flooded lubricated condition: 93lbf. contact loads.

TRACTION VS SLIP

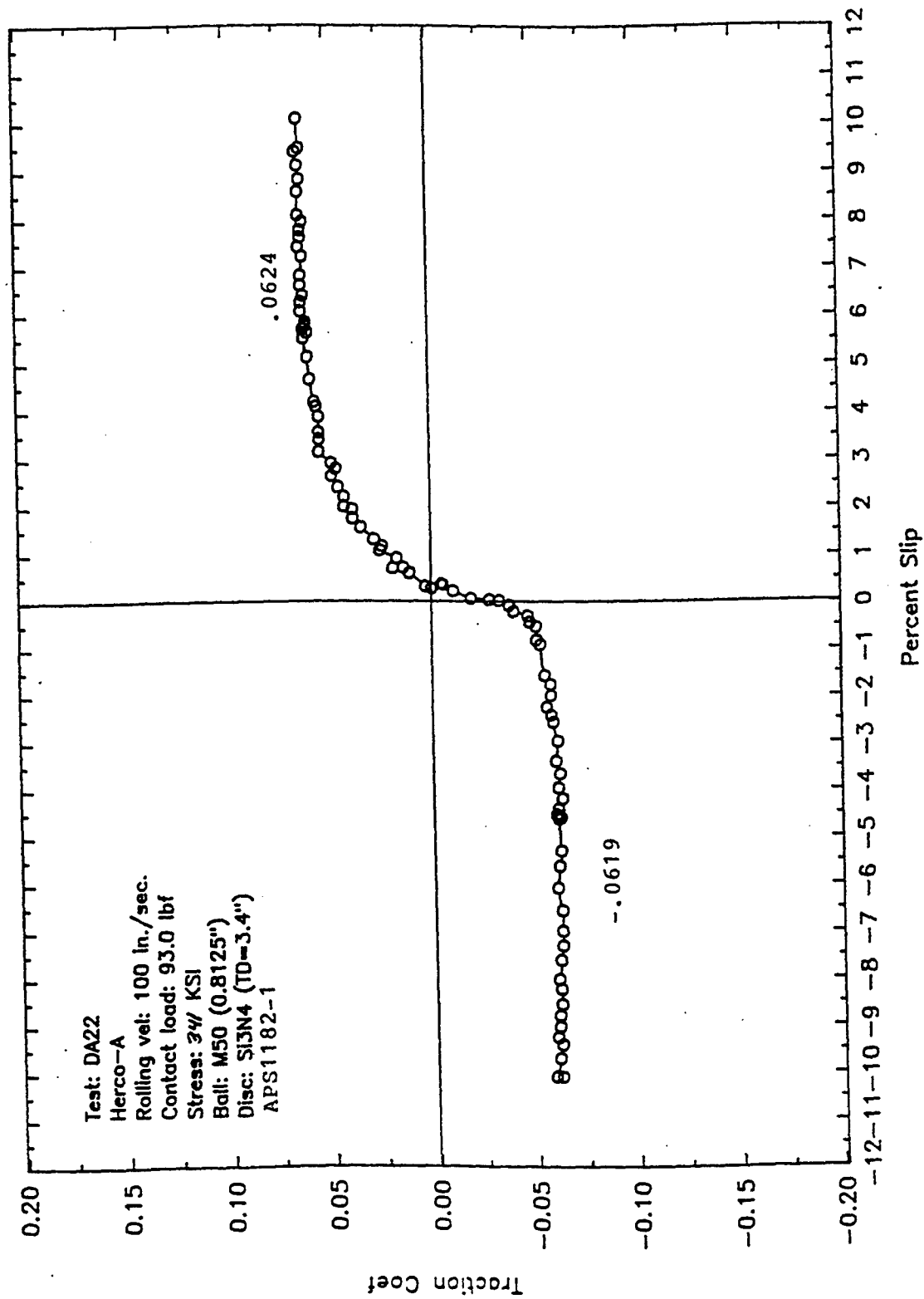


Figure 33b: Traction curve for M50 ball run against Dow Chemical self-reinforced Si₃N₄ (APS 1182-1); 93 lbf contact loads.

6.3.2 Starved Lubrication

During liquid lubrication of a contact, if there is insufficient lubricant at the inlet zone where the EHD fluid film is generated, the contact is said to be starved. In a such situation, the lubricant fluid film thickness is substantially lower than the EHD full-film thickness. Under a severe or fully starved condition, often referred to as parched lubrication, there is effectively no oil in the inlet zone. The lubrication of the contact is then dependent only on the absorbed layer of fluid on the contacting surface.

Under oil starvation, extensive interaction between the contacting surfaces is expected. This will result in wear and, in the extreme case, could lead to loss of surface integrity.

The goal of the starved lubrication test reported here was to evaluate the performance of an all-steel contact in comparison to a hybrid Si_3N_4 -on-steel contact under this severe and inadequately lubricated contact condition.

6.3.3 Experimental Details

The starved lubrication tests were conducted on the WAM3 machine with the following parameters:

- Ball specimens: M50 and Si_3N_4 (13/16" dia. finished)
- Disc specimens: M50 ($R_a = 6 \mu\text{in}$)
- Contact Stress: 320 Ksi
- Rolling velocity: 100, 75 in/sec
- Contact Slip: Variable
- Temperature: Ambient RT ($\approx 23^\circ\text{C}$)
- Relative Humidity: 67%
- Test duration: 3600 seconds (1 hr)
- Lubricant: ETO-25

6.3.4 Procedure

Clean ball and disc specimens were mounted on their respective spindles and were thoroughly wetted with the lubricant. A fully formulated ester based aviation oil, Exxon Turbo oil 25 (ETO 25), was used as the lubricant. Lubricant starvation was created by spinning-off excess oil from the specimen surface prior to testing. This was done by rotating the ball and the specimens at 200 in/sec for 1 min., after which only a thin film of the lubricant was left on the specimen surfaces. The amount of residual oil on the surface is both a function of the rotating speed and time.

Following the spin clear procedure, the ball and disc specimens were set to a rolling speed of 100 in/sec and loaded to a contact stress of 300 ksi. The first 200 sec of test time was operated under pure rolling condition. At 200 seconds, 5% contact slip was introduced. At every subsequent 300 sec the contact slip was increased by 5% until 50% slip is attained at 2900 seconds. Tests

were terminated at 3600 sec (1hr). This test procedure progressively increases the severity of contact with time by increasing the shear strain/stress imposed at the contact interface. Because the contact is under lubricant starvation, significant interaction between the ball and disc surfaces occur, which makes the role of the materials in the tribological performance more dominant. Therefore, differences are expected between the all-steel and the hybrid contact test results.

6.3.5 Results and Discussion

Figure 34a shows the traction behavior for the hybrid Si_3N_4 ball and M50 steel disc test. With the introduction of contact slip, the traction coefficient increased to about 0.06. Beyond this point, the traction coefficient showed a generally decreasing trend throughout the duration of the test, ending with a value of about 0.04. Furthermore, the traction coefficient showed a serrated pattern throughout the test. The serration does not appear to coincide with the contact slip increase. It is probably connected with the events occurring at the contact interface.

The traction behavior for the steel-on-steel test is shown in Figure 34b. The traction behavior was very similar to that of the hybrid contact. The traction coefficient was slightly higher with the all-steel contact and the frequency of serration was considerably lower than for the Si_3N_4 -on-steel hybrid contact.

Examination of the surfaces in both test showed some significant differences. Figure 35 shows the SEM micrograph of the worn surfaces of the M50 steel ball and the Si_3N_4 ball. With the steel ball, there was significant wear and surface damage, as shown in Figure 35a. Little or no wear and minimal damage was observed on the Si_3N_4 ball surface (Figure 35b). These results show a better tribological durability in terms of the extent of damage by the hybrid contact compared to an all-steel contact under starved lubrication.

The disc surfaces run against a steel ball and a Si_3N_4 ball have similar appearance. There was polishing wear of the ridges and some formation of surface films, presumably from the additives in the lubricating oil film. The disc ran against a Si_3N_4 ball that appeared to show more polishing wear and less surface film.

The decreasing trend in the traction coefficient for both the all-steel and hybrid contacts was a consequence of the frictional heating of the contact interface and of topographical run-in. As the contact slip was increased, the sliding speed at the contact interface increased resulting in higher frictional heating. The interface increase in temperature was accompanied by a decrease in its shear strength and, hence, traction. Under starved lubrication, both the thin lubricant layer and interaction of the ball and disc specimen surface features contributed to the traction characteristics.

A significant difference between the traction characteristic of the all-steel and hybrid contact for hybrid contact is a pronouncement of serration in the traction coefficient of the hybrid contact. This means that the traction/friction force at the contact interface varies more with time in the hybrid contact. Such behavior is usually associated with stick-slip phenomenon or a discrete mechanisms/process for accommodating shear strain at the contact interface. An example of

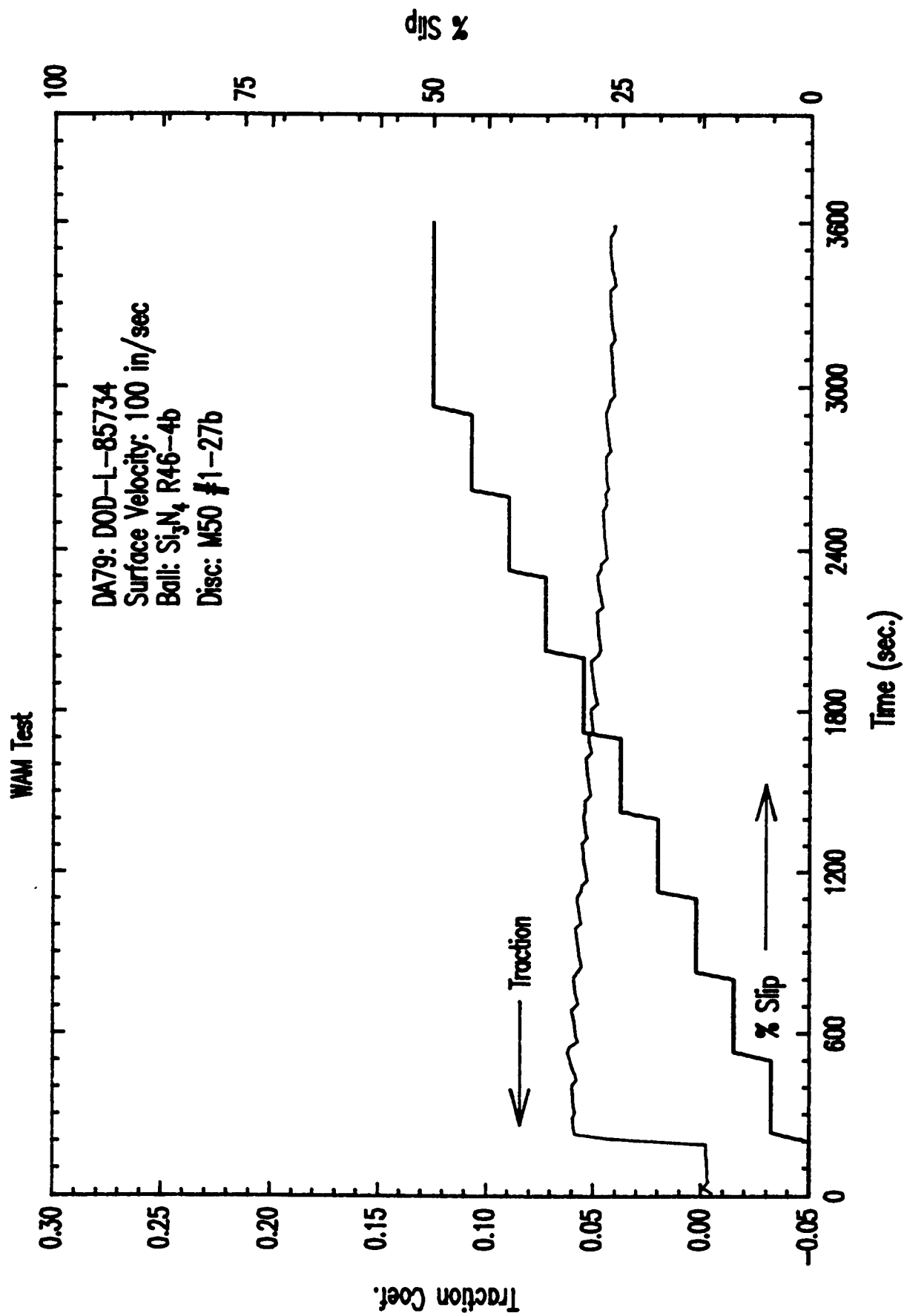


Figure 34a

Traction behavior during starved lubrication tests with hybrid contact

<DA79.SPW>

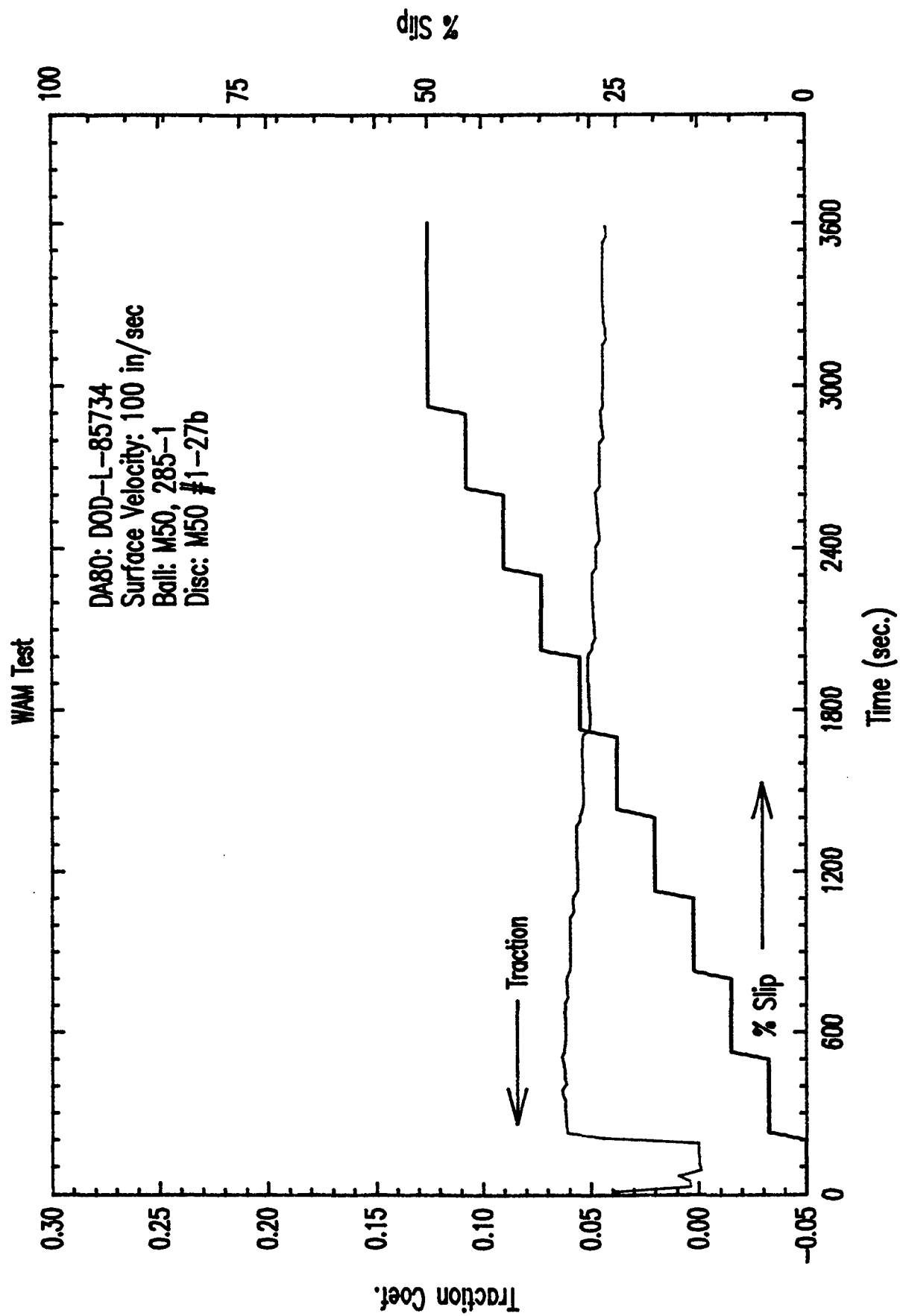
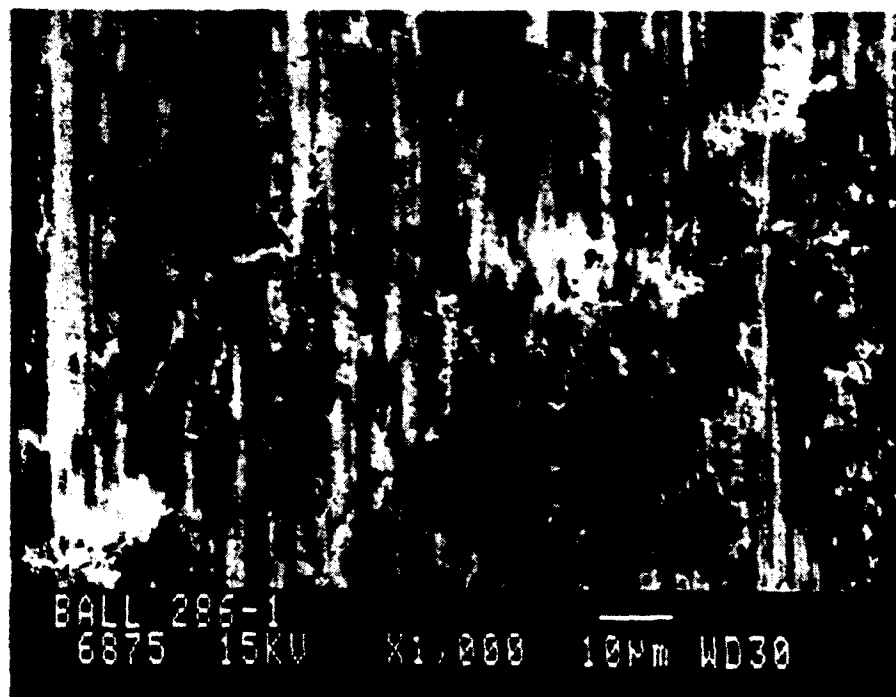


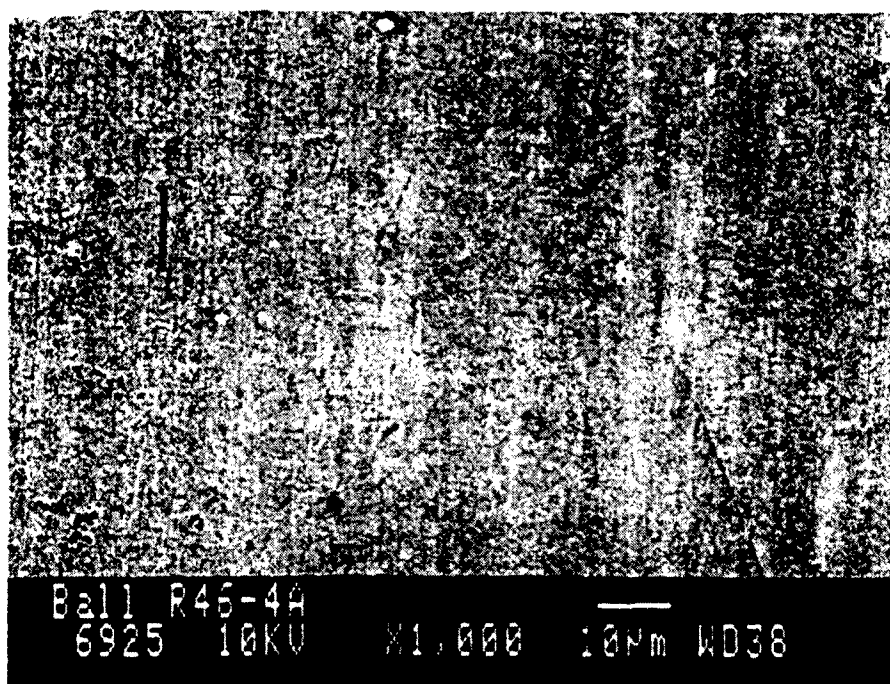
Figure 34b

Traction behavior during starved lubrication tests with all-steel contact.

<DA80.SPW>



(A)



(B)

Figure 35 Ball worn surface after starved lubrication test
(a) M50 steel and (b) Si_3N_4

such a mechanism is the formation of discrete, often parallel, surface cracks. In the all-steel contact, the traction serration is not as pronounced. The exact reason for this difference in the degree of traction serration is not fully understood at this point. This may be connected with the surface film formation and removal, or differences in the mechanism of the accommodation of interfacial shear strain imposed by the introduction of contact slip. Whatever the reason, this difference has an implication for practical application. Hybrid bearings made of Si_3N_4 ball and steel races may be more susceptible to a jerky or noisy running under starved lubrication when compared to all-steel bearings. Less wear occurred in the hybrid pair, compared to the all-steel contact pair, in spite of the similarity of their traction coefficient values. The higher hardness of Si_3N_4 made it more resistant to abrasive wear. While there were a lot of scratches and indentation damage on the steel ball, only superficial damage was observed on the Si_3N_4 ball in the present tests. Film formation from the oil additives as well as oxide formation on the disc surfaces provided some protection against severe wear or damage.

6.3.6 Summary

The tribological performance of a Si_3N_4 /M50 steel hybrid pair and a M50/M50 steel pair were evaluated under starved lubrication condition with a fully formulated ester based aviation oil. Starvation was created by spinning clear excess oil from the specimen surface prior to testing. Both the hybrid and the all-steel pairs exhibited similar magnitude of traction coefficient. They both also showed an overall decreasing trend in the traction with increasing contact slip. This was associated with contact interface frictional heating with higher slip. The hybrid contact showed a more pronounced serrated pattern in its traction coefficient suggesting some form of stick-slip phenomenon. This could have a significant implication for hybrid bearings under starved lubrication. The bearing may be noisy under such condition.

There was very little wear or damage on the Si_3N_4 ball, while abrasive scratches and indentation damage were seen on the steel ball. Also, film formation from the lubricant additives occurred on the steel ball and disc, but no such film was observed on the Si_3N_4 ball.

6.4 Load Capacity Test

Usually, load carrying capacity (LCC) is used to describe oil lubricant performance under severe contact conditions. The load carrying capacity of an oil is the maximum load (or contact pressure) that the lubricant can sustain without catastrophic failure of the lubricated surfaces. In assessing the LCC of different oils, the tests are conducted with the same material, test parameters, and procedure. The performance of each oil is then judged by the failure load during the test with the oil. Failure in load capacity tests (LCT) occurs by a scuffing mechanism that is often accompanied by a sudden increase in the traction coefficient and noise level.

Wedeven Associates (WAI) developed a load capacity test procedure to qualify the oils for the Navy. The load capacity rating from this procedure shows a good correlation with the Ryder gear test rating, the standard qualification test for Navy. In the WAI test method, the contact between the ball and disc is operated under a given rolling (R) and sliding (S) velocities. With adequate supply of lubricant, the contact load is increased in step fashion until scuffing occurs.

Although the load capacity test is currently being used to evaluate oil performance, the ultimate failure at the interface during the test actually occurred in the materials. Therefore, the test methodology could be used to evaluate the propensity of different combinations of contact materials to catastrophic failure. The goal of the following tests was to evaluate and compare the scuffing and surface damage characteristics of an all-steel and a Si_3N_4 -steel hybrid contact pairs with the same oil.

6.4.1 Experimental Details

The load capacity tests for M50/M50 steel contact pair and Si_3N_4 /M50 contact pair are conducted on the WAM3 machine. Following are the test parameters.

Ball specimen: M50 and Si_3N_4 (TSN-03H)

Disc specimen: M50 ($R_a = 6 \mu\text{in}$)

Rolling Velocity: 200, 150, 100 in/sec.

Sliding Velocity: 400 in/sec.

Temperature: Ambient RT.

Contact Load: Variable

Lubricant: Ester basestock oil (Herco-A); fully formulated aviation oil (ETO-25)

Relative Humidity: 63%

6.4.2 Procedure

Clean ball and disc specimens are mounted on the appropriate spindle and set to the desired rolling and sliding velocities. The standard LCC test procedure currently used by WAI for qualification of MIL-L-23699 oils is conducted at a rolling (entraining) velocity (R) of 200 in/sec and a sliding velocity (S) of 400 in/sec. The contact load is increased progressively every 60 sec (1 min) by 4 lbs. Until scuffing occurs. The oil is supplied by continuous drip feeding. The traction coefficient and the specimen temperatures are continuously monitored during the test. The load at which the scuffing occurs is judged to be a measure of the LCC of the oil. To further characterize the two kinds of contacts, the effect of the variation of rolling velocity (R) on the LCC is also evaluated. At the conclusion of each test, the ball and the disc surfaces are examined to assess the extent and the nature of damage. In some cases, duplicate tests are run for repeatability.

6.4.3 Results and Discussion

A summary of the results of the load capacity tests with all-steel and Si_3N_4 /steel contact pairs for the two kinds of oil used in conducting the tests is displayed in a bar chart form in Figure 36. Under all the conditions tested, the hybrid contact has a much higher LCC than the all-steel contacts. Details of the results for each oil are now presented.

6.4.3.1 Basestock Oil (Herco-A)

Figure 37 shows the results for a LCC test run with the ester basestock oil (Herco-A) with a

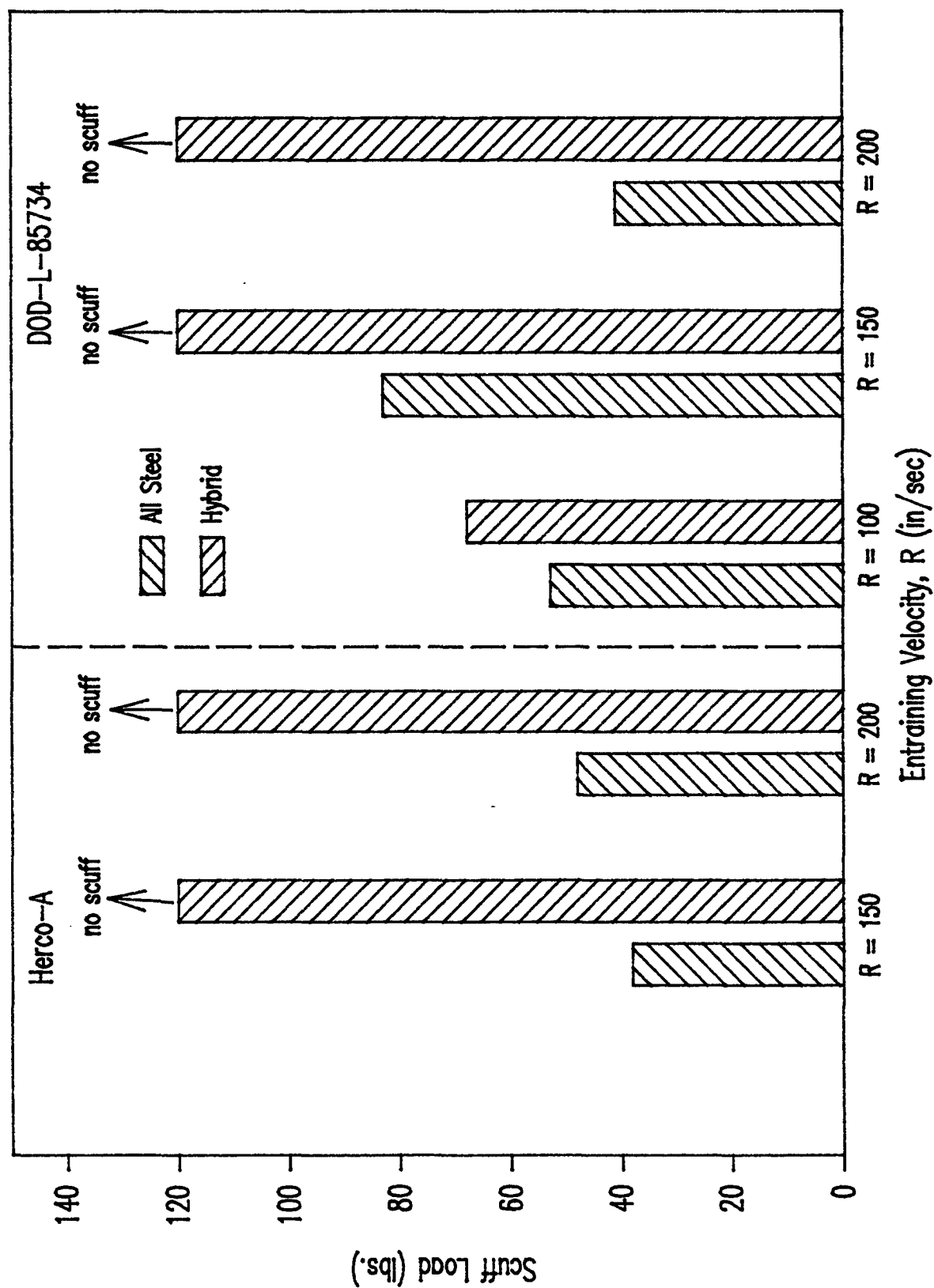


Figure 36 Load Capacity Comparison of All-Steel and Hybrid Contacts

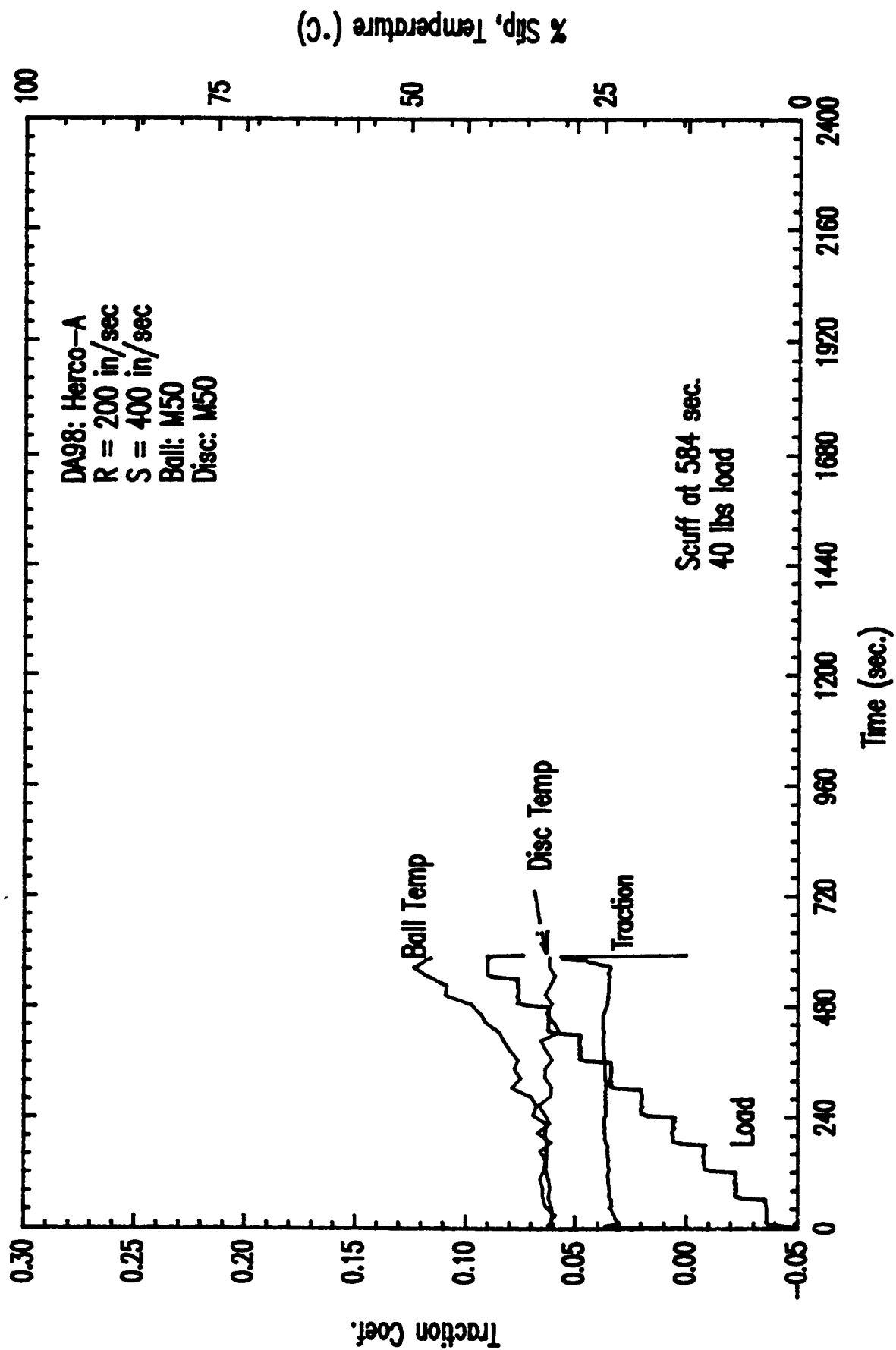


Figure 37 All-steel load capacity test

<DA98.SPW>

smooth M50 ball and M50 steel disc. Scuffing occurred at 40 lbs. and 56lbs for the duplicate tests. The traction behavior and the specimen temperatures in both test were very similar to one another. The ball temperature increased more rapidly due to its lower mass in comparison to the disc. At the scuffing point, when the tests were terminated, the traction coefficient and the specimen temperature showed a sudden increase.

The results for hybrid contact Si_3N_4 ball on M50 disc under the same test conditions and procedure are shown in Figure 38. Two tests were also conducted for this material combination. Both test ran to a load of 120 lbs. (which is taken as the upper load) limit without failure as determined by occurrence of scuffing. The traction coefficient and the specimen temperature behavior in the duplicate tests were very similar to one another. During these tests, the traction coefficient showed some transitions and periodic spikes. These were due to the occurrence of micro-scuffing and polishing of local surface disturbances. Compared with the all-steel contact of Figure 37, the hybrid contact tremendously increased the load carrying capacity of the ester basestock fluid.

In order to quantify the relative load carrying capability of an all-steel and a hybrid contact, it was useful to run both configurations to failure by scuffing. The tests that were conducted at $R=200$ in/sec and $S=400$ in/sec resulted in failure of the steel-on-steel configuration but not for the Si_3N_4 on steel configuration. Reducing the entraining velocity R will decrease the fluid film thickness between the ball and the disc surfaces. This will reduce the scuffing load as a result of increased interaction between the two surfaces. A test of each was therefore conducted at R of 150 and S of 400 for steel-on-steel and the Si_3N_4 on steel configuration. Figure 39 shows the results of the tests. For the all-steel contact, scuffing occurred at a load of 36 lbs. (Figure 39a) whereas the Si_3N_4 /steel contact ran to 120 lbs., again without scuffing (Figure 39b). These results show that the hybrid contact configuration increased the load carrying capacity of ester basestock oil by a factor of more than 3 compared to an all-steel contact.

6.4.3.2 Formulated Oil

Load carrying capacity tests were also conducted with a fully formulated DOD-L-85734 aviation oil (ETO-25) containing a blend of additives. Tests were run with a M50 steel on steel contact and with hybrid contacts of Si_3N_4 balls and M50 steel discs.

Results of tests run at speeds of $R=100$ in/sec and $S=400$ in/sec are shown in Figure 40. For the steel-on-steel contact, failure by scuffing occurred at 40 lbs. (Figure 40a). The traction coefficient during the tests was nearly steady at 0.062 with some small fluctuation, especially as the load was changed. For the hybrid contact (Figure 40b), the test ran to 108 lbs. Without failure. The traction coefficient started at about 0.065, increased gradually over the first few load stages to a peak value of about 0.068, after which the traction coefficient decreased steadily throughout, with the test ending with a value of about 0.020 at 108 lbs. There were some spikes in the traction curve due to micro-scuffing. The ball and disc temperature increased rapidly at the early stages but approached a steady value towards the end of the test. The decrease in traction coefficient and its effect on frictional heating offset that of the load increase.

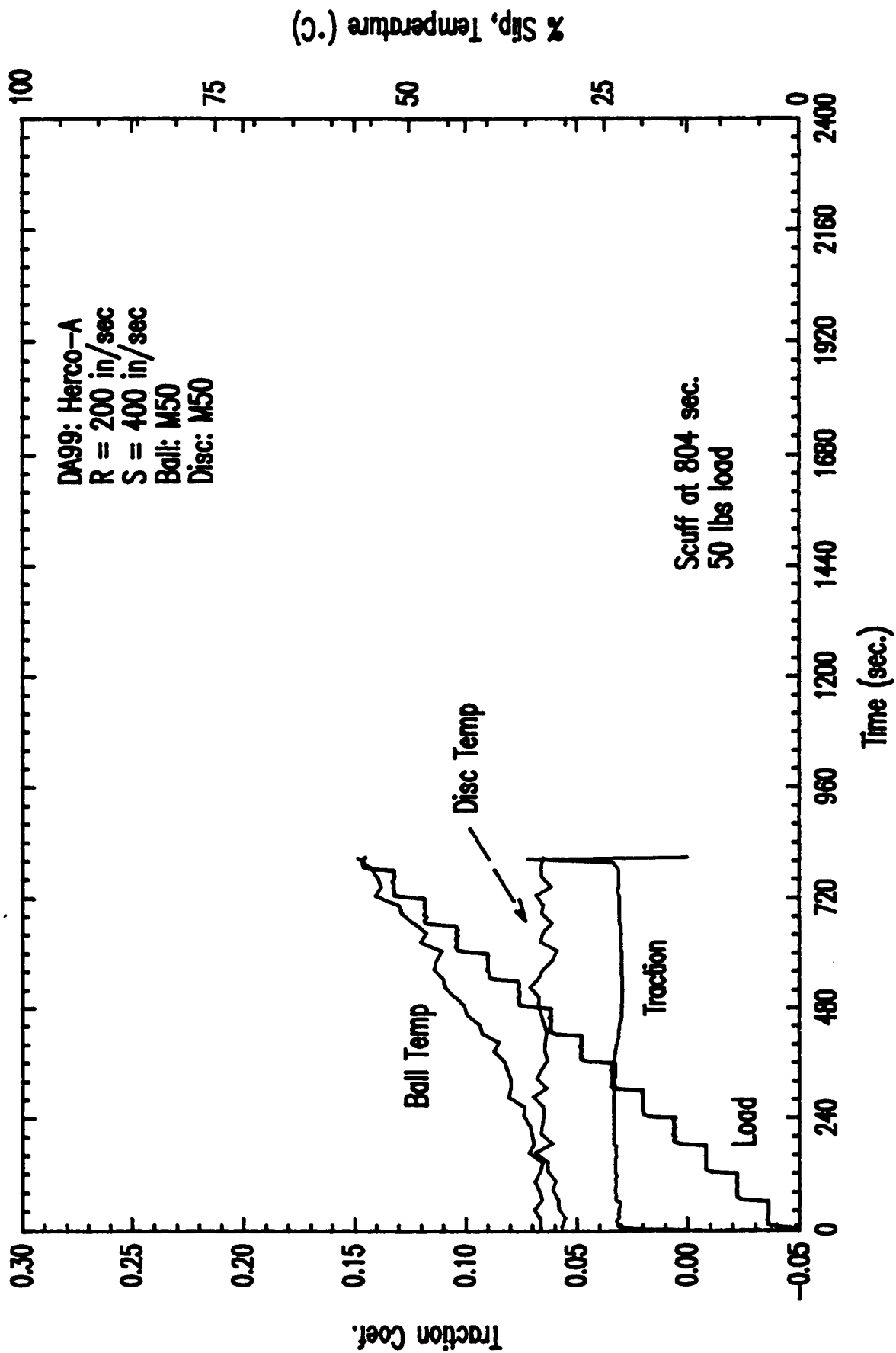


Figure 38 Hybrid Load Capacity Test

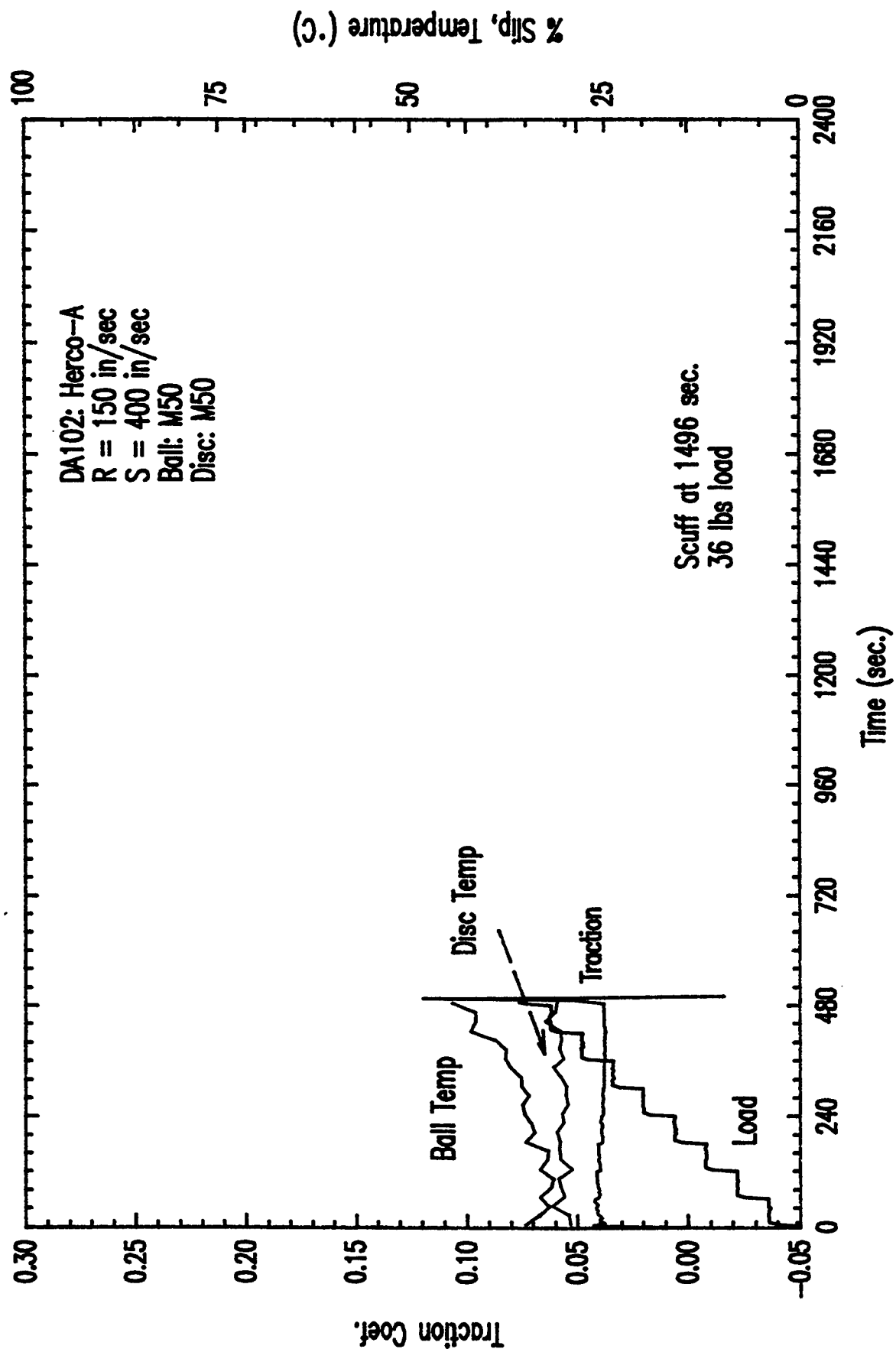


Figure 39a All-steel load capacity test

<DA102.SPW>

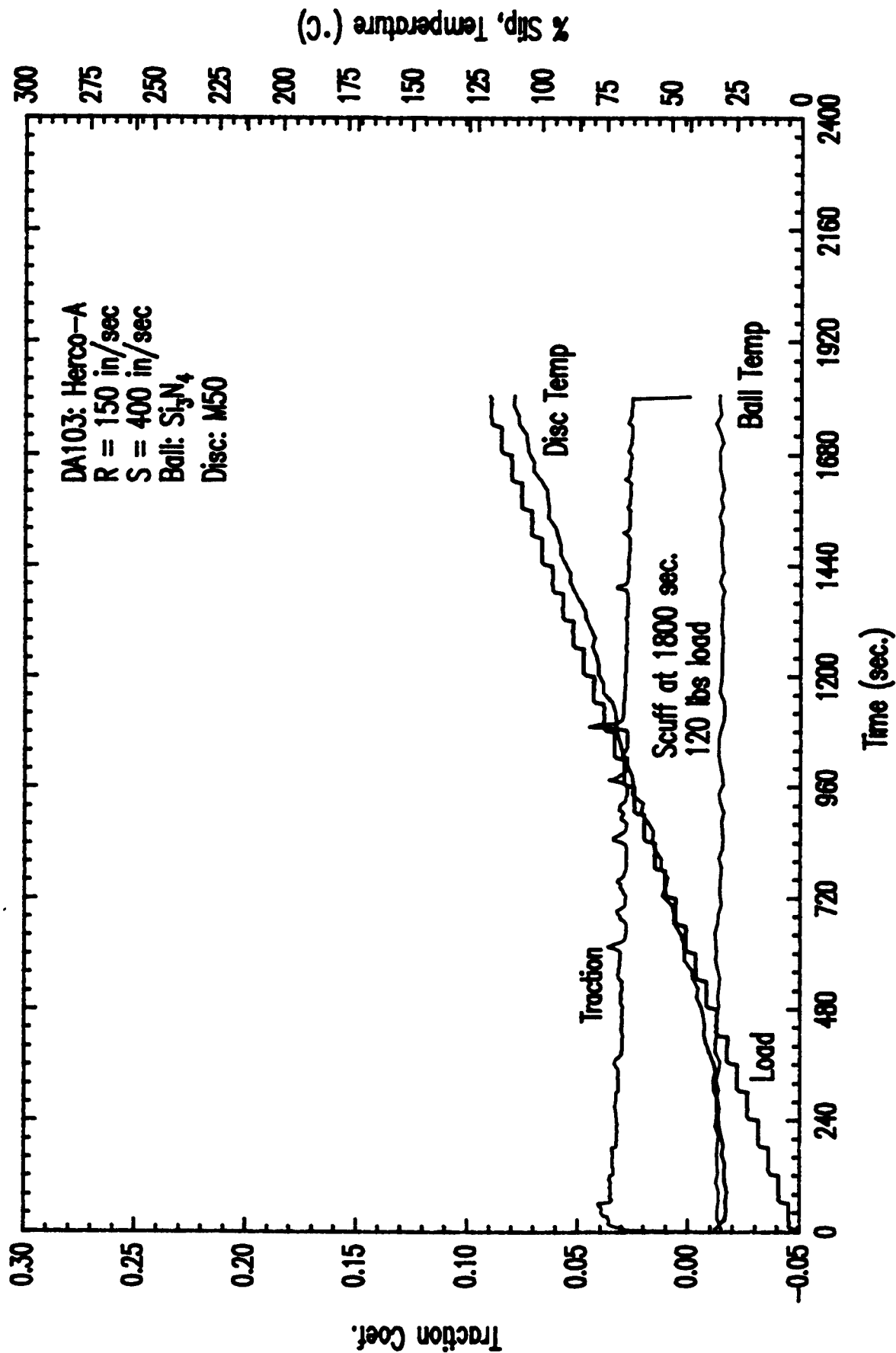


Figure 39b Hybrid load capacity test

<DA103.SPW>

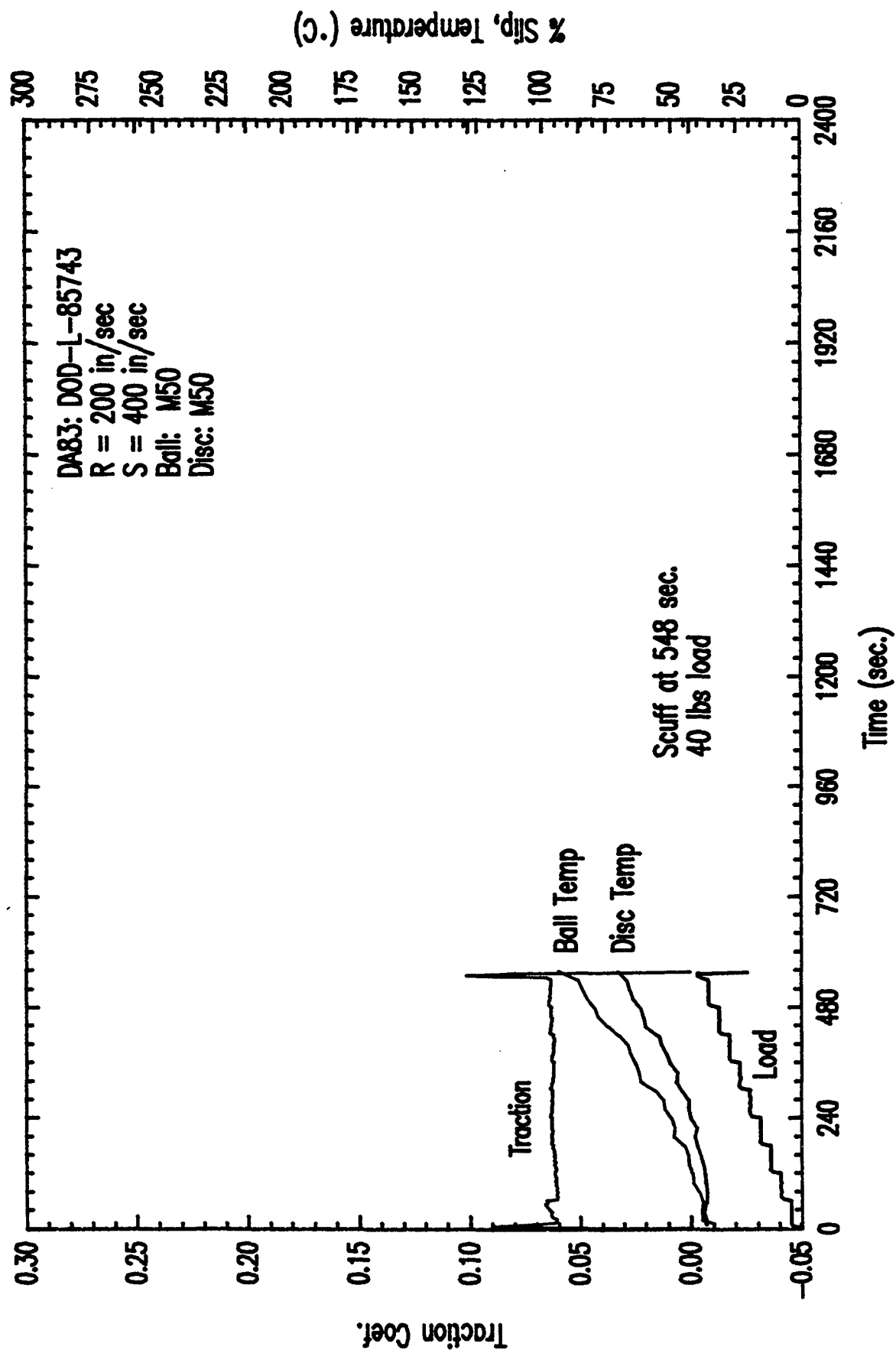
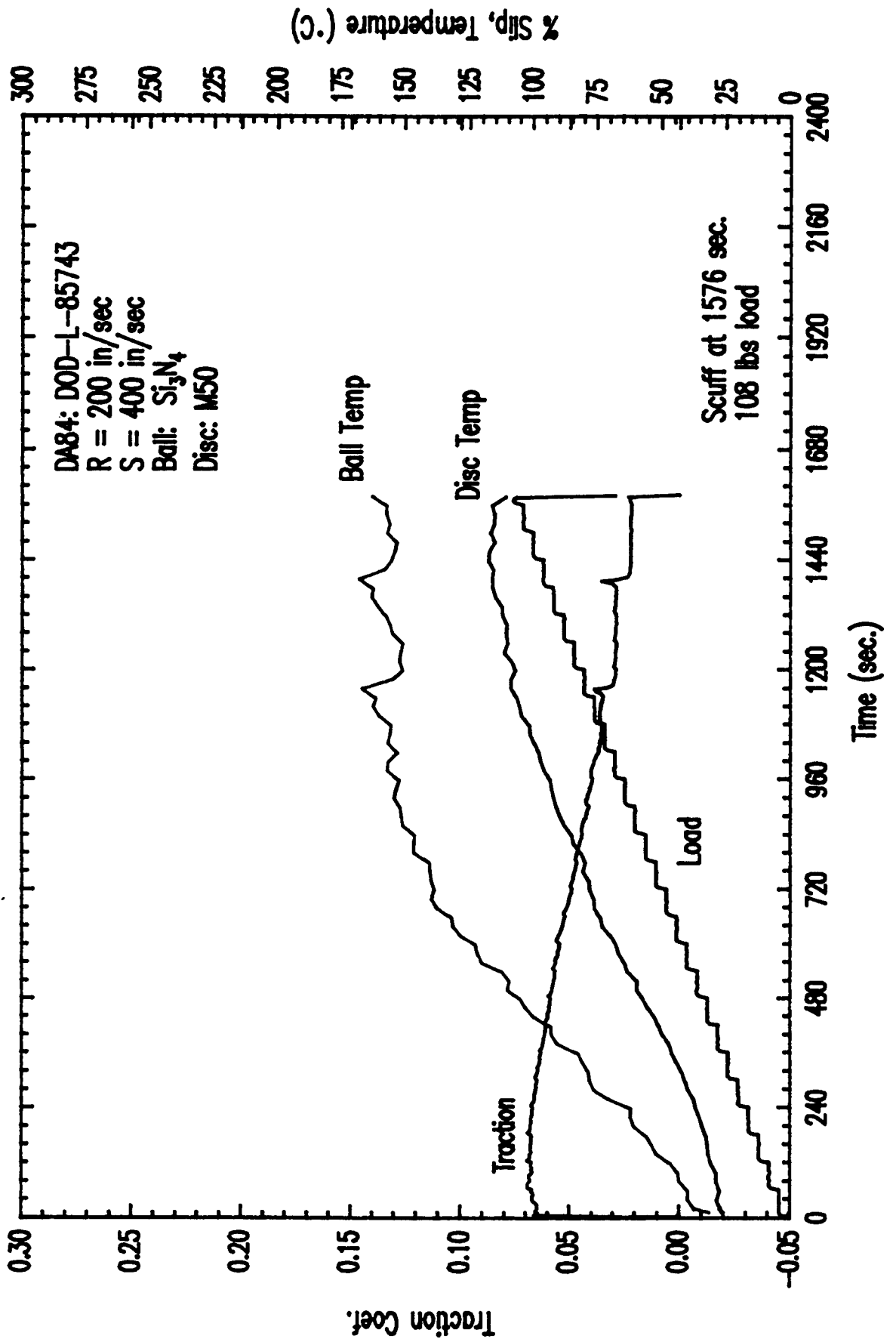


Figure 40 All-steel load capacity test with formulated oil

<DA83.SP.W>



<DA84.SPW>

Figure 40b Hybrid load capacity test with Si_3N_4 ball

A set of tests was also conducted at $R=150$ in/sec and $S=400$ in/sec in order to accelerate the failure process by starting with a smaller fluid film thickness. Results of the tests are shown in Figure 41. For the steel on steel contact, scuffing occurred at a load of 80 lbs. The traction coefficient showed an increasing trend in the early stages of the test, reached a maximum and was on a decreasing trend when failure occurred (Figure 41a). For the Si_3N_4 on steel hybrid contact, no scuffing occurred up to the terminal load of 120 lbs. The traction coefficient shed a trend very similar to the one for steel on steel contact except for the spikes due to micro-pitting (Figure 41b).

The last set of tests was conducted with speeds of $R=100$ in/sec and $S=400$ in/sec, reducing further the initial fluid film thickness. Under this condition the all-steel test failed at 52 lbs. and the hybrid contact of Si_3N_4 ball on steel disc failed at 68 lbs. The traction behavior in both tests was very similar to one another. Examination of the ball specimen surfaces at the conclusion of the tests showed some significant differences between the failed steel and the Si_3N_4 balls. Abrasive wear and material removal by spalling occurred on the steel ball (Figure 42a). For the Si_3N_4 ball, however, there was extensive transfer of material from the steel disc (Figure 42b). At the point of failure, it is conceivable that contact interface indeed involved steel on steel interaction rather than Si_3N_4 on steel interactions.

There were two areas in which the hybrid and the all-steel contacts show some similar behavior during the load capacity test. These were traction behavior and friction heating characteristics. For the basestock oil, the traction coefficient in both M50-on-M50 contact remained nearly constant during the test. In some cases, a sudden decrease to a lower steady value occurred. Similarity in hybrid contact of Si_3N_4 -on-M50, the traction coefficient remains nearly steady. At higher loads, occasion traction spikes, some of which are accompanied by a decrease in traction coefficient, occurred. This kind is traction behavior in both the all-steel and hybrid contacts is due to the fact that contact interface in both cases is being condition topographically. The transition in traction coefficient at higher loads is a result of decrease in h/σ ratio due to the lower roughness of the contact interface. The effect is more pronounced in the hybrid contacts because the Si_3N_4 ball can produce quicker and smoother topography on the steel counter face. This is due to the higher hardness of Si_3N_4 and the fact that the contact stress in hybrid contact is higher than all steel contact under the same load.

With fully formulated oil, the traction behavior in hybrid and all steel contact was also similar. In both cases, the traction coefficient increased in the early load stage, reached a maximum and decreased until failure or termination of the test. The traction behavior results from the anti-wear additives in the oil preserving the surface topography of the disc. As the load is increased, the EHD fluid film thickness decreases, due for the most part to the lowering of the fluid viscosity by frictional heating. Because of this film thickness decrease and very little change in surface topography, the specimen surface features will make more contribution to the shear strength of the interface resulting in higher traction. Eventually, wear of the surface features will occur, which will improve the EHD lubrication and, consequently, the traction coefficient decrease until scuffing occurs.

This similarity of behavior between the traction of hybrid and all steel contacts in both the

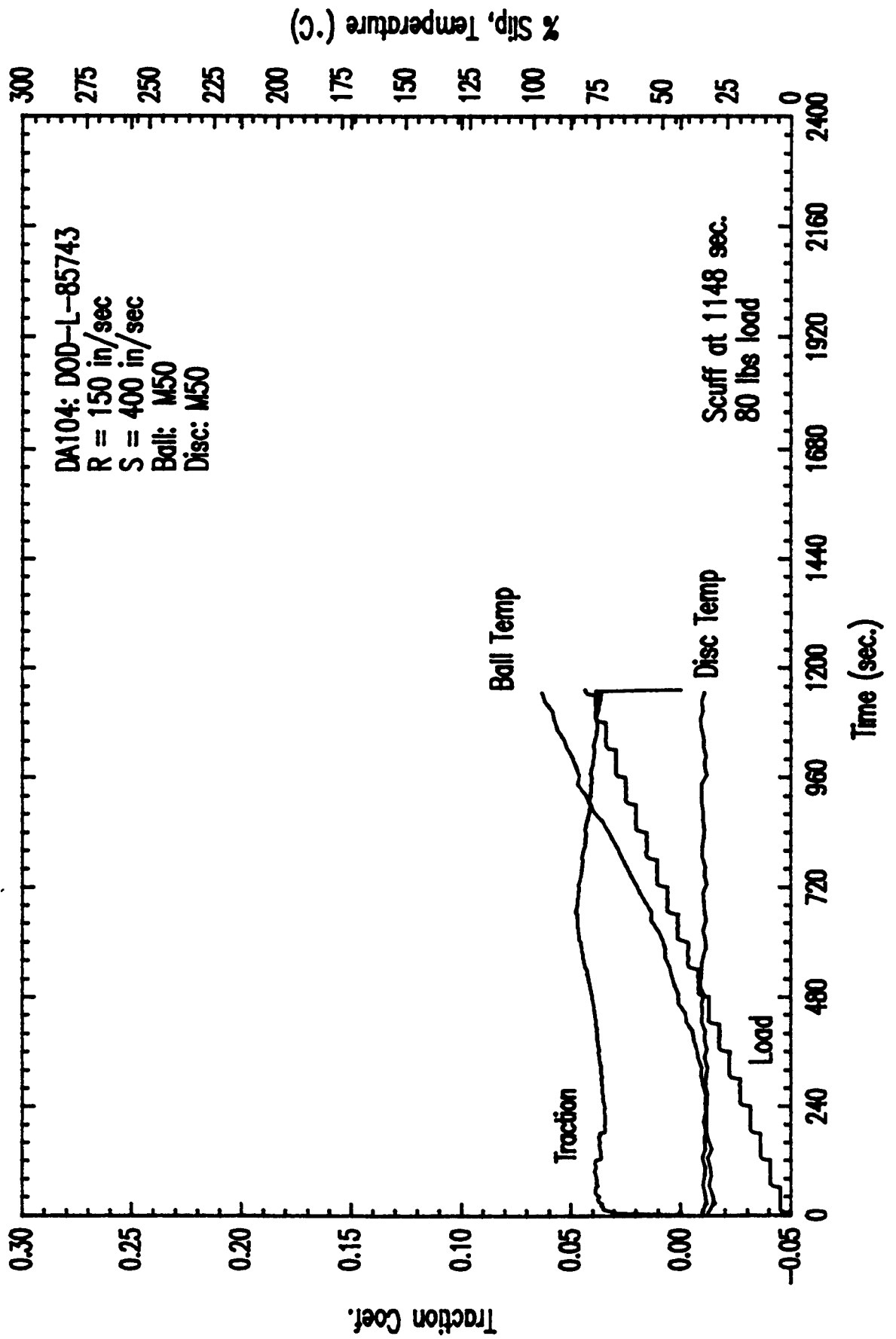
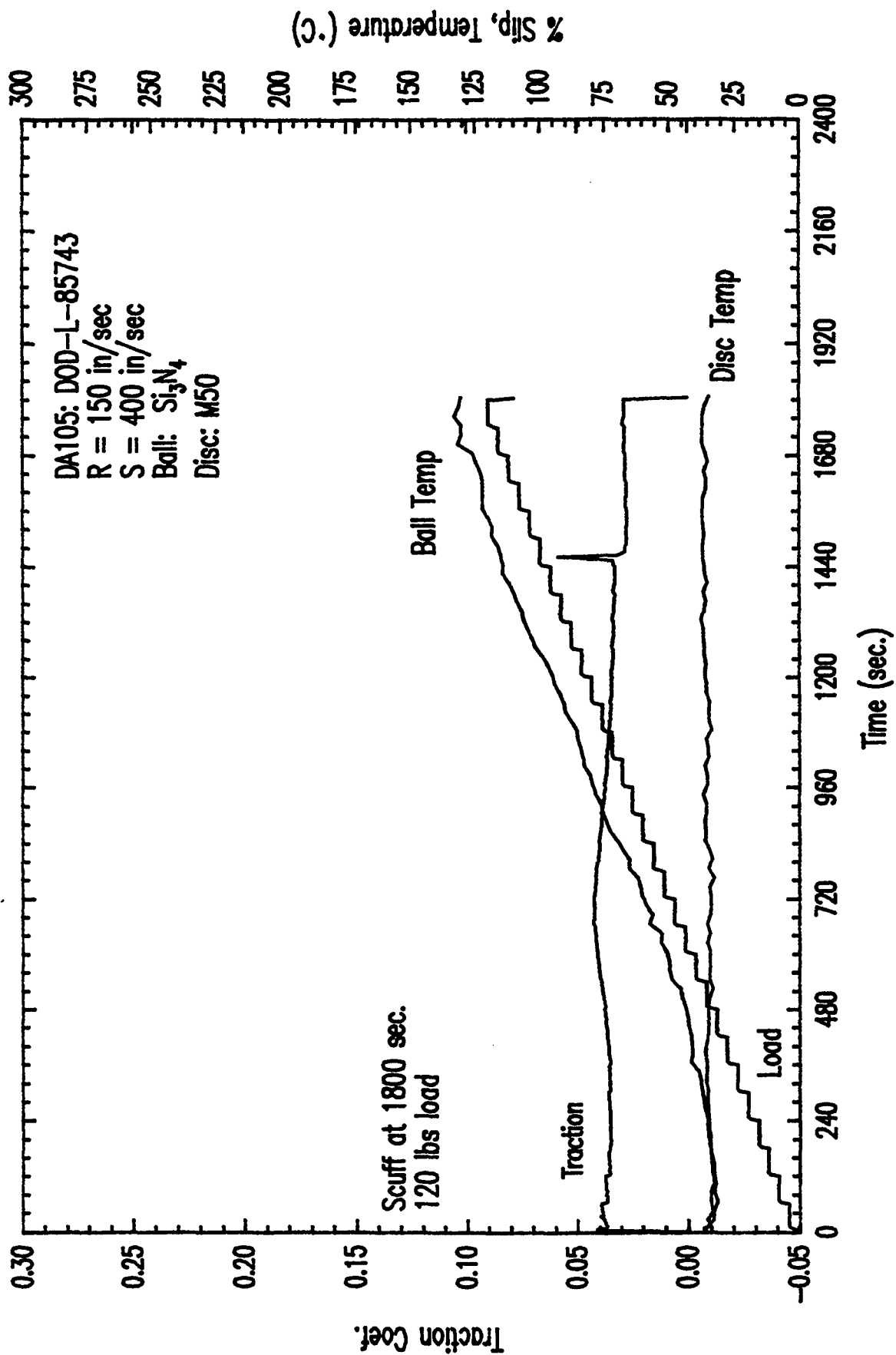
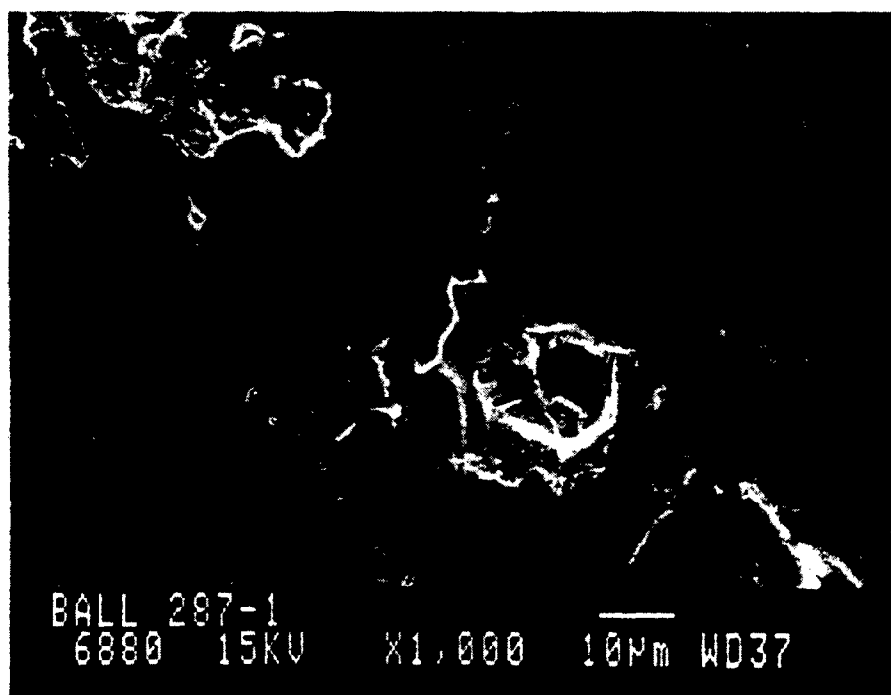


Figure 41c All steel load connected with simulated ball and disc R = 150 in/sec

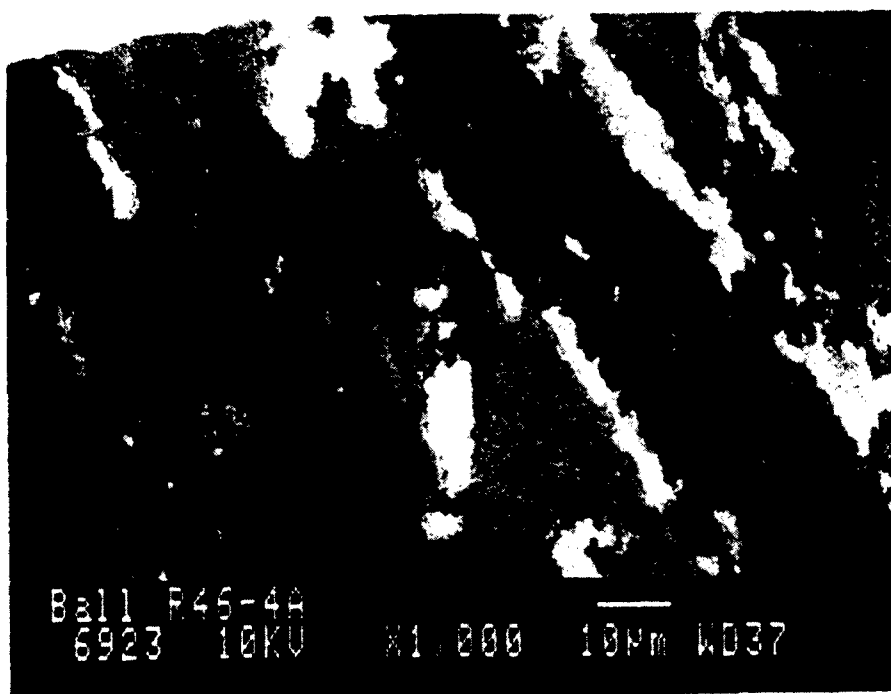


<DA105.SPW>

Figure 41b Hybrid load capacity test with formulated oil and R = 150 in/sec



(A)



(B)

Figure 42 Ball worn surface after load capacity test
(a) M50 steel and (b) Si_3N_4

basestock and fully formulated oils suggest similar tribological phenomena occurring in both contact with regards to interaction with, and the role of lubricating oil. Although Si_3N_4 material is more chemically inert, the interaction between the oil additives in the formulated oil and the steel disc surface of hybrid contact is adequate to produce the same tribological phenomena as in the all steel contacts.

The other similar behavior between the all-steel and hybrid contacts involved the frictional heat characteristics. Under the same condition of load, rolling and sliding velocities, the measured ball and disc specimen temperatures for Si_3N_4 on M50 and M50 steel-on-M50 steel were about the same. As discussed above, the traction coefficient in both contact pairs are similar. Therefore the rate of frictional heat generation in both hybrid and all-steel contacts are going to be similar, since the rate of heat generation $q = \mu P_{av} v$; where μ = friction coefficient, P_{av} = average nominal contact pressure, and v is the sliding velocity.

The frictional heat is dissipated by conduction and it is governed by the thermal conductivity of the contacting materials. Due to similarities in the thermal conductivity's of the Si_3N_4 material and the M50 steel material (33 w/mk for Si_3N_4 and 30 w/mk for M50 steel), the thermal dissipation and, hence, the specimen temperatures are expected to be similar. This is what we observed. If the thermal conductivity of the steel material component is significantly different from that of Si_3N_4 (for example 52100 bearing steel with thermal conductivity of 61 w/mk) then one would expect different thermal characteristics between the all steel and hybrid contacts.

All the reasons for the higher load carrying capacity of hybrid contact compared to all steel contacts when lubricated by the same oil is not fully understood yet, but it must be connected with the failure mechanisms during load capacity testing. In our tests, the failure point, which we termed scuffing, is characterized by high traction, relatively loud noise and loss of surface integrity.

The exact mechanisms scuffing are still a subject of debate and certainly not fully understood. There are several theories and criteria for occurrence of scuffing available in the literature. All the existing theories can be divided into three broad groups, (1) thermal, (2) plasticity, and (3) lubricant breakdown.

(1) Thermal: It has been suggested that when the surface temperature reaches a certain value, scuffing will occur [9,10]. This critical temperature is assumed to be the point at which desorption of the lubricant film or changes in lubricant mechanism of scuffing invokes thermoelastic instability at the contact interface. It is suggested that surface roughening is caused by local expansion from frictional heating, which eventually increases the severity of contact, and, consequently, initiate scuffing failure. There are other thermally based scuffing theories, which will not be discussed here.

(2) Plasticity: It has been proposed that scuffing will occur when the surface asperities are plastically deformed beyond a certain strain level [16]. Recent studies however have shown that a lubricated contact interface can sustain a much larger amount of pressure than proposed by the model without scuffing [17]. It has also been suggested that

scuffing is initiated by plastic roughening of the contact interface.

(3) Lubricant Breakdown: Scuffing theories based on lubricant breakdown suggests that when the lubricant film thickness is smaller than a certain critical value, scuffing will be initiated. It is hypothesized that under the condition of subcritical lubricant film thickness, local cold welding of the contacting surfaces will occur. This is local surface welding is associated with scuffing.

None of the above theories and criteria, can adequately explain the reason for the much higher load carry capacity of hybrid as compared to an all steel contacts. It is generally accepted that the scuffing process involves intense frictional heating, and is promoted by high sliding velocity and high contact pressure. Also, phenomenologically, scuffing involves gross and often severe plastic damage of the contact interface. Under high strain-rate compressive stress, adiabatic strain localization can occur. This strain localization generally is manifested in the form of bands of intense local shear. It requires high strain rate (sliding speed), high compressive stress, and high temperature. These are the same conditions required for scuffing. Could it be that scuffing, is due to local shear band formation resulting from adiabatic strain localization at the contact interface in the regions below the surface films? This is plausible scuffing mechanism the is worth further investigation.

If local shear band formation below the surface films is indeed the mechanism for scuffing, the higher load capacity of hybrid contact can be explained in terms of the higher shear strength of the "composite" material of the contact interface. Eventually the shear strain in the steel component alone will reach a critical value and scuffing will occur. In all-steel contacts where both the ball and the disc surfaces can plastically deform, the critical shear strain will be reached sooner by the contact interface.

Whatever the reason for the higher load carrying capacity of hybrid contact it has a major implication for lubrication of hardware that encounters severe contact conditions. Such hardware will require oil with several additives to protect the surface against catastrophic failure if it is made of all steel contact pairs. On the other hand, 'cleaner' basestock oil may be able to provide same degree of surface preservation for hybrid contact pairs.

6.4.4 Summary

Load carrying capacity tests were conducted with an ester basestock and a fully formulated aviation oils for a steel-on-steel contact and a Si_3N_4 -on-Steel hybrid contacts. For both oils, the hybrid contacts showed a much higher load carrying capacity than the all-steel contacts. The traction behaviors for the two types of contacts were very similar to one another, which suggest similar kinds of film formation especially on the disc in both contacts. The thermal characteristics for the all-steel and the hybrid contact pairs were very similar to one another. This was due to their similarity of thermal conductivity of M50 steel and Si_3N_4 materials. The superior load carrying capacity of hybrid contacts has a major technological implication in that hardware, such as bearings made of hybrid Si_3N_4 -steel contact pairs can be adequately lubricated by 'cleaner' basestock oils.

6.5 Oil-Off Test

For aircraft applications, it is desirable that the bearings be able to run for some period of time after oil flow interruption (oil-off). In fact, some bearings have oil-off run time requirement. The reason for this requirement or desire is obvious. Should the oil supply of an aircraft bearing be interrupted in mid-flight, additional running time of the bearing to allow safe landing is more than desirable.

In this study, comparative evaluation of the performance of Si_3N_4 ball and 440C stainless steel disc content pair and 440C Steel-on 440C Steel pairs under the oil off condition was conducted. Several lubricants covering a wide range of chemical compositions were evaluated. Most the evaluated oils were the ones used primarily in aviation and aircraft industry.

6.5.1 Experimental Details

The oil-off tests were conducted on WAM1 machines using the following test parameters.

Ball: 440C, Si_3N_4 (1/2" diameters).

Disc: 440C, ($R_a = 3\mu$ in).

Load: 51 lbs.

Temperature: 100°C

Starting Rolling Velocity: 100 in/sec.

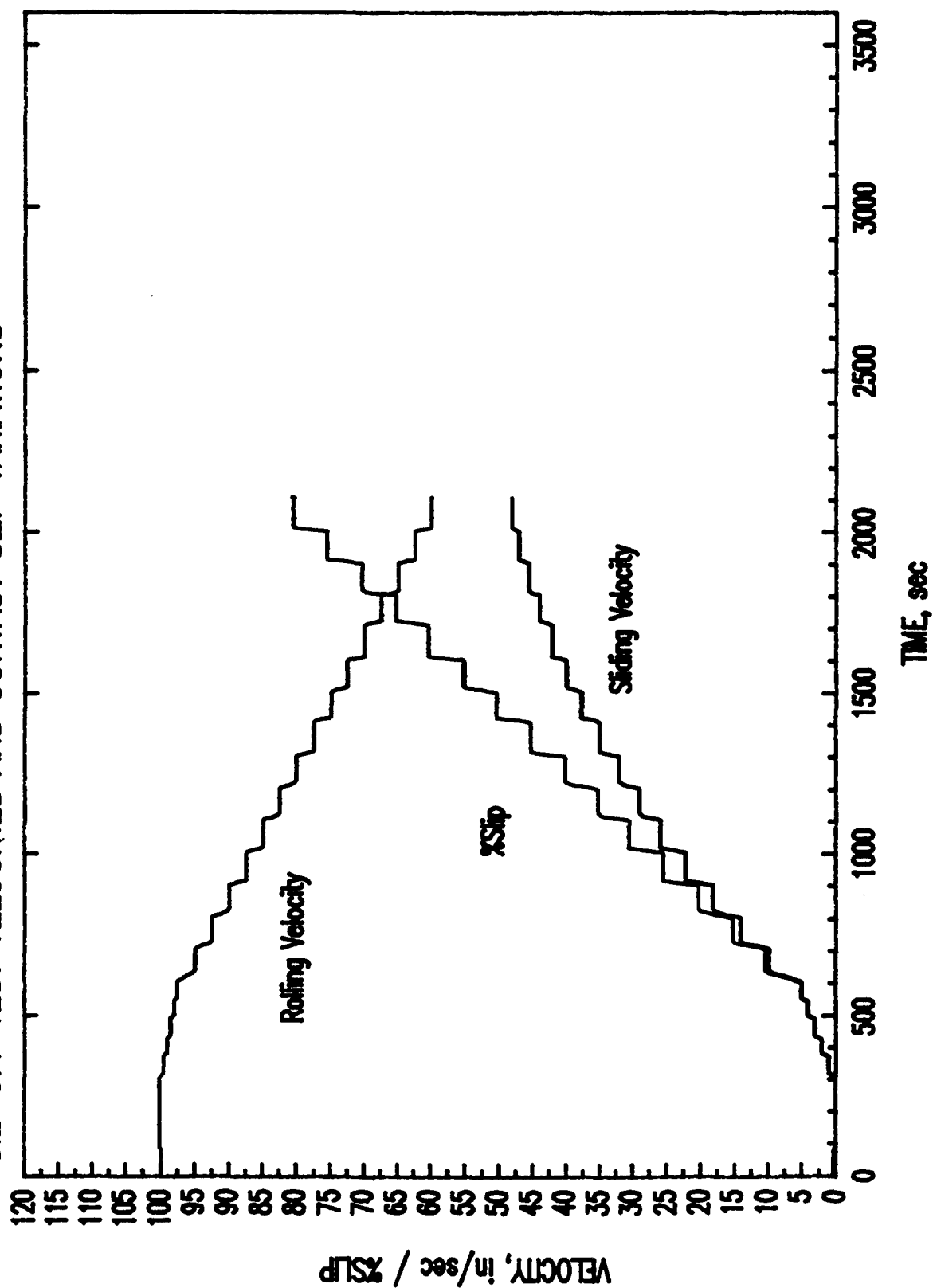
Oil Supply: drip feed at 11 ml/hr for 300 seconds

6.5.2 Procedure

The ball and disc specimens are mounted on their respective spindles and heating to the desired temperature of 100°C. Both the ball and the disc specimens are set into motion at 100 in/sec. The oil is drip fed onto the disc at a rate of 11 ml/hr. The contact is loaded to 51 lbs. and operated under pure rolling at 100 in/sec for 300 sec, at which point the oil supply is turned off. This is done in order to simulate a Hertzian contact similar to a typical bearing application. In order to accelerate the failure process at the contact interface, the severity of contact is gradually increased. This is accomplished by decreasing the rolling velocity, which will have the effect of reducing the EHD lubricant film thickness. Sliding is also introduced at the same time, resulting in the shearing of the contact interface and frictional heating. Figure 43 shows the variation of the rolling and sliding velocities with the resulting contact slip percent during the oil-off test. The increase in contact severity is continued until failure, which is characterized by sudden increase in traction coefficient.

During each test, the traction coefficient and the specimen temperatures are continuously monitored. At the conclusion of each test, the ball and disc specimen surfaces are examined to characterized the nature and severity of damage. Tests are run with five different oils that span different molecular structures. The durability and the performance of each contact pair under oil-off condition are judged by the time and slip level to failure.

OIL-OFF TEST VELOCITIES AND CONTACT SLIP VARIATIONS



6.5.3 Results and Discussion

A typical plot of the traction coefficient, contact slip and specimen temperatures during the oil-off test is shown on Figure 43. The figures, which are from the test with fully formulated ester based aviation oil (ETO-25) show that the hybrid contact pair of the Si_3N_4 ball and 440C disc ran for a much longer time and much higher contact slip before failures. A summary of the test results for all the oils evaluated is shown in Table 7. The contact slip level at which failure occurs is also shown on Figure 45.

From these results, a pattern that is consistent for all the oils evaluated is the higher failure slip for the hybrid compared to all-steel contact pairs. Details of the results for each kind of oil will now be presented.

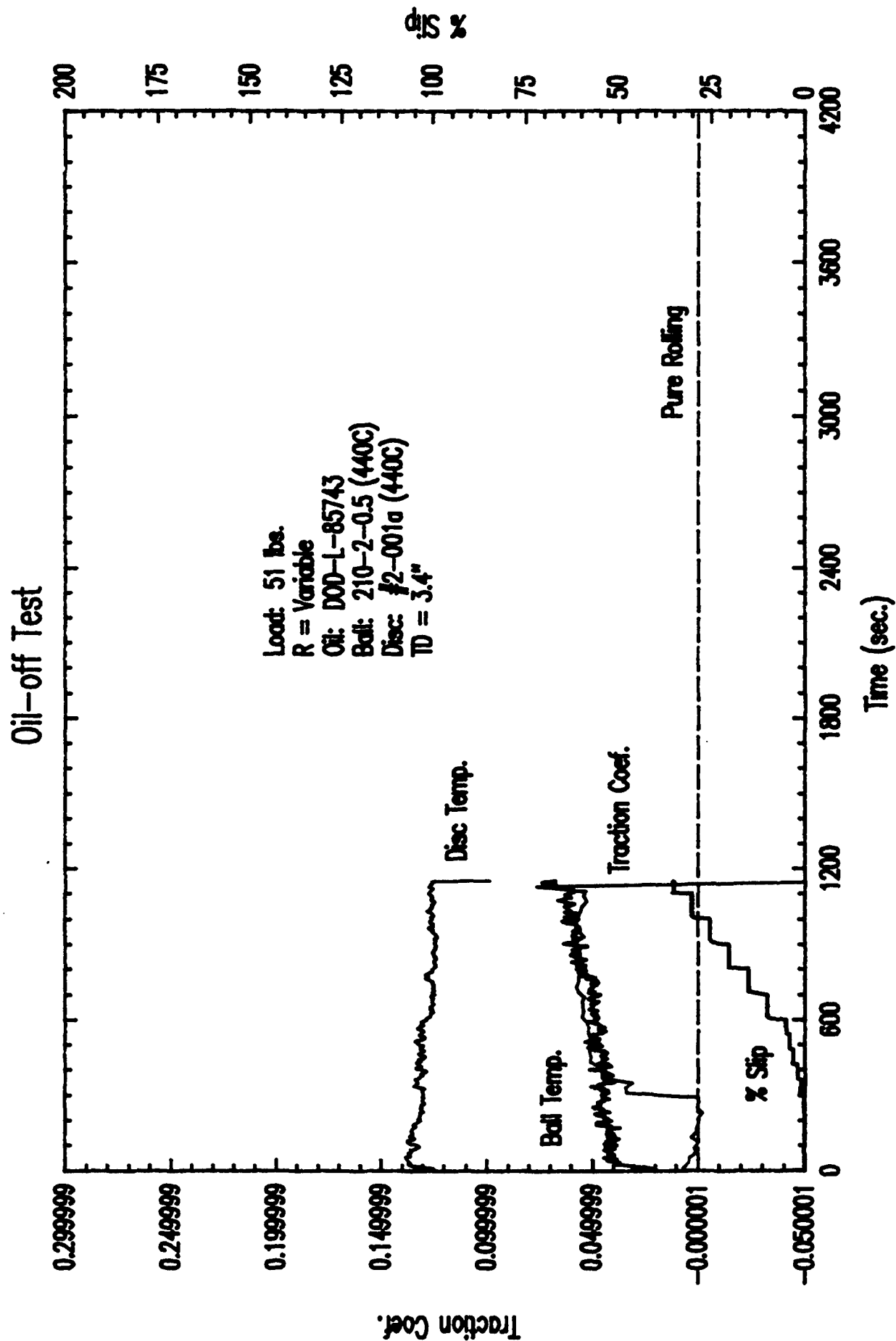
6.5.3.1 Ester Oils

In both the formulated and the basestock ester based oil, the hybrid contact showed much higher levels of durability under the oil off conditions. For the basestock, the all-steel contact failed at 15% slip while the Si_3N_4 -steel hybrid pair failed at 75% slip. The average traction coefficient in both kinds of contacts was comparable at about 0.05. For the formulated oil, the failure slip was higher for both all-steel and hybrid contacts (35% for all-steel and 85% for hybrid) when compared to the basestock oil. This improvement reflects the effect of the additives in providing better protection for the contact surface against catastrophic failure. As expected, the improvement in the steel-on-steel contact was more pronounced than the hybrid contact. This is because both surfaces are chemically interacting with the oil additives in the all-steel pair, while only the steel disc surface is involved in the hybrid contact pair. Nonetheless, the hybrid contact still performs much better than the all-steel contact in the formulated oil.

The failure mechanism during the oil-off test with the ester fluids is scuffing. Figure 46 shows the surfaces of the specimens after failure. For the all-steel contact pair, both the ball and the disc surfaces show severe wear and damage typical of scuffing phenomenon (Figure 46a). For the hybrid contact pair, on the other hand, the damage on the ball consist primarily of metal transfer (Figure 46b). The damage on the disc consists of some wear, but mostly plastic flow. The damage on the disc can be characterized as micro-scuff. In the hybrid contact pair, the damage is much milder compared to the all-steel pairs in spite of being subjected to a more severe contact conditions.

6.5.3.2 PFPE Fluid (Krytox 143AB)

In the tests run with this fluid, the hybrid contact of Si_3N_4 ball and 440C disc also showed better performance compared to the all-steel 440C-on-440C contact. The hybrid contact failed at 95% slip while the all-steel pair failed at 75%. This fluid produced higher durability of contact interface than ester based fluid, even the formulated one. The average traction coefficients with the PFPE fluid, however, were significantly higher than the ones with ester based fluid (0.1 for PFPE, 0.055 for ester fluid). The higher traction was observed with both the all-steel and the hybrid contact pairs. A significant implication of this higher traction coefficient is the higher rate



<test72.spw>

Figure 44a All-steel contact pair

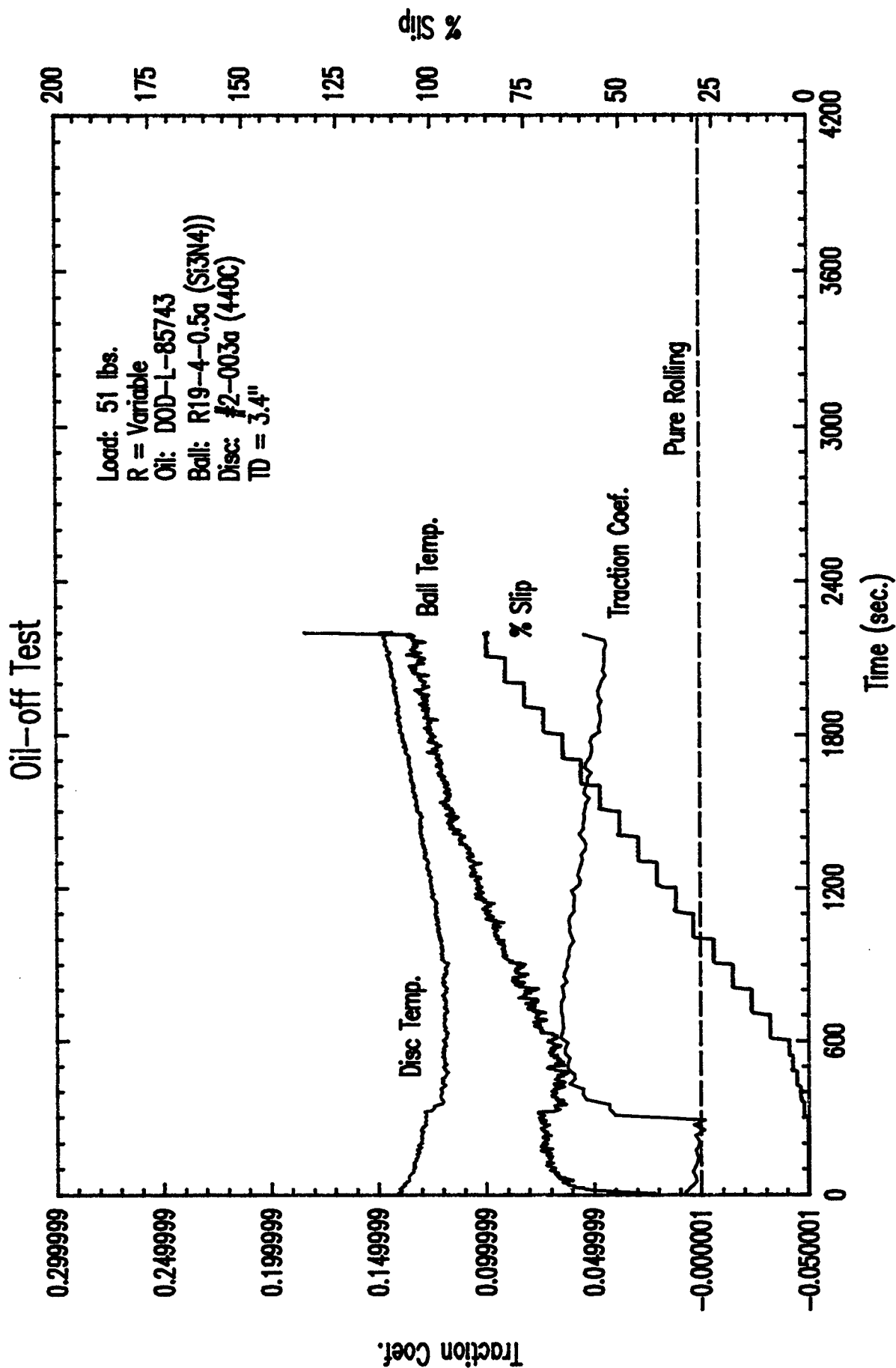


Figure 44b Hybrid contact pair

<TEST74.app>

SUMMARY CHART OF OIL-OFF TESTS

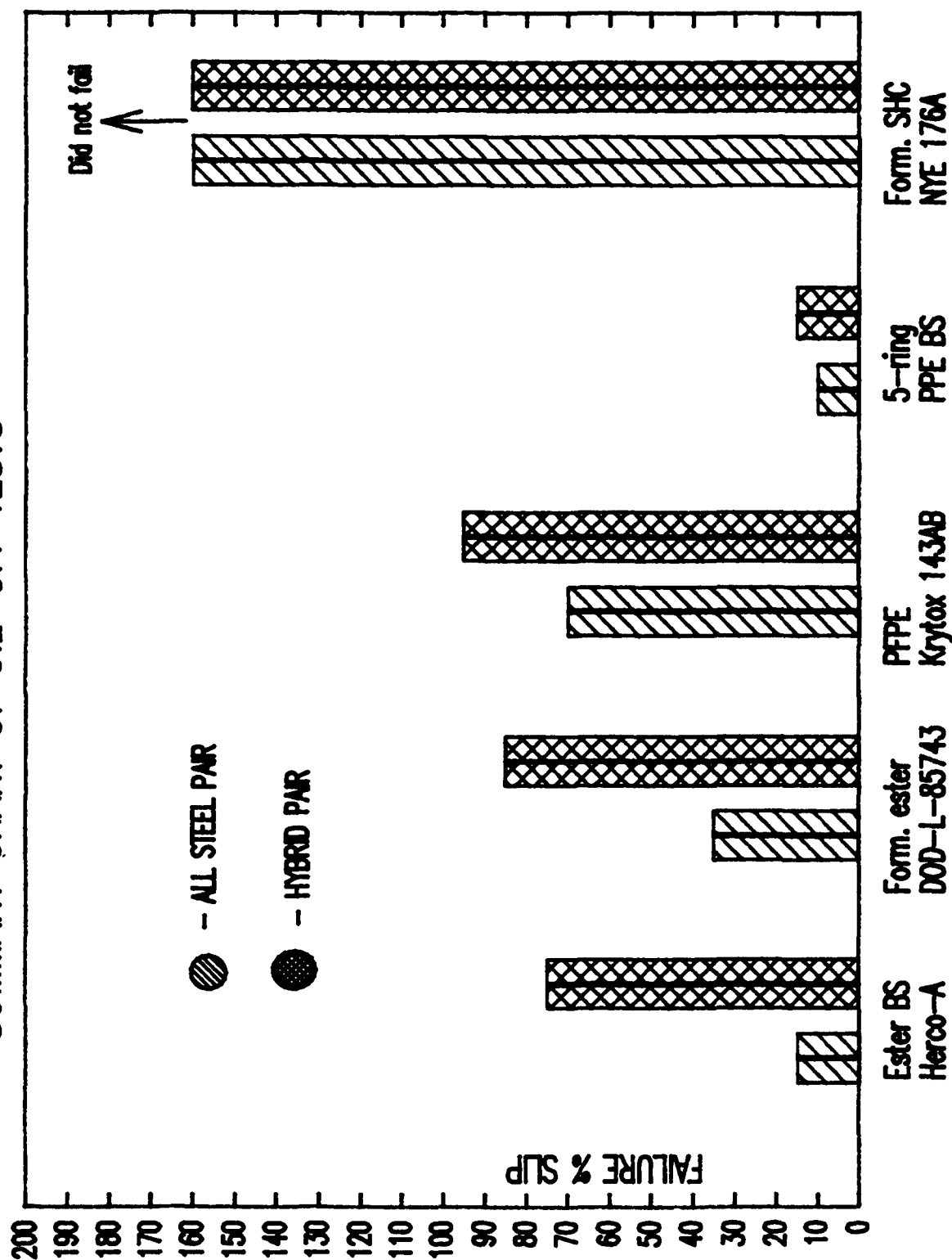


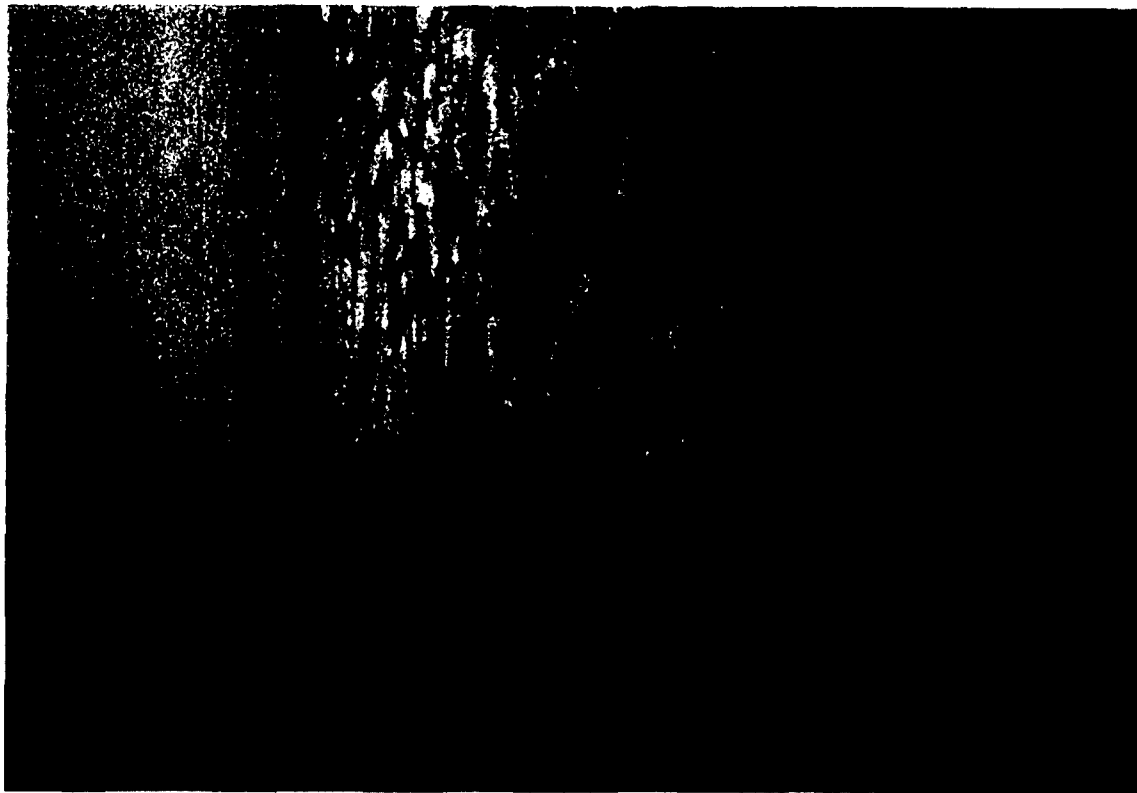
Figure A5 Summary chart of hybrid and all-steel contacts during oil-off tests

<OFFBWLSPW>

Table 7

Oil - Off Test Results Table

| Oil | Material Combination | Failure Slip (Time) | Average Traction Coef. | Max. Ball Temp. (°C) | Max. Disc Temp. (°C) | Comments |
|---------------------------------|--|--------------------------|------------------------|----------------------|----------------------|--|
| Esther B.S. (Herco-A) | 440C Steel On 440C Steel | 15% (700 sec) | 0.048 | 75 | 100 | Severe wear and damage on ball. Surface distress and cracking on disc. |
| | Si ₃ N ₄ On 440C Steel | 75% (1945 sec) | 0.056 | 94 | 105 | Massive metal transfer to ball and severe wear on disc. |
| Formulated Ester based (ETO-25) | 440C On 440C | 35% (1140 sec) | 0.06 | 95 | 100 | Severe wear and gross surface damage on ball and disc. |
| | Si ₃ N ₄ On 440C | 85% (2198 sec) | 0.055 | 105 | 110 | Massive metal transfer to ball and severe wear on disc. |
| PFPE (Krytox 143AB) | 440C On 440C | 70% (1782 sec) | 0.09 | 130 | 110 | Severe wear and film on ball and disc. |
| | Si ₃ N ₄ On 440C | 95% (2380 sec) | 0.11 | 160 | 140 | Small amount of metal transfer and patches of larger transfer that is oxidized on the ball. Gray film and other color films on disc. |
| 5-Ring PPE B.S. | 440C On 440C | 10% (760 sec) | 0.055 | 70 | 100 | Brownish and gray film and some wear on the ball. Wear and gray film on the disc. |
| | Si ₃ N ₄ On 440C | 15% (780 sec) | 0.055 | 75 | 100 | Patches of small amount of metal transfer and Hertzian cracks on all. Severe wear and patches of gray film. |
| Formulated SHC (NYE 176A) | 440C On 440C | 160% no scuff (3600 sec) | 0.032 | 100 | 100 | No wear on ball or disc. Continuous brownish film on ball. |
| | Si ₃ N ₄ On 440C | 160% no scuff (3600 sec) | 0.031 | 84 | 100 | No wear on ball or disc, but continuous brown film on both. |



Steel Ball

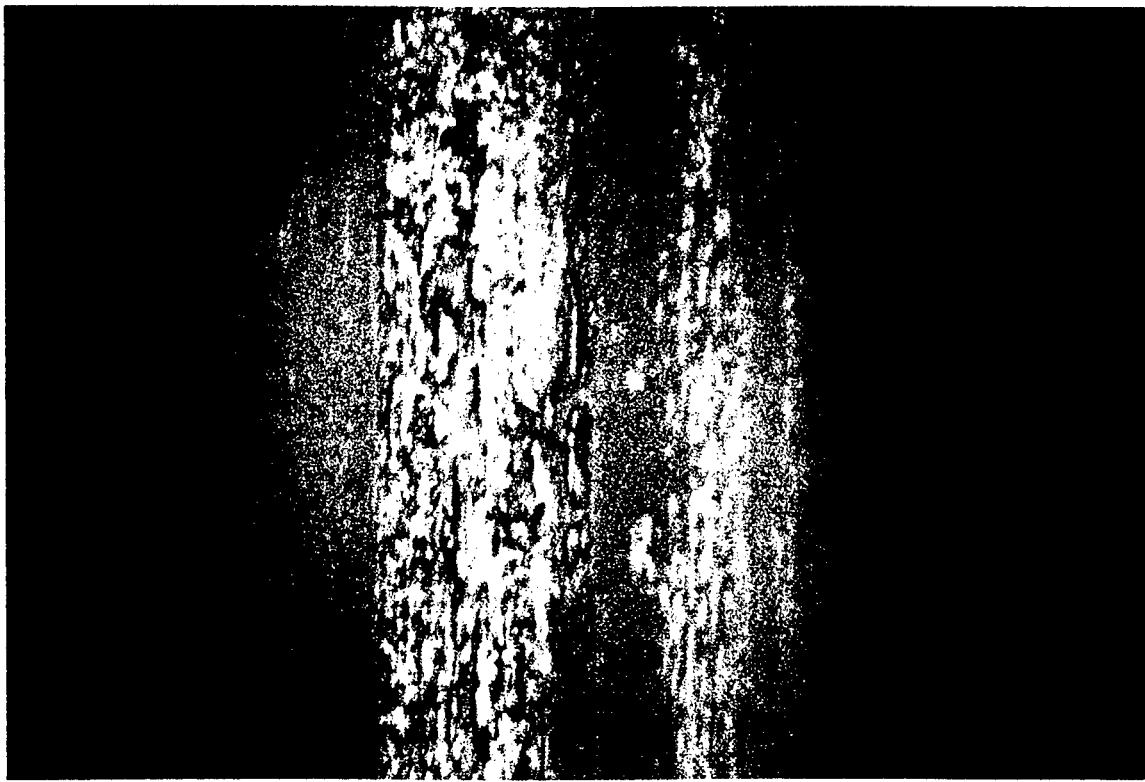
200 μ m



Steel Disc

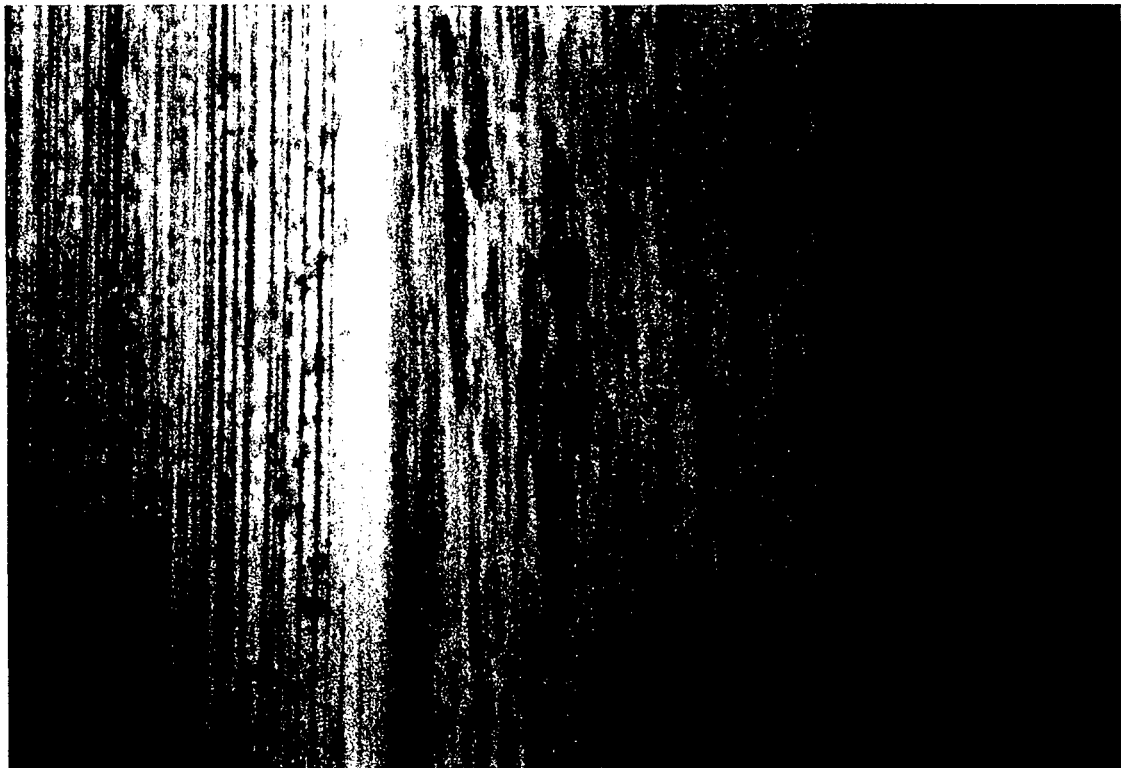
200 μ m

Figure 46a Oil-off test with Herco-A for all-steel pair



Si₃N₄ Ball

200 μm



Steel Disc

200 μm

Figure 46b Oil-off test with Herco-A for hybrid pair

of frictional heat generation that will ensue. Bearings run with PFPE under oil-off conditions will be running hotter than bearings lubricated with ester fluid under similar condition.

The failure process in the all-steel contact pair involves the formation of surface film and wear. There appears to be some evidence of scuffing on the disc surface as well (Figure of 47a). In the hybrid contact pair, there is metal transfer onto the Si_3N_4 ball and perhaps some abrasive wear as indicated by the presence of some fine scratches (Figure 47b). The steel disc shows some film formation, plastic flow and wear. The films on the steel surfaces in both the all-steel and the hybrid contacts are most likely a complex mixture of reaction and degradation product of the lubricant and iron (Fe). It is a well documented fact that PFPE degradation and decomposition is catalyzed by the steel surface [18-20]. Less film is observed in the hybrid contact pair, again due to the fact that only one of the surfaces is involved in the surface reaction and chemical interaction.

6.5.3.3 Polyphenylether (PPE)

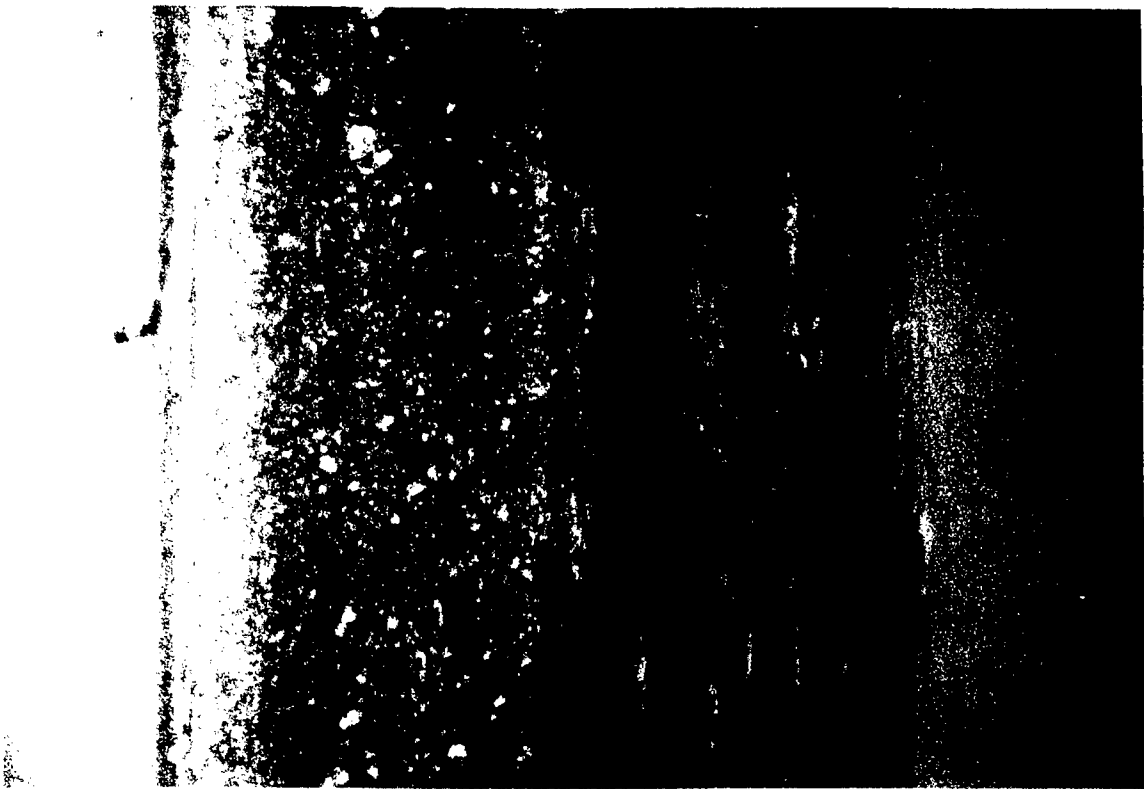
Among all the fluids evaluated, the PPE lubricated contacts showed the least durability under the oil-off condition (Figure 45). Even with this relatively poor performing fluid, Si_3N_4 -steel hybrid contact showed a higher durability than the all-steel contact. The hybrid contact failed at 15% contact slip, while the all-steel contact failed at 10%. In both kinds of contact pairs, the average traction coefficient prior to failure was about 0.055.

Examination of the specimen surfaces shows that the failure mechanism in the all-steel and the hybrid contacts are quite different. For the all-steel contact (Figure of 48a), both the ball and the disc surfaces are covered with a film, presumably oxide. The PPE fluids are known to cause oxidation of steel surfaces and perform very poorly as a lubricant under boundary conditions. The severe tribological contact conditions of the oil-off test are certainly under boundary lubrication regime. It appears the rate of oxide growth at the contact interface is the life limiting process for the all-steel contact pair tested with this fluid. In the Si_3N_4 /steel hybrid contact on the other hand, there is very little evidence of oxide growth. Instead, the failure process involves metal transfer onto the Si_3N_4 and formation of Hertzian cracks on the ball (Figure of 48b). The damage on the disc consists of some wear and plastic flow, but no evidence of oxides.

6.5.3.4 Synthetic Hydrocarbon (Formulated)

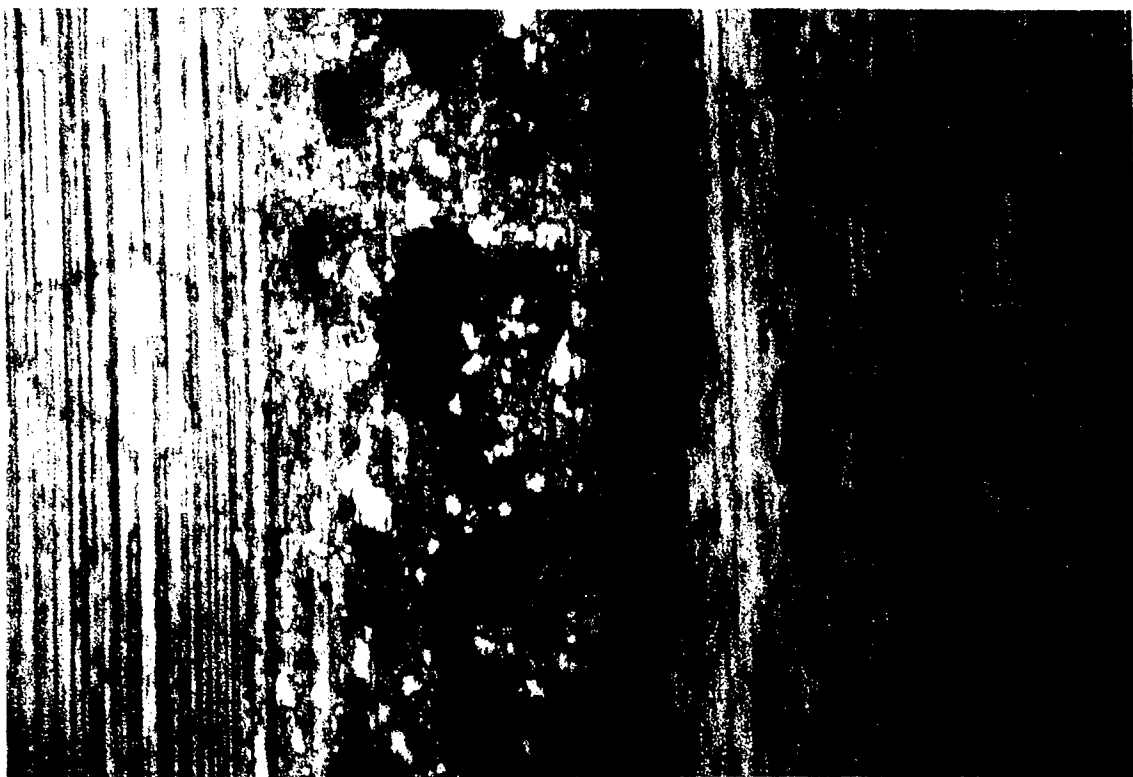
Among the five oils evaluated with the current oil-off test procedure, the fully formulated synthetic hydrocarbon is the only one in which failure did not occur either for the all-steel or the hybrid contact pairs. Plots of test data for both the steel-on steel and the Si_3N_4 -on steel contact pairs are shown in Figures 49a and 49b, respectively. In both cases, the traction coefficient remained relatively low. It decreased with increasing contact slip as expected due to increase in frictional heating. Compared to the other fluids the average traction coefficient with this fluid was also very low, with a value of about 0.03. The low traction coefficient would translate to lower shear stress and lower frictional heating at the contact interface.

Examination of the ball and disc surfaces provided some indication as to the excellent



Steel Ball

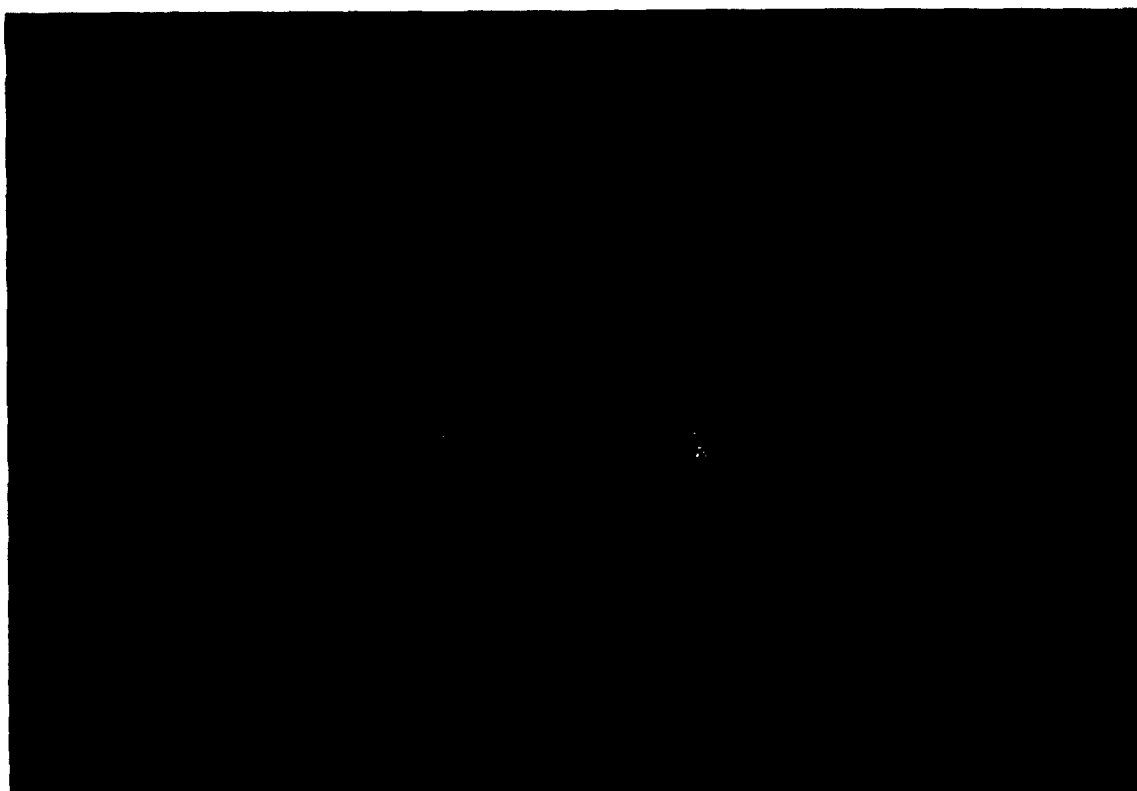
200 μ m



Steel Disc

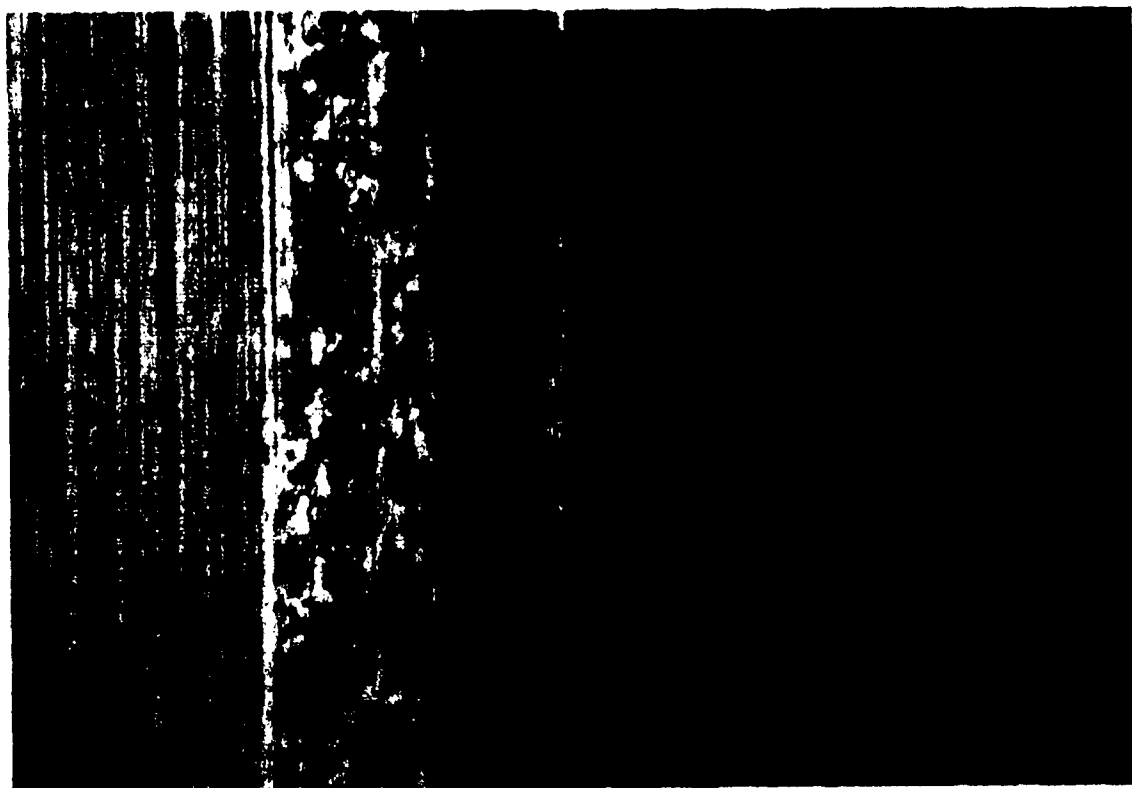
200 μ m

Figure 47a Oil-off test with Krytox 143AB for all-steel pair



Si₃N₄ Ball

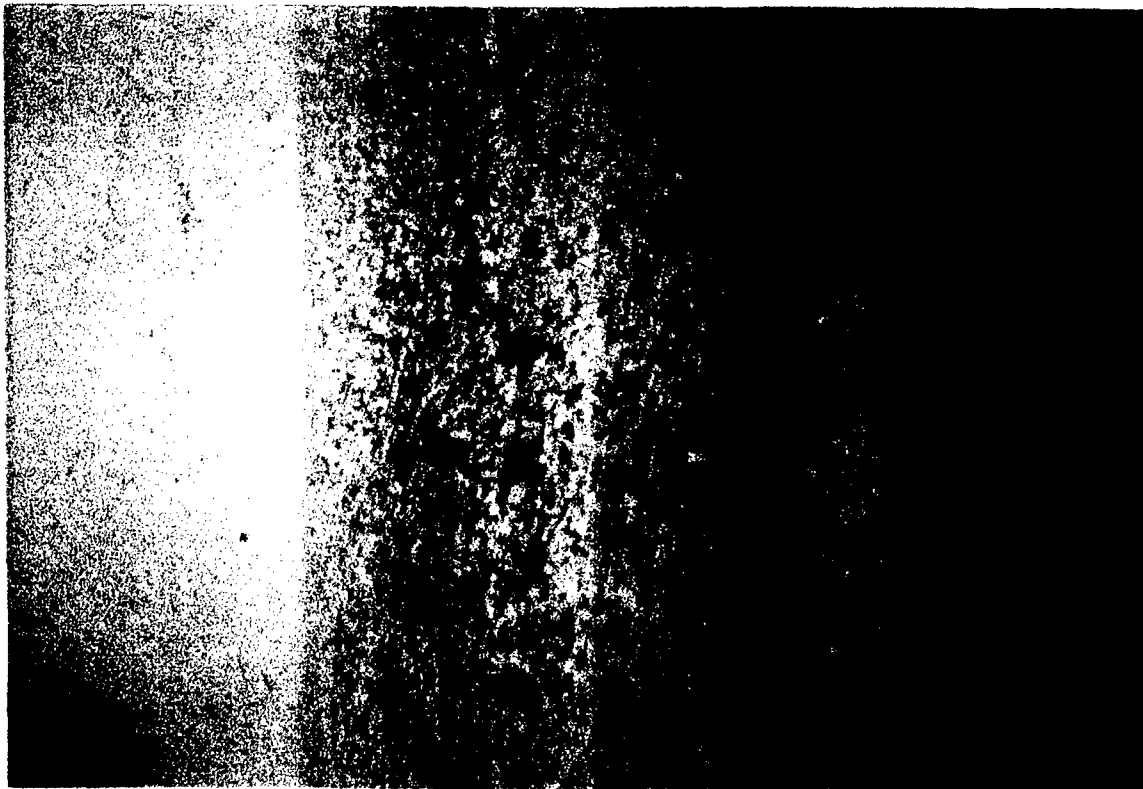
200 μm



Steel Disc

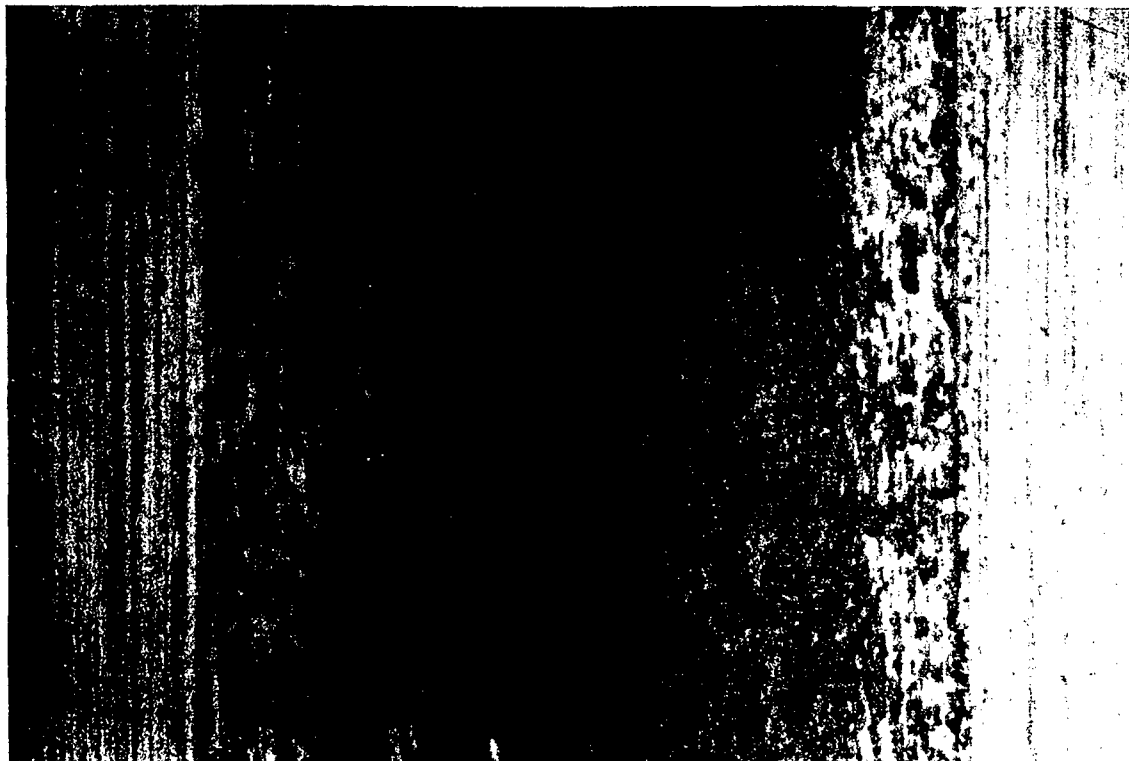
200 μm

Figure 47b Oil-off test for hybrid contact with Krytox 143AB



Steel Ball

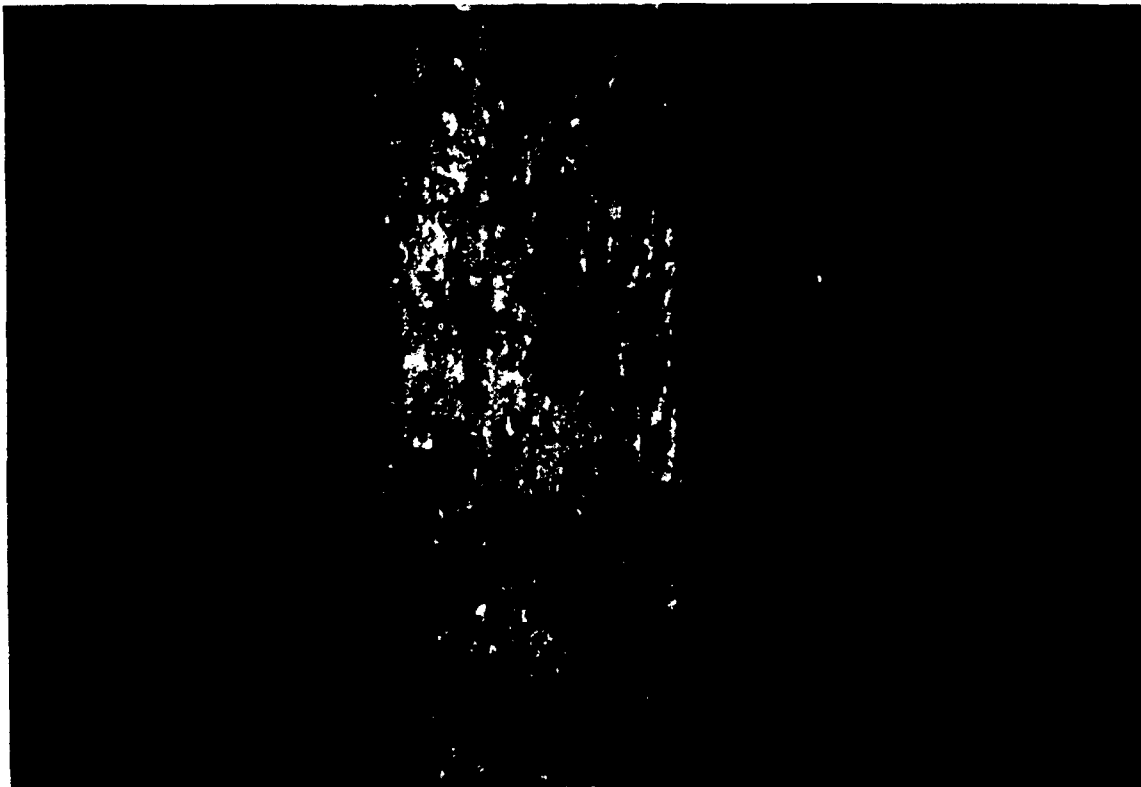
200 μ m



Steel Disc

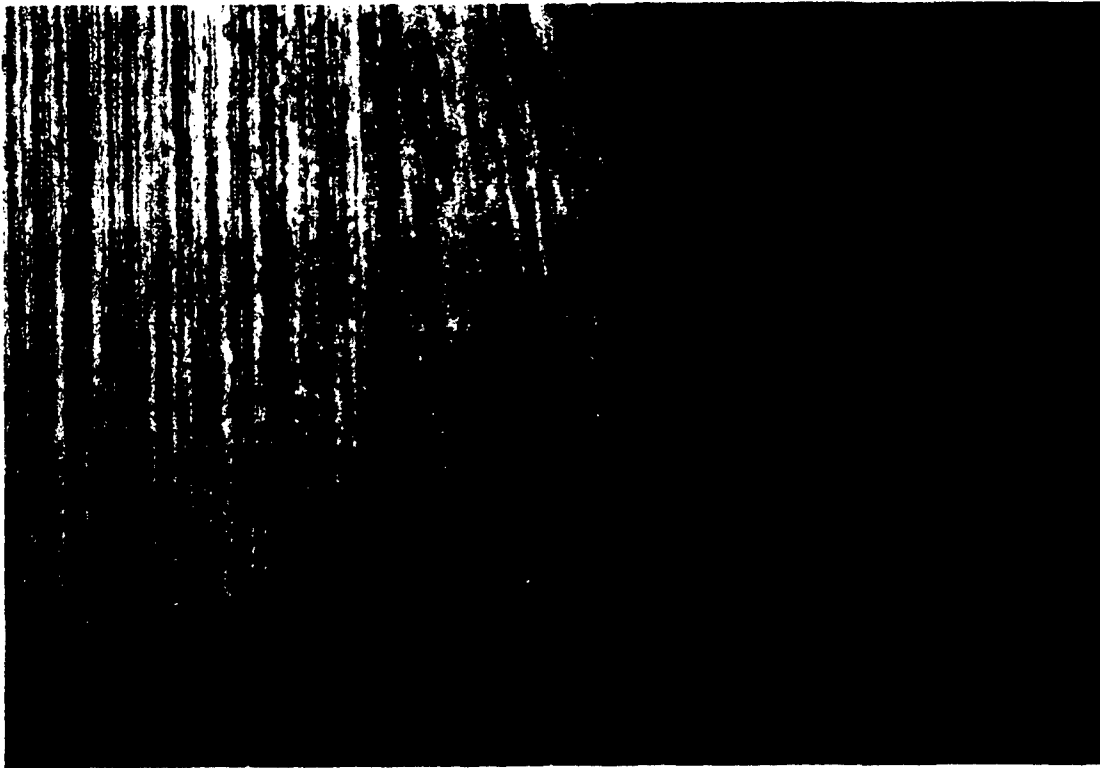
200 μ m

Figure 48a Oil-off with PPE B.S. for all-steel pair



Si₃N₄ Ball

|-----|
200 μm



Steel Disc

|-----|
200 μm

Figure 48b Oil-off test with PPE B.S. for all Hybrid pair

Oil Off Test

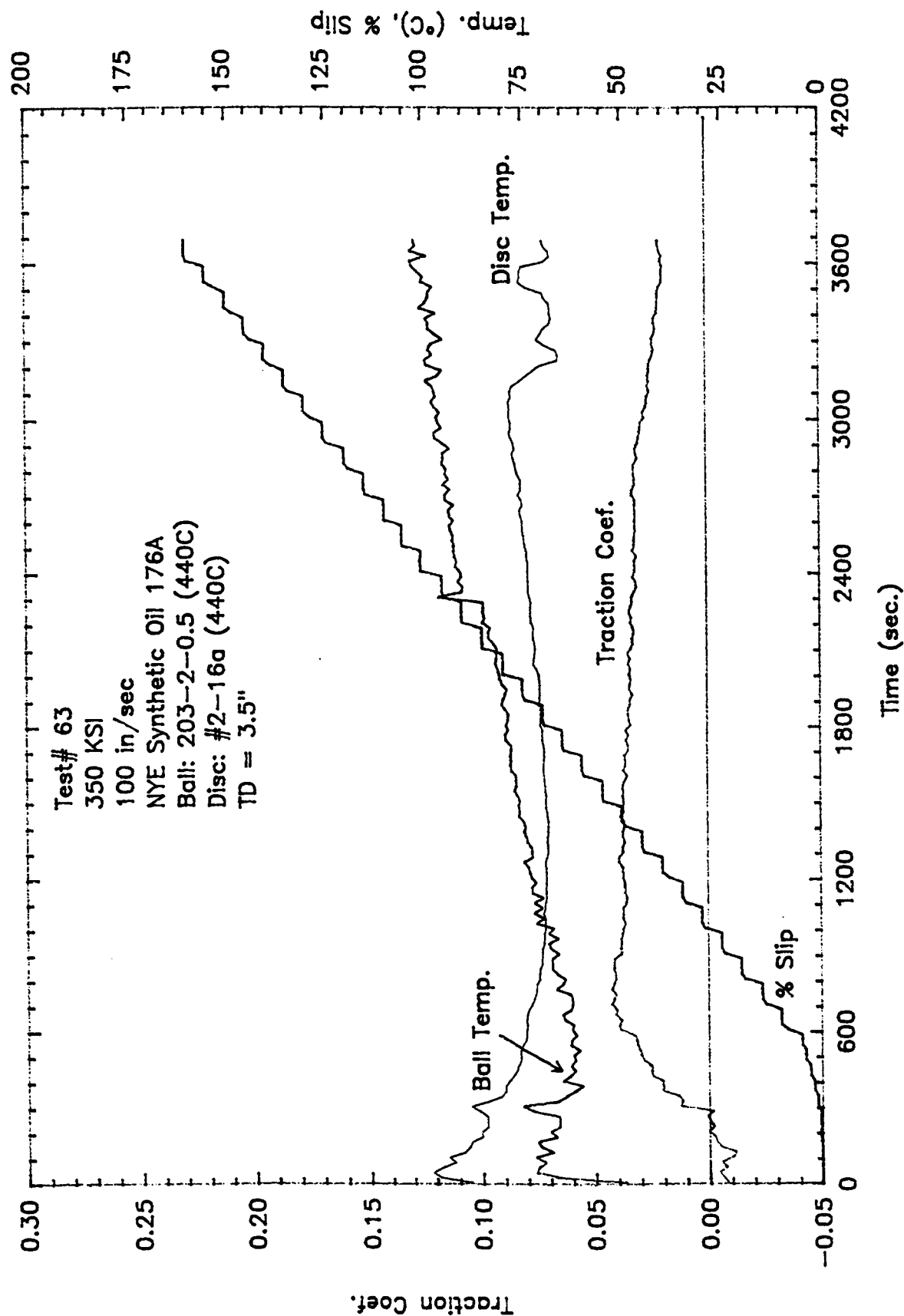


Figure 49a Oil-off test with the formulated synthetic hydrocarbon oil for all-steel

Oil Off Test

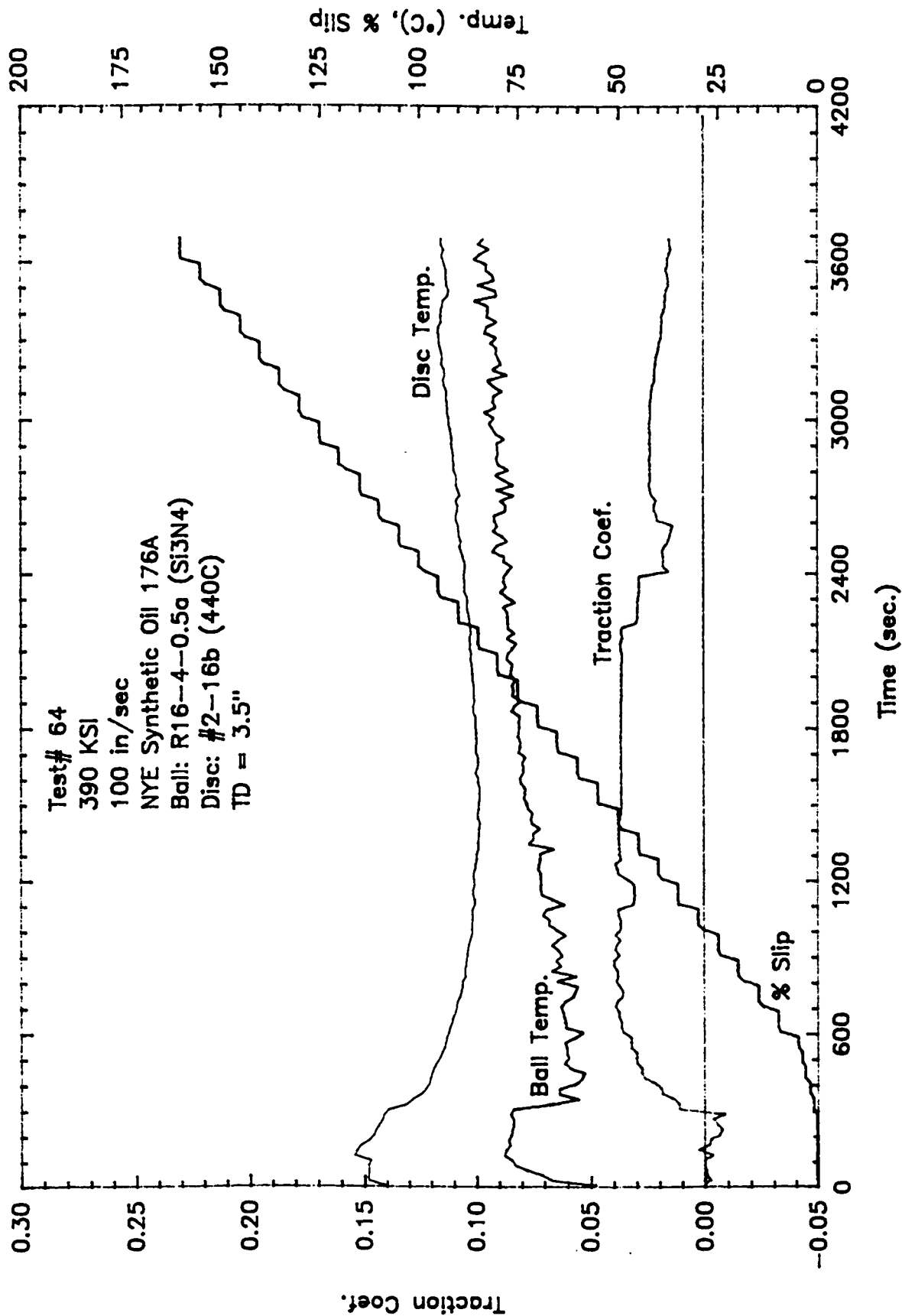


Figure 401. Oil off test with the formulated synthetic hydrocarbon oil for hybrid

performance of this oil. In both all-steel (Figure 50a) and the hybrid (Figure 50b) contact pairs, there was no wear or little change on the disc surface. Both the steel and the Si_3N_4 ball surfaces were covered with a brownish film. Although the exact nature and compositions of these films are not known, they were formed from the proprietary additive package in the oil. The films were formed perhaps by a combination of chemical reaction and physical absorption/deposition. This conclusion is based on the fact that a good film is formed on the Si_3N_4 ball in spite of its relatively low chemical reactivity. There appears to be more film on the steel ball, an indication of its higher chemical reactivity

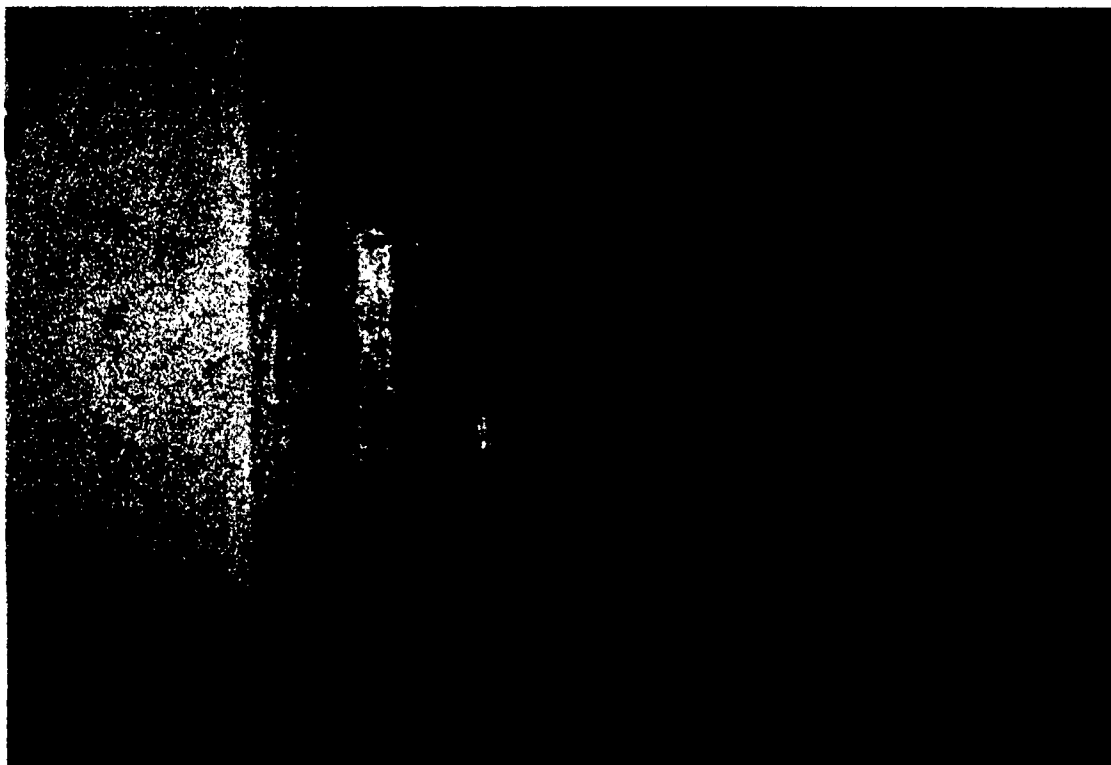
Whatever the mechanism of the film formation with this oil, the role of the film is indeed the key to the excellent performance of the oil under oil-off conditions. The film, probably formed early during the test is thick enough to physically separate the ball and the disc surfaces, thereby preventing wear on the disc or ball surface. The film also has a low shear strength, thereby accommodating the shear imposed by the high contact slip and hence a low traction coefficient. The film appears durable enough in that it protected both the ball and the disc surface against failure even after the oil has been turn-off. This oil, NYE 176A, has achieved the goal of surface chemical conditioning proposed under Task II of this effort

6.5.4 Summary

Tribological performance and durability of an all-steel and Si_3N_4 -on-steel hybrid contact pairs were evaluated under the oil off condition using five different oils. In all cases, the hybrid contact pair of Si_3N_4 ball and steel disc showed much higher durability and tribological performance compared to the all-steel contact pair. Among all the oils evaluated, the best performance is by the fully formulated synthetic hydrocarbon, and the worse performance was by the 5-ring PPE basestock fluid. The failure mechanisms also varied depending on the type of oil. In ester based oils, the all-steel contact pair failed by a scuffing mechanism while the hybrid pair failed by massive metal transfer onto the Si_3N_4 ball surface and plastic flow with wear on the steel disc. In the PFPE fluid, the failure process involved surface film formation from the fluid degradation and reaction with the steel surfaces. There appeared to be some evidence of scuffing also. For hybrid contact pair, metal transfer onto the Si_3N_4 ball was also prevalent in addition to film formation on the steel surface. The failure of the all-steel contact pair in the PPE fluid was by massive oxide build up. For the hybrid contact pair on the other hand, there was little or no oxide build up. Instead there was massive metal transfer onto the Si_3N_4 ball and formation of Hertzian cracks. The synthetic hydrocarbon formed durable boundary films in both the all-steel and hybrid contact pairs. The film protected the surfaces against wear and damage and also provided a low traction coefficient. Whatever the lubricant used for bearing lubrication, the hybrid bearing consisting of Si_3N_4 rolling elements and steel races will give a much better performance under oil-off conditions based on the results presented above.

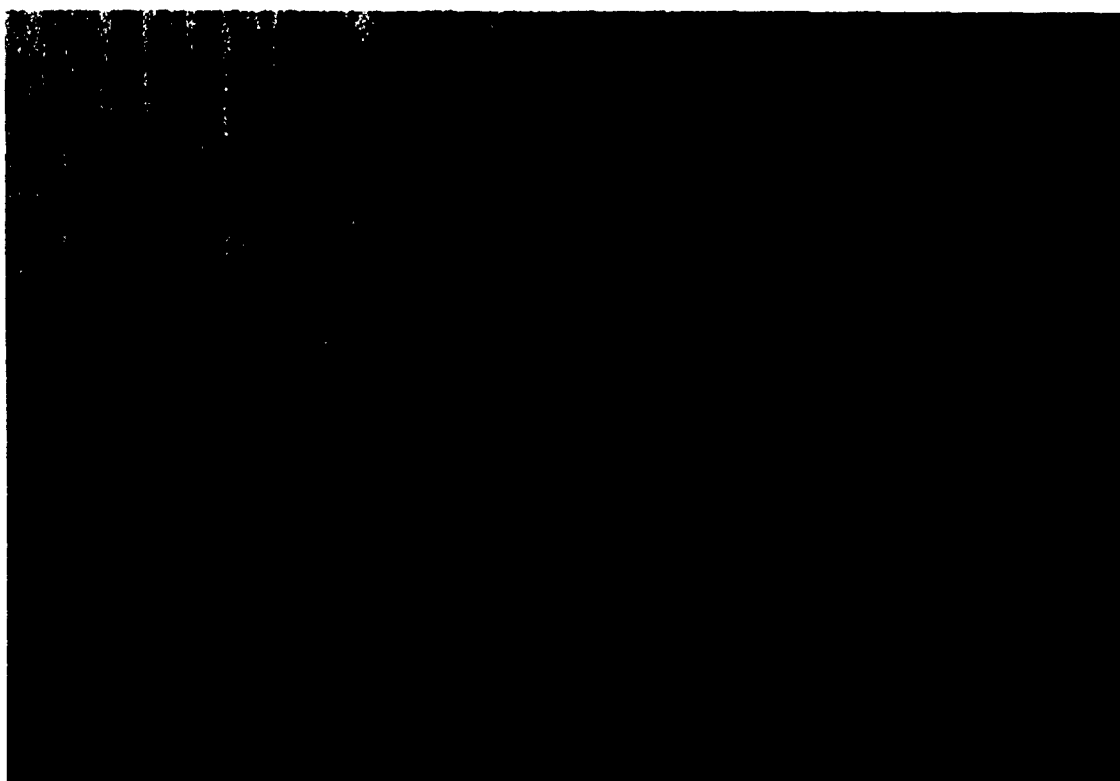
6.6 Grease Lubrication Test

A number of rolling element bearings were lubricated with grease. Grease is a semi-solid consisting of two or more components. There is a fluid phase that forms the lubricating fluid film and there is a thickener. Most greases also contain additives to improve tribological



Steel Ball

200 μm



Steel Disc

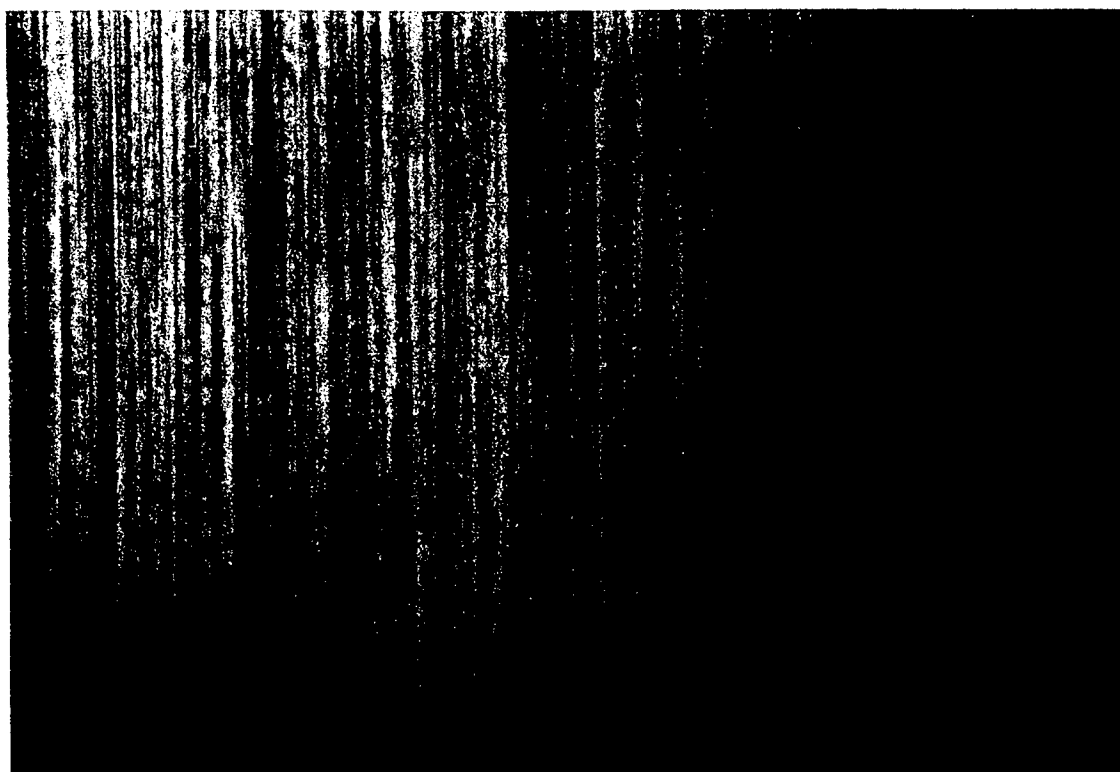
200 μm

Figure 50a Oil-off test with NYE 176A for all-steel pairs



Si₃N₄ Ball

200 μm



Steel Disc

200 μm

Figure 50b Oil-off test for Hybrid contact with oil NYE 176A

performance. The fluid phase in greases consists primarily of mineral or petroleum oils and synthetic fluids. Thickeners are often metallic soaps. The blends of additives used in greases are similar to the ones used in formulating oils. Commonly used additives include extreme pressure (EP), antiwear, friction modifier, oxidation and rust inhibitors.

Because greases are physically semi-solids, they are capable of resisting deformation and have considerable ability to remain at the contact interface. Lubrication with grease has many advantages. It eliminates auxiliary equipment for pumping or circulation oil, resulting in both size and weight reduction of components. In addition, only a small amount of grease is required for effective lubrication. Greases are particularly preferred over oil lubrication in applications where frequent lubrication service is difficult.

Since many of the all-steel bearings which can be replaced by hybrid bearings are likely to be grease lubricated, it was useful to do a comparative evaluation of the tow material combination performance when lubricated with grease. For this purpose, tests were run with all-steel and Si_3N_4 -steel contact pairs with five different greases. The primary goal of the tests was to evaluate the tribological durability of the tow kinds of contacts under grease lubrication.

6.6.1 Test Details

All of the grease lubrication tests were run on the WAM3 machine. Details of the test machine have been previously described. The tests were run with the following parameters:

Ball: Si_3N_4 , M50 steel (13/16" diameter, smooth)

Disc: M50 steel ($R_a=3\mu\text{in}$)

Rolling Velocity: 100 in/sec

Load: 20 lbs.

Temperature: Ambient (frictional heating occurs during test)

Table 8 shows the five test greases with their composition (fluid and thickener) and viscosity at 40 °C. The selection of test greases represents the advanced, high performance formulations. The selection also covers a wide range of the base fluids and thickeners.

6.6.2 Procedure

Tests were run using steel ball-on-steel disc and Si_3N_4 ball-on-steel disc contact configurations for each of the greases. At the beginning of each test, the grease being evaluated was generously applied to the disc surface. With the ball and disc surface velocities set to 100 in/sec, the contact was loaded to 20 lbs. The first 300 sec of each test was operated under pure rolling. The severity of contact was then gradually increased through the introduction of contact slip. This was done in a predetermined manner. Between 300 and 600 sec, the contact slip was increased by 5% ever 5 minutes. This was continued until the failure of the contact interface. The grease was not re-circulated during the test.

The failure point was determined by a sudden rise in the traction coefficient. Failure was often accompanied by a loud noise. The durability of the all-steel and the hybrid contact pairs was

Table 8 Various Grease Material Properties

| Grease | Fluid Type | Thickener | Viscosity at 40 °C (cSt) |
|---------------------|-------------------|------------------|-------------------------------------|
| Amoco Rykon | Mineral Oil | Urea | 129.0 |
| Texaco Premium | Mineral Oil | Lithium Soap | 129.0 |
| Krytox 240 AB | PFPE | Teflon | 85.0 |
| Mobilith SHC 100 | Synthetic HC | Lithium Soap | 100.0 |
| Kluber Petamo | PPE / Ester | Urea | 60.0 |

judged by the contact slip level at which failure occurs. The time to failure was also noted. During each test, the traction coefficient and the specimen temperature was continuously monitored. At the conclusion of each test, the ball and disc surfaces were examined to assess the nature and extent of the damage.

6.6.3 Results and Discussion

Figures 51a and 51b show plots of the data during the test with Krytox 240AB grease for the all-steel and hybrid contacts, respectively. These figures are typically representative of the data for all the grease tests. The traction coefficient increased rapidly with the introduction of contact slip, reaching a maximum value of 3% slip for both all-steel and hybrid contacts. Once at the peak value (about 0.13 for all-steel and 0.14 for hybrid), the traction coefficient remained nearly steady during the test. In the hybrid test there were periodic rises ("spikes") in traction, followed by a quick decrease to the steady value.

The ball and disc temperature trends in both the all-steel and hybrid contact pairs were very similar. In both cases, the specimen temperature increases gradually with time. This was expected since the sliding speed increases with contact slip. For nearly steady traction and constant load test, the rate of frictional heating, and, hence, the temperature increased linearly with the amount of slip. The temperature increased more rapidly in the ball than in the disc because of the smaller mass of the ball specimen.

Figure 51 shows that the hybrid contact pair lubricated with the Krytox 240AB is more durable than the all-steel pair tested with the same grease. This was not the case in the tests run with the other greases. A summary of results for all the pairs tested with grease is shown in Table 9. For all of the five greases, the average traction coefficient for the hybrid contact pair was always slightly higher than that of the corresponding all-steel pairs. This could be due to a higher contact pressure in the hybrid test, since the tests were run at the same load of 20 lbs. The higher pressure would increase the severity of interaction between the surfaces and hence high traction.

A plot of the slip level at failure for each test grease is shown in Figure 52. The Si_3N_4 /steel hybrid pair performed better than all-steel pair when lubricated with the Krytox 240AB grease. In Mobilith SHC 100 grease, there was no difference in the performance of the hybrid and all-steel contact pairs. In the other three greases, the all-steel contact showed better performance. The relative performance of the all-steel and hybrid contacts in various test greases could also be explained by the operating lubrication mechanisms.

Lubrication by grease is accomplished by the base fluid and the additives present. The thickener serves as a reservoir for the oil. Because greases are semi-solid, they do not flow easily back into the contact pathway without re-circulation. Consequently, grease lubricated surfaces tend to run starved without an auxiliary means of pushing the grease back into the contact pathway. Under starved lubrication, the additive chemistry will dominate the tribological performance. In the current grease tests, there was no re-circulation. Better performance of the all-steel contact compared to the hybrid contact with greases: Amoco Rykon, Kluber Petomo, and Texaco Premium may be the result of EP additives working on two steel surfaces, instead of one for the

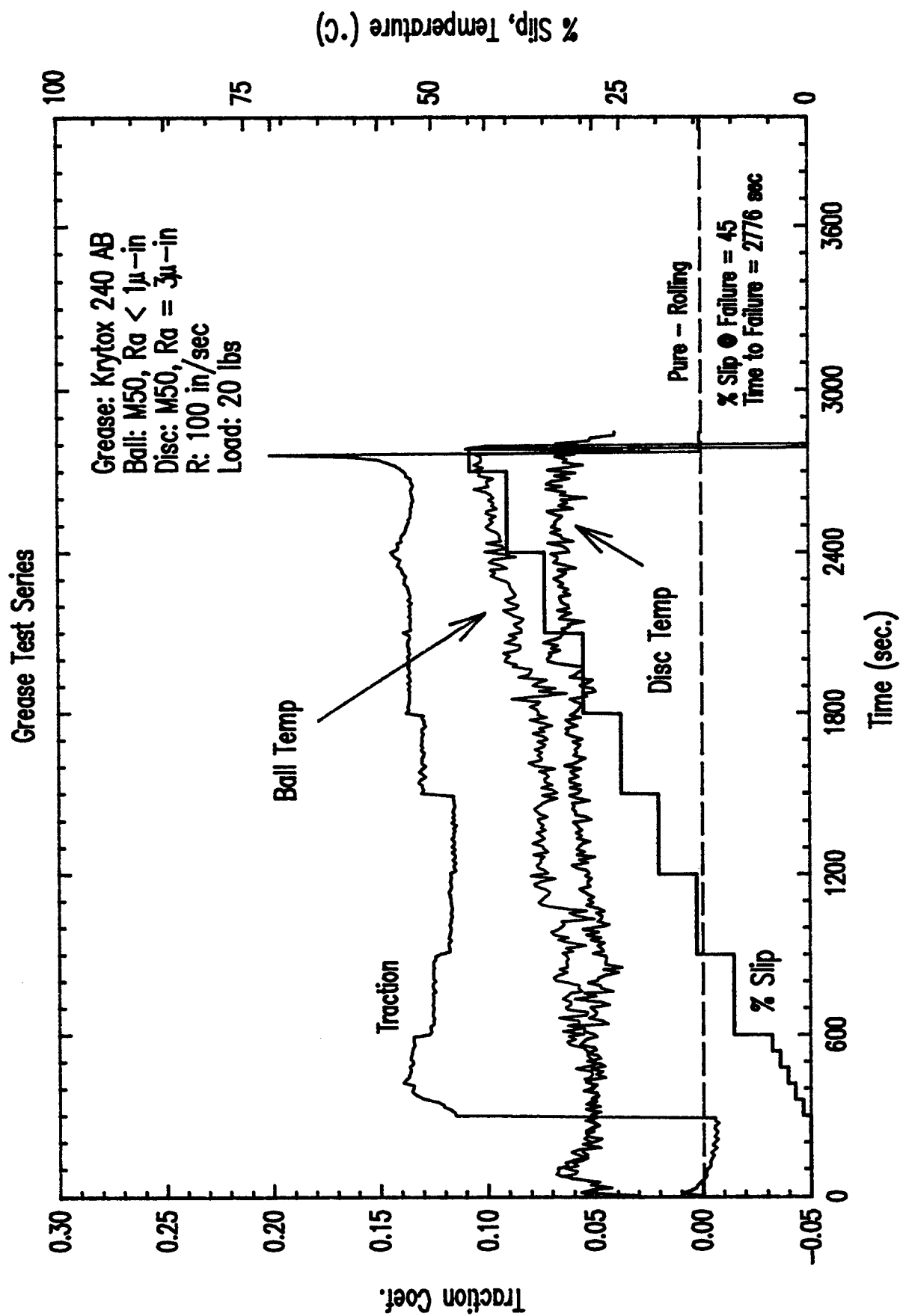


Figure 51a All-steel contact grease lubrication test

<DA111.SPW>

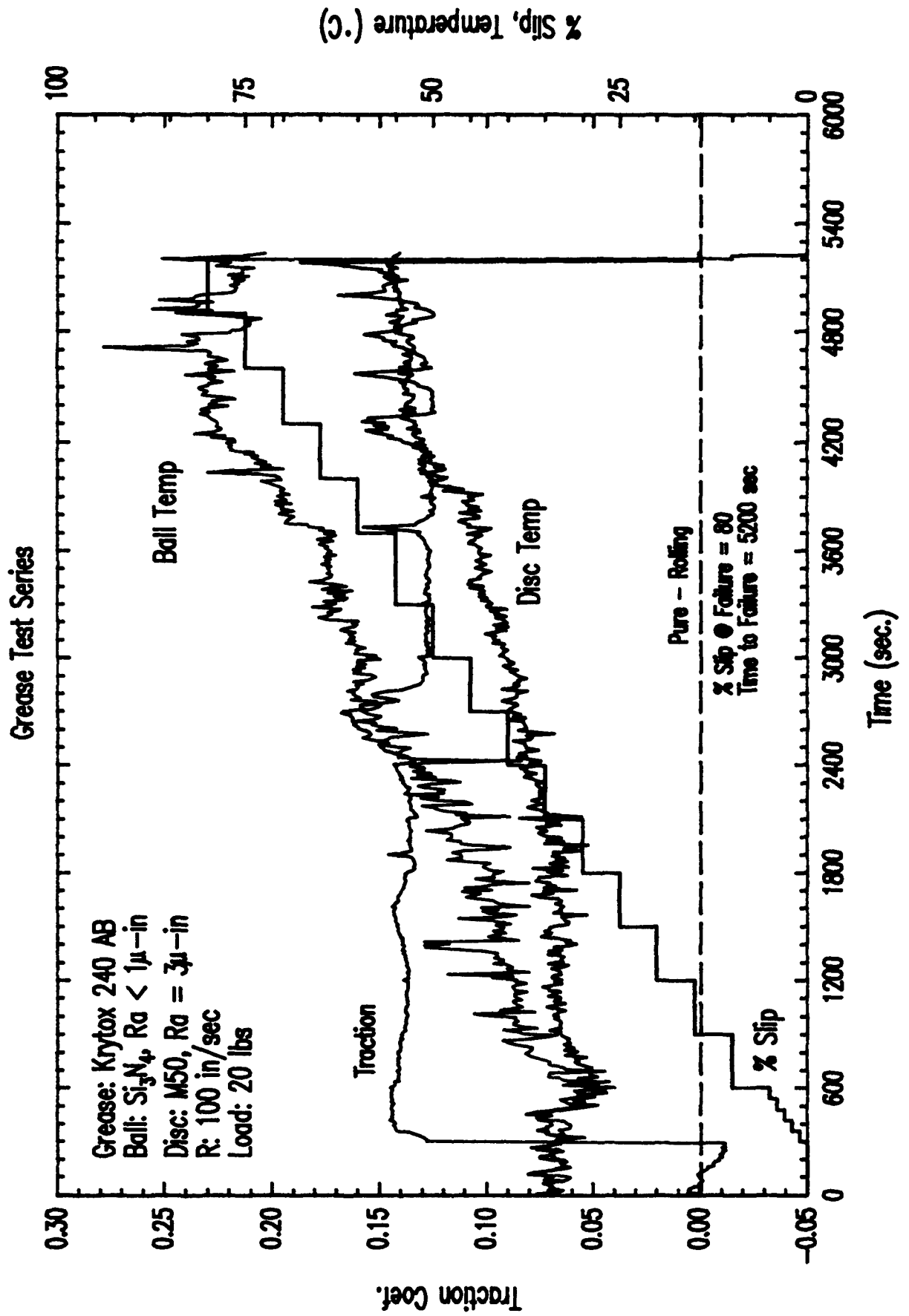


Figure 51b Hybrid contact grease lubrication test

SUMMARY CHART OF GREASE LUBRICATION TESTS

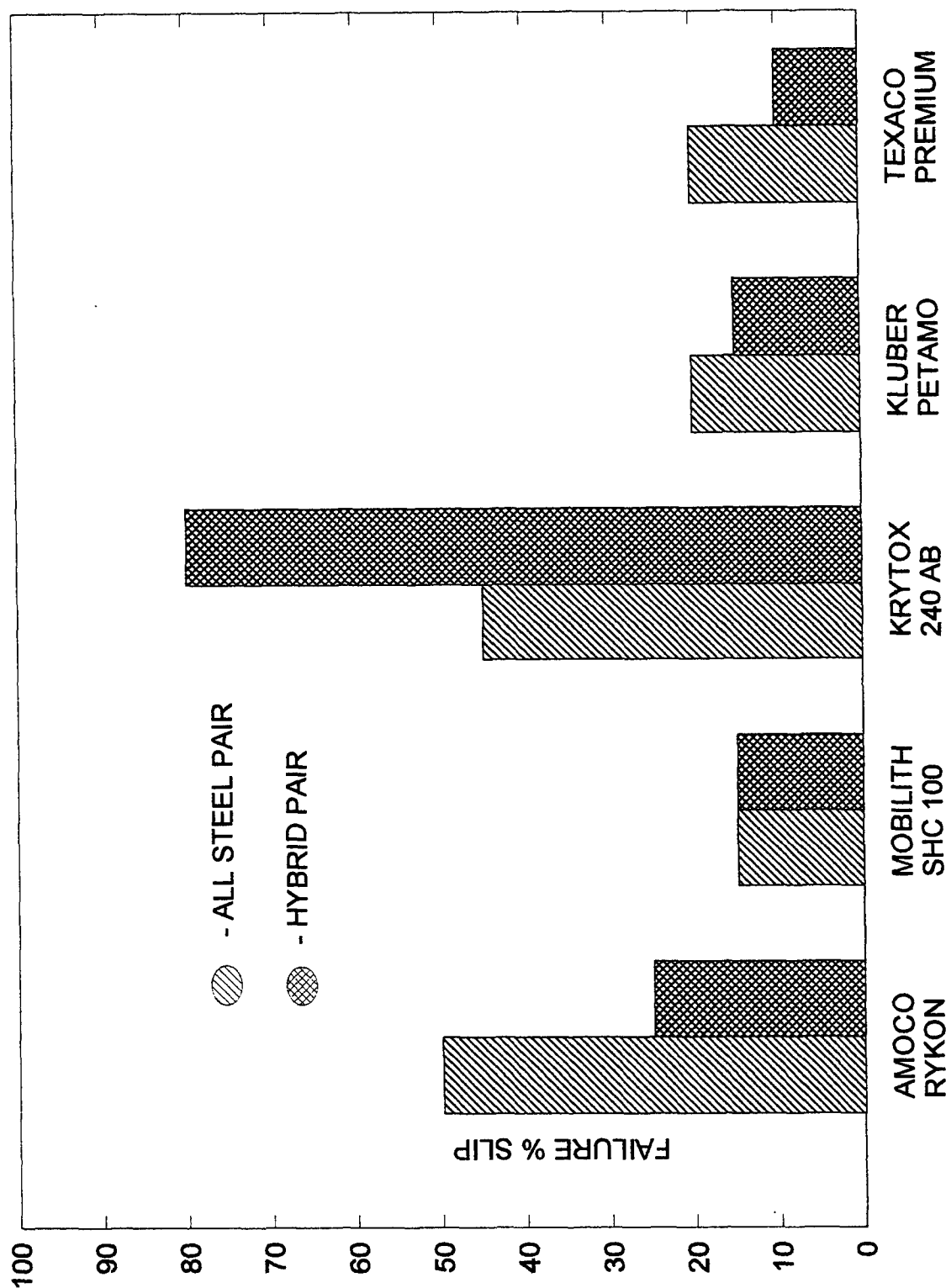


Figure 52 Summary Chart of Grease Lubrication Tests

<Darpabar.spw>

GREASE LUBRICATION RESULTS

Table 9

| GREASE | MATERIAL COMBINATION | FAILURE SLIP (TIME) | AVERAGE TRACTION COEFF. | MAX BALL TEMP. (°C) | MAX DISC TEMP. (°C) | COMMENTS |
|------------------|----------------------|---------------------|-------------------------|---------------------|---------------------|---|
| AMOCO RYKON | M50 STEEL | | | | | |
| | - ON - | | | | | |
| | M50 STEEL | 50% (3095 sec) | 0.078 | 44 | 31 | Film on ball and patchy film on disc. No wear in either Specimens. |
| | SI3N4 | | | | | |
| MOBILITH SHC 100 | - ON - | | | | | |
| | M50 STEEL | 25% (1776 sec) | 0.112 | 40 | 32 | No wear or damage on ball and disc. Occasional patchy film on ball and disc. |
| | - ON - | | | | | |
| | M50 STEEL | 15% (975 sec) | 0.100 | 34 | 30 | Traction Coefficient increased continually throughout test from 0.07 at 1% slip to 0.12 at failure. Continuous films on ball and disc. |
| KRYTOX 240AB | SI3N4 | | | | | |
| | - ON - | | | | | |
| | M50 STEEL | 15% (972 sec) | 0.110 | 40 | 31 | T.C. increased continuously during the test start at 0.07 at 1% to 0.17 at 15%. No damage or wear on ball and disc; some film on disc. |
| | - ON - | | | | | |
| KRYTOX 240AB | M50 STEEL | 45% (2776 sec) | 0.130 | 44 | 32 | Test was loud. Wide track on ball, with film. Film and no polishing wear on disc. |
| | - ON - | | | | | |
| | M50 STEEL | 80% (5200 sec) | 0.142 | 82 | 55 | Occasional Traction spikes with loud contact. Film on ball. More polishing wear and film on disc. |
| | SI3N4 | | | | | |
| KLUBER PETAMO | - ON - | | | | | |
| | M50 STEEL | 20% (1150 sec) | 0.100 | 35 | 31 | Continuous film on ball and disc tracks. |
| | - ON - | | | | | |
| | M50 STEEL | 15% (954 sec) | 0.115 | 38 | 31 | T.C. increased continually during the test with a start value of 0.09 at 1% slip to 0.20 at failure. No wear on ball and disc. Film on disc. |
| TEXACO PREMIUM | SI3N4 | | | | | |
| | - ON - | | | | | |
| | M50 STEEL | 20% (1275 sec) | 0.105 | 34 | 30 | Continuous film on ball, no wear but streaky film on disc. Traction Coeff. increased very slow during test until final failure. |
| | - ON - | | | | | |
| TEXACO PREMIUM | M50 STEEL | 10% (894 sec) | 0.120 | 37 | 31 | Traction Coeff. increased continuously during test starting at 0.096 at 1% ending at 0.20 at 10% slip. Isolated metal transfer to ball. Film on disc. |
| | - ON - | | | | | |
| | M50 STEEL | | | | | |
| | SI3N4 | | | | | |

hybrid contact.

Although a general conclusion cannot be drawn from the present results because of its limited scope; it appears the type of thickener also has a significant effect on grease performance. The grease with Urea thickener seems to enhance the performance of both all-steel and hybrid contacts compared to Lithium soap. This is illustrated by the results from tests with Amoco Rykon and Texaco Premium. Both greases contained the same type of fluid, with the same viscosity. The Amoco grease with Urea thickener showed a better performance than the Texaco grease with Lithium soap thickener.

The Krytox 240AB grease showed a different behavior compared to the other greases. It showed a significantly better performance than the other greases. It was also the only one in which the hybrid contact pair performed better than the all-steel pair. There are two plausible reasons for this peculiar behavior of the Krytox grease. Since most (if not all) of the common additives are insoluble in the PFPE base fluid, the grease contains no additives. As a result, the hybrid contact pair performed better than the all-steel contact with the effect of the additives removed. Second, the Teflon thickener in the grease was a solid lubricant. There is, therefore, a synergism between the liquid lubricating action of the base fluid phase and the solid lubrication by the thickener. This accounts for the good performance of the grease for both all-steel and hybrid contacts. In fact, a study has shown that incorporation of Teflon (PTFE) particles into a Lithium soap-based grease increased its tribological performance [21].

Examination of the specimen surfaces at the conclusion of each test showed some similarities and some differences between the all-steel and hybrid contact pairs. In both cases, there was no large scale wear in terms of material removal. Formation of surface films was also a common occurrence in both the all-steel and the hybrid contacts. Figures 53 and 54 show the hybrid and all-steel pairs respectively run with the Mobilith SHC 100 grease. Although both tests failed at about the same point, there was considerably more film on the all-steel surfaces. In fact, there was no film on the Si_3N_4 ball from the hybrid test. In all five greases tested, there was always more film formation in the all-steel contact pairs when compared to the hybrid.

The exact nature and role of these surface films on the grease performance is not clear at this point. If they are oxides, which they appear to be, their presence can significantly degrade the lubricating grease over time. As the films are worn, they will get incorporated into the grease, thereby reducing its effectiveness. Lack or reduction of film formation in the hybrid contact pair would be beneficial to the long term durability of the grease.

From the results of the present grease lubrication tests, it is clear that the hybrid bearing can be lubricated with grease as well as the all-steel bearings. Lack of possible grease degrading oxide film in the hybrid bearing could be a significant advantage. The use of Teflon containing grease, such as Krytox 240AB, is particularly recommended for the lubrication of hybrid bearings.

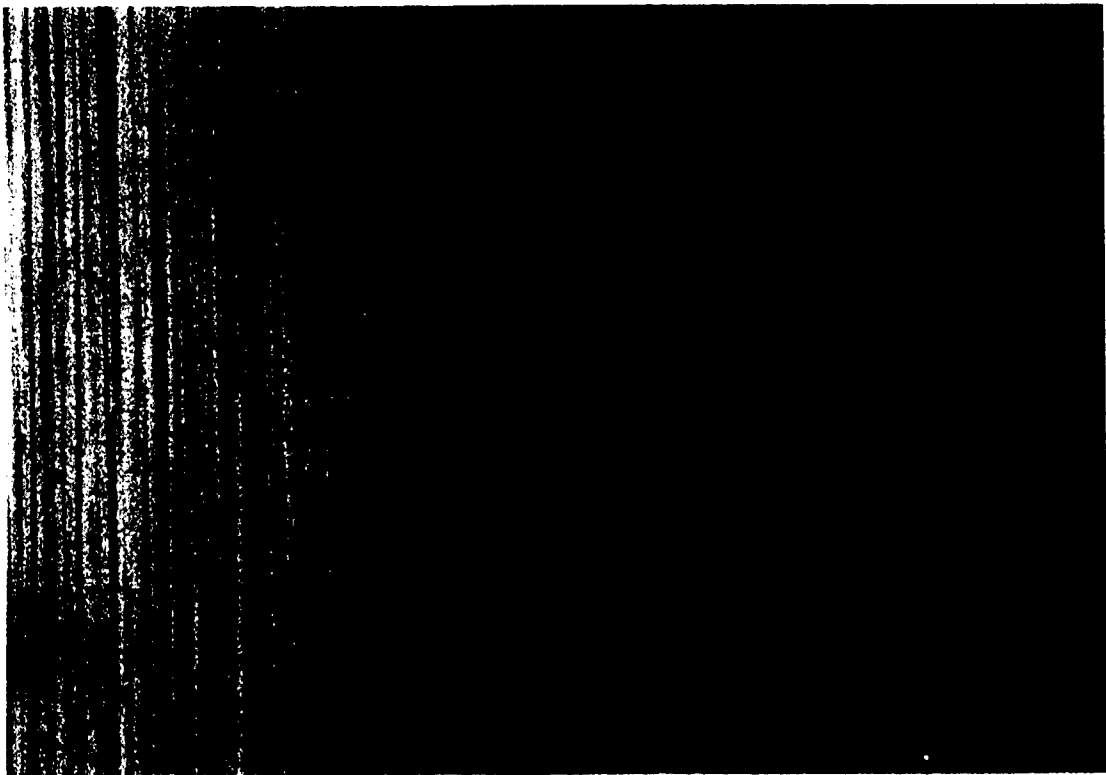
6.6.4 Summary

The tribological performances of steel-on-steel contacts and Si_3N_4 -on-steel contacts lubricated



Si₃N₄ Ball

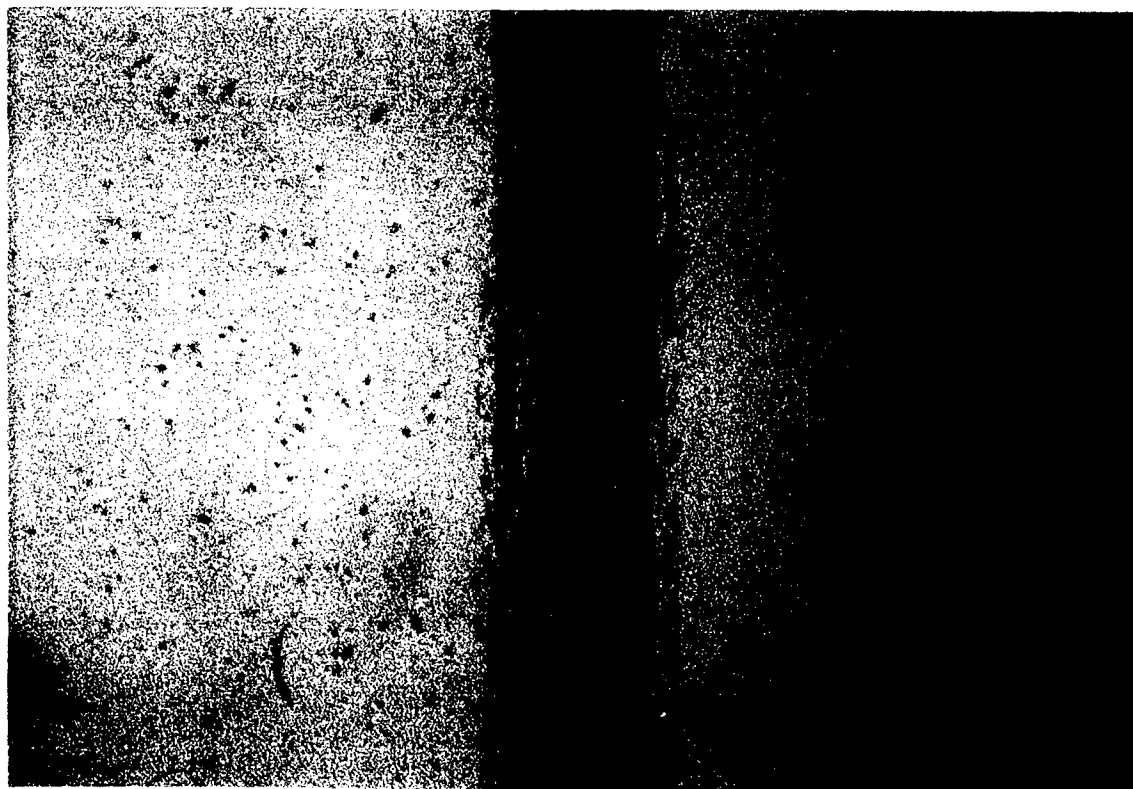
200 μm



Steel Ball

200 μm

Figure 53 Mobilith SHC 100 grease lubricated hybrid contact pair



Steel Ball

200 μ m



Steel Disc

200 μ m

Figure 54 Mobilith SHC 100 grease lubricated all steel contact pair

with grease were evaluated. This was done by assessing the durability of each contact with five different greases. The test procedure involved a progressive increase in the severity of contact until failure. Hybrid contacts showed better durability than all-steel contacts in only the test run with Krytox 240AB grease. In the other four greases, the all-steel contacts shed slightly better or about the same durability as the hybrid. This comparative behavior is rationalized in terms of the effect of the grease's EP additives under the starved lubrication condition of the test. The better performance of hybrid contact in the Krytox grease is attributed to the lack of additive, and the synergistic effect of solid and liquid lubrication. The failure process in all the tested greases involved the formation of an oxide layer on both ball and disc surfaces. Much more film was formed in the all-steel contact pair compared to the hybrid pair. It is concluded that hybrid bearings consisting of Si_3N_4 rolling elements and steel races can be effectively lubricated with grease. A substantial performance gain is expected when the bearing is lubricated with Krytox grease, compared to an all-steel bearing.

6.7 Performance Mapping

Most of the tribological components are, in general, usually lubricated with oil or grease. Failure of such components in service is often connected with the inadequate performance of the lubricant. It is always useful from a design standpoint to be able to assess, or at least estimate, the expected performance of a lubricated component. A comprehensive evaluation of the performance attributes of lubricated contact is therefore desirable.

There are three broad regimes of fluid lubrications, viz.: hydrodynamic, elastohydrodynamic (EHD), and mixed film or boundary regime. The operating contact kinematics and the lubricant physical properties determine the lubrication regime. Under hydrodynamics and full-film EHD lubrication, the surfaces are completely separated by the lubricant film. Under such conditions, the lubricant's rheological properties govern the performance and behavior of the lubricated contact. In mixed film and boundary lubrication regime, there is direct interaction between the surfaces. Then the chemical properties of the oil and the material surface properties determine the performance. Contact severity beyond the boundary regime, or the breakdown of the boundary chemical films, could result in a catastrophic failure. The nature and properties of the boundary films and the properties of the contacting surfaces govern this failure process.

Evaluation of the performance characteristics of all-steel and hybrid lubricated contacts under various lubrication regimes will be a useful exercise. This is in fact necessary if all-steel bearings are going to be replaced with hybrid ones. The designers need to know that the lubrication approach that works for the all-steel bearings will also work equally as well for the hybrid bearings. The goal of the task reported here was to evaluate the tribological performance attributes of all-steel and hybrid contacts under various lubrication regimes.

6.7.1 Approach

The operating lubrication regime is determined by the ration of lubricant film thickness to the composite roughness of contacting surfaces, i.e., h/σ or the so-called λ ratio. When $\lambda > 3.0$,

hydrodynamic lubrication operates. For $1 < \lambda < 3$, EHD lubrication operates. Whenever $\lambda < 1$, the contact is under fixed film or boundary lubrication regime. The lubricant film thickness (h) is determined by the oil rheological properties (primarily viscosity and pressure-viscosity coefficient) and the operating parameters, particularly the entraining or rolling velocity. When sliding is imposed on the contact, shear strain ensues, which could result in wear when the surfaces are touching. Sliding also produces frictional heating, which will alter the lubricant film physical and rheological properties. These properties are strongly dependent on temperature.

Wedeven Associates has developed a method of "mapping" the various operating lubrication regimes in a contact [22]. This is done by operating a lubricated contact over a range of values of rolling (R) and sliding (S) velocities in a series of tests. The operating regimes during each test are identified. The results are then displayed as a plot of S and R, on which various lubrication regimes are shown. Each test is denoted as a data point on the map.

This approach can also be used to display other tribological failure mechanisms in terms of some operating parameters. The interest here is the lubrication performance mapping for hybrid and all-steel contacts. Therefore, the standard Wedeven Associates method will be used. Both all-steel and hybrid contacts will be evaluated with the same lubricant. The effect of Si_3N_4 substitution for steel on lubricated contact performance under various regimes can then be effectively assessed.

6.7.2 Test Details

All the tests for performance mapping are run on the WAM3 machine. The unique capability of the machine to independently control the entraining (rolling) velocity and the sliding velocity is essential in performance mapping methodology. The tests are run with the following parameters:

Ball: M50 Steel, Si_3N_4 (smooth, $R_a \approx 0.3 \mu\text{in}$)
Disc: M50 Steel ($R_a \approx 2 \mu\text{in}$)
Stress: 300 ksi
Entraining (rolling) Velocity: 30, 100, 170 in/sec
Sliding Velocity: Variable
Temperature: Ambient Room Temperature (frictional heating of specimen occurs during test)
Lubricant: Synthetic Ester basestock (Herco-A)

6.7.3 Procedure

A series of 10 min. tests are run at three different selected entraining (rolling) velocities, R, and various sliding velocities, S. For a given R, the severity of contact is increased I subsequent tests in the series by increasing the sliding velocity S. Increase in contact severity is continued until failure by scuffing or severe wear occurs. At the end of each test, the specimen surfaces are examined to assess occurrence of wear and to quantify its amount. The test results are then displayed as a plot of sliding velocity (S) vs. rolling velocity (R). Each test is identified as a data point. The lubrication regime operating during each test is identified on the plot or "performance

map.” For example, tests, which show no evidence of wear or direct interaction between the specimen surfaces, define the EHD lubrication regime.

The lubricant is drip-fed onto the disc specimen throughout the duration of each test. The traction coefficient and the specimen temperatures are continuously monitored during each 10 min. test. Temperature measurements are made by trailing thermocouples. At the conclusion of each test, the specimen surfaces are examined with an optical microscope to characterize wear and other changes on the surface.

6.7.4 Results and Discussion

Hybrid contact also showed a larger mixed film lubrication regime compared to the all-steel contact. This reflects the higher durability of Si_3N_4 /steel hybrid contact, over the all-steel contacts under low h/σ conditions. Furthermore, better topographical run-in of the steel disc surface by the Si_3N_4 ball will expand the mixed-film lubrication regime. Combination of the EHD and mixed film lubrication expansion in the hybrid contact pair, coupled with the higher durability of Si_3N_4 /steel interface, produced a significantly higher scuffing boundary when compared to an all-steel contact. This is also consistent with the load capacity test results presented earlier in this report.

The average traction coefficients during each test used in the tribological performance mapping a all-steel and hybrid contact pairs are shown in Figures 56a and 56b, respectively. The trends of the traction variation with the sliding velocity in both kinds of contact pairs are essentially the same. In general, the average traction coefficient decreases with increasing sliding velocity in a near exponential manner to a steady value of about 0.026. The first of each 10 minute test series with both the all-steel and hybrid contacts started with a n average traction coefficient of about 0.063 to 0.068.

The traction trends in Figures 56a and 56b reflect the changes in surface topography and the effect of frictional heating as the sliding velocity increased in subsequent tests. Topographical run-in during the earlier test reduced the surface roughness and hence resulted in improved EHD lubrication, which decreased the traction coefficient during the subsequent tests. Also, as sliding velocity S increased, the rate of frictional heating increased. The resulting increase in contact interface temperature lead to a decrease in the interface shear strength, which also reduced the traction. The combined effect of topographical changes and frictional heating was responsible for the near exponential decrease in traction coefficient.

Increase in frictional heating with sliding velocity will also decrease the effective oil film viscosity. This will reduce the fluid film thickness, thereby decreasing the h/σ ratio. The effect will be to increase the level of interaction between the surfaces and, hence, the surface contribution to traction. The result is an increase in the traction coefficient. Thus, higher frictional heat at the contact interface produces two opposing effects on traction behavior. When these two opposite effects nullify each other, the traction coefficient is expected to be less sensitive to S . This is perhaps responsible for the near steady values of the traction coefficient at high S .

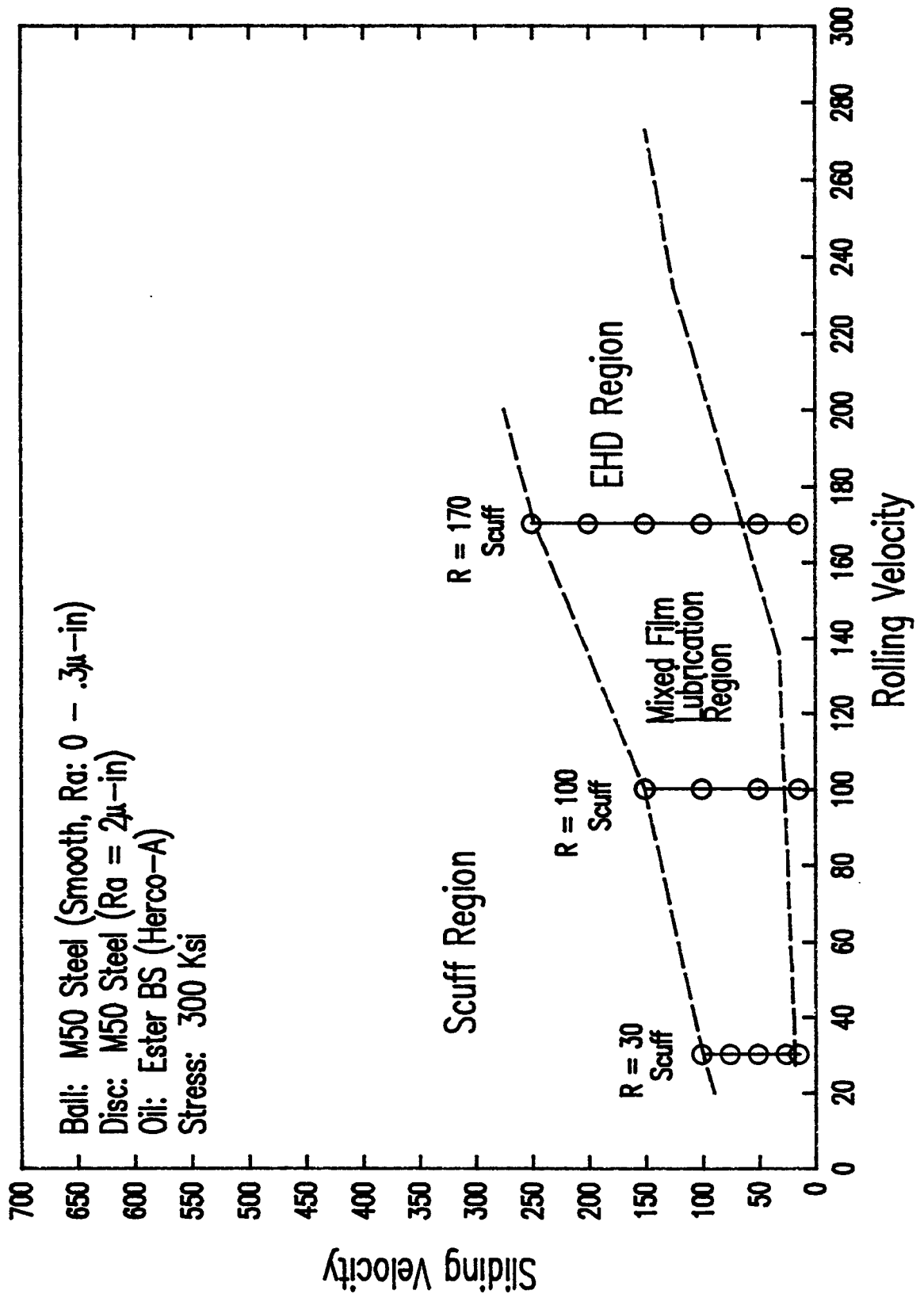


Figure 55a Performance map for all-steel contact

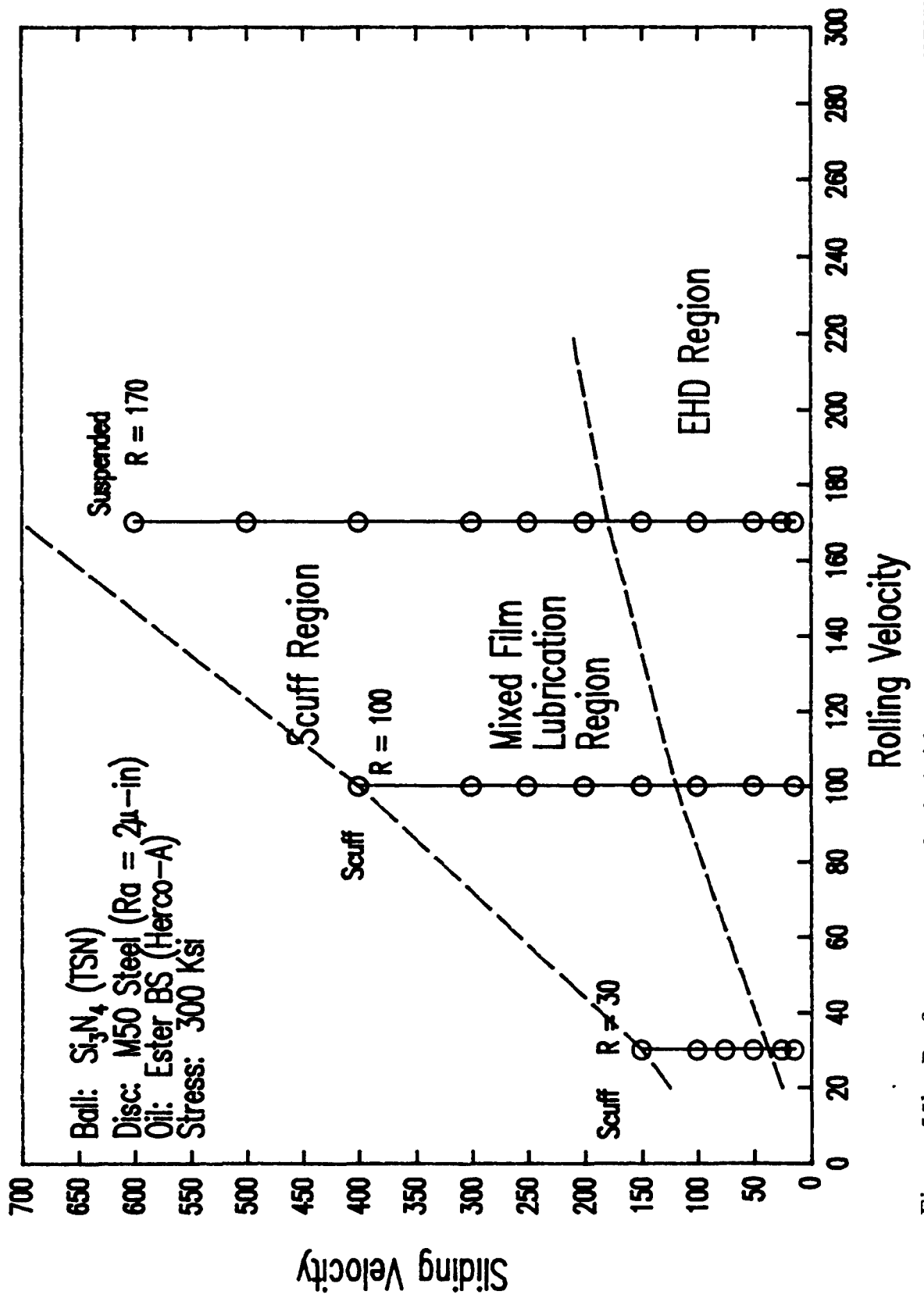


Figure 55b Performance map for hybrid contact pair

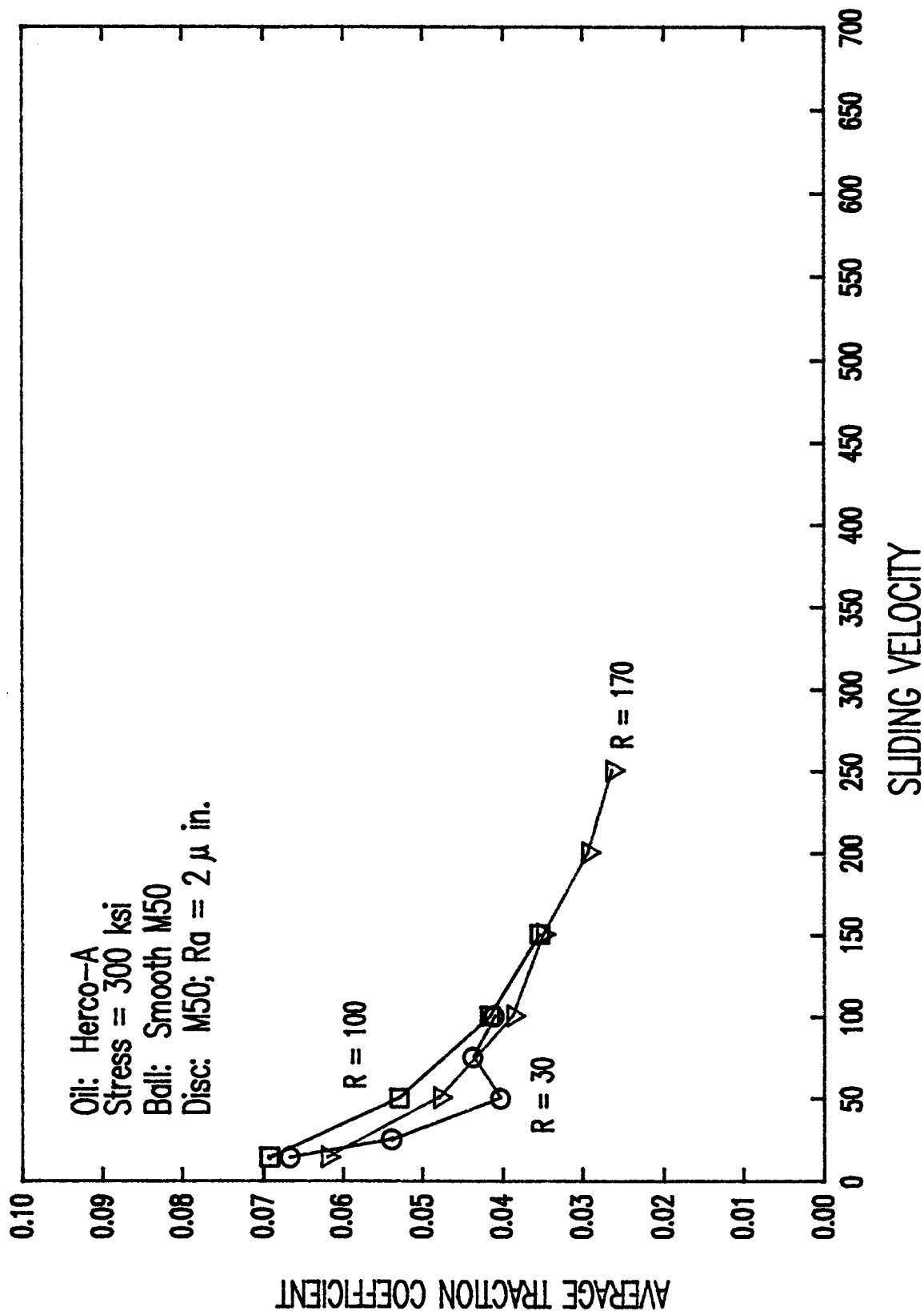


Figure 56a Average traction coefficient as a function of sliding velocity for all-steel

<DARPATR3.SPW>

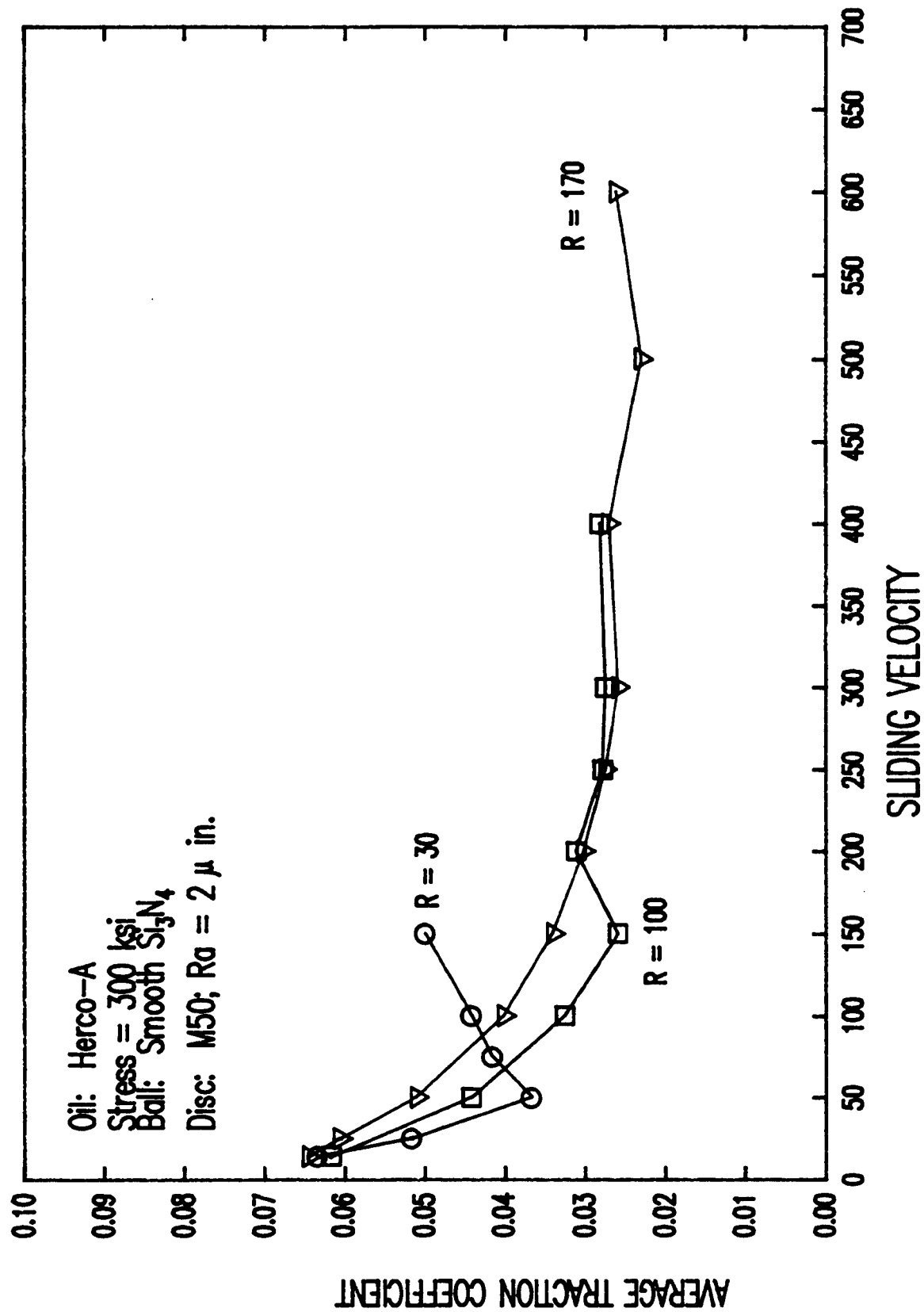


Figure 56b Average traction coefficient as a function of sliding velocity for hybrid

A peculiar deviation occurred in the traction behavior of the hybrid contact pair test series at an R of 30 in/sec (Figure 56b). After the initial decrease of traction with increasing S, up to 50 in/sec, the average traction coefficient then increased with S. This change in the traction trend was observed to coincide with the occurrence of transfer of disc metallic steel material onto the Si_3N_4 ball surface. The extent of this transfer increased with S until scuffing finally occurred.

The thermal characteristics of the all-steel and hybrid contact pairs during performance mapping are shown in Figures 57a and 57b, respectively. The figures are plots of average ball temperatures during each 10 minute test as a function of a frictional heat input parameter $\text{TC} \times \text{S}$. The rate of frictional heat generation $q = \mu P_{av} S$, where μ is the traction coefficient (TC). P_{av} is the average contact pressure and s is the sliding velocity. Since all the performance mapping tests are run under constant nominal stress, the parameter $\text{TC} \times \text{S}$ is a good indicator of the rate of frictional heat input into the contact interface.

Figure 57 shows that the ball temperatures have a near linear dependence on the heat input for both all-steel and hybrid contact pairs. The magnitudes of the ball temperature in both contact pairs are also similar. These are all expected. With the frictional heat dissipation at the contact interface assumed to be by thermal conduction (a very reasonable assumption), a linear variation with heat input is expected. Also, with the thermal conductivity of Si_3N_4 and the M50 steel being very similar, the magnitude of temperatures in both kinds of ball s is expected to be similar. Figure 57b shows, however, that deviation occurs at some points in the linearity of the Si_3N_4 ball temperature with the frictional heat input parameter during the hybrid tests. This deviation is due to the occurrence of metal transfer from the disc onto the Si_3N_4 ball surface. The presence of a transfer layer modified the thermal characteristics of the ball surface, particularly with regards to heat conduction. In the absence of metal transfers, the thermal characteristics of all-steel and hybrid contact pairs are very similar to one another.

The failed surfaces of the all-steel and the hybrid contact pairs tested at $R=30$ in/sec are shown in Figures 58 and 59, respectively. In the preceding tests before failure, a grayish film forms on the ball surface and polishing wear occurred on the disc for the all-steel contact pair. For the hybrid pair, there was no wear on the ball but a progressive increase in metal transfer in subsequent tests. Polishing wear also occurred on the disc. The extent of polishing wear on the hybrid contact pair was more than that in the equivalent all-steel test. The failed ball and disc surfaces in the all-steel pairs look very much alike (Figure 58). There was severe damage and roughening, which is characteristic of scuffing phenomena. In the hybrid contact pair, on the other hand, there was massive metal transfer, but no wear on the Si_3N_4 ball. The damage on the steel disc involved scuffing, but with less roughening compared to the all-steel pair (Figure 59).

The progression of damage at higher rolling velocities of 100 and 170 in/sec was also similar to the one at R of 30 in/sec. The failed surfaces at $R=100$ in/sec were similar to the ones in Figure 58 and 59. At the rolling velocity of 170 in/sec, scuffing occurred in the test series with all-steel pairs, while the hybrid pair was suspended without scuffing. Figures 60 and 61 show the failed all-steel and suspended hybrid surfaces respectively. There was a typical scuffing appearance in the all-steel pair, in addition to some film on the ball surface (Figure 60). In the hybrid pair, there was some metal transfer onto the Si_3N_4 ball and significant damage to the disc surface. In

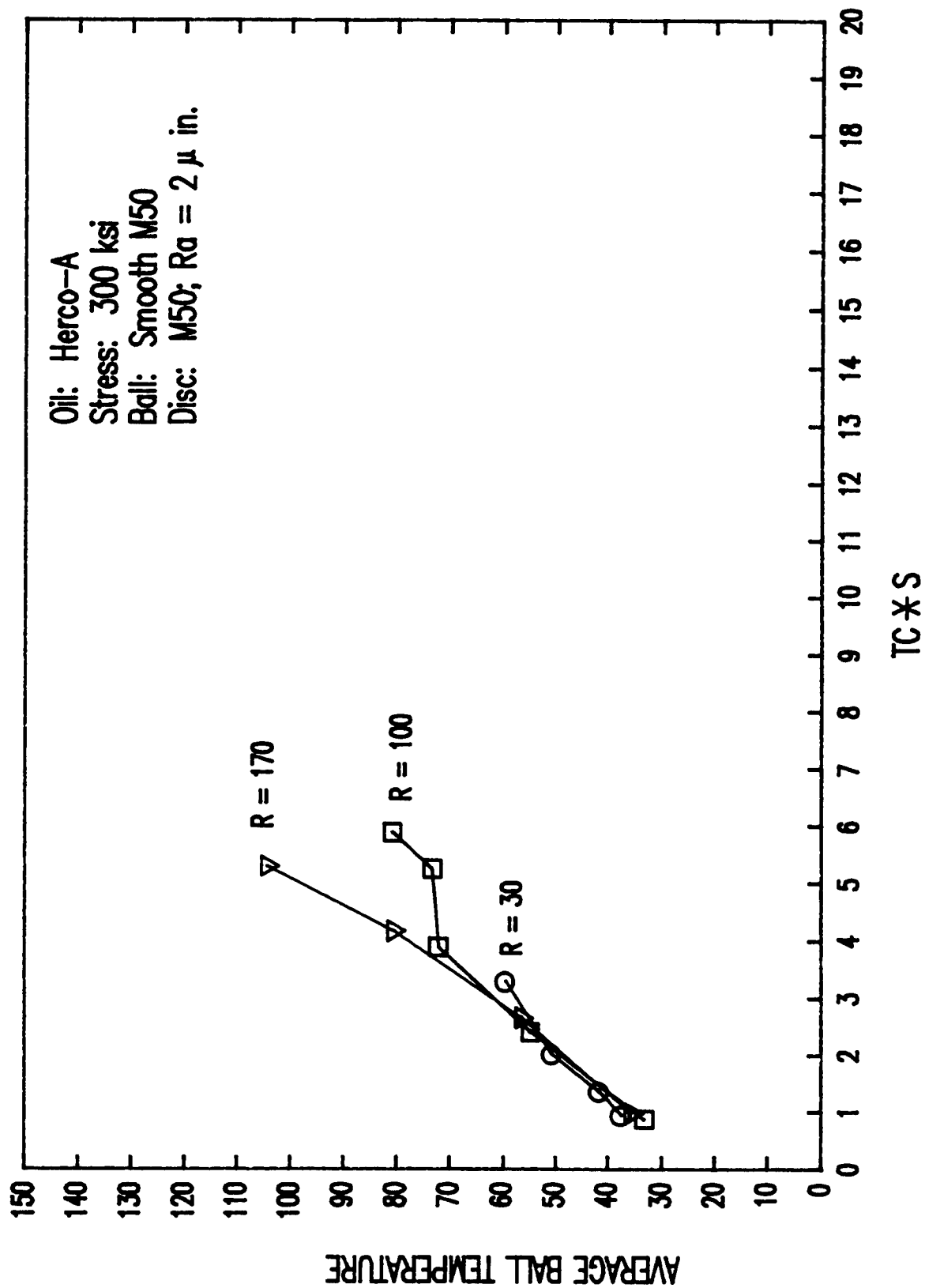
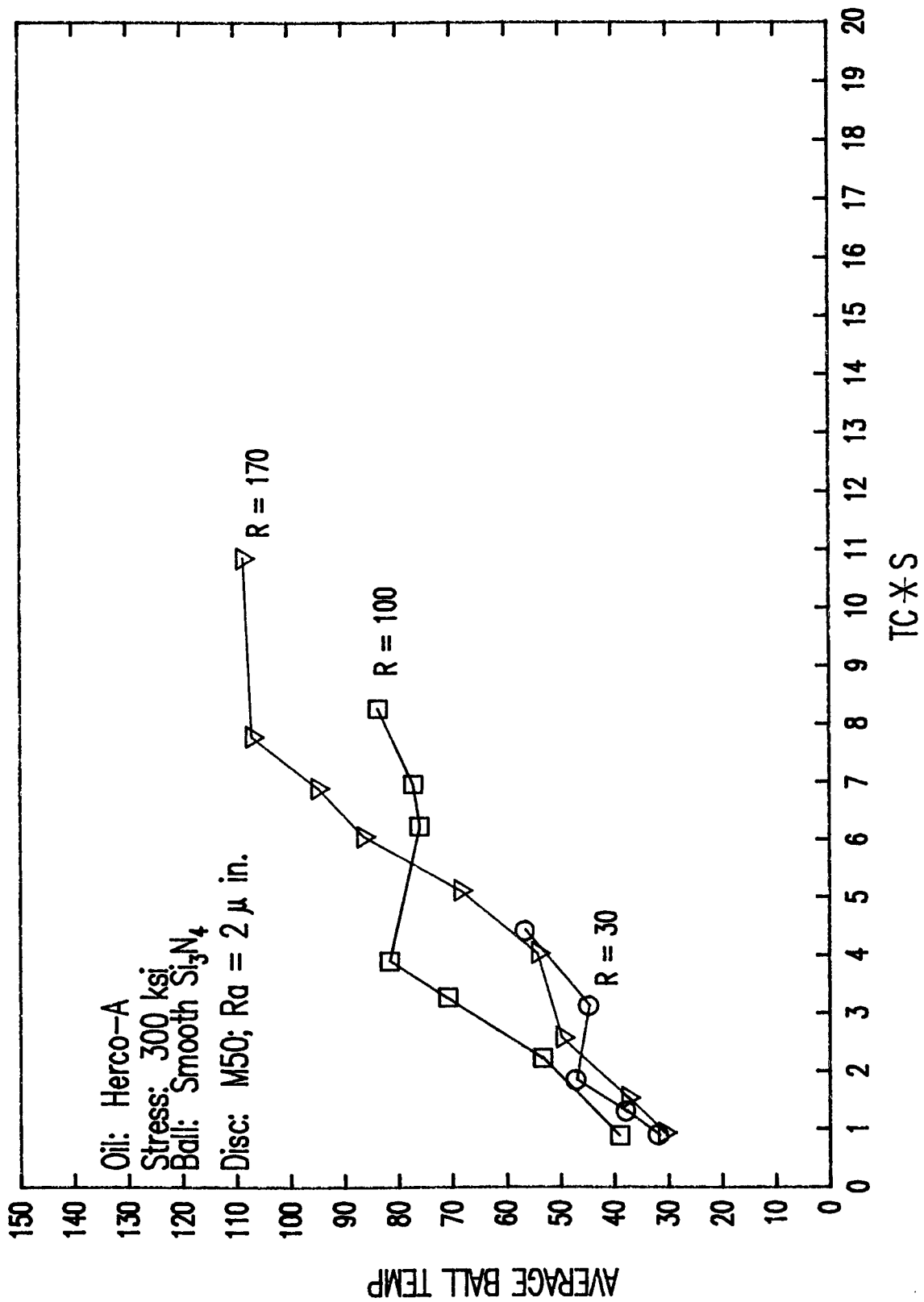
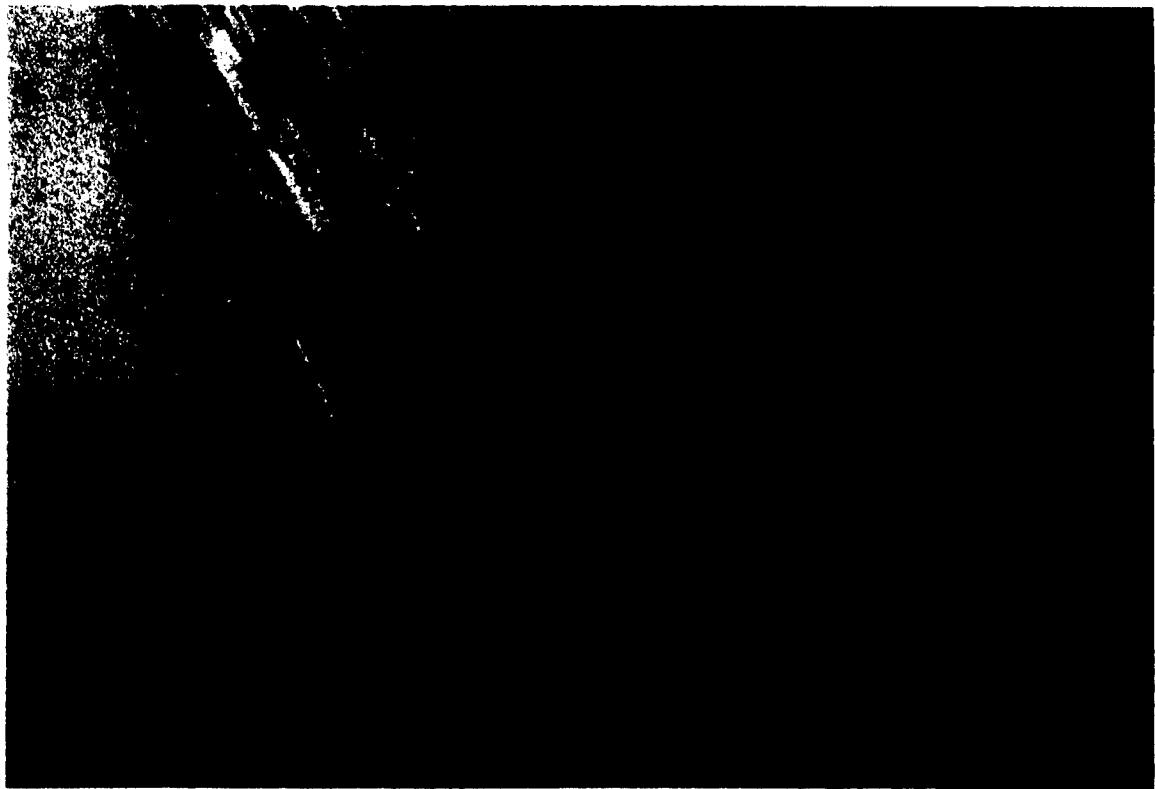


Figure 57a Ball temperature as a function of friction heat input for all-steel



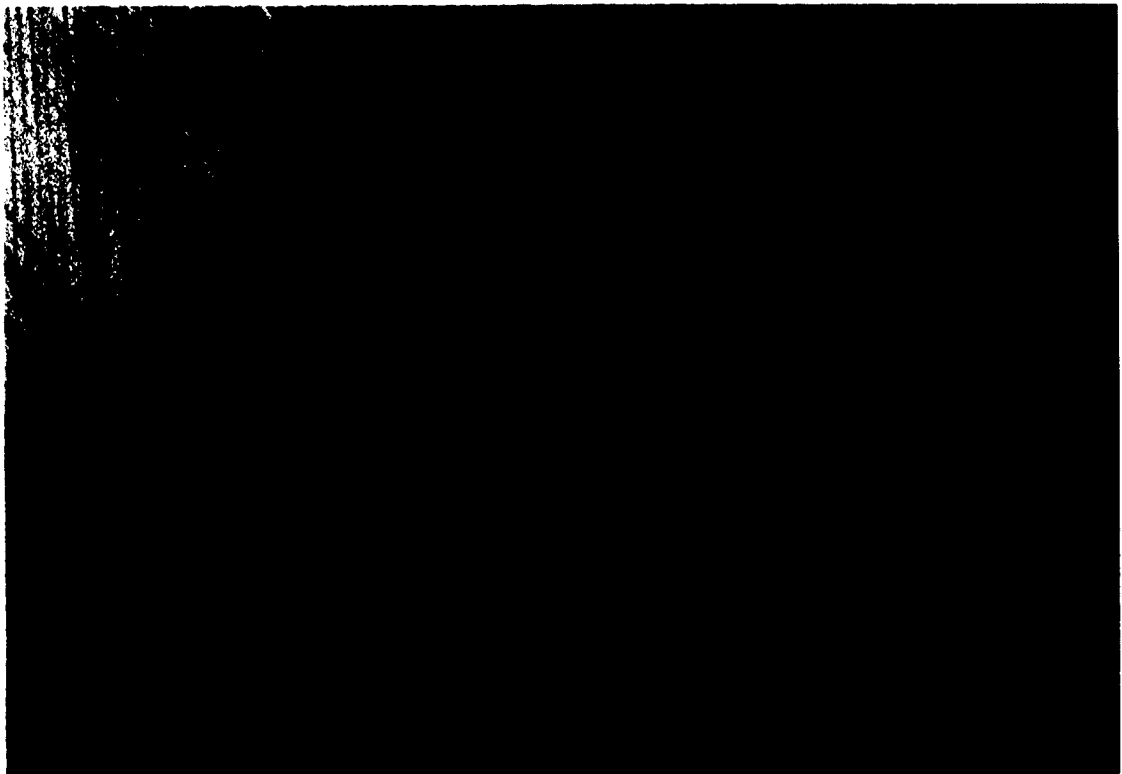
<DARPA/ELSPW>

Figure 57b Ball temperature as a function of friction heat input for hybrid



Steel Ball

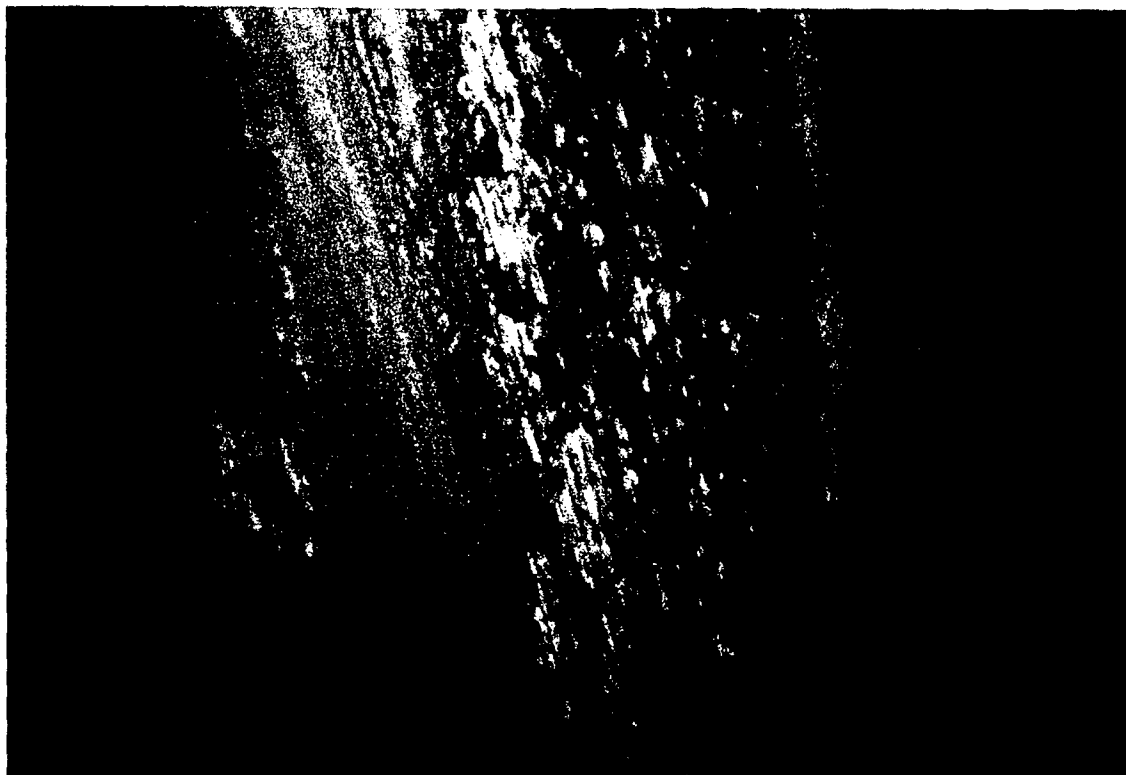
|-----|
200 μm



Steel Disc

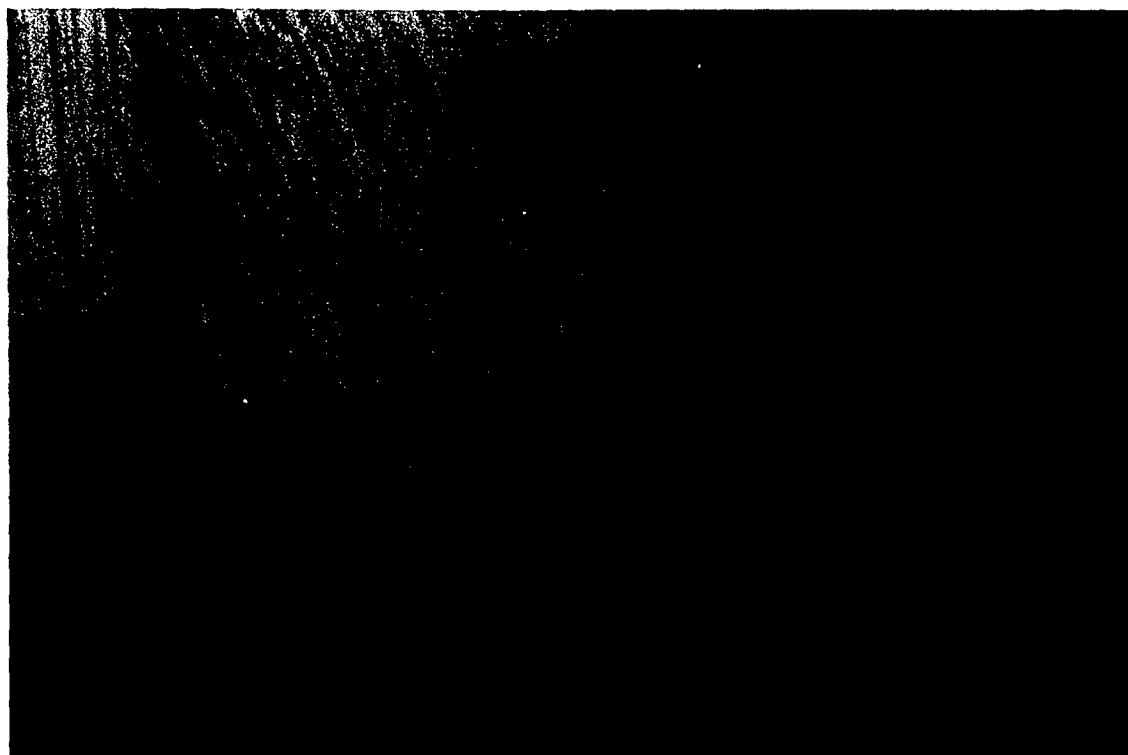
|-----|
200 μm

Figure 58 Ball and disc in all steel contact for performance map at $R=30$ in/sec after failure.



Si_3N_4 Ball

200 μm



Steel Disc

200 μm

Figure 59 Ball and disc in hybrid contact for performance map at $R=30$ in/sec after failure. Oil: Herco-A



Steel Ball

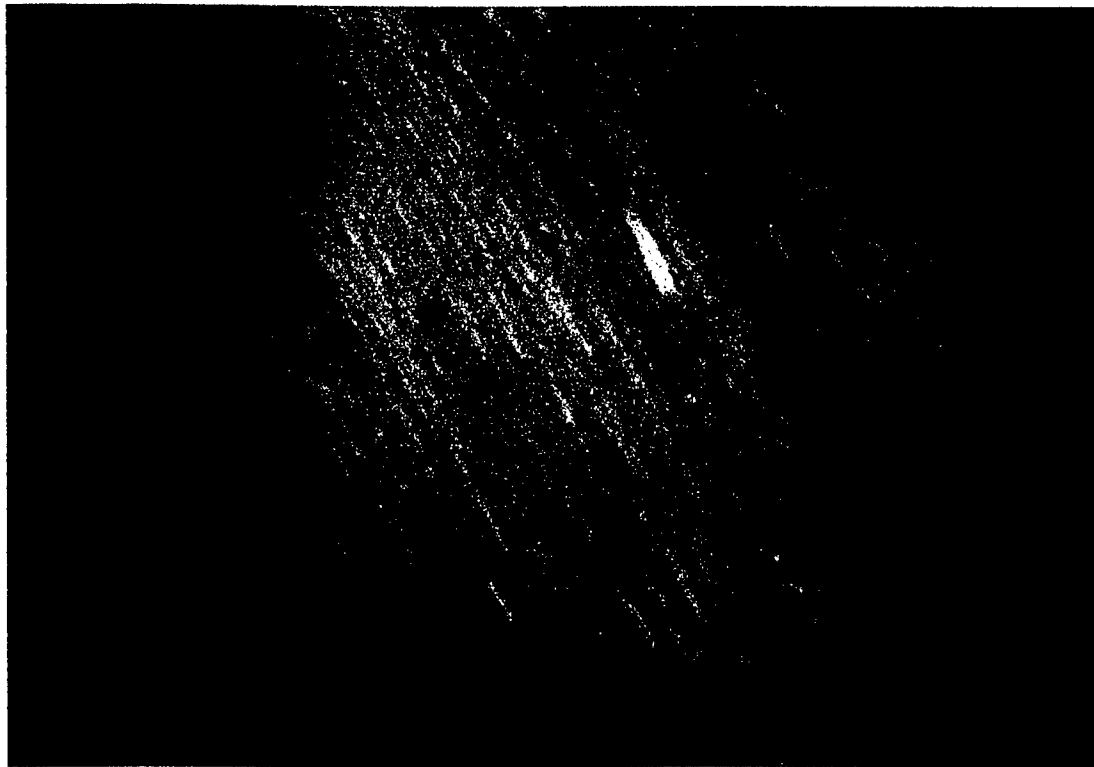
200 μ m



Steel Disc

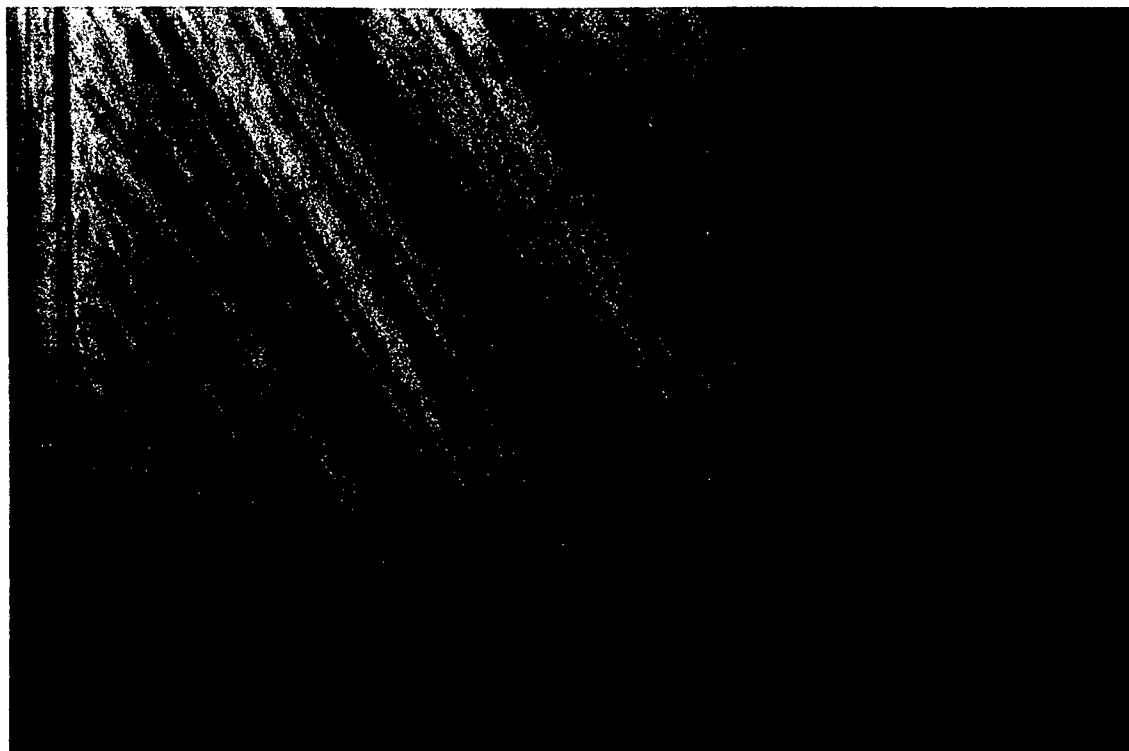
200 μ m

Figure 60 Ball and disc in all-steel contact for performance map at $R=170$ in/sec after failure. Oil: Herco-A



Si₃N₄ Ball

200 μm



Steel Disc

200 μm

Figure 61 Ball and disc in hybrid contact for performance map at
R=170 in/sec. Contact did not fail. Oil: Herco-A

fact, the disc surface had a scuffed appearance, although the usual traction transition and rapid temperature rise, characteristics of the scuffing process, did not occur.

6.7.5 Summary and Implications of Performance Mapping Results

A comparative tribological performance map was done for all-steel and hybrid contact pairs. This was done by running a series of tests under various rolling, which controls lubricant film thickness, and sliding, which controls interfaced shear strain, velocities. Using a synthetic ester basestock oil, the various lubrication regimes of EHD and mixed film regions were significantly expanded in the hybrid contact pairs compared to the all-steel pairs. It was also observed that the traction and the thermal characteristics of both the hybrid and all-steel pairs were very similar under similar contact kinematics. This would suggest that existing oils, even the poor ones, can be used to effectively lubricate hybrid bearings with performance gain. It would also allow the design of smaller hybrid bearings, but with the same performance level as current larger all-steel ones. This would also enable hybrid bearing to operate under a much more severe condition without the risk of catastrophic tribological failure.

It was also observed that hybrid contacts can run satisfactorily without high traction or excessive heating, even when the steel disc surfaces appeared scuffed. This observation has a major practical implication for hybrid bearing lubrication. Such bearings do not require the heavily formulated and often “dirty” oils for satisfactory performance. In fact, a basestock oil will effectively lubricate a hybrid bearing.

7. Conclusions

1. A run-in finishing methodology has been successfully developed for Si_3N_4 balls and Si_3N_4 and steel disc surfaces. Using a single element contact of a ball-on-disc, polishing wear mode is invoked on the ball and/or disc contact area without the use of abrasive particles. In the procedure, the ball and disc contact is operated under combined rolling and sliding conditions and lubricated with a working fluid.
2. The working fluid plays a significant role in the run-in finishing process. Water-containing fluids were observed to accelerate the run-in finishing process in ball and disc surfaces of Si_3N_4 . The presence of a peroxide (hydrogen peroxide in this study) or a hydroxide (sodium hydroxide in this study) produces another material removal mechanism, which involves spalling in addition to polishing wear.
3. The Si_3N_4 ball chemistry and/or original surface topography appears to have a significance on the run-in finishing process. Different rates of finishing are observed in the Toshiba TSN-03H and Cerbec NBD200 Si_3N_4 balls when tested with the same working fluids. The two materials differ in their sintering-aid additives and the original surface condition of their blanks.
4. The good run-in finishing of Si_3N_4 materials obtained with the water-containing working fluids involves two concurrent mechanisms. The presence of water in oil (emulsion) degrades the EHD film-forming capability of the oil, thereby creating inadequate lubrication. Tribochemical reactions also occur on the Si_3N_4 surface in the presence of water. The synergistic effect of inadequate EHD lubrication and tribochemical reaction creates a smooth topography in the contact area.
5. The presence of some metallic coatings accelerates the run-in finishing process in a steel disc. Soft metallic coatings, notably Ag and Cu, also act as boundary film under marginal lubrication, thereby improving the tribological performance of Si_3N_4 and coated disc contacts. Polymeric coatings, specifically PTFE, were also observed to be an effective boundary film for hybrid contacts of Si_3N_4 balls and steel discs.
6. Fully formulated synthetic hydrocarbon (SHC) oils (NYE 176A) were observed to form a well-pronounced brown film on both Si_3N_4 ball and steel disc surfaces during severe contact conditions. The presence of this surface film prevented catastrophic failure of the contact interface.
7. Extensive comparative evaluation of the tribological performance of an all-steel and a Si_3N_4 -on-steel hybrid contact was done with different types of tests. The hybrid contact showed much better performance than an all-steel contact under starved lubrication and oil-off tests. The load carrying capacity of oils was also increased substantially by a hybrid contact when compared to an all-steel contact. The conditions required for EHD and mixed-film lubrication regimes in terms of entraining and sliding velocities are significantly expanded in the Si_3N_4 and steel contact pair when compared to the steel-on-steel contact.

8. The much superior performance of the hybrid contact when compared to the al-steel contact under poor lubrication conditions suggests that heavily additized oils may not be necessary for satisfactory lubrication of hybrid bearings. In view of the ever-increasing regulatory requirements for "cleaner" oils, this is a major advantage of hybrid bearings and perhaps other lubricated hybrid components.

8. Recommendations

1. The run-in finishing methodology developed for Si_3N_4 ball and disc was the steel disc surface in the present effort used only the working fluid to produce the smooth topography. Current ball finishing and for the most part raceway finishing operations all use abrasives. A simultaneous use of a good run-in fluid with abrasive particles is expected to produce a synergistic effect between the two processes. An investigation of Si_3N_4 finishing with abrasives and a good run-in fluid is therefore recommended.
2. In the current study, an effect of Si_3N_4 ball material chemistry and original surface condition on the run-in finishing process was observed. A more detailed study of the effect of these two parameters on the Si_3N_4 ball finishing operations is recommended.
3. Formation of surface film occurred on both Si_3N_4 ball and steel disc surfaces during oil-off tests with the formulated SHC (NYE 176A) oil. Further investigation of the mechanisms of this film formation is recommended. Evaluation of the formation of such film in Si_3N_4 -on- Si_3N_4 contact is also recommended. Findings from such an investigation can provide the key to the formulation of oils specifically for hybrid and/or all-ceramic lubricated components.
4. The failure mechanisms in the hybrid contact of the Si_3N_4 ball and steel disc appear to be substantially different from the all-steel contact. The differences are particularly noticeable under the catastrophic failure condition of scuffing encountered in the load capacity, oil-off, and performance mapping tests. A better understanding of the failure mechanisms is required and studies aimed at a better elucidation of the lubricated hybrid contact failure processes are highly recommended.

9. References

1. J. Lange: "NDI/NDE of Silicon Nitride Ceramics," ARPA Ceramic Bearing Technology Annual Review Meeting Proceedings. May 26-27, 1994.
2. T. Sugita, K. Ueda and Y. Kanemura: "Material Removal Mechanism of Silicon Nitride during Rubbing in Water," *Wear*, 97, (1984) 1-8.
3. M.G. Gee: "The Formation of Glass in the Wear of Reaction-Bonded Silicon Nitride," *J. Phys. D: Appl Phys* 25, (1992) A182-A188.
4. T. E. Fischer and H. Tomizawa: "Interaction of Tribochemistry and Microstructure in the Friction and Wear of Silicon Nitride," *Wear*, 105 (1985) 29-45.
5. D. C. Barker, G. J. Johnston, H. A. Spikes and T. F. Bunemann: "EHD Film Formation and Starvation of Oil-In-Water Emulsions," *STLE Trib. Trans.* 36, (1993), 565-572.
6. D. Zhu, G. Biresaw, S. J. Clark and T. J. Kasun: "Elastohydrodynamic Lubrication with O/W Emulsion," *ASME J. Trib.*, 116 (1994) 310-320.
7. A. Dyson: "The Failure of Elastohydrodynamic Lubrication of Circumferentially Ground Discs," *Proc. ImechE.* 190., (1976) 52-76.
8. S. Singhal: "Asperity Welding – An Aspect of Scuffing of a Lubricated Sliding Contact," *Wear*, 24 (1973) 391-394.
9. H. Blok: "Theoretical Study of Temperature Rise at Surfaces of Actual Contact under Oiliness Lubricating Conditions," *Proc. ImechE, Gen. Disc. Lubr.* (1937) 222.
10. J. R. Barber: "Thermoelastic Instabilities in the Sliding of Conforming Solids," *Proc. Roy. Soc. Lond.* A312 (1969) 381-394.
11. W. Hirst and J. V. Stafford: "Transition Temperature in Boundary Lubrication," *Proc. Inst. Mech. Eng., Lond.* 186 (1972) 179.
12. H. A. Spikes and A. Cameron: "Scuffing as a Desorption Process," *SLE Trans.* 17 (1974) 92-96.
13. Y. Tanita, T. Mine and K. Nakajima: "Tribological Reaction Generated on Ceramic-Steel Couples under Boundary Lubrication," *ASME J. Trib.* 112, (1990) 637-642.
14. F. R. Morrison, J. I. McCool, T. M. Yonushonis and P. Weinberg: "The Load-Life Relationship for M50 Steel Bearings with Silicon Nitride Ceramic Balls," *Lubr. Engr.* 4, (1984) 153-159.

15. S. M. Schrader and E. E. Pfaffenberger: "Performance of Hybrid Ball Bearings in Oil and Jet Fuel," STLE Trib. Trans. 35 (1992) 389-396.
16. K. Kim and K. C. Ludema: "A Correlation Between Low Cycl Fatigue Properties and Scuffing Properties of 4340 Steel," ASME J. Trib. 117, (1995), 617-621.
17. K. C. Ludema: "A Review of Scuffing and Running-in of Lubricated Surfaces," Wear, 100, (1984), 315-331.
18. S. Mori and W. Morales: "Decomposition of perfluoroalkylpolyethers (PFPE) in Ultra-High Vacuum under Sliding Conditions," STLE Trib. Trans., 33, (1990), 325-332.
19. D. J. Carre: "Perfluoroalkylpolyehter Oil Degradation: - Influence of FeF_3 Formation on Steel Surfaces under Boundary Conditions," ASLE Trans., 29, (1986), 121-125.
20. P. C. Herrera-Fierro, W. R. Jones and S. V. Pepper: "Interfacial Chemistry of a Perfluoropolyether Lubricant Studied by XPS and TDS," NASA TM105840, (1992).
21. T. Stolarski and O. Olszewski: "An Experimental Study of the Frictional Mechanism in a Journal Bearing Lubricated with Grease Containing Powdered PTFE," Wear, 39, (1976), 377-387.
22. L. D. Wedeven, G. E. Totten and R. J. Bishop: "Performance Map Characterization of Hydraulic Fluids," SAE 941752.